THE REGULATION OF ADULT NEUROGENESIS BY RB FAMILY PROTEINS

BENSUN CAMBELL FONG

Thesis submitted to the University of Ottawa

in partial Fulfillment of the requirements for the

Doctor of Philosophy in Cellular and Molecular Medicine

Department of Cellular and Molecular Medicine

Cellular and Molecular Medicine Program

Faculty of Medicine

University of Ottawa

2022

For Linda Jui

For Sui Yee Fong

For Borisine Kusey

ABSTRACT

A complex regulatory framework underlies the generation of newborn neurons in the adult mammalian brain, including the lifelong maintenance of neural stem cell (NSC) quiescence and instructing NSC entry to and exit from quiescence. Future therapies targeting endogenous repair of the aging or afflicted brain, including neurodegenerative pathologies, rely on present efforts to define and characterize the mechanisms underlying the regulation of adult NSC fate. In this dissertation, we demonstrate a requirement for the Rb/E2F axis in the regulation of the molecular program instructing adult NSC quiescence and activation, with a potential role in the impaired hippocampal function observed in Alzheimer's disease pathology. While Rb plays a role in the production and survival of hippocampal newborn neurons, we identify a collective requirement for Rb family proteins – pRb, p107 and p130 – as well as their targets, E2F family transcriptional activators E2F1 and E2F3, in the regulation of NSC quiescence and activation. We further demonstrate that this is mediated through pivotal factors REST and ASCL1, identified as direct molecular targets of the Rb/E2F axis, and that REST inactivation can partially rescue NSC depletion following Rb family loss. We finally demonstrate impaired NSC activation and a return to quiescence in the 3xTG-AD model of Alzheimer's disease, with altered expression of Rb/E2F genes observed within cell population-specific defects. Ultimately, this work addresses the key issue of how transcriptional signatures of quiescence and activation among adult NSCs are co-ordinated with cell cycle control, and demonstrates that Rb family proteins serve as master regulators of the molecular program instructing adult NSC exit from and re-entry into quiescence.

ACKNOWLEDGMENTS

I've never preferred short acknowledgments sections amounting to the rather trite phrase of *"It takes a village"*. In August 2013, whilst sprawled on my parents' couch after a pretty difficult CrossFit WOD, I received an interview request from Dr. Ruth Slack, in which she enclosed Julian et al., *Cell Stem Cell* 2013 for me to read. This won't go on too long, but to just say that "the rest was history" and reel off a list of names would diminish just how life-altering that e-mail became.

A doctorate can make for a lonely, introspective experience; not to mention completing it amid an *unprecedented global pandemic*. I likened it early on to "chasing an adrenaline rush" you can only really get from sorting YFP-expressing cells you can see under a microscope and reproduce on a western blot, to getting an e-mail back from StemCore that after countless tries you finally have six samples whose RQN is 9 (and those were adult NSCs, not embryonic). Those rushes empower you to fail once more, maybe a little better each time, and to drive you as you wait for the door to ACVS to unlock at 6:01 AM (enough time to genotype the E13.5 embryos) or as you redo the differentiation assay and see if this set of chromatin may be sufficient. The evening I sat at our kitchen table and finally pieced together how significant that one gene (which I'd spent countless hours of analysis glazing past) would be to my story, Dominique was in awe at seeing *that rush* in person. Yet those moments can be weeks or months apart. What makes the difference is the training environment, and the people you can count on to help you achieve that forward momentum, and to whom you can lend a hand while waiting, and maybe even build something amazing together.

During my graduate training, Dr. Ruth Slack has been the one constant and an eternal source of support. I am humbled by the many opportunities she has afforded me, including training at the very cutting edge of regenerative medicine. I have appreciated the progress I feel I have made as a scientist, and it could not have happened without the collegial atmosphere she has fostered through our weekly meetings and, presently, at-times multi-hour-long discussions over Zoom. Whatever intensity I have had, whatever progress or publications I have made, were my attempts to honour the commitment that Ruth has made to me for the past eight-plus years. And for someone who has repeatedly referenced "turning into a pumpkin" at a given deadline, I hope that this very long journey has borne work worthy of her encouragement. I am grateful that her insistence I always put my family and a balanced life first has left me with zero regrets inside or out of her lab.

I must next acknowledge Jason MacLaurin and Smitha Paul. Besides Ruth, no one has had a greater impact on my development as a scientist. I am indebted to you both for the years of long conversations, of contributions to this research, and for shaping my character. I have appreciated every lesson and every opportunity to process and to evolve through your everyday guidance.

To those who came before me, I hope that this dissertation does you proud. To Alysen Lougheed, who provided my initial training and taught me to honour the mice we use, as "every mouse must have a purpose". To Dr. Devon Svoboda and Dr. Lisa Julian, both of whom convinced me to pursue a PhD, and whose examples I most tried to live up to as a scientist: ever curious, always enjoying the experience. To Dr. Renaud Vandenbosch, who began the Rb-TKO project, and whose encoura*gements et conseils ont continué à être ressentis de 5800 kilomètres*. To Dr. Noël Ghanem, the beating heart who spurred me on. To Dr. David Patten and Dr. Delphie Dugal-Tessier, whose shaping the lab's stalwart culture helped me mature as a scientist. And Prof. Mireille Khacho, who taught me invaluable lessons in character, collaboration, and encouraging trainee development.

This work was performed alongside very talented scientists who joined the lab after me, each of whom helped shape this work. I am proud to have collaborated with them and even more proud to consider them my friends. Mohamed Ariff Iqbal has been my lab brother in crisp pastel dress shirts, and from our fateful meeting at CAN in 2015, I have admired his research attitude and valued our chats over coffee. This would make Maria Bilen my younger lab sister, though only in age and not in the sheer wisdom and fortitude that define her. Chapters 2 and 3 were only possible through close collaboration with Dr. Iman Chakroun and Dr. Yubing Liu, who I was pleased to have initially met during their time in the Alexandre Blais Lab but whose counsel has been invaluable as members of the Slack Lab. To Jingwei, Amaal and Vanessa, I have enjoyed everything you have brought to our lab and the congenial culture you have helped further.

With the defense of this dissertation, I will be pleased to join the ranks of those who left the lab before me, each of whom carries pride in their Slack Lab training. To Raghda Ragaie Gemae, my confident lab sister and my biggest supporter in those early years, who I also must thank for bringing Dominique into my life. To Joelle Azzi, whose tenacity was inspiring and whose ChIPs were works of art. To Joseph Bastasic, who I was proud to have supervised as an Honours student prior to his MSc and who brought so much to the Rb-TKO project. To the genuine Daniel O'Neil whose capacity for good is as great as his technical skill. To Dr. Ujval Anil Kumar and Dr. Richard Harris, who demonstrated the importance of mindfulness and joy in pursuing research excellence.

I would like to acknowledge the support of my Thesis Advisory Committee, Dr. Marc Ekker, Dr. Stephen Gee, Dr. Jing Wang, formerly Dr. Alexandre Blais, and that of lab colleagues Dr. Nastaran Ahmadi, Dr. Jacob Wong, Ruthann Duivesteyn, Kristen Stephens, Zach Roberts, and Jacob Cuthbert, as well as Dr. Anthony Carter, Dr. Jason Fernandes and Dr. Fernando Ortiz, and the CMM (Blanche Dinelle, Marie-Florence Lafontant, Christina Sardella) and ACVS staff.

Within the walls of RGN, I appreciated the support and camaraderie from a number of friends, including Dr. Mariana Gomez-Smith, Dr. Jagroop Dhaliwal, Dr. Vera Tang, Dr. Maheen Ceizar, Dr. Aswin Hari, Wissam Nassrallah, Dr. Chloë van Oostende-Triplet, Redaet Daniel, Victoria Racher, and Dr. Steffany Bennett. Outside of the walls of RGN, I appreciated the same from friends Olivier Richard, Amy Thiffault, Sheina Perth, Dr. Rim Khazall, Dr. Robert Caratun, Dr. Itai Malkin, Dr. Jason Fernandes, Dr. Imogen Coe, Dr. Krishana Sankar, and Dr. Tara Moriarty.

I would like to acknowledge the boundless support of my parents, Dr. Ken Fong and Mrs. Elizabeth Kusey, who I updated every Sunday night during dinner / 49ers half-time, my excellent role model of a sister, Dr. Jenna Fong, and my aunt Joan Taichman in addition to my extended family.

I would also like to acknowledge those who passed during this academic journey, including my great-grandmother Sui Yee Fong (Bak bak), who I was lucky to spend a memorable final day with in 2014, and my grandmother Borisine Kusey (Baba), who at 100 years old fought COVID-19 and won before passing peacefully this July. I would like to specially acknowledge Linda Jui, whose life devoted to research, as conveyed by her loving family, became a model for my commitment.

Finally, Dominique. I started this on my own, but we finished it together. No more PubMed/ bioRxiv alerts, Excel lookups, or long-distance date nights while slide-mounting. At least until the next chapter of my scientific career. Until then, you and Ella finally have my undivided attention.

Addendum, April 2022

I would also like to acknowledge the contributions of my Thesis Examiners in preparation for, and during my successful defence of this thesis on March 22, 2022, as chaired by Dr. Morgan Fullerton. I appreciated being able to engage Dr. Alexandre Blais, Dr. Marc Ekker, Dr. Diane Lagace and my external examiner Dr. Leigh Anne Swayne in a highly-anticipated academic discussion, and despite being required to do so virtually via Zoom, the exhilarating experience did not disappoint.

I am honoured to join each of them, as well as Dr. Ruth Slack, as a Doctor of Philosophy.

TABLE OF CONTENTS

LIST OF FIGURES AND TABLES

LIST OF ABBREVIATIONS

^{14}C	carbon-14
3xTG-AD	triple-transgenic model (APP KM670/671NL (Swedish), MAPT P301L, PSEN1 M146V)
AC3	activated caspase-3
ACVS	Animal Care & Veterinary Service
AD	Alzheimer's disease
Aldoc	aldolase C, fructose-bisphosphate
aNSC	activated neural stem cell
Apoe	apolipoprotein E
APP	amyloid beta precursor protein
Aqp4	aquaporin 4
Ascl1	achaete-scute family bHLH transcription factor 1
ATP	adenosine triphosphate
Aβ	amyloid beta
bHLH	basic helix–loop–helix
Bmp	bone morphogenetic protein
Bmp6	bone morphogenetic protein 6
BrdU	5-bromo-2'-deoxyuridine
BRG1	Brahma-related gene-1 / SMARCA4
C57/BL6	C.C. Little strain 57, substrain 6
CA1	cornu ammonis subfield division 1
CA3	cornu ammonis subfield division 3
Ccna2	cyclin A2
CD133	prominin 1
Cdc20	cell division cycle 20
Cdc6	cell division cycle 6
CDK	cyclin-dependent kinase
cDNA	complementary DNA
ChIP	chromatin immunoprecipitation
CIHR	Canadian Institutes of Health Research
CIP	CDK interacting protein
CKI	cyclin-dependent kinase inhibitor
CNS	central nervous system
CoREST	REST corepressor
CTDSP1	CTD small phosphatase 1
DAPI	4',6-diamidino-2-phenylindole
DBD	DNA binding domain

Dbi	diazepam binding inhibitor
Dcx	doublecortin
DEG	differentially-expressed gene
DG	dentate gyrus
DGC	dentate gyrus granule cells
DKO	Double knockout
DMEM	Dulbecco's Modified Eagle Medium
DNA	deoxyribonucleic acid
DNE	dentate neuroepithelium
DNMT	DNA methyl-transferase
dNSC	dormant neural stem cell
DP	differentiation-related polypeptide protein
dpi	days post-induction
DREAM	Drosophila orthologues of pRb, E2F and dMyb
DYRK1A	dual specificity tyrosine phosphorylation regulated kinase 1A
E	embryonic day
E1A	adenovirus early region 1A
E2F	E2 factor
$E2F^{TD}$	E2F transactivation domain
EdU	5-Ethynyl-2'-deoxyuridine
EGFR	epidermal growth factor receptor
Egfr	epidermal growth factor receptor
ER	estrogen receptor
ERK	extracellular regulated MAP kinase
EYFP	stop-Enhanced yellow fluorescent protein
Ezh2	enhancer of zeste 2 polycomb repressive complex 2 subunit
F12	Nutrient Mixture F-12
FACS	fluorescence activated cell sorting
Fgf2	fibroblast growth factor 2
Fgfr3	fibroblast growth factor receptor 3
Flox	flanked by LoxP
Foxg1	forkhead box G1
FVB/N	Friend Virus B NIH Jackson
G0 phase	gap phase 0
G1 phase	gap phase 1
G2 phase	gap phase 2
GABA	gamma-Aminobutyric acid
GCN	granule cell neuron

GEPCOT	$Glast^{mid}EGFR^{high}PlexinB2^{high}CD24^{-/low}O4/PSA\text{-}NCAM^{-/low}Ter119/CD45^{-}$
GFAP	glial fibrillary acidic protein
GFP	green fluorescent protein
H^3	tritiated (tritium)
HD	Huntington's disease
HDAC	histone deacetylase
Hes1	hes family bHLH transcription factor 1
Hes5	hes family bHLH transcription factor 5
Hey1	hairy/enhancer-of-split related with YRPW motif 1
Hopx	HOP homeobox
hPLAP	human phospholipase A2 activating protein
HPV	human papillomavirus
HUWE1	HECT, UBA and WWE domain containing E3 ubiquitin protein ligase 1
IACUC	Institutional Animal Care and Use Committee
ID4	inhibitor of DNA binding 4, HLH protein
Id4	inhibitor of DNA binding 4
INK4	inhibitors of CDK4
iPSC	induced pluripotent stem cells
Jak2	Janus kinase 2
kb	kilobase
Ki67	antigen Ki-67 (Kiel, clone 67)
KIP	kinase inhibitory protein
KO	knockout
L1cam	L1 cell adhesion molecule
LIN52	lin-52 DREAM MuvB core complex component
Lpar1	lysophosphatidic acid receptor 1
LZ	leucine zipper
M phase	mitosis phase
MAPT	microtubule-associated protein tau
MB	marker box
MEF	mouse embryonic fibroblasts
miRNA	microRNA
Mms22l	MMS22 like, DNA repair protein
mSin3A	SIN3 transcription regulator family member A
Mycn	MYCN proto-oncogene, bHLH transcription factor
Nanog	Nanog homeobox
NeuN	neuronal nuclei (RNA binding protein, fox-1 homolog 3)
NeuroD1	neuronal differentiation 1

NFT	neurofibrillary tangles
NLS	nuclear localization signal
NPC	neural precursor cell
Npm1	nucleophosmin 1
NRSE	neuron-restrictive silencer element
NRSF	neuron-restrictive silencer factor
NSC	neural stem cell
NTG	non-transgenic
OB	olfactory bulb
Oct4	POU class 5 homeobox 1
p107	retinoblastoma-like 1
p130	retinoblastoma-like 2
p21	cyclin-dependent kinase inhibitor 1
Pax6	paired box 6
PBS	phosphate buffered saline
PCNA	proliferating cell nuclear antigen
PD	Parkinson's disease
Pdfgrb	platelet derived growth factor receptor, beta polypeptide
PEI	polyethylenimine
PFA	paraformaldehyde
Pin1	peptidyl-prolyl cis/trans isomerase, NIMA-interacting 1
pRb	retinoblastoma protein
Prox1	prospero homeobox 1
PSEN	presenilin
Pttg1	pituitary tumor-transforming gene 1
qNSC	quiescent neural stem cell
R26	ROSA26 locus
Rb	retinoblastoma
RBC	retinoblastoma C-terminal domain
RBN	retinoblastoma N-terminal domain
RE1	repressor element-1
REST	RE1-silencing transcription factor
RFP	red fluorescent protein
RGL	radial glia-like
RMS	rostral migratory stream
RNA	ribonucleic acid
RP	radial precursor
Rpl4	ribosomal protein L4

S phase	synthesis phase
S100β	S100 protein, beta polypeptide, neural
SEM	standard error of the mean
SGZ	subgranular zone
Shh	sonic hedgehog signaling molecule
SIN3A	SIN3 transcription regulator family member A
Socs3	suppressor of cytokine signaling 3
Sox11	SRY-box transcription factor 11
Sox2	SRY-box transcription factor 2
Sox4	SRY-box transcription factor 4
SRR2	SOX2 regulatory region 2
STD	standard deviation of the mean
Suz12	SUZ12 polycomb repressive complex 2 subunit
SWI/SNF	SWItch/Sucrose Non-Fermentable
Tam	tamoxifen
TAP	transiently-amplifying progenitors
TBI	traumatic brain injury
Tbr2	T-box brain protein 2 (eomesodermin)
Tfgbr3	transforming growth factor, beta receptor III
THC	triple-heterozygous control
TKO	triple knockout
TMZ	temozolomide
TRIM28	tripartite motif containing 28
Tuj1	class III beta-tubulin
UMAP	Uniform Manifold Approximation and Projection
UMI	unique molecular identifier
V-SVZ	ventricular-subventricular zone
VEGF	vascular endothelial growth factor
VZ	ventricular zone
Waf	wild-type p53-activated fragment
wpi	weeks post-induction
YFP	yellow fluorescent protein

And you, good yeoman,
Whose limbs were made in the Ruth Slack Laboratory, show us here
The mettle of your pasture: let us swear
That you are worth your breeding; which I doubt not;
For there is none of you so mean and base,
That hath not noble lustre in your eyes.
I see you stand like greyhounds in the slips,
Straining upon the start. The game's afoot:

Henry V, Act Ill, Scene I
(modified)

Chorus Lines 4-5 (not reproduced here)

Dua Lipa, *Dua Lipa*, Track No. 6
(verbatim)

CHAPTER 1

GENERAL INTRODUCTION

1. Adult Neurogenesis

Neural stem cells (NSCs) are the source of all neurons, glial and oligodendrocyte cells in the CNS, comprised of the brain and spinal cord. As with any stem cell, NSCs fit a semantic definition of a multipotential, self-renewing cell that sits atop the lineage hierarchy, maintains an immature state over a long duration, and is able to differentiate to generate these specialized cell types (Kooy and Weiss, 2000). In mammals, where tissue growth is limited to the embryonic and early postnatal periods, NSC numbers decline as the majority differentiate and disappear from most regions of the CNS – a key exception being adult NSCs, which continue to persist in a few well-defined areas of the mammalian brain throughout life.

Adult neurogenesis is the life-long process by which adult NSCs, continuously maintained in a relatively-quiescent state (Morshead et al., 1994), undergo activation, differentiation, long-distance migration and commitment, to generate terminally-differentiated mature neurons capable of survival and integration into surrounding circuitry (Bonaguidi et al., 2016). Whereas developmental neurogenesis exists to establish neural circuits, adult neurogenesis serves to modify circuits by inducing neural plasticity – the process through which the CNS responds to intrinsic or extrinsic stimuli through structural reorganization.

The modulation of neural plasticity through the generation of adult-born neurons shapes the CNS throughout life. In the olfactory bulb, continuous reorganization of the interneuron network fine-tunes the processing of olfactory sensory information, which becomes resolved into temporal and spatial patterns (Lledo and Valley, 2016). Adult hippocampal neurogenesis plays significant roles pertaining to hippocampal cognitive function: these include learning and the encoding and consolidation of memories, reviewed in (Toda and Gage, 2017), as well as guiding the efficiency of spatial navigation (Yu et al., 2019). Adult-born hippocampal neurons possess a

special role in pattern separation – the computational process through which firing patterns amongst groups of neurons are discriminated and encoded as distinct memories: experimental augmentation improves behavioural performance in differentiating between overlapping contexts (Sahay et al., 2011). In deeper neurobiological analysis of memory, adult neurogenesis has been shown to be as important for memory persistence – as in, remembering – as it is for memory transience – as in, forgetting (Richards and Frankland, 2017). Recent work has established prominent sex-specific functions for adult neurogenesis under stress conditions, as blocking neurogenesis under aversive temperatures caused female rats to learn faster and male rats to learn slower, relative to controls, in behavioural tests of spatial learning (O'Leary et al., 2021).

A complex process, adult neurogenesis relies on tight regulation by a broad array of cell-autonomous and non-cell autonomous partners, including the input of surrounding niche factors, transcriptional actors to be discussed in this thesis, epigenetic actors reviewed in (Sheehy et al., 2021), as well as interneurons and long-range inhibitory projecting neurons (Song et al., 2013; Yun et al., 2019).

In mammals, adult neurogenesis has been best established in two discrete neurogenic niches we will next examine in-depth: the ventricular-subventricular (also *subependymal*) zone (V-SVZ) lining the lateral ventricles, as well as the subgranular zone (SGZ) of the hippocampal dentate gyrus (DG). They share key similarities, as each niche possesses a population of stem (in the SGZ, alternately: *stem-like, "precursor"*) cells with a radial glial morphology, which can give rise to discrete neuronal, oligodendrocyte and/or glial cell types, proceeding through a multi-stage process marked by temporal expression of distinctive protein markers. To generate neurons in either niche, neurogenesis begins by activating these NSCs, which divide to form an intermediate cell type referred to as transiently-amplifying progenitors, which, after rapid proliferation,

differentiate to form neuroblasts. Neuroblasts subsequently exit the cell cycle, and commit to a post-mitotic neuronal fate (Ming and Song, 2011).

For the purposes of further elaboration, we will focus discussion and illustrations on a rodent, and specifically a murine, model of adult mammalian neurogenesis, resulting in neurons capable of functional synaptic integration. Nevertheless, it is important to note that gliogenesis accompanies neurogenesis in each niche: this includes the generation of adult-born astrocytes as well as oligodendrocyte progenitor cells, which in turn give rise to adult-born oligodendrocytes. There is diversity between the niches, as gliogenic progeny of V-SVZ NSCs are predominantly oligodendrocyte precursors, while SGZ NSCs generate astrocytes alone (Bond et al., 2015).

1.1 Adult Neurogenesis in the V-SVZ

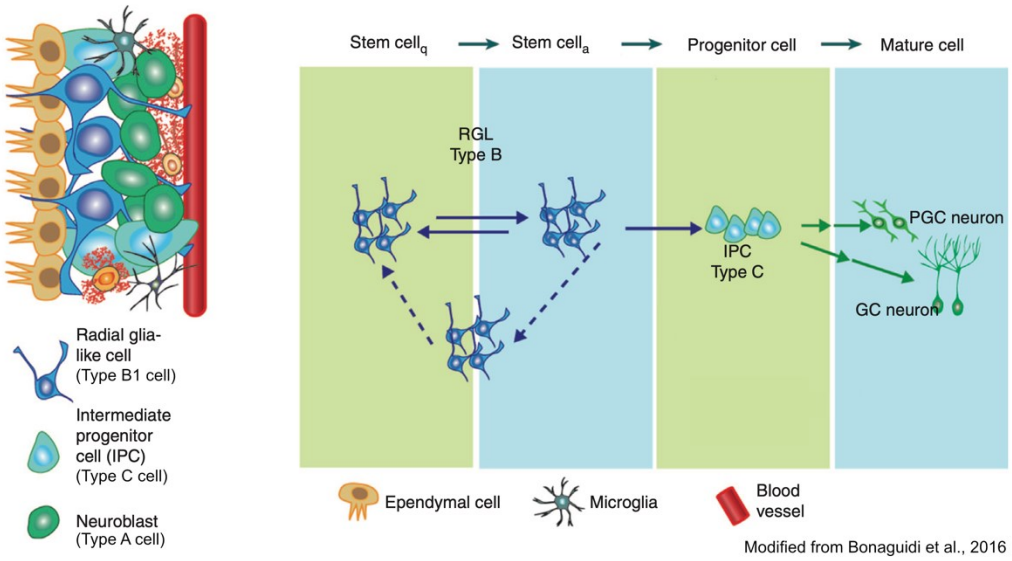

Adult NSCs in the V-SVZ observe a “set-aside” model, as they diverge from the developmental NSC pool during mid-embryonic development. While developing NSCs continue to divide rapidly, adult V-SVZ NSCs slow their cell cycle between E13.5 and E15.5, and become characterized by p57 expression and slow cell divisions before ultimately generating a majority of

NSCs in the young adult V-SVZ (Fuentealba et al., 2015; Furutachi et al., 2015). In contrast with developmental NSCs, whose rapid division is dependent on Notch-dependent oscillatory expression of Hes1 and Hes5, the slow division of adult V-SVZ NSCs is dependent on accumulation of Notch and Hey1 through cell cycle arrest (Harada et al., 2021).

V-SVZ NSCs form neuroblasts capable of migration – in chains – along the rostral migratory stream toward the olfactory bulb. There, they migrate radially to become either GABAergic granule interneurons or dopaminergic periglomerular interneurons (Carleton et al., 2003) and participate in olfactory sensory function (Imayoshi et al., 2008).

Adult neurogenesis in the V-SVZ is characterized by progression through the following key cell types: Type B1 NSCs (distinguished from Type B2 niche astrocytes), Type C progenitors, and finally Type A neuroblasts.

1.1.1 Type B1 NSCs

In the V-SVZ, Type B1 NSCs extend two processes: a primary cilium extends through an ependymal cell layer separating the V-SVZ from the lateral ventricle, while a basal process extends, terminating on blood vessels (Mirzadeh et al., 2008). In contrast with NSCs in the SGZ, this allows V-SVZ NSCs to contact both ventricular cerebrospinal fluid and the vascular network, thereby exposing them to secreted signaling factors including noggin and VEGF. Type B1 NSCs characteristically express Nestin, GFAP and CD133/Prominin-1, and maintain apical-basal polarity. They closely resemble RGLs found in the developing brain, both in morphology and conservation of a characteristic gene signature (Borrett et al., 2020). Recent work has determined that Type B1 NSCs divide primarily symmetrically: the majority undergo consuming divisions to generate intermediate transiently-amplifying Type C progenitors, while approximately 20-30%

divide to generate two Type B1 NSCs (Obernier et al., 2018). In contrast against SGZ NSCs (Pilz et al., 2018), this suggests that V-SVZ neurogenesis uncouples self-renewal from differentiation.

Though previously believed to represent a homogeneous group, recent studies have demonstrated heterogeneity amongst Type B1 NSCs. Basal NSCs are believed to comprise the largest NSC pool in the postnatal V-SVZ and the main source of adult-born OB interneurons, while apical NSCs are believed to act as Notch-dependent gatekeepers of niche proliferation and neurogenesis (Baur et al., 2020). Two broad non-overlapping populations of Type B1 NSCs are believed to mark distinct dorsal and ventral neurogenic lineages, indicative of region-specific regulation (Cebrian-Silla et al., 2021).

1.1.2 Type C progenitors and Type A neuroblasts

Type C progenitors, which characteristically express Tbr2 and ASCL1, divide asymmetrically several times before giving rise to migrating Type A neuroblasts, which divide symmetrically and characteristically express Dcx. As compared with slowly-dividing Type B1 NSCs, these populations possess a shorter cell cycle time (Morshead and Kooy, 1992). Type A neuroblasts move along each other, forming chains ensheathed by Type B2 astrocytes (Lois et al., 1996), and migrate tangentially along the RMS. Clonal analysis has suggested that – 6 days following retroviral labelling – only 25% of proliferating cells in the SVZ proceed with migration as Type A neuroblasts along the RMS, whereas 15% remain in the V-SVZ and the majority (60%) undergo apoptosis (Morshead et al., 1998); nevertheless, the surviving, migratory portion represents tens of thousands of migrations daily (Lois and Alvarez-Buylla, 1994). Motility distinguishes Type A neuroblasts from the sessile Type B/C cells, and its dynamics have been extensively investigated (James et al., 2011; Kim et al., 2009; Nam et al., 2007).

1.2 Adult Neurogenesis in the SGZ

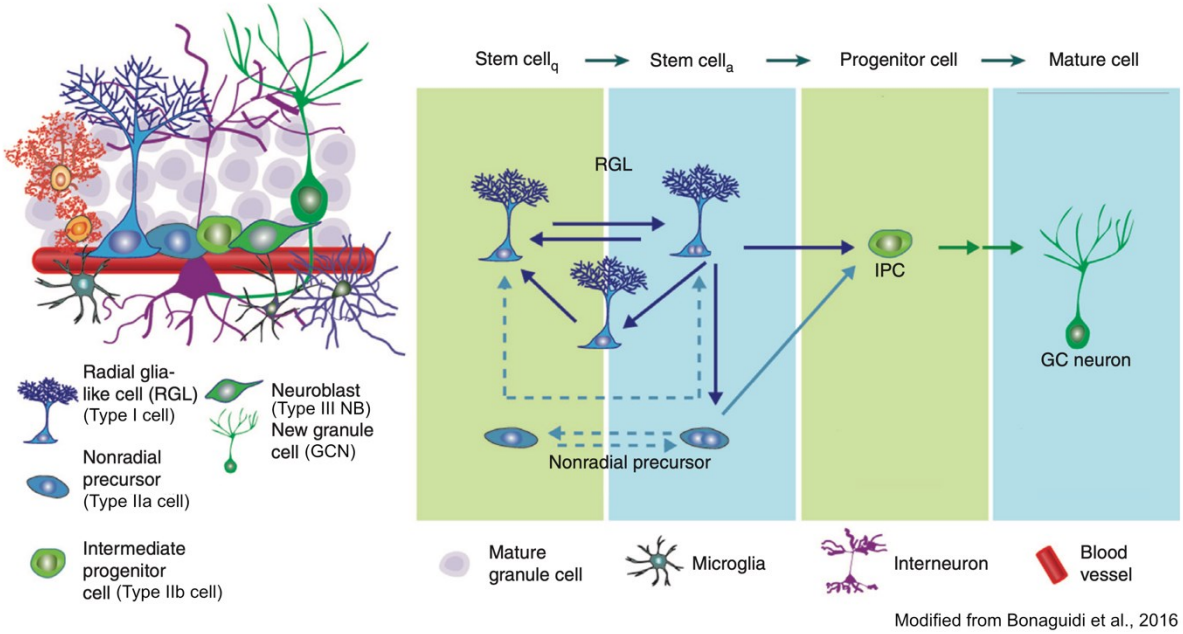

Adult NSCs in the SGZ observe a "continuous" model – and are considered an extension of developmental NSCs – as dentate neurons throughout development and adulthood originate from a common Hopx-expressing precursor population; this population originates during early embryonic development and is maintained throughout life (Berg et al., 2019).

SGZ NSCs, located at the border between the inner granule cell layer and the hilus, produce neuroblasts capable of tangential migration. This is followed by their development into immature neurons, which migrate radially into the granule cell layer and mature into glutamatergic dentate granule cell neurons (GCNs). These GCNs integrate into the hippocampal trisynaptic circuit, in which granule cells receive input from neurons of the entorhinal cortex and extend projections to CA1 and CA3 neurons (Zhao, 2006).

Stable functional integration occurs 4 weeks after birth, and adult-born neurons are mature by 2 months old, viewed as equivalent to the broader neuronal population. Selection, pruning and integration in the interim defines the "critical period" for plasticity pertaining to memory encoding

and retrieval (Gu et al., 2012), and participation in learning and memory, including pattern separation (Imayoshi et al., 2008). Recent work by Jason Snyder's group has established distinct relative features of adult-born SGZ neurons reflecting greater spine density, larger presynaptic terminals, and greater contacts on inhibitory neurons (Cole and Snyder 2020).

Adult neurogenesis in the SGZ is characterized by progression through the following key cell types: Type I NSCs, Type IIa and IIb progenitors, and finally Type III neuroblasts.

1.2.1 Type I NSCs

In the SGZ, Type I NSCs are defined by Nestin and GFAP expression, as well as expression of self-renewal gene Sox2. They possess a radial glial-like morphology, resembling developmental progenitors. Type I NSCs divide generally through asymmetric "self-renewing" divisions, generating one Type I NSC and either one Type IIa progenitor (Suh et al., 2007) or an astrocyte. Some Type I NSCs divide symmetrically, generating either two Type I NSCs in an "amplifying" division, or two Type IIa progenitors in a "consuming" division (Bonaguidi et al., 2011; Götz and Huttner, 2005; Pilz et al., 2018). This decision is believed to stem from multiple mechanisms, including the input from Shh (Favaro et al., 2009) and Notch pathways (Shimojo et al., 2008). Reminiscent of the developmental program governing embryonic progenitors, Type I NSCs that divide repeatedly become progressively restricted in their capacity to self-renew (Pilz et al., 2018).

1.2.2 Type IIa and IIb progenitors

Type IIa transiently-amplifying progenitor cells are distinctly defined by Tbr2 and ASCL1, in addition to continued Sox2 expression. The distinction between glia-like Type IIa from IIb progenitors is neuronal determination, reflected in IIb cells by expression of Dcx and NeuroD1.

At this stage, there is very low Sox2, and colocalization between Sox2 and Dcx is only seen in weakly-Dcx Type IIb cells: this reflects a transition from self-renewal ability towards neuronal determination (Suh et al., 2007). Type IIb progenitors divide mostly symmetrically, but also asymmetrically, to form neuroblasts (Pilz et al., 2018).

1.2.3 Type III neuroblasts

Type III migratory neuroblasts express Prox1, a marker for neuronal commitment, continue to express Dcx and NeuroD1, and lack Sox2 expression entirely. These neuroblasts exit the cell cycle, entering a terminal differentiation phase and losing all proliferative potential. Post-mitotic neurons are subsequently identified using Rbfox3/NeuN (in later stages, Calbindin and Calretinin), while continued Prox1 expression commits neurons to a GCN and not a CA3 pyramidal neuron fate (Lavado et al., 2010).

Altogether, adult neurogenesis is a dynamic process suited to thorough examination. In particular, the mouse model of adult neurogenesis – amenable to cell culture as it is to quantification – affords wide availability of transgenic lines, allowing researchers to target specific cell types all the while offering substantial brain complexity with a short gestation period. However, we will move from mice for the next chapter, and discuss the context for why adult NSCs are worthy of study in-depth: their pertinence and relevance to us humans.

2. Adult NSCs in Context

2.1 A Historical View

In 1913 – *a century exact prior to the start of this thesis* – Santiago Ramon y Cajal defended the fatalistic premise that following development, adult mammalian neurogenesis was not possible:

> "Once development was ended, the fonts of growth and regeneration of the axons and dendrites dried up irrevocably. In adult centers, the nerve paths are something fixed and immutable: everything may die, nothing may be regenerated."
>
> (Cajal, 1913) *as translated from Spanish in 1928*

This dogma – in line with manifest evidence that, unlike damage to tissues from skin to muscle, damage to the CNS is often permanent – has been refuted over the past sixty years, with adult neurogenesis gaining acceptance largely due to improved methodology. Altman and Das presented the first anatomical evidence of tymidine-H^3-labeled newborn cells in the postnatal rat hippocampus (Altman, 1962; ALTMAN and DAS, 1965), later shown to have ultrastructural characteristics of neurons (Kaplan and Hinds, 1977). Retrospectively, an earlier challenge by Smart, who observed incorporation of thymidine-H^3 labeling into dividing cells in the mouse V-SVZ, regrettably underestimated the role of migration along the RMS and missed the generation of OB neurons (Smart, 1961).

Functional adult neurogenesis would be first demonstrated by Nottebohm's work with songbirds, using histology and behavioural studies to demonstrate functional integration of newborn neurons associated with new seasonal birdsong (Alvarez-Buylla and Nottebohm, 1988; Goldman and Nottebohm, 1983), and revealing ongoing neural plasticity.

In 1992, pioneering experimental work by Reynolds and Weiss demonstrated self-renewal and multipotency of NSCs derived from striatal cells of the adult mouse brain (Reynolds and Weiss, 1992). In 1994, Morshead would demonstrate that the ependymal and subependymal layers of the periventricular region was the source of neurosphere-forming cells, with Chiasson later specifying the subependymal layers alone (Chiasson et al., 1999; Morshead et al., 1994). Together with advancements in labeling techniques, including birth-dating of proliferating cells using thymidine analogue BrdU (Kuhn et al., 1996) and labelling of newborn cells using GFP (Praag et al., 2002), by the new millennium there had been a shift towards a dynamic view of the adult mammalian brain.

2.2 Of Mice and Humans

Following a series of publications leaving rodents and climbing the evolutionary ladder to non-human primates (Gould et al., 1997, 1999; Kornack and Rakic, 1999), in 1998 Eriksson and Gage demonstrated the first evidence of adult hippocampal neurogenesis in humans (Eriksson et al., 1998). Since that time, there has been significant debate regarding whether NSCs persist past development and maintain the capacity to produce functional newborn neurons in the adult human brain.

As adult-born neurons have not been detected in the human olfactory bulb (Bergmann et al., 2012), study in humans has virtually entirely focused on SGZ hippocampal neurogenesis. In 2013, Spalding and Frisén used ^{14}C dating to demonstrate that the human hippocampus is able to generate new neurons at a significant rate throughout adulthood and until old age, with only a modest age-related decline relative to the dramatic decline previously observed in rodents (Imayoshi et al., 2008; Spalding et al., 2013).

Five years after Spalding's publication, two publications would rekindle the debate, similarly analyzing the presence of immature neuronal markers (including Dcx) in humans, but reporting opposing findings. Sorrells et al., of Arturo Alvarez-Buylla's group, suggested that newborn neurons are absent or very rare in the human hippocampus (Sorrells et al., 2018). In contrast, Boldrini et al, of J. John Mann's group, concluded that large numbers of new neurons continue to be produced (Boldrini et al., 2018), a finding repeated by other groups (Moreno-Jiménez et al., 2019; Tobin et al., 2019). Parades would subsequently respond by defending the Alvarez-Buylla group's methodology, suggesting that Boldrini et al. employed improper stereology, refuting concerns over post-mortem delay, and highlighting dramatic inter-patient variability going back to Spalding's initial ^{14}C measurements (Paredes et al., 2018). Finally, following the initial submission of this thesis, Franjic et al. reported in 2022 that the trajectory from neural progenitors to granule cells observed in rodents was homologous in pigs and macaques, but not humans (Franjic et al., 2022).

The reignited controversy, reviewed extensively elsewhere (Denoth-Lippuner and Jessberger, 2021; Duque and Spector, 2019), has therefore prompted discussion of whether adult neurogenesis is relevant to human physiology and disease. Does the presence of thousands of Dcx-expressing immature neurons equate to functional relevance? Moreover, does Dcx expression suggest the presence of dividing newborn neurons, or merely a retained immature profile extended throughout life? With these questions outstanding, and deficits in translation between rodents and humans always a concern, one might argue that a safer area of study into human neurogenesis might eschew the adult altogether, and focus in on developmental disorders such as schizophrenia (Ye et al., 2017) and childhood brain injury (Dadwal et al., 2015).

2.3 Of Endogenous Repair

Throughout adulthood, insults to the CNS result in a limited neurogenic response, suggesting regenerative and reparative roles for NSCs, reviewed in (Beckervordersandforth and Rolando, 2020). In response to ischaemia, there is a robust increase in neurogenesis, reviewed in (Ceanga et al., 2021). NSC proliferation occurs within days of injury and subsides between 3-5 weeks, while Dcx-positive neuroblasts continue to proliferate a year post-ischemia (Thored et al., 2006) and BrdU-labelled NeuN-positive adult-born neurons migrate near the lesion, originating from the V-SVZ. Traumatic brain injury (TBI) has a multi-faceted response, activating NSCs and stimulating progenitor proliferation and neuroblast survival (Zheng et al., 2013).

This is contrasted with a decrease in neurogenesis associated with human neurodegenerative pathologies. Patients with Alzheimer's disease (AD), Parkinson's disease (PD) and Huntington's disease (HD) present with similar early symptoms – including depression, anxiety, and cognitive dysfunction – linked to impaired hippocampal or olfactory function (Winner and Winkler, 2015). Recent work has demonstrated the influence of SGZ neurogenesis in AD pathology specifically, as end-stage patients (Braak V-VI; neocortical involvement) show a sharp decline in neuroblast number, relative to negligeable differences in healthy patients (Moreno-Jiménez et al., 2019). This is consistent with reported impairment of both neural precursor proliferation and neurogenesis in the 3xTG-AD mouse model of AD as early as 2 months of age. While these deficits are sustained throughout life as late as 11 and 18 months of age, they notably predate onset of the accumulation of amyloid plaques and neurofibrillary tangles used as diagnostic markers of AD progression (Hamilton et al., 2010, 2015; Rodríguez et al., 2008, 2009).

Limited neurogenic responses are also observed in human pathologies. GFAP-expressing NSCs are observed in the V-SVZ of PD patients, with transcriptomic alterations in

neurotransmitter signalling and a notably aerobic metabolic profile suggesting NSC activation (Berge et al., 2011; Donega et al., 2019). Proliferating NSCs are further observed in the V-SVZ of HD patients, though they fail to mature into functional neurons (Curtis et al., 2003).

Taken together, these findings suggest that while the adult CNS may possess the potential to replenish damaged neurons by guiding the proliferation and differentiation of NSCs, it is either unable to mount a sufficient response, or impaired as a result (or potential cause?) of disease pathologies. Therapies targeted at enhancing this response and/or the originating niche can, and should, remain a focus of adult neurogenesis research. However, the mechanisms regulating them require further study, and are presently confounded by a lack of knowledge regarding the fundamental regulatory mechanisms – partners and pathways alike – that guide adult neurogenesis.

For instance, while the number of NSCs drops in the aging brain, the smaller NSC population is protected from total depletion by an increase in quiescence (explored next) driven by the surrounding niche. This quiescence nevertheless comes at a cost of making aged NSCs more resistant to activation – restoring only 44% of the TMZ-ablated population relative to 92% in the younger control – thereby negatively affecting the potential to regenerate the afflicted brain (Kalamakis et al., 2019). Acknowledging the usefulness of a "parking brake" preserving NSCs in a deeply quiescent state, in the crisis event of a CNS insult, how might we be able to turn it off and drive neurogenesis in the direction of endogenous repair?

Any long-term inquiry seeking potential endogenous therapies is currently reliant on efforts to define and characterize the mechanisms underlying the maintenance of NSCs and growth and development of adult-born neurons. Only then can the modulation of adult neurogenesis through established therapeutic targets begin its journey from bench to bedside. Next, we will descend the evolutionary ladder to the murine model of adult neurogenesis to explore regulation of NSC fate.

3. Regulation of Adult NSC Fate

During adult neurogenesis, NSCs undergo significant molecular and morphological change. At each stage, NSCs experience both cell-intrinsic / cell autonomous and niche-dependent / non-cell autonomous mechanisms, regulating the transition to the next cellular state. This ideally culminates in adult-born neuronal selection and integration into the neural circuitry, but may alternately result in entry into senescence – a degenerative cell state characterized by irreversible cell cycle arrest, cell death, or as we will next discuss, a return to the originating state of adult NSCs: quiescence.

3.1 Quiescence and Activation

Quiescence is defined as a state of reversible cell cycle arrest – reviewed in (Urbán et al., 2019a) – generally in the G0 phase of the cell cycle, but also in G2 (Otsuki and Brand, 2018). Similar to terminally-differentiated and senescent cells, quiescent NSCs (qNSCs) are non-proliferative; by contrast, quiescence allows adult NSCs to reversibly re-enter the cell cycle under physiological conditions.

Quiescence is crucial to maintain the adult NSC pool over extended periods, preventing the exhaustion of NSC proliferative potential. Kippin et al. first demonstrated that p21 loss in adult forebrain NSCs led to a short-term expansion of the NSC pool between 2-8 months, followed by a dramatic depletion of the NSC population by 16 months (Kippin et al., 2005). This finding suggested that cell cycle regulators including p21 – which are the subject of Section 5 – contribute to NSC quiescence, which is necessary for the maintenance of the NSC pool throughout life. The low metabolic state of qNSCs, including low rates of RNA and protein synthesis, allows them to avoid the accumulation of damage to DNA, proteins and mitochondria, thereby preserving

genomic integrity (Cheung and Rando, 2013). The transition from a proliferative state to a quiescent state represents a developmental milestone reflecting the transition from a developmental radial glial NSC phenotype to an adult NSC phenotype.

Though qNSCs have been classically identified simply by the lack of proliferation marker expression, we now conceptualize quiescence as an actively-maintained process. qNSCs are highly sensitive to their local signaling environment, employing a primary cilium that functions as a signaling hub; these are further assembled during re-entry into quiescence and upon cell cycle exit (Guemez-Gamboa et al., 2014). Quiescence can also be modulated by surrounding neuronal activity, including projections from surrounding mossy cells (Yeh et al., 2018). Transcriptomic profiles reveal enrichment in transcripts related to cell signaling, cell-cell communication, cell adhesion, and the extracellular matrix (Basak et al., 2018). Counter to the classical view of passive quiescence, these profiles emphasize that qNSCs compute a diverse array of inhibitory and stimulating inputs when ultimately choosing to maintain a quiescent state.

Moreover, the transition towards activation (and therefore enrichment of gene transcripts involved in ribosomal and RNA synthesis, as well as DNA repair) requires more than merely cell cycle entry. Recent transcriptomic analyses (Artegiani et al., 2017; Basak et al., 2018; Hochgerner et al., 2018; Llorens-Bobadilla et al., 2015) have demonstrated molecular diversity amongst qNSCs that do not currently support subpopulations but have identified characteristic markers reflecting a transition through “deep quiescence” and “shallow quiescence” (also, *primed quiescent*) ahead of NSC activation. This is accompanied by significant physiological changes including a metabolic shift from glycolysis to oxidative phosphorylation (Beckervordersandforth 2017).

In the V-SVZ, qNSCs further lack EGFR expression, defining a subpopulation of GFAP+/CD133+ NSCs which, upon activation, upregulate both EGFR and Nestin (Codega 2014). Recalling that a minority – 20-30% – of Type B NSCs divide symmetrically to generate two NSCs (rather than Type C progenitors), this activated population is capable of returning to quiescence: reactivation occurs on average within three weeks, but can take place after up to one year (Obernier et al., 2018). FACS has been used to examine the distinction between V-SVZ NSCs and neurosphere-initiating cells, with the latter referred to as GEPCOT ($Glast^{mid}EGFR^{high}PlexinB2^{high}CD24^{-/low}O4/PSA\text{-}NCAM^{-/low}Ter119/CD45^{-}$) and contrasted against quiescent pre-GEPCOT cells (Mich et al., 2014). Recent work has demonstrated a high similarity between developing forebrain RPs and adult qNSCs – there, referred to as "dormant" or dNSCs – which reacquire a RP-like transcriptional state upon activation. This study has proposed a common ground state for all forebrain and V-SVZ NSCs, influenced throughout development and adulthood by the surrounding niche environment (Borrett et al., 2020).

In the SGZ, qNSCs are identified by expression of Hopx. In a continuous process originating during development, dentate precursor cells enter quiescence to become qNSCs during the second postnatal week. At this time, qNSCs acquire the morphology of adult NSCs and the DG has acquired its adult structure (Berg et al., 2019) Upon activation, Type I NSCs are progressively restricted in self-renewal capacity (on average persisting for 9.6 days, and dividing 2.3 times), and often pause between divisions for a period ranging from several days to weeks in a short-term quiescence (Pilz et al., 2018). This function is believed to preserve the SGZ NSC pool, and thereby extend neurogenesis throughout life.

4. Transcriptional Regulation of Adult NSC Fate

Regulating the balance between NSC quiescence and activation is crucial for sustaining the brain's neurogenic capacity throughout life. This balance determines the overall rate of neurogenesis, ensures a maintained population of NSCs, and preserves capacity for endogenous response to a CNS insult. Here, we will review two master transcriptional regulators of neurogenesis, and examine their impact on maintaining this balance. Signal integration of niche inputs (Vicidomini et al., 2020), and other major regulatory pathways that direct NSC fate – including Notch, Wnt, Sonic Hedgehog and Bmp – in addition to epigenetic and small RNA/miRNA regulation, have been reviewed elsewhere (Esteves et al., 2020; Gonçalves et al., 2016; Hsieh, 2012; Urbach, 2019).

4.1 REST

REST (RE1-Silencing Transcription factor, also *NRSF; Neuron-Restrictive Silencer Factor*) is a Krüppel-type zinc finger transcription factor. First identified in parallel by David Anderson's group (Schoenherr and Anderson, 1995) and Gail Mandel's group (Chong et al., 1995), it has been extensively investigated as a highly-expressed repressor of neural genes in non-neuronal tissues (Ballas et al., 2005). However, REST silences only a minority of gene targets (Belyaev et al., 2004), and is presently viewed as a negative regulator instead of a silencer, offsetting positive regulators to modulate gene expression in different cell types, including adult postmitotic neurons (Palm et al., 1998).

Acting as a transcriptional repressor, REST binds to a 21-23bp motif (RE1, also *NRSE; Neuron-Restrictive Silencer Element*) on genes encoding fundamental neuronal traits, including neurite outgrowth and guidance, ion channels, synaptic vesicle proteins/trafficking/release, and

neurotransmitter receptors (Bruce et al., 2004; Mortazavi et al., 2006; Sun et al., 2005). REST active repression relies on recruitment of a wide variety of both corepressors, including at its N-terminus with SIN3A/HDAC complex (Roopra et al., 2000) as well as at its C-terminus with cofactor CoREST (Andrés et al., 1999), and interacting proteins, including TRIM28 (Lee et al., 2016).

While the breadth of REST downstream targets is increasingly well understood, its upstream regulators are barely known, particularly regarding adult neurogenesis. During neurogenesis, REST is stabilized by CTDSP1, while ERK1/2-dependent phosphorylation promotes REST degradation in a Pin1-dependent manner (Nesti et al., 2014). *In ovo* results from the chick spinal cord suggest that canonical Wnt signaling directly controls REST expression (Nishihara et al., 2003). In embryonic neural progenitors, REST is a target of both Oct4 and Nanog (Loh et al., 2006), is directly upregulated by the Bmp pathway (Kohyama et al., 2010), and work *in vitro* has implicated the Notch pathway via Hes1 (Abderrahmani et al., 2005).

REST possesses multiple roles in neurodegenerative disease pathologies, reviewed by (Hwang and Zukin, 2018; Mampay and Sheridan, 2019), including ischaemia (Calderone et al., 2003), Huntington disease, Parkinson's disease (Kawamura et al., 2019), epilepsy (McClelland et al., 2014), and notably Alzheimer's disease. *In vitro* NSC models of AD – including patient-derived – demonstrate modifications in REST-regulated gene networks stemming from decreased RE1 binding; the defects begin with decreased NSC self-renewal, premature differentiation and accelerated synapse formation, and persist into a post-mitotic neuronal stage (Meyer et al., 2019).

4.1.1 REST and Adult NSC Fate

In adult NSCs, REST demonstrates an overall requirement for maintaining the NSC population and orchestrating stage-specific neuronal differentiation. Notably, REST restricts the expression of SoxC proteins Sox4 and Sox11 (Bergsland et al., 2006), which are essential for SGZ neuronal differentiation and directly control the activity of neuron-specific gene promoters, including Dcx, in adult NSCs (Mu et al., 2012). This stands in contrast with development, where REST maintains genomic integrity through chromatin remodeling; precocious REST deletion in developing NSCs results in catastrophic DNA damage and apoptosis (Nechiporuk et al., 2016).

In the SGZ, REST demonstrates biphasic expression over the course of neurogenesis. In (Gao et al., 2011), Jenny Hsieh's research group demonstrated that REST is expressed in Type I and Type II NSCs and intermediate progenitors, where it recruits CoREST and mSin3A to prevent precocious neuronal differentiation. REST is downregulated in a subset of ASCL1-expressing activated NSCs and the majority of NeuroD1-positive neuroblasts, resulting in neuronal commitment; it is later upregulated during terminal differentiation. Conditional REST deletion resulted in decreased long-term neuronal survival, including a diminished GCN population, linked to a transient increase and subsequent decrease of the Type I NSC population.

These results suggested a requirement for REST in maintaining SGZ NSC quiescence and preserving the qNSC population. In (Mukherjee et al., 2016), a follow-up study by Hsieh's group next identified distinct requirements for REST in qNSCs (referred to as QNPs) and Type II progenitors (referred to as TAPs). Lentiviral-mediated REST deletion in qNSCs reflected a requirement for REST in maintaining quiescence, as deletion resulted in increased NSC activation and short-term progenitor proliferation. By contrast, retroviral-mediated REST deletion reflected a requirement for REST in maintaining progenitor proliferation and number, thereby preventing

precocious differentiation. They further identified unique REST targets involved in ribosome biogenesis, including Npm1 and Rpl4, and cell cycle regulation, including Mms22l and Cdc20, whose expression in qNSCs promoted activation.

While REST function in adult NSCs has been examined mostly in the SGZ, similar roles have been demonstrated in the V-SVZ. Transcriptomic studies have demonstrated a significant overlap between genes enriched in activated V-SVZ NSCs and genes regulated by REST. *In vitro*, REST knockdown inhibits neurosphere growth, cell proliferation, and triggers precocious cell differentiation in the presence of growth factors. Together, these suggest a similar requirement for REST in both neurogenic niches, in addition to de-repression of REST targets upon V-SVZ NSC activation (Soldati et al., 2015).

In summary, REST possesses context-specific functions during adult neurogenesis, which appears to be highly similar between the V-SVZ and the SGZ. REST possesses an early requirement in maintaining NSC quiescence, a medial requirement maintaining progenitor proliferation and preventing precocious differentiation, and a late requirement promoting neuronal survival. Next, we will examine a more focused function for ASCL1 in NSCs.

4.2 ASCL1

ASCL1 (achaete-scute family bHLH transcription factor 1, also Mash1; *mammalian achaete scute homolog-1*) is a pro-activation factor expressed in both neurogenic niches. Lowly expressed in V-SVZ B cells and SGZ Type I cells, its expression increases as cells transition to a progenitor stage (Kim et al., 2011). ASCL1 expression is oscillatory, and is suppressed by similarly oscillatory expression of the Notch target Hes1 – albeit with larger peaks and troughs in qNSCs as compared to activated NSCs (Sueda et al., 2019).

In the SGZ, ASCL1 is required for qNSC responsiveness to activating signals (including kainic acid, a glutamate receptor agonist), as NSC activation first leads to ASCL1 expression, leading to subsequent exit from quiescence. Modulation of ASCL1 expression suggests a major requirement: lowered expression reduces NSC proliferation, while inactivation blocks exit from quiescence entirely, and led to no new progenitor or GCN production. This is mirrored in the V-SVZ, where ASCL1 deletion results in severe decreases to the activated NSC and Dcx-expressing neuroblast populations. ChIP analyses on SGZ NSCs demonstrated ASCL1 direct regulation of cell cycle genes including cyclin D2 (Andersen et al., 2014).

Recent work has further established a role for ASCL1 – through its degradation – in NSC return to quiescence. ASCL1 is restricted to proliferating SGZ NSCs due to elimination from qNSCs in a E3 ubiquitin ligase HUWE1 and repressor ID4-dependent manner, with a downstream impact on cyclin D accumulation. This suggests a dynamic role for expression and degradation of ASCL1 in regulating NSC return to quiescence (Urban et al., 2016). A follow-up study demonstrated that, with age, increasing degradation of ASCL1 by HUWE1 co-ordinates the maintenance of the qNSC population: this leads the majority of activated NSCs to return to shallow quiescence by 6 months, and lifelong-quiescent NSCs (also, *dormant NSCs*) to enter deeper quiescence (Harris et al., 2021).

These transcription factors, REST and ASCL1, represent two key regulators providing transcriptional control of NSC fate. Next, we will cover an additional regulatory paradigm controlling NSC quiescence and activation, and examine the involvement of cell cycle regulators.

5. Cell Cycle Regulation of Adult NSC Fate

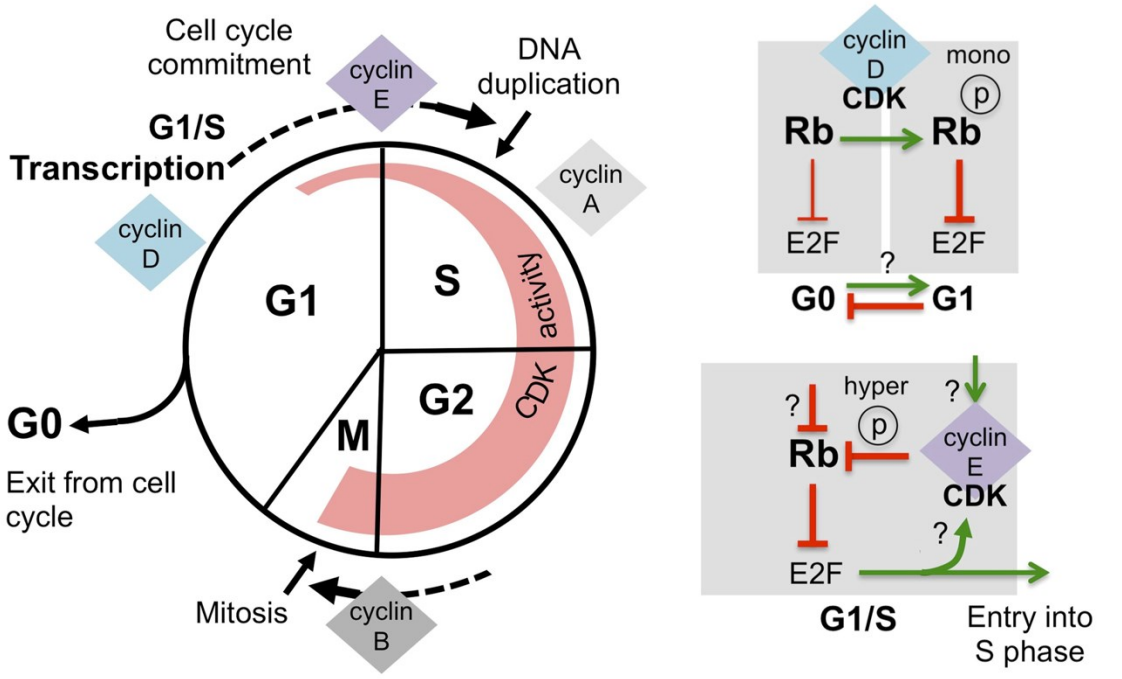

Modified from Bertoli et al., 2014

The cell cycle is a complex process, and its fine regulation is essential for NSC development, differentiation, proliferation and death along the progression of adult neurogenesis, extensively reviewed in (Urbach, 2019). Briefly, the cell cycle involves a mitosis (M) phase and a DNA synthesis (S) phase separated by two gap phases, G1 and G2. The G1 phase is the longest phase and represents the main period of cell growth, preparing the cell before passing to the S phase. Cells are also able to arrest in G1 phase, or may exit the cell cycle into a G0 state that is either temporary (during quiescence) or permanent (during terminal differentiation).

Progress through the cell cycle is regulated at checkpoints that ensure essential events of each phase are completed before the cell enters the following phase. This regulation involves the sequential expression, activation and inhibition of cell cycle proteins, which include cyclins, cyclin-dependent kinases (Cdks), and two families of cyclin-dependent kinase inhibitors (CKIs). Notably, the cyclin A/Cdk1 complex promotes S/G2 progression, while the cyclin B/Cdk1

complex promotes G2/M transition. However, the cell cycle regulators that regulate the critical G1/S phase transition – and represent the focus of this thesis – are **the Rb/E2F axis**.

5.1 The Rb/E2F Axis

In the canonical model of Rb/E2F function, the G1/S transition is dependent on the phosphorylation of **Rb family proteins: pRb, p107 and p130**. Briefly, the cyclin D/Cdk4/6 complex promotes G1 arrest by mono-phosphorylating and activating Rb family proteins in early G1. At the late G1 restriction point, the cyclin E/Cdk2 complex promotes G1/S progression by hyper-phosphorylating and inactivating Rb family proteins (Bertoli and Bruin, 2014; Narasimha et al., 2014). Rb family proteins become re-activated through dephosphorylation between the end of mitosis and early G1 through phosphatase action of the PP1-Spinophilin holoenzyme, reviewed in (Verdugo-Sivianes and Carnero, 2021). This allows **E2F family transcription factors** to bind to the promoters and activate expression of genes required for entry into S phase. The activity of these cyclin/Cdk complexes is inhibited by 2 families of CKIs: the INK4 family (p16, p15, p19 and p18), which specifically regulate G1/S progression by inhibiting Cdks4/6, and the Kip/Cip inhibitors (p21, p27 and p57), which regulate G1 arrest by inhibiting Cdk2.

Research over the past twenty years, by our laboratory and others, have established significant requirements for the Rb/E2F axis beyond simple regulation of S phase entry, discussed next and reviewed in (Chen et al., 2009b; Julian and Blais, 2015; McClellan and Slack, 2006). Broadly, these include regulation of the DNA damage response, the G2/M transition, cellular differentiation and apoptosis – including during developmental neurogenesis (Lee et al., 1994) – chromatin reorganization, and lipid metabolism. Extending the role of Rb/E2F families well

beyond cell cycle regulation, these functions carry profound significance to the regulation of adult neurogenesis.

We will begin by discussing the composition of the Rb family, comprised of three unique members, as well as the composition of the E2F family, comprised of eight genes, two of which (E2F3 and E2F7) give rise to two distinct protein isoforms.

5.2 Rb family Proteins

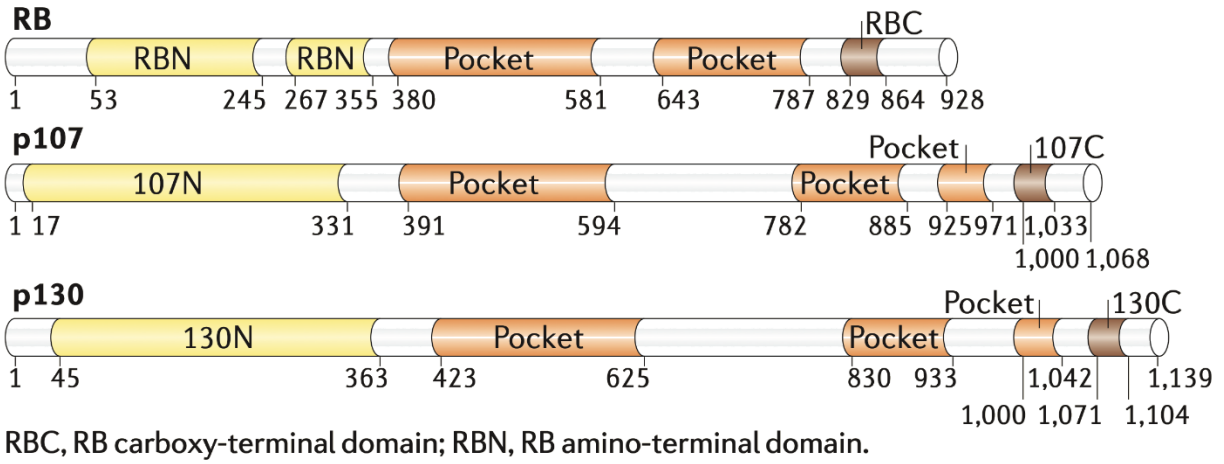

Rb family proteins operate at the core of the canonical cell cycle pathway, representing a point of convergence for cyclin, Cdk and CKI regulation of the G1 restriction point (Dick and Rubin, 2013). The Rb family is named for its initial member, (**pRb**), encoded by the retinoblastoma gene Rb1, whose genetic locus was first associated in 1976 with a hereditary eye cancer termed retinoblastoma (Francke and Kung, 1976). In 1987, Rb1 would become the first tumour suppressor gene to be cloned (Lee et al., 1987), and following studies would identify Rb1 deletions and/or mutations in many other tumors and tumor cell lines, including osteosarcomas, small cell lung carcinomas, breast cancers and bladder carcinomas (Dyson et al., 1989). **p107** and **p130** are

paralogs of pRb, encoded respectively by genes Rbl1 and Rbl2 (i.e. *Rb-like*), and represent the other two proteins within the Rb family.

Structurally, pRb comprises a structured N-terminal domain (RBN), an intrinsically disordered C-terminal domain (RBC), linker sequences containing Cdk-dependent phosphorylation sites (Burke et al., 2012) and, notably, a central "pocket" structure. This pocket, which defines Rb family proteins as "pocket proteins", is formed by A and B subdomains – each resembling a cyclin fold with three additional helices – which interact with each other to form a single structural unit (Lee et al., 1998). The domain structure of p107 and p130 is highly similar, with consistent N-terminal (107N/130N) and C-terminal (107C/130C) domains together with the shared pocket structure. While pRb shares approximately 25% sequence identity with either, p107 and p130 share approximately 54% identity (Dick and Rubin, 2013; Liban et al., 2016; Mulligan and Jacks, 1998).

5.2.1 Rb family Function

The classical function of Rb family proteins is to inhibit E2F transactivation, which it mediates through two mechanisms. In the first, *inhibition of activation*, Rb family proteins bind the E2F transactivation domain ($E2F^{TD}$) using a highly conserved region of the pocket, preventing its interaction with the core transcriptional machinery (Helin et al., 1993a). The pocket also contains a L-X-C-X-E-binding cleft targeted by DNA tumor viruses – including HPV, Adenovirus and Polyomavirus – with the pocket being initially identified as the minimal region necessary to bind viral L-X-C-X-E-containing oncoproteins such as HPV E7 (Dyson, 1998). DNA tumor viruses bind Rb family proteins to inactivate its ability to repress cell proliferation, mediating viral

oncogenic transformation in what is referred to as the "viral hypothesis" of cancer (Dyson et al., 1989; Felsani et al., 2006).

Rb family proteins are further able to bind and regulate multiple protein interactors through their modular domains. pRb interaction with chromatin-modifying and histone-modifying enzymes have been identified, mediated through the L-X-C-X-E-binding cleft (Brehm and Kouzarides, 1999) – these include histone deacetylases (HDACs) HDAC1/2, DNA methyl-transferases DNMT1/2, and ATP-dependent SWI/SNF modifiers (Brehm et al., 1998; Dunaief et al., 1994; Robertson et al., 2000). This represents the second mechanism of E2F control, *active repression*, as the pRb/E2F complex subsequently binds to the promoters of E2F targets and can recruit chromatin remodelers (including HDACs and BRG1 (Brehm et al., 1998; Dahiya et al., 2000) to mediate transcriptional silencing. Similarly, p107 and p130 employ the L-X-C-X-E-binding cleft to recruit large repressive complexes including the DREAM complex: the Drosophila orthologues of pRb, E2F and dMyb (Forristal et al., 2014). Though it does not contain an L-X-C-X-E motif, the suboptimal L-X-S-E-X-L sequence on DREAM subunit LIN52 is able to pair with the phosphate at nearby S28 to bind the cleft with high affinity (Guiley et al., 2015). The DREAM complex represents a druggable target for Rb family protein inactivation: the drug harmine has been employed to recapitulate the phenotype associated with compound p107/p130 loss through phosphorylation of DREAM subunit DYRK1A (Forristal et al., 2014; Göckler et al., 2009)

While all three Rb family proteins control cell proliferation, regulate E2F transcription factors and become inactivated by cyclin/Cdk complexes (Stengel et al., 2009), there are notable distinctions between them. While pRb is constitutively expressed in all cells, p107 is generally restricted to uncommitted cycling cells and p130 is predominant in quiescent and differentiating cells (Mulligan and Jacks, 1998). While pRb is expressed throughout G0/G1/S phase, p107 forms

E2F complexes at late G1 and S phases (Shirodkar et al., 1992), and p130 forms E2F complexes during the quiescent G0 and early G1 phases (Smith et al., 1996). In response to p53-mediated downregulation of cell cycle genes, pRb and p130 co-operate to repress G1/S transition, with p107 providing repression in their absence; by contrast, p107 and p130 alone repress G2/M transition, with p107 repression specifically restricting entry into M phase (Schade et al., 2019).

Along with the observation that only pRb is commonly associated with tumor formation (Knudsen and Knudsen, 2008), these results suggest that the Rb family proteins are not functionally redundant. Study of sequence homology in other species have revealed that many pRb-related genes in non-mammals resemble p107 and p130, suggesting the presence of an ancestral Rb1 gene, replaced more recently by modern Rb1; this would suggest that the tumor suppressor function of pRb is a more recent evolutionary adaptation (Wirt and Sage, 2010). Moreover, while overexpression of all three Rb family proteins is sufficient to induce growth arrest in G1 (Dyson, 1998), studies in epithelial and neural tissues during early-embryonic development demonstrate cell ability to exit the cell cycle despite Rb family protein deletion (Wirt et al., 2010). This suggests that the Rb family operates within a broader regulatory network to control G1/S progression, wherein parallel repression pathways exist to regulate the target genes of our next topic, E2F family transcription factors.

5.3 E2F family Transcription Factors

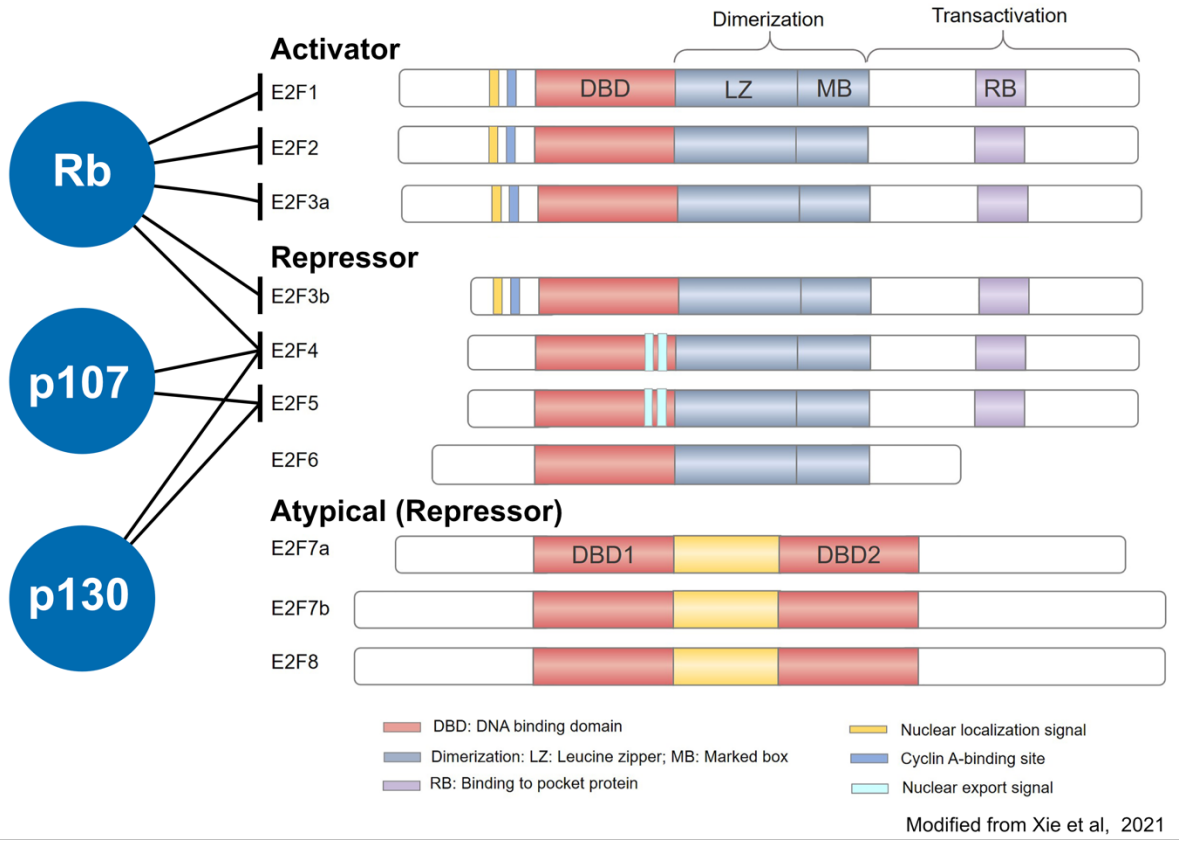

E2F family transcription factors (E2Fs) serve as critical downstream effectors of Rb family function. E2Fs are generally subdivided into two categories based on their functional properties: the *activator E2Fs* E2F1/2/3a are transcriptional activators, while the *repressor E2Fs* E2F3b/4/5/6/7a/7b/8 are transcriptional repressors. E2Fs heterodimerize with one of two Differentiation-related Polypeptide proteins – most commonly DP1 but also DP2 (Girling et al., 1993; Komori et al., 2018) – whose interaction is required to maximize E2F transactivation through stable binding to DNA sites (Helin et al., 1993b). The exceptions to this are repressor E2Fs E2F7a/7b/8, further distinguished as *atypical* repressor *E2Fs* due to prominent structural differences explored below.

Classically viewed as positive regulators of genes required to promote S phase entry, our understanding of E2F family function has evolved substantially over the past 35 years. E2F was

defined in adenovirus-infected cells as a cellular transcription factor required for the early region 1A (E1A) transforming protein to mediate the transcriptional activation of the viral E2 promoter; hence, E2 Factor (Kovesdi et al., 1986). Through co-purification and identification, researchers would rapidly establish E2F as among the first known binding partners of pRb (Bagchi et al., 1991; Chellappan et al., 1991). Its function promoting cell proliferation through trans-activation of S phase genes, in turn inhibited by pRb through direct binding (Helin et al., 1993a), would be soon connected mechanistically with specific E2F targets required for DNA replication (Hsiao et al., 1994; Leone et al., 1998). Presently, we view E2Fs at the centre of a core transcriptional network, touching on multiple aspects of cell fate, including DNA repair (Ren et al., 2002), cell cycle progression and apoptosis (DeGregori and Johnson, 2006), metabolism (Blanchet et al., 2011), and differentiation (Cuitiño et al., 2019).

5.3.1 Activator E2Fs

The primary role of activator E2Fs E2F1/2/3a is to **promote** the expression of E2F target genes, including DNA polymerase α and cyclins E/A (Lundberg and Weinberg, 1998). Together with repressor E2Fs, they possess a winged-helix DNA binding domain (DBD), a DP binding domain comprised of a leucine zipper (LZ) and a marked box (MB), as well as the C-terminus $E2F^{TD}$ transactivation domain whose interaction with Rb family proteins has been previously described. Activator E2Fs are distinguished by a longer N-terminus, containing a nuclear localization signal (NLS) to promote nuclear translocation (Müller et al., 1997), as well as a binding site through which cyclin A exerts inhibition during S/G2 phases (Krek et al., 1995).

Following the initial isolation of E2F1, E2F2 and E2F3 were first isolated in 1993 (Lees et al., 1993). E2F3 would be later resolved into two distinct transcripts, with the longer E2F3a acting

as a transcriptional activator (Adams et al., 2000; Leone et al., 2000). Activator E2Fs are maximally expressed from late G1 to early S phase – with E2F1 increasing 15-fold at the G1/S-boundary – correlating with their requirement to promote S phase entry as well as progression (Hsiao et al., 1994). pRb preferentially binds activator E2Fs (Saavedra et al., 2002) and activator E2F loss is sufficient to suppress the proliferative phenotype associated with pRb loss (Tsai et al., 1998). In contrast, E2F1 demonstrates a further function in the regulation of apoptosis and the suppression of cell proliferation, as E2F1-null mice demonstrate a phenotype of aberrant cell proliferation with age (Field et al., 1996).

Though activator E2Fs are considered part of the Rb tumor suppressor pathway, acting to mediate Rb control of the G1/S phase transition, multiple studies have demonstrated that activator E2Fs can also function as tumor suppressors, as well as oncogenes, in a tissue-specific manner. E2F1 acts upstream of p53 and signals p53-dependent apoptosis to suppress tumor formation (Pan et al., 1998), re-introduction of E2F2 into T-cell lymphomas stimulates tumor cell apoptosis (Opavsky et al., 2007), and loss of E2F3 promotes development and metastasis of medullary thyroid tumours (Ziebold et al., 2003).

5.3.2 Repressor E2Fs

The primary role of repressor E2Fs is to **repress** E2F target gene expression. In contrast with the late-G1/S phase expression of activator E2Fs, they are defined by ubiquitous expression in quiescent cells, and throughout the cell cycle (Leone et al., 2000).

Repressor E2Fs can be classified into two groups; in the first, *canonical* repressor E2Fs E2F3b/4/5/6 possess distinct structural differences, though generally resemble activator E2Fs. With the exception of E2F3b, they lack either a NLS or a cyclin A-binding site, and rely on Rb

family proteins for nuclear translocation (Verona et al., 1997). Though E2F3b shares significant structural similarities with E2F3a, its truncated transcript lacks 5' regulatory elements common to activator E2Fs, and it forms repressive complexes in quiescent cells (Adams et al., 2000; Leone et al., 2000). E2F4 and E2F5 are necessary for Rb family protein-mediated G1 arrest (Gaubatz et al., 2000), and possess bipartite nuclear export signals (NES) that mediate their export to the cytoplasm during cell cycle entry from quiescence (Gaubatz et al., 2001). They possess roles in the differentiation of specific lineages, as E2F4 loss results in developmental defects in hematopoiesis and gut development (Rempel et al., 2000), while loss of E2F5 results in choroid plexus defects leading to hydrocephalus formation by 3-4 weeks (Lindeman et al., 1998). Though E2F4 induces ectopic proliferation similar to E2F1, it lacks any tumor-suppressor function (Wang et al., 2000) and acts solely as an oncogene, promoting pituitary and thyroid tumor development (Lee et al., 2002b). Finally, E2F6 further lacks an $E2F^{TD}$ transactivation domain, and is presumed to repress E2F-responsive genes independently of Rb family proteins (Cartwright et al., 1998).

pRb, in addition to binding activator E2Fs, binds repressor E2Fs E2F3b and E2F4. In quiescent cells, pRb functions as a transcriptional repressor through a pRb-E2F3b complex, repressing targets including cyclin E (Leone et al., 2000). In cycling cells, pRb-E2F4 complexes account for the majority of endogenous E2F activity (Moberg et al., 1996).

p107 and p130 preferentially bind repressor E2Fs 4 and 5, in contexts consistent with their expression patterns. In cycling cells, p107-E2F4 complexes are most highly expressed during S phase (Zini et al., 2001) and target the promoters of actively transcribing genes (Wirt and Sage, 2010). In quiescent and senescent cells, p130/E2F4 complexes – including the DREAM complex – as well as p130 / E2F5 complexes, are most highly expressed during G0 and G1 phase to repress genes that promote cell cycle re-entry (Chen et al., 2008; Litovchick et al., 2007). Under conditions

of growth arrest, p130 and E2F4 co-operatively repress genes involved in cell cycle control, but also mitochondrial and metabolic genes, many co-regulated by NRF1 (Cam et al., 2004).

The second group of repressor E2Fs, *atypical* repressor E2Fs 7a/7b/8, are set apart structurally from other E2Fs (Bruin et al., 2003; Christensen et al., 2005; Stefano, 2003). Similar to E2F6, atypical repressor E2Fs lack an $E2F^{TD}$ transactivation domain, acting independently of Rb family proteins; by contrast with E2F6, they further lack DP binding domains. In contrast with E2F3 isoforms, E2F7a and E2F7b are produced through alternate splicing of the primary transcript (Stefano, 2003). Atypical E2Fs form homo- and hetero-dimers with one-another and are believed to serve as a critical fine-tuning mechanism to modulate E2F target genes, including on E2F1. While the use of inducible E2F7-flox and E2F8-flox mice demonstrated no significant developmental defect resulting from individual protein loss, combined ablation of E2F7 and E2F8 resulted in massive apoptosis and early-embryonic (E11.5) lethality. This was associated with an increase in E2f1 and p53, as apoptosis was rescued following deletion of either; atypical E2Fs were also found directly bound to target promoters including E2F1 (Li et al., 2008). Recent work has further demonstrated tissue-specific roles for atypical E2Fs as both oncogenes and tumor suppressors: while they act co-operatively with Rb to prevent liver tumorigenesis, their long-term expression independent of Rb enhances spontaneous lung tumorigenesis (Moreno et al., 2021).

5.4 Functional Compensation within Rb and E2F Families

While the preceding sections defined our current understanding of binding preferences amongst Rb family proteins and E2F family transcription factors, it is important to consider functional compensation in specific contexts, as with the tissue-specific functions demonstrated by activator, repressor and atypical E2Fs, acting as both oncogenes and tumor suppressors.

Rb family proteins demonstrate functional compensation in multiple systems. Following Rb inactivation, p107 and p130 enforce the G2/M phase checkpoint in myoblasts (Blais et al., 2007). p107 and p130 are able to interact with activator E2Fs in the absence of Rb (Lee et al., 2002a), notably in testicular sertoli cells (Rotgers et al., 2014); p107 and E2F3 can even interact under physiological conditions, to control Fgf2 expression in neural progenitors (McClellan et al., 2009). In hematopoietic and liver tissues, inactivation of all three Rb family members demonstrates distinct requirements from inactivation of Rb alone, reflecting a compound requirement in regulating stem cell quiescence, preventing cell-intrinsic myeloproliferation and hepatocellular carcinoma formation (Viatour et al., 2008, 2011a). This was later associated with positive regulation of Jak2 signaling through the E2F-mediated transactivation of Jak2-inhibitor Socs3 (Kim et al., 2017). In the absence of pRb or pRb/p130, p107 is ectopically upregulated during late retinal development, though it is haploinsufficient to rescue the effects of pRb/p130 deficiency (Ajioka et al., 2007).

Compound Rb family protein knockouts are also more severe than single knockouts (Classon et al., 2000; Hurford et al., 1997). Germline deletion of pRb is embryonic lethal due to hypoxic stress and muscle differentiation defects, and pRb-deficient embryos terminate by E15.5 (Jacks et al., 1992). p107-deficient and p130-deficient embryos are viable and fertile on a C57BL/6 genetic background, but in Balb/cJ mice lead to impaired growth and termination by E13, respectively (LeCouter et al., 1998a, 1998b). Rb family-deficient embryos terminate by E11 (Wirt et al., 2010). Compound deletion of p107/p130 results in death immediately after birth, related to defects in bones and cartilage (Cobrinik et al., 1996), while deletion of either with pRb results in neonatal death (Lee et al., 1996; Sage, 2000).

E2F transcription factors also possess some degree of functional compensation, beyond their classifications as activators or repressors. Chong et al. demonstrated that, in contrast to their role as transcriptional activators in proliferating cells, activator E2Fs function as pRb-associated transcriptional repressors in differentiating cells, in order to silence E2F target genes and facilitate cell cycle exit. Notably, pRb inactivation in this context resulted in a functional switch for activator E2Fs from repressors to their canonical role as transcriptional activators, resulting in E2F target super-activation (Chong et al., 2009). In the retina, and in contrast with observations in fibroblasts, retinal progenitor cells and activated Müller glia are able to proliferate in the absence of activator E2Fs1/2/3, though this is accompanied by elevated apoptosis. This tissue-specific dispensability for cell division is believed to result from functional compensation by MYCN (Chen et al., 2009a).

Importantly, this suggests that activator E2Fs may possess context-specific abilities and broadly serve as both activators and repressors. In line with this, repressor E2F4 can act as a transcriptional activator in mouse ES cells, interacting with chromatin regulators to promote gene activation and expression of cell cycle genes, independent of Rb family proteins (Hsu et al., 2019).

5.5 Cell Cycle Regulators and Adult Neurogenesis

Several studies have revealed crucial requirements for cell cycle proteins in adult NSC fate, in coordination with fate determinants and differentiation factors, reviewed in (Fong and Slack, 2017). Cdk6 regulates G1 length to mediate the expansion of differentiating adult-born progenitors (Beukelaers et al., 2011), while adult genetic ablation of cyclin D2 results in a SGZ devoid of proliferating cells and neuroblasts (Kowalczyk et al., 2004). Furthermore, cyclin D1/Cdk4 complex overexpression in the SGZ induces expansion of the activated NSC and progenitor

populations at the expense of differentiation (Artegiani et al., 2011), though Cdk4 alone appears to be dispensable *in vivo* (Beukelaers et al., 2011).

CKIs $p21^{Waf1}$, $p27^{Kip1}$ $p57^{Kip2}$ have been thoroughly investigated for their roles regulating cell cycle exit, differentiation and migration. $p21^{Waf1}$ maintains an activated, non-differentiating population of V-SVZ qNSCs, preventing niche exhaustion through E2F-mediated modulation of Bmp2 expression (Kippin et al., 2005; Porlan et al., 2013), and represses NSC self-renewal through direct repression of Sox2 at its downstream SRR2 enhancer (Marqués-Torrejón et al., 2013). $p21^{Waf1}$ further suppresses proliferation in differentiating adult-born SGZ neurons (Pechnick et al., 2008). $p27^{Kip1}$ is dispensable in V-SVZ NSCs, but promotes progenitor cell exit (Doetsch et al., 2002). In the SGZ, $p27^{Kip1}$ regulates quiescence and cell cycle exit in immature GCNs (Andreu et al., 2015; Qiu et al., 2009), and prevents expansion of the activated NSC population, acting downstream of Bmp4, and may also be involved in promoting neuronal differentiation by repressing Sox2 (Li et al., 2012). Finally, $p57^{Kip2}$ is required to maintain the developmentally-originating RGLs that become V-SVZ qNSCs, as well as to maintain the SGZ qNSC population; $p57^{Kip2}$ downregulation is further required for exercise-induced NSC activation (Furutachi et al., 2013, 2015).

5.6 The Rb/E2F Axis and Adult NSC Fate

The Rb/E2F axis possesses a wide range of functions relevant to adult NSC fate, reviewed in (Julian and Blais, 2015), reflecting a broader role as essential regulators of stem cell fate in other tissues (Sage, 2012).

In the V-SVZ, p107 suppresses adult NSC self-renewal by downregulating the Notch pathway though direct Hes1 repression, favouring neuronal differentiation and commitment

(Vanderluit et al., 2004, 2007). While a requirement for p107 pertaining to quiescence remains to be clarified, high Notch activity promotes NSC quiescence (Chapouton et al., 2010; Sueda et al., 2019). p107 further binds E2F3 isoforms E2F3a and E2F3b, which hold opposing roles in directly targeting self-renewal factor Sox2 at its proximal promoter region, in activated NSCs (Julian et al., 2013).

p130 represents the *dark horse* of the Rb family, though it is believed to be involved in NSC differentiation and survival. During iPSC differentiation, p130 forms a repressive complex with E2F4 and SIN3A to repress Sox2 expression via its SRR2 enhancer, potentially in synergy with similar repression by $p27^{Kip1}$ (Li et al., 2012). p130 has been further implicated in the regulation of cortical neuronal death and survival through E2F4-mediated repression of pro-apoptotic genes (Liu et al., 2005).

5.6.1 Rb and Adult NSC Fate

pRb itself carries the most curious implications of the three. pRb is required for adult post-mitotic neuronal survival, acting to maintain continuous cell cycle repression (Andrusiak et al., 2012). pRb-E2F complexes further mediate neuronal quiescence through LXCXE-independent chromatin remodeling (Andrusiak et al., 2014). However, a similar role for pRb in adult NSCs remains unknown.

A recent publication (Naser et al., 2016) by our collaborators demonstrated roles for pRb in adult V-SVZ/OB neurogenesis both consistent with, and distinct from, those we had previously reported in the embryonic cerebral cortex during development (Ferguson et al., 2002; MacPherson et al., 2003). Consistent with development, pRb does not appear to regulate self-renewal of adult NSCs, and is required to control progenitor proliferation in the adult V-SVZ and RMS. However,

the authors were not able to detect a role for pRb in maintaining NSC quiescence, and pRb-deficient immature granule cell neurons did not demonstrate any apparent defects in differentiation or rostral migration. While pRb loss led to an increase in OB neurogenesis, it was abrogated one month later by increased apoptosis, consistent with apoptosis similarly seen in the developing telencephalon following pRb loss (Ferguson et al., 2002).

While this demonstrates a requirement for Rb in the long-term survival of adult-born OB interneurons, it further suggests that Rb may also play an important role in the regulation of adult DG neurogenesis. In Chapter 2, published as (Vandenbosch et al., 2016), we hypothesized that Rb may have distinct functions in the regulation of DG neurogenesis and examined its role in the production of dentate granule cell neurons during embryonic and adult neurogenesis.

Findings following Chapter 2, together with findings from (Naser et al., 2016), suggest that pRb is dispensable in maintaining NSC quiescence and may not serve as the main cell cycle regulator governing adult NSCs. This prompts the question: if pRb alone is dispensable to regulate quiescence and activation fate in the adult NSC population, then how are these fates linked with cell cycle control? Mindful of the functional compensation established in Section 5.4, both between Rb family proteins as well as their E2F family transcription factor targets, this question is the subject of Chapter 3.

As neurodegenerative disease pathologies demonstrate deficits in neuronal differentiation and neuronal cell number, we are interested in how the regulation of adult neurogenesis may become impacted, or may even be implicated, in mouse models of neurodegeneration. In Chapter 4, we assess the regulation of NSC quiescence and activation in the 3xTG-AD model of Alzheimer's Disease. We chose this model due to its consistency with findings from human AD pathology, as described in Section 2.3.

Statement of Objectives

The primary objective of this thesis is to determine the requirement of Rb family proteins during adult neurogenesis. The main body of this thesis comprises of three manuscripts, with one published and two in submission.

In Chapter 2, published as (Vandenbosch et al., 2016), we tested the hypothesis that Rb possesses distinct requirements in SGZ neurogenesis, pertaining to the generation and survival of dentate granule cell neurons during developmental and adult neurogenesis.

In Chapter 3, we tested the hypothesis that the Rb/E2F axis is a master regulator of adult NSCs, and functions as an on/off switch instructing the cellular and transcriptomic changes that instruct quiescent and activated states. This continued our inquiry into Rb function in adult SGZ neurogenesis from Chapter 2, expanded to establish the requirement for Rb/E2F axis in a system free of functional overlap, and broadening the scope to further encompass adult neurogenesis in both the V-SVZ and SGZ. At time of thesis submission, this manuscript is being revised for submission for publication as Fong et al., 2022.

Finally, in Chapter 4, we tested the hypothesis that NSC quiescence and activation states are altered in the 3xTG-AD model of Alzheimer's Disease. Together with unpublished findings outlined in Appendix I implicating the involvement of Rb family proteins and their E2F targets, this notably expands our inquiries into Rb/E2F regulation of NSC fate to a pathological context. At time of thesis submission, this manuscript is being revised for submission as a bioRxiv pre-print as Liu et al., 2022.

CHAPTER 2

Renaud Vandenbosch, Alysen Clark, **Bensun C Fong**, Saad Omais, Carine Jaafar, Delphie Dugal-Tessier, Jagroop Dhaliwal, Diane C Lagace, David S Park, Noël Ghanem, and Ruth S Slack. RB regulates the production and the survival of newborn neurons in the embryonic and adult dentate gyrus. *Hippocampus*. 2016 Nov;26(11):1379-1392. Doi: 10.1002/hipo.22613.

BCF performed several revision experiments, including immunohistochemical staining and quantification of adult brain sections, as well as validation of Rb deletion with qPCR. These contributions are reflected in the final publication as Figure 5C. BCF contributed to the writing and revision of the manuscript.

RB regulates the production and the survival of newborn neurons in the embryonic and adult dentate gyrus

Renaud Vandenbosch[1,3], Alysen Clark[1], Bensun C. Fong[1], Saad Omais[2], Carine Jaafar[2] , Delphie Dugal-Tessier[1], Jagroop Dhaliwal[1], Diane C. Lagace[1], David S. Park[1], Noël Ghanem[2,4] and Ruth S. Slack[1,4]

[1]Department of Cellular & Molecular Medicine, University of Ottawa, Ottawa, ON, Canada

[2]Department of Biology, American University of Beirut, Beirut, Lebanon

[3]Present address: Developmental Neurobiology Unit, GIGA-Neurosciences, University of Liège, Liège, Belgium.

[4]Co-corresponding authors

Running Title: RB controls Dentate Neurogenesis

Key Words: adult neurogenesis, hippocampal development, cell cycle, survival

Number of text pages: 28

Number of figures: 7 + 5 Supplemental Figures in Supporting Information

Table: 1 in Supporting Information

Acknowledgments:. We thank Jason G. MacLaurin, Linda Jui and Sawsan Al Lafi for excellent technical assistance. This work was supported by CIHR grants to R.S.S and grants from the University Research Board (URB) at AUB to N.G. R.V. was supported by postdoctoral fellowships from the Vision 2010 strategic plan of the University of Ottawa, the Alzheimer Society of Canada, the Heart and Stroke Foundation of Canada and by travel awards from the Léon Fredericq Funds (University of Liège, Belgium) and Wallonie-Bruxelles International.

Corresponding authors:

Ruth S. Slack; Tel: +1 613 562 5800 x 8458; E-mail: rslack@uottawa.ca

Noël Ghanem; Tel: +961 1 350000 x 3915; E-mail: ng13@aub.edu.lb

Abstract

In mammals, hippocampal dentate gyrus granule cells (DGCs) constitute a particular neuronal population produced both during embryogenesis and adult life, and play key roles in neural plasticity and memory. However, the molecular mechanisms regulating neurogenesis in the dentate lineage throughout development and adulthood are still not well understood. The retinoblastoma protein (RB), a transcriptional repressor primarily involved in cell cycle control and cell death, plays crucial roles during cortical development but its function in the formation and maintenance of DGCs remains unknown. Here, we show that loss of RB during embryogenesis induces massive ectopic proliferation and delayed cell cycle exit of young DGCs specifically at late developmental stages but without affecting stem cells. This phenotype was partially counterbalanced by increased cell death. Similarly, during adulthood, loss of RB causes ectopic proliferation of newborn DGCs and dramatically impairs their survival. These results demonstrate a crucial role for RB in the generation and the survival of DGCs in the embryonic and the adult brain.

Introduction

Dentate granule cells (DGCs), one of the major types of excitatory neurons found in the hippocampus, are densely packed in the granule cell layer of the dentate gyrus (DG), and play key roles in learning and memory as well as epileptogenesis (Kesner, 2013). In contrast to the majority of neurons of the mammalian CNS which are born during embryogenesis, DGCs are continuously produced from mid-gestation to old age, including in humans (Ernst and Frisén, 2015). During embryonic development, DGCs arise from neural precursor cells (NPCs) located in a discrete part of the ventricular zone (VZ) of the dorsal pallium, the dentate neuroepithelium (Li and Pleasure, 2007), whereas postnatally-born DGCs develop locally from NPCs anchored in a specialized niche of the DG, the subgranular zone (SGZ) (Rolando and Taylor, 2014).

A better understanding of the molecular mechanisms orchestrating DGCs production could contribute to the development of novel strategies aimed at replacing neurons following brain disorders or injury. Neurogenesis occurs under the control of extrinsic and intrinsic factors, including transcription factors, epigenetic regulators and components of the cell cycle machinery. However, the specific contribution of each family of cell cycle regulators to the production of the large repertoire of neurons and glial cells remains to be fully elucidated. Moreover, the exquisite coordination between precursor proliferation, cell cycle exit and differentiation in the DG lineage is not well understood, and the same regulators could have different functions during development and adulthood (Urbán and Guillemot, 2014). Some members of the cell cycle machinery have been shown to play a crucial role in the generation of DGCs. For example, $p27^{Kip1}$, an inhibitor of cyclin-dependent kinases (Cdks), acts as a dual regulator of NPCs quiescence and cell-cycle exit of immature DGCs in the adult hippocampus (Qiu et al., 2009; Andreu et al., 2015). Cdk6 specifically drives the expansion of transit-amplifying progenitors in the postnatal DG (Beukelaers et al.,

2011), whereas its binding partner cyclin D2 is essential for DGCs production after birth but not during embryonic development (Kowalczyk et al., 2004). In the canonical cell cycle pathway, the point of convergence between cyclins, Cdks and Cdk inhibitors is the phosphorylation and inactivation of the retinoblastoma protein (RB). RB is a key regulator of cell cycle progression controlling the G1/S transition. Upon phosphorylation by Cdk–cyclin complexes, RB dissociates from bound E2F transcription factors, liberating them to regulate expression of genes essential for cell cycle progression, differentiation and cell death (Iaquinta and Lees, 2007). Importantly, we and others have previously demonstrated that loss of RB induces ectopic proliferation of neuroblasts and enhanced neurogenesis in the embryonic cerebral cortex (Ferguson et al., 2002; MacPherson et al., 2003), suggesting that RB may also play an important role in the regulation of DG neurogenesis. Moreover, we have recently shown that RB controls progenitor proliferation in the adult subventricular zone (SVZ) and rostral migratory stream (RMS), and is required for long-term survival of adult-born interneurons in the olfactory bulb (OB)(Naser et al., 2016).

In this study, we have hypothesized that RB may have distinct functions in the regulation of DG neurogenesis and thus, have examined its role in the production of DGCs during embryonic and adult neurogenesis. We show that deletion of RB expands the number of DGCs produced during late embryogenesis by inducing massive proliferation of young DGCs that is coupled to increased apoptosis at late developmental stages. In the adult DG, acute loss of RB does not affect NPCs quiescence but induces ectopic proliferation of newborn DGCs and dramatically reduces their survival. Taken together, our data demonstrate a crucial role for RB as a regulator of DGCs production and, more importantly, their survival in the embryonic and adult DG.

Material and Methods

Animals and Treatments

All experiments were approved by the Animal Care Ethics Committee of the University of Ottawa and adhered to the Guidelines of the Canadian Council on Animal Care and the Institutional Animal Care and Use Committee (IACUC) of the American University of Beirut. Rb^{lox} (Marino et al., 2000), Foxg1-Cre (Hébert and McConnell, 2000), $E2f1^{-/-}$ (Field et al., 1996) and $E2f3^{lox}$ (Wu et al., 2001) mice were maintained on a FVB/N background. Rb^{lox}; Nestin-CreERT2 (Cicero et al., 2009); R26-stop-enhanced yellow fluorescent protein (YFP) (Srinivas et al., 2001) mice were maintained on a mixed FVB/N X 129Sv/J X C57/BL6 background. Animals were genotyped according to standard protocols with previously published primers. All Foxg1-Cre and Nestin-CreERT2 animals used were heterozygotes for Cre expression. In all experiments, both females and males were used. For embryonic studies, the time of plug identification was considered to be day 0.5. For adult studies, 6-8 week old mice were used. For Cre induction in adult NestinCreERT2 animals, mice were administered tamoxifen (TAM) at 150 mg/kg/d for 5d (intraperitoneally; dissolved in 10% EtOH/90% sunflower oil). To analyze cell proliferation in the adult brain, NestinCreERT2 mice were given a single injection of BrdU (100mg/kg, i.p) ten days after the end of TAM treatment and euthanized 2h later. To analyze cell proliferation in the embryonic brain, pregnant mothers were given a single injection of BrdU (100mg/kg, i.p) and euthanized 30min or 1h later. For birth dating experiments, NestinCreERT2 mice were treated with BrdU for three consecutive days after the end of TAM treatment (100 mg/kg/day i.p., 3 days) and euthanized four weeks later.

Tissue processing and Immunostaining

Tissue was fixed as previously described (Fortin et al., 2001; Mcclellan et al., 2007). Cells were fixed for 20 minutes at room temperature with 4% PFA. Embryonic brains were sectioned at 14µm on slides. Adult brains were sectioned as free-floating sections at 30µm for NestinCreERT2 animals (1-in-9 series) or 40µm for animals injected with retroviruses (1-in-6 series). Prior to immunolabeling, when necessary, sections underwent antigen retrieval for 15 minutes at 95°C in Target Retrieval Solution (S1699-Dako). To perform BrdU detection, DNA was denaturated with 2N HCl for 30 min at 37°C followed by 0.1M borate buffer pH 8.5 for 10 min. Sections or cells were incubated overnight at 4°C with primary antibodies (see Table 1 in Supporting Information for the complete list of primary antibodies used) diluted in 1x PBS containing 0.1% Triton, 0.1% Tween 20 and 5% normal donkey serum (blocking solution) and incubated for 1 hour at room temperature in blocking solution with secondary antibodies coupled to Alexa Fluor-488, Cy3 or Dylight-649 dyes (Jackson ImmunoResearch) along with 4',6-diamidino-2-phenylindole (DAPI) (Sigma) or Hoechst (Invitrogen) stain. Slides were coverslipped with Immunomount (Genetex). Images for quantifications of double or triple labeled sections were taken using a Zeiss 510 meta confocal microscope. Quantifications of $BrdU^+$, $AC3^+$, $Cre:GFP^+$ and RFP^+ cells in the adult DG were performed on an Olympus BX-51 microscope. For cell culture, cells were imaged using a Zeiss AxioImager (M2 Microscope with Axiovision software). Images were analyzed using ImageJ (Schneider et al., 2012).

Cresyl Violet Staining

Cresyl violet staining procedures were performed as previously described (Sirkin, 1983).

Cell Quantification and Statistical Analysis

For cell quantification in the embryonic DG, counts were performed using confocal images on a minimum of 3-4 sections from each brain that had been leveled rostra-caudally based on cresyl violet or DAP/Hoechst staining, and values were expressed per section or per mm^2. To determine the percentage of proliferating $Ki67^+$ cells in each cell population, a minimum of 100 cells per animal were counted. For BrdU, AC3 and YFP/DCX/Ki67 counts in the DG of adult NestinCreERT2 mice, every ninth section throughout the DG was quantified and counts were summed and multiplied by 9 to generate an estimate of the total number of cells in the DG. To quantify the percentage of double and triple labeled cells in NestinCreERT2 animals, a minimum of 50 YFP^+ $Sox2^+$ (Fig. 5B), 50 YFP^+ $NeuroD1^+$, 50 YFP^+DCX^+ and 100 YFP^+ (Fig. 5C-E) cells per animal were counted at similar rostro-caudal levels of the DG. To assess the density of $NeuroD1^+/YFP^+$ cells (Fig. 5F), counts were performed on 8 fields per animal, located at similar rostro-caudal levels of the DG and expressed as a number of cells per μm^3 (size of the field: 225 µm x 225 µm x 10 µm). To quantify the survival of Cre:GFP infected neurons, a minimum of 50 RFP^+ cells per animal were quantified and assessed for the expression of Cre:GFP per animal. To quantify the proliferation of Cre:GFP infected neurons, a minimum of 50 GFP^+ cells per animal were quantified and assessed for the expression of Ki67. For the *in vitro* differentiation assay, 50 $Tuj1^+$ cells per embryo and per timing were evaluated for the presence of BrdU. Statistical analysis was performed using Prism software (GraphPad Software). Unpaired, two tailed Student's T-tests or one-way ANOVA tests were performed for all results with a minimum 95% confidence threshold. Unless otherwise stated, all data is presented as the arithmetic mean, plus or minus the standard error of the mean (mean ± SEM). For each experiment, a minimum of n=3 animals per genotype were used.

Cell Culture

Embryonic DG NPCs were obtained by dissection of the dentate neuroepithelium at E14.5 (Clarke and van der Kooy, 2011) Neurosphere and *in vitro* differentiation assays were performed as previously described (Vanderluit et al., 2004; Babu et al., 2007). Adult NPCs were isolated from the brain 5 days after the last tamoxifen injection and cultured as previously described (Naser et al., 2016). At passage 2 and after dissociation, YFP^+ single cells were sorted using an automated cell sorter (BD FACS Aria SORP cell sorter) and processed for Western blot analysis.

Retroviral vectors, virus preparation and stereotaxic injections

The retroviral vectors cytomegalovirus immediate early enhancer-chicken β-actin hybrid-Cre recombinase: green fluorescent protein (CAG-Cre:GFP) and CAG-red fluorescent protein (RFP) were generous gifts from F. Gage (Salk Institute, La Jolla, CA) and were previously described (Tashiro et al., 2006). Retroviruses were generated using an all-transient transfection approach. 293T cells were transfected with a mixture containing three separate plasmids, including capsid (CMV-vsv-g), viral proteins (CMV-gag/pol), and retroviral vectors using Polyethylenimine (PEI). Virus-containing supernatant was harvested twice, 48h and 96h after transfection, and concentrated by two rounds of ultracentrifugation. Viral titers ranged between 0.5 and 5 x 10^7 colony-forming units (cfu) ml-1. $Rb^{lox/+}$, $Rb^{lox/lox}$, $Rb^{lox/lox}$;$E2f1^{-/-}$, $Rb^{lox/lox}$;$E2f3^{lox/lox}$ were anesthetized with isoflurane and stereotaxically injected with 1.5 µl of the same 1:1 mixture of CAG-Cre:GFP and CAG-RFP retroviruses into the left and right DG. Coordinates were (in mm): -0.7 anterior/posterior ± 1.2 medial/lateral from bregma and −1.9 dorsal/ventral from dura.

Western blot analysis

Protein lysates were isolated from dissected hippocampal tissue at E17.5 and from neurospheres derived from adult brains, and, Western blot analyses were performed as previously described (Naser et al., 2016) using antibodies against total RB (BD-Pharmingen, San Diego, CA, Cat#554136, 1:250) and GAPDH (Santa Cruz, sc-25778, 1:1000). The secondary antibodies used are: goat anti-mouse (sc-2005, Santa Cruz 1:2500) and goat anti-rabbit (sc-2004, Santa Cruz, 1:2500).

Results

Embryonic development of the dentate gyrus in the absence of RB

The role of RB and its family members has been examined in the development of pyramidal neurons in the cerebral cortex (Ferguson et al., 2002; Oshikawa et al., 2013) and the migration of GABAergic interneurons (Ferguson et al., 2005; Andrusiak et al., 2010), however its importance in the formation of DGCs during development and adulthood remains elusive. To address the role of RB in the development of the DG, we crossed mice carrying conditional *Rb* floxed alleles with mice expressing the Cre recombinase from the endogenous Foxg1 locus, thus inducing loss of RB in the whole telencephalon including the DG, starting at embryonic day (E)10.5 (Hébert and McConnell, 2000). Since Foxg1-Cre;$Rb^{lox/lox}$ (Foxg1-RB KO) mice die at birth from respiratory failure (Ferguson et al., 2002; Mcclellan et al., 2007), we analyzed the consequences of deletion of RB on the DG at E18.5, when lamination of the hippocampus is nearly complete. First, we confirmed the deletion of RB by Western blot analysis using protein lysates extracted from hippocampi of Foxg1-Cre;$Rb^{lox/+}$ (Foxg1-RB Ctrl) and Foxg1-RB KO littermates at E17.5 (Fig. 1A). Compared to Foxg1-RB Ctrl, histological analysis of Foxg1-RB KO brains revealed an increase in the cellularity of the Cornu Ammonis (CA) regions of the hippocampus, CA1 and CA3 as well as the DG (Fig. 1B). In addition, the dorsal blade of the granule cell layer (gcl) was clearly identifiable in Foxg1-RB KO brains (Fig. 1B), suggesting that production of DGCs occurs in the absence of RB. This was confirmed by the presence in both genotypes of cells co-expressing Prox1, a specific marker of DGCs, and NeuroD1, a marker of young hippocampal neurons (Fig. 1C), but with a significant increase in the number of $Prox1^{+}NeuroD1^{+}$ cells in Foxg1-RB KO brains compared with littermate controls (Fig. 1D). The number of $Prox1^{+}NeuroD1^{+}$ cells was also increased in the absence of RB at E16.5 (Supporting Information Fig. S1). In addition, we observed

a delay in the morphological development of the dorsal blade of the gcl at this age. Altogether, these results indicate the presence of enhanced DGC neurogenesis following loss of RB.

The expansion of the DGC population could be due to increased cell proliferation and/or decreased cell death, two well-characterized functions that are controlled by RB. To test this, we stained for Ki67 and activated caspase 3 (AC3) and assessed cell proliferation and cell death, respectively. Our results revealed a 3-fold increase in the numbers of $Ki67^+$ cells found in the DG at E18.5 in the absence of RB (Fig. 2A), and this was paralleled by a significant but less dramatic increase in $AC3^+$ cells and $NeuroD1^+AC3^+$ cells (Fig. 2B) following loss of RB at the same age. Similar results were observed at E16.5 (Suppl. Figs. S2 and S3). We next asked whether loss of RB affects proliferation and/or apoptosis at E14.5, when DGCs have not been produced yet. Interestingly, we found no change in the percentage of $Sox2^+$ (a marker of NPCs) cells co-expressing either Ki67 (Fig. 2C) or in the number of $AC3^+$ in the dentate neuroepithelium (DNE) in the absence of RB at this age (Fig. 2D). Accordingly, there was no difference in the total number of $Sox2^+BrdU^+$ double-labeled cells found in the VZ/SVZ of the whole hippocampal primordium at the same age in development (30min. BrdU pulse, Suppl. Fig. S4). However, we noticed ectopically proliferating $BrdU^+$ cells in the future CA1-CA3 areas of Foxg1-RB KO embryos compared with controls (Suppl. Fig. S4; white arrows), probably corresponding to immature hippocampal pyramidal neurons. This was consistent with our previous results (Fig. 2C; $Ki67^+Sox2^-$ cells; white arrows). Altogether, these results indicate that loss of RB specifically leads to an increase in the number of DGCs produced at later stages in development (between E16.5 and E18.5) compared with controls, and this is likely due to enhanced cell proliferation that occurred after E14.5. Moreover, the survival of newly generated DGCs is affected by the loss of RB in the embryonic hippocampus.

To determine whether the increase in cell proliferation observed in the absence of RB was cell-

type specific or not, we co-labeled with Ki67 and markers of distinct cell populations including Sox2, Tbr2 (a marker of intermediate progenitors) and NeuroD1 at E18.5. Quantifications revealed no difference in the percentages of $Sox2^+$ or $Tbr2^+$ cells co-expressing Ki67 between genotypes (Fig. 3A-B), however, there was a dramatic increase in the percentage of $NeuroD1^+$ cells co-expressing Ki67 both at E16.5 and E18.5 (Fig. 3C)**.** This increase in the number of proliferating immature hippocampal neurons was confirmed by double labeling with NeuroD1/BrdU at E16.5 (1h BrdU pulse), and, was coupled to an increase in the number of $NeuroD1^+$ cells co-expressing the M-phase marker phospho-histone H3 (PH3) at the same age (Fig. 3C and Suppl. Fig. S5). These data clearly indicates that, in the developing DG, loss of RB leads to cell cycle deregulation e.g. delayed cell cycle exit resulting in the production of more newborn DGCs. We cannot rule out, however, the possibility that this phenotype could be associated with cell non-autonomous defects following loss of RB and/or may result from neuronal cycle re-entry of newborn DGCs rather than a delayed cell cycle exit. To answer this question, we performed *in vitro* neurosphere assays by isolating cells from E14.5 DNE of Foxg1-RB Ctrl and Foxg1-RB KO brains and assessing the number of colony-forming cells in culture. In accordance with our *in vivo* results, these assays indicated no change in the number of colony-forming cells in the absence of RB, thus ruling out the presence of more NPCs in the RB mutant DG compared with controls (Fig. 4A). Next, we performed differentiation assays coupled to incorporation of BrdU in order to determine whether the enhanced proliferation observed *in vivo* could be due, at least partially, to delayed cell cycle exit. Cells isolated from the E14.5 DNE were plated in monolayers, then induced to differentiate in the presence of BrdU. To overcome the low number of neurons that are normally generated from the differentiation of DG neuroepithelial cells (Clarke and van der Kooy, 2011), all monolayers were differentiated for a total of 7 days and BrdU was added at regular intervals

starting at various time-points throughout differentiation. Cultures were then co-stained for Tuj1, a marker of the neuronal specific beta III-tubulin, and BrdU. The number of $BrdU^+$ cells present in the Tuj1 population was used to assess cell cycle exit. As a result, the percentage of $Tuj1^+/BrdU^+$ cells was very low and similar in both genotypes when BrdU was added at late stages of differentiation e.g. day 5 and day 7 of culture (Fig. 4B), suggesting that RB-deficient $Tuj1^+$ cells are able to exit properly the cell cycle. However, when BrdU was added 24h post-differentiation, we observed a 2-fold increase in the percentage of $Tuj1^+/BrdU^+$ cells in the absence of RB compared to controls. Moreover, while very few $Tuj1^+BrdU^+$ cells were detected in control cultures when BrdU was added on day 3 of differentiation, many $Tuj1^+/BrdU^+$ cells were still detectable in RB-null cultures, confirming indeed the presence of a delay in cell cycle exit (Fig. 4C).

Taken together, our results showed that RB does not seem to regulate proliferation of stem/progenitor cells during DG development but is required for the proper cell cycle exit e.g. timing of exit of newly born DGCs.

Loss of RB impairs neurogenesis in the adult DG

Considering that previous studies have shown that RB plays context-dependent and time-dependent functions during embryonic and adult neurogenesis (Ghanem et al., 2012; Naser et al., 2016), we next questioned whether RB has an essential role in adult hippocampal neurogenesis. Given that Foxg1-RB KO are perinatal lethal, we crossed Rb^{lox} mice with Nestin-CreERT2/R26-stop-enhanced yellow fluorescent protein (YFP) mice to generate Nestin-CreERT2; $Rb^{lox/+}$; $Rosa26^{YFP/+}$ (RB iNes-Ctrl) and Nestin-CreERT2; $Rb^{lox/lox}$; $Rosa26^{YFP/+}$ (RB iNes-KO). In these mice, the *Nestin* promoter and second intron drive the expression of the Cre recombinase fused to

a modified estrogen receptor (CreERT2; fusion protein) in NPCs. Upon administration of the estrogen congener tamoxifen (TAM), CreERT2 recombines DNA sequences flanked by loxP sites, thus allowing the expression of YFP and deletion of *Rb* in Nestin-expressing NPCs and their progeny. Ten days after TAM treatment (Fig. 5A), we found that 80-85% of $Sox2^+$ NPCs found in the SGZ positive for YFP (RB iNes-Ctrl: 83.87±4.501; RB iNes-KO: 82.89±3.171, n=3, mean ± SD), validating the efficiency of our model. In addition, we extracted proteins from YFP-expressing neurospheres derived from the adult brain and confirmed by Western blot that the Cre recombination was successful *in vivo* (Fig. 5A). To assess the overall consequences of RB deletion on cell proliferation in the DG, we first counted the total number of $BrdU^+$ cells in the DG after a 2h BrdU pulse and found no significant difference in results between genotypes 10d post-deletion of RB (RB iNes-Ctrl:894 ± 187.6; RB iNes-KO: 990 ± 148.2, n=3, mean ± SD). Next, we determined whether RB is required to maintain the quiescence of adult NPCs in the DG at the same age: thus, we performed triple labeling with Sox2, YFP and Ki67 ten days after TAM treatment but did not observe any difference in the percentage of $YFP^+/Sox2^+$ co-labeled with Ki67 between genotypes either (Fig. 5B). In order to assess whether RB deficiency affects the cell cycle kinetics of newborn DGCs in the adult DG as seen during development, we euthanized animals 5 weeks after TAM treatment (Fig. 5A) and co-stained for YFP, Ki67 and NeuroD1 or Doublecortin (DCX), simultaneously. Then, we determined the percentage of YFP^+ immature DGCs undergoing proliferation in a population of 50 to 60 YFP^+ cells. Our results showed a slight (but not significant) increase in the percentage of $YFP^+/NeuroDl^+$ or YFP+/DCX^+ cells co-expressing Ki67 between RB iNes-Ctrl and RB iNes-KO animals (NeuroD1: RB iNes-Ctrl: 6,968 % ± 2,087 ; RB iNes-KO: 8,213 ± 1,405; DCX: RB iNes-Ctrl: 5,872% ± 1,789; RB iNes-KO: 8,151 ± 1,886, n = 3, mean ± SD). Owing to the low number of proliferating cells in the adult DG, we quantified the total number

of $YFP^+/DCX^+/KI67^+$ cells to confirm our previous results and found a doubling of this population in the absence of RB (Fig. 5C). Altogether, these data suggest that RB is not essential to maintain NPCs quiescence but controls cell proliferation of newborn immature DGCs in the adult DG.

In the adult hippocampus, newborn DGCs become integrated into the DG circuitry within 4-5 weeks after their birth (Kempermann et al., 2004). To assess the ability of RB-deficient NPCs to give rise to mature DGCs, we co-labeled YFP^+ cells with NeuroD1 and the ubiquitous neuronal marker NeuN at 5 weeks post-TAM, and quantified the percentage of recombined cells expressing NeuN but not NeuroD1 (e.g. mature DGCs). Interestingly, we detected a significant reduction in the percentage of YFP^+ neurons co-expressing NeuN only ($NeuroD1^-/NeuN^+$) in RB iNes-KO compared to RB iNes-Ctrl mice (Figs. 5D-E). In addition, the density of $NeuroD1^+/YFP^+$ young DGCs cells was decreased in the absence of RB compared with controls at this age (Fig 5F). Altogether, these findings indicate that loss of RB reduces significantly the capacity of adult hippocampal NPCs to produce mature DGCs, possibly due to a lack of long-term survival of young DGCs.

RB is required for the survival of adult-born DGCs

To investigate whether RB is required for the survival of adult-born DGCs, we performed a long-term birth dating experiment whereby we injected RB iNes-Ctrl and RB iNes-KO mice with BrdU for three consecutive days after TAM treatment and euthanized the animals 4 weeks later, when maturation of adult-born DGCs is mostly completed (Fig. 6A). As a result, we observed a dramatic reduction in the total number of $BrdU^+$ cells found in the DG in the absence of RB (almost a 3 fold decrease) compared with controls, and this was paralleled with an increase (although not significant) in the number of $AC3^+$ cells (Fig. 6B), indicating that RB-deficient newborn DGCs

are less prone to survive than their control counterparts. To confirm these findings and determine the time window during which newborn DGCs die, we stereotaxically injected *Rb*$^{lox/+}$ (RB Ctrl) and *Rb*$^{lox/lox}$ (RB KO) mice with a mixture of two retroviruses, one expressing Cre:Green fluorescent protein (Cre:GFP) and one control retrovirus encoding for the red fluorescent protein (RFP) (Fig. 6C). This approach allowed us to quantify the fraction of double-labeled cells among the RFP-labeled cells at different time points, and in doing so determine the influence of the deletion of RB on the number of newborn cells, regardless of discrepancies in the number of infected cells overall (Jagasia et al., 2009). First, we confirmed that RB regulates proliferation of adult-born DGCs by quantifying the percentage of GFP$^+$ cells co-expressing Ki67. About 13-15% of GFP$^+$ cells were Ki67$^+$ at 7 and 14dpi in the absence of RB while only few (2%) double-labeled cells were detected in control animals (Fig. 6D). Moreover, while the fraction of GFP-RFP double-labeled cells among the RFP-labeled population did not differ between genotypes at 7 and 14 days post-injection (dpi), it was greatly reduced at 28dpi in RB-deficient animals in comparison with controls (Fig. 6E). Altogether, the above data strongly demonstrates that RB is indeed essential for the survival of newborn neurons in the adult DG, probably through inhibition of the cell cycle machinery.

E2f1, but not E2f3, acts downstream of RB to control survival of adult-born DGCs

To determine the molecular mechanisms by which RB controls survival of adult-born DGCs, we crossed *Rb*$^{lox/lox}$ mice with mice lacking either E2f1 or E2f3, two transcription factors acting as regulatory targets of RB signaling. We then performed stereotaxic injection of Cre:GFP and RFP retroviruses in the DG of *Rb*$^{lox/lox}$; *E2f1*$^{-/-}$ (RB-E2f1 DKO) and *Rb*$^{lox/lox}$; *E2f3*$^{lox/lox}$ (RB-E2f3 DKO) mice and quantified the number of surviving cells at 28 dpi (Fig. 7A). We found that E2f1

deficiency partially rescued the survival of RB-deficient cells, but no rescue was observed in RB E2f3 DKO mice (Fig. 7B), suggesting that E2f1 acts downstream of RB to regulate the survival of adult-born DGCs.

Discussion

In the present study, we have uncovered a central role for RB in DGCs production and survival in the embryonic and adult hippocampus. Our data have several important implications regarding the intrinsic mechanisms that govern DGCs production throughout life. First, loss of RB leads to an expansion of the number of DGCs produced during embryonic development as a result of delayed cell cycle exit specifically in this population, whereas it mainly causes ectopic proliferation of newborn DGCs in the adult brain. Second, we found that RB is required for the survival of adult-born DGCs, a role that is partially mediated through its interaction with E2f1. Although we report also increased apoptosis in RB-null DGCs during late development, it is still unknown how loss of RB impacts this population after birth due to perinatal lethality.

Presently, few studies have focused on the role of cell cycle genes during dentate neurogenesis. Using the Foxg1-Cre line and distinct markers of the glutamatergic lineage as well as *in vitro* assays, we have demonstrated that RB is specifically needed to ensure proper cell cycle exit in young DGCs, but is not required at earlier time-points in the lineage e.g. regulation of stem and progenitor cells in the VZ/SVZ of the dentate neuroepithelium (Figs 2, 3 and Suppl. Fig. S4). Importantly, this was also true for progenitors giving rise to the Ammon horn, suggesting that the increase of cellularity observed in this region is primarily due to increased proliferation of newborn pyramidal neurons. Interestingly, this phenotype is reminiscent of the ectopically proliferating newborn neurons observed in the developing cortex of Foxg1-RB KO mice (Ferguson et al., 2002), suggesting a conserved role for RB in the control of cell cycle exit in young neurons produced in the proliferative zones of the dorsal telencephalon. The ectopic proliferation of newborn DGCs in the RB-deficient brains was partially counterbalanced by enhanced apoptosis at late developmental stages. Given the important role of RB in the control of cell proliferation and apoptosis, our results

cannot distinguish at this point whether DGCs apoptosis during development is a direct consequence of the deletion of RB and/or a secondary effect associated with ectopic proliferation. On the other hand, since RB is virtually absent from all cells in the telencephalon of Foxg1-RB KO, we cannot rule out the possibility that the latter defect could result from is cell non-autonomous phenomenon. Future studies may aim to address this question by using different Cre-drivers or, alternatively, by creating a targeted knock-out of RB in the dentate neuroepithelium using *in-utero* electroporation.

We found that acute deletion of RB in adult hippocampal NPCs does not disrupt their quiescence. This result is consistent with data coming from the hematopoietic field, where deletion of RB does not affect the cell cycle of adult hematopoietic stem cells (Walkley and Orkin, 2006). These data suggest that RB does not control self-renewal in the hippocampal aNSCs. Alternatively, the role of RB in early NPCs may be masked by compensatory roles of other RB family proteins such as p107 and/or p130. The generation of a triple KO mouse model for all three pocket proteins in future studies will contribute to a better understanding of the distinct roles played by these pocket proteins in the maintenance and development of adult NPCs. Similarly to the developing DG, we observed ectopic proliferation of young DGCs following loss of RB in the adult hippocampus, implying that some aspects of the intrinsic cell cycle machinery may be conserved between embryonically- and adult-born DGCs. On the other hand, we have clear evidence that RB-deficient DGCs born during late embryonic development undergo ectopic divisions leading to an expansion of the hippocampus. While this scenario could be plausible in the adult brain, our data cannot rule out that other possibilities such as the absence of RB in adult-born DGCs could lead to sporadic cell cycle re-entry and subsequent cell death as previously observed in cortical neurons (Andrusiak et al., 2012). In fact, cell-type specific effects associated with loss of RB have been well

documented in the retina (Chen et al., 2004; MacPherson et al., 2004) and linked to the differential expression of p107 and p130 in distinct cell types and lineages.

Loss of RB induces cell death in a tissue-specific and cell-type-specific manner as seen with other defects such as the control of cell proliferation and cell cycle exit. For instance, loss of RB alone or in combination with p107 in the retina results in considerable apoptosis of rod photoreceptors but is compatible with horizontal interneurons and amacrine neurons differentiation and survival (Chen et al., 2004; MacPherson et al., 2004; Zhang et al., 2004; Ajioka et al., 2007; Martins et al., 2011). In agreement with previous studies demonstrating an essential role for RB in the survival of adult cortical neurons (Andrusiak et al., 2012), we found that adult-born DGCs do not survive in the absence of RB (Fig. 6). Moreover, using the same genetic approach, we have recently shown that RB is required for the long-term survival of adult-born OB interneurons but does not control quiescence of NSCs in the adult SVZ (Naser et al., 2016), thus highlighting a conserved role for RB both the SGZ and SVZ/OB. Given all the above and since phosphorylation of RB and re-entry in the cell cycle are frequently associated with the course of development of several neurodegenerative disorders, understanding the molecular basis of RB-dependent survival in different types of CNS neurons is important.

In the embryonic CNS, loss of either E2f1 or E2f3 can almost entirely rescue ectopic proliferation and apoptosis observed in germline RB KO mice (Saavedra et al., 2002). However, the role of these E2f activators in RB KO cells is still controversial since apoptosis observed in germline RB KO animals is partially due to a cell non-autonomous effect. Using conditional rather than germline RB KO models, we have previously demonstrated that RB regulates the survival of a subset of Cajal Retzius cells within the marginal zone of the developing cortex through both E2f1 and E2f3 (Mcclellan et al., 2007). Using a similar strategy, we showed here that E2f1 deficiency,

but not E2f3, partially rescues the survival of adult-born DGCs following loss of RB, indicating that E2f1 and E2f3 are not interchangeable downstream of the RB signaling pathway in this cell type. Moreover, the E2f1-dependent rescue was only partial, suggesting that other mechanisms, either E2f-related or not, are involved in the survival of RB-deficient DGCs. Similarly, it was shown that, upon loss of both RB and p107 in the retina, E2f1, but not E2f2 or E2f3, causes death of rod, bipolar and ganglion neurons, whereas E2f2 is required and sufficient for cone death (Chen et al., 2007; 2013).

Our study revealed a central role for the cell cycle regulator RB in the control of the DGCs production and survival during development and adulthood. We also highlight that the core cell cycle machinery actively contributes to the functional heterogeneity found in embryonic versus adult precursors.

References

Ajioka I, Martins RAP, Bayazitov IT, Donovan S, Johnson DA, Frase S, Cicero SA, Boyd K, Zakharenko SS, Dyer MA. 2007. Differentiated horizontal interneurons clonally expand to form metastatic retinoblastoma in mice. Cell 131:378–390.

Andreu Z, Khan MA, GonzÁlez-Gómez P, Negueruela S, Hortigüela R, San Emeterio J, Ferrón SR, Martínez G, Vidal A, Fariñas I, Lie DC, Mira H. 2015. The Cyclin-Dependent Kinase Inhibitor p27(kip1) Regulates Radial Stem Cell Quiescence and Neurogenesis in the Adult Hippocampus. Stem cells (Dayton, Ohio) 33:219–229.

Andrusiak MG, Mcclellan KA, Dugal-Tessier D, Julian LM, Rodrigues SP, Park DS, Kennedy TE, Slack RS. 2010. Rb/E2F Regulates Expression of Neogenin during Neuronal Migration. Mol Cell Biol 31:238–247.

Andrusiak MG, Vandenbosch R, Park DS, Slack RS. 2012. The retinoblastoma protein is essential for survival of postmitotic neurons. Journal of Neuroscience 32:14809–14814.

Babu H, Cheung G, Kettenmann H, Palmer TD, Kempermann G. 2007. Enriched monolayer precursor cell cultures from micro-dissected adult mouse dentate gyrus yield functional granule cell-like neurons. PLoS ONE 2:e388.

Beukelaers P, Vandenbosch R, Caron N, Nguyen L, Belachew S, Moonen G, Kiyokawa H, Barbacid M, Santamaría D, Malgrange B. 2011. Cdk6-dependent regulation of G(1) length controls adult neurogenesis. STEM CELLS 29:713–724.

Chen D, Chen Y, Forrest D, Bremner R. 2013. E2f2 induces cone photoreceptor apoptosis independent of E2f1 and E2f3. Cell Death Differ.

Chen D, Livne-bar I, Vanderluit JL, Slack RS, Agochiya M, Bremner R. 2004. Cell-specific effects of RB or RB/p107 loss on retinal development implicate an intrinsically death-resistant cell-of-origin in retinoblastoma. Cancer Cell 5:539–551.

Chen D, Opavsky R, Pacal M, Tanimoto N, Wenzel P, Seeliger MW, Leone G, Bremner R. 2007. Rb-mediated neuronal differentiation through cell-cycle-independent regulation of E2f3a. PLoS Biol 5:e179.

Cicero SA, Johnson D, Reyntjens S, Frase S, Connell S, Chow LML, Baker SJ, Sorrentino BP, Dyer MA. 2009. Cells previously identified as retinal stem cells are pigmented ciliary epithelial cells. Proceedings of the National Academy of Sciences 106:6685–6690.

Clarke L, van der Kooy D. 2011. The adult mouse dentate gyrus contains populations of committed progenitor cells that are distinct from subependymal zone neural stem cells. STEM CELLS 29:1448–1458.

Ernst A, Frisén J. 2015. Adult neurogenesis in humans- common and unique traits in mammals. PLoS Biol 13:e1002045.

Ferguson KL, McClellan KA, Vanderluit JL, McIntosh WC, Schuurmans C, Polleux F, Slack RS. 2005. A cell-autonomous requirement for the cell cycle regulatory protein, Rb, in neuronal migration. EMBO J 24:4381–4391.

Ferguson KL, Vanderluit JL, Hébert JM, McIntosh WC, Tibbo E, MacLaurin JG, Park DS, Wallace VA, Vooijs M, McConnell SK, Slack RS. 2002. Telencephalon-specific Rb knockouts reveal enhanced neurogenesis, survival and abnormal cortical development. EMBO J 21:3337–3346.

Field SJ, Tsai FY, Kuo F, Zubiaga AM, Kaelin WG, Livingston DM, Orkin SH, Greenberg ME. 1996. E2F-1 functions in mice to promote apoptosis and suppress proliferation. Cell 85:549–561.

Fortin A, Cregan SP, MacLaurin JG, Kushwaha N, Hickman ES, Thompson CS, Hakim A, Albert PR, Cecconi F, Helin K, Park DS, Slack RS. 2001. APAF1 is a key transcriptional target for p53 in the regulation of neuronal cell death. The Journal of Cell Biology 155:207–216.

Ghanem N, Andrusiak MG, Svoboda D, Lafi Al SM, Julian LM, McClellan KA, De Repentigny Y, Kothary R, Ekker M, Blais A, Park DS, Slack RS. 2012. The Rb/E2F pathway modulates neurogenesis through direct regulation of the Dlx1/Dlx2 bigene cluster. Journal of Neuroscience 32:8219–8230.

Hébert JM, McConnell SK. 2000. Targeting of cre to the Foxg1 (BF-1) locus mediates loxP recombination in the telencephalon and other developing head structures. Dev Biol 222:296–306.

Iaquinta PJ, Lees JA. 2007. Life and death decisions by the E2F transcription factors. Curr Opin Cell Biol 19:649–657.

Jagasia R, Steib K, Englberger E, Herold S, Faus-Kessler T, Saxe M, Gage FH, Song H, DC L. 2009. GABA-cAMP Response Element-Binding Protein Signaling Regulates Maturation and Survival of Newly Generated Neurons in the Adult Hippocampus. Journal of Neuroscience 29:7966–7977.

Kempermann G, Jessberger S, Steiner B, Kronenberg G. 2004. Milestones of neuronal development in the adult hippocampus. Trends Neurosci 27:447–452.

Kesner RP. 2013. An analysis of the dentate gyrus function. Behav Brain Res 254:1–7.

Kowalczyk A, Filipkowski RK, Rylski M, Wilczynski GM, Konopacki FA, Jaworski J, Ciemerych MA, Sicinski P, Kaczmarek L. 2004. The critical role of cyclin D2 in adult neurogenesis. The Journal of Cell Biology 167:209–213.

Li G, Pleasure SJ. 2007. Genetic regulation of dentate gyrus morphogenesis. Prog Brain Res 163:143–152.

MacPherson D, Sage J, Crowley D, Trumpp A, Bronson RT, Jacks T. 2003. Conditional mutation of Rb causes cell cycle defects without apoptosis in the central nervous system. Mol Cell Biol 23:1044–1053.

MacPherson D, Sage J, Kim T, Ho D, McLaughlin ME, Jacks T. 2004. Cell type-specific effects of Rb deletion in the murine retina. Genes & Development 18:1681–1694.

Marino S, Vooijs M, van Der Gulden H, Jonkers J, Berns A. 2000. Induction of medulloblastomas in p53-null mutant mice by somatic inactivation of Rb in the external granular layer cells of the cerebellum. Genes & Development 14:994–1004.

Martins RAP, Davis D, Kerekes R, Zhang J, Bayazitov IT, Hiler D, Karakaya M, Frase S, Gleason S, Zakharenko SS, Johnson DA, Dyer MA. 2011. Retinoblastoma (Rb) regulates laminar dendritic arbor reorganization in retinal horizontal neurons. Proc Natl Acad Sci USA 108:21111–21116.

Mcclellan KA, Ruzhynsky VA, Douda DN, Vanderluit JL, Ferguson KL, Chen D, Bremner R, Park DS, Leone G, Slack RS. 2007. Unique Requirement for Rb/E2F3 in Neuronal Migration: Evidence for Cell Cycle-Independent Functions. Mol Cell Biol 27:4825–4843.

Naser R, Vandenbosch R, Omais S, Hayek D, Jaafar C, Lafi Al S, Saliba A, Baghdadi M, Skaf L, Ghanem N. 2016. Role of the Retinoblastoma protein, Rb, during adult neurogenesis in the olfactory bulb. Sci Rep 6:20230.

Oshikawa M, Okada K, Nakajima K, Ajioka I. 2013. Cortical excitatory neurons become protected from cell division during neurogenesis in an Rb family-dependent manner. Development 140:2310–2320.

Qiu J, Takagi Y, Harada J, Topalkara K, Wang Y, Sims JR, Zheng G, Huang P, Ling Y, Scadden DT, Moskowitz MA, Cheng T. 2009. p27Kip1Constrains Proliferation of Neural Progenitor Cells in Adult Brain Under Homeostatic and Ischemic Conditions. STEM CELLS 27:920–927.

Rolando C, Taylor V. 2014. Neural Stem Cell of the Hippocampus: Development, Physiology Regulation, and Dysfunction in Disease. Curr Top Dev Biol 107:183–206.

Saavedra HI, Wu L, de Bruin A, Timmers C, Rosol TJ, Weinstein M, Robinson ML, Leone G. 2002. Specificity of E2F1, E2F2, and E2F3 in mediating phenotypes induced by loss of Rb. Cell Growth Differ 13:215–225.

Schneider CA, Rasband WS, Eliceiri KW. 2012. NIH Image to ImageJ: 25 years of image analysis. Nat Meth 9:671–675.

Sirkin DW. 1983. Critical defatting of frozen brain sections for optimal differentiation with the cresyl violet stain. Stain Technol 58:121–122.

Srinivas S, Watanabe T, Lin CS, William CM, Tanabe Y, Jessell TM, Costantini F. 2001. Cre reporter strains produced by targeted insertion of EYFP and ECFP into the ROSA26 locus. BMC Dev Biol 1:4.

Tashiro A, Sandler VM, Toni N, Zhao C, Gage FH. 2006. NMDA-receptor-mediated, cell-specific integration of new neurons in adult dentate gyrus. Nature 442:929–933.

Urbán N, Guillemot F. 2014. Neurogenesis in the embryonic and adult brain: same regulators, different roles. Front Cell Neurosci 8:396.

Vanderluit JL, Ferguson KL, Nikoletopoulou V, Parker M, Ruzhynsky V, Alexson T, McNamara SM, Park DS, Rudnicki M, Slack RS. 2004. p107 regulates neural precursor cells in the mammalian brain. The Journal of Cell Biology 166:853–863.

Walkley CR, Orkin SH. 2006. Rb is dispensable for self-renewal and multilineage differentiation of adult hematopoietic stem cells. Proc Natl Acad Sci USA 103:9057–9062.

Wu L, Timmers C, Maiti B, Saavedra HI, Sang L, Chong GT, Nuckolls F, Giangrande P, Wright FA, Field SJ, Greenberg ME, Orkin S, Nevins JR, Robinson ML, Leone G. 2001. The E2F1-3 transcription factors are essential for cellular proliferation. Nature 414:457–462.

Zhang J, Gray J, Wu L, Leone G, Rowan S, Cepko CL, Zhu X, Craft CM, Dyer MA. 2004. Rb regulates proliferation and rod photoreceptor development in the mouse retina. Nat Genet 36:351–360.

Figure Legends and Figures

Figure 1. Deletion of RB leads to an expansion of the number of DGCs. (A) Western blot analysis confirming the absence of RB in the hippocampus in Foxg1-Cre RB KO animals compared with Foxg1-Cre RB controls at E17.5. (B) Cresyl violet staining of Foxg1-Cre RB Ctrl and Foxg1-Cre RB KO hippocampi at E18.5, illustrating the increased hippocampal cellularity in the absence of RB. (C) Single-plane confocal images of NeuroD1 (red), Prox1 (green) and merged NeuroD1/Prox1 (yellow) staining in the DG at E18.5, illustrating the increased number of DGCs in the absence of RB. (D) Histogram showing the number of $NeuroD1^{+}Prox1^{+}$ cells per section in Foxg1-Cre RB Ctrl and Foxg1-Cre RB KO at E18.5. Scale bar = 200 μm. Data in (C) are presented as mean ± SEM and were analyzed by a Student's t test. N = 4 animals for FoxG1-Cre RB Ctrl and n = 3 animals for FoxG1-Cre RB KO. *, p <0 .05. Abbreviations: gcl, granule cell layer; DG, Dentate Gyrus; CA, cornus ammonis.

Figure 2. Loss of RB enhances cell proliferation and apoptosis in the DG during late development but not at earlier time-points. (A, B) Single-plane confocal images of DAPI/Ki67 (A) and NeuroD1/AC3 (B) double staining in the DG of Foxg1-Cre RB Ctrl and Foxg1-Cre RB KO at E18.5, with histograms showing the number of $Ki67^{+}$ per section (A) and the number of $AC3^{+}$ or $AC3^{+}NeuroD1^{+}$ cells per section (B). (C, D) Single-plane confocal images of Ki67/Sox2 (C) and Sox2/AC3 (D) double staining in the DNE of Foxg1-Cre RB Ctrl and Foxg1-Cre RB KO at E14.5, with histograms showing the percentage of $Sox2^{+}$ cells co-expressing Ki67 (C) and the number of $AC3^{+}$ per section (D), respectively. White arrows in (B) point to $AC3^{+}$ cells and the yellow arrow in (B) points to the double-labeled $AC3^{+}NeuroD1^{+}$ cell showed in insets. White arrows in (C) point to ectopically proliferating $Ki67^{+}$ cells found in the future CA1-CA3 area.

Yellow arrows in (D) point to $AC3^+$ cells. Scale bar = 50 μm. Histograms are presented as mean ± SEM and were analyzed by a Student's t test. For Figure 2A-2B, n = 4 animals for FoxG1-Cre RB Ctrl and n = 3 animals for FoxG1-Cre RB KO. For Figure 2C-2D, n = 3 animals per genotype. **, $p < 0.005$; ***, $p < 0.001$. Abbreviations: DNE, dentate neuroepithelium; LV, lateral ventricle.

Figure 3. Deletion of RB specifically increases proliferation of NeuroD1$^+$ cells in the embryonic DG. (A, B) Single-plane confocal images of Sox2/Ki67 (A) and Tbr2/Ki67 (B) double staining in the DG of Foxg1-Cre RB Ctrl and Foxg1-Cre RB KO at E18.5, with histograms showing the percentages of $Sox2^+$ cells co-expressing Ki67 (A) and $Tbr2^+$ cells co-expressing Ki67 (B), respectively. (C) Single-plane confocal images of NeuroD1/Ki67 double staining in the DG of Foxg1-Cre RB Ctrl and Foxg1-Cre RB KO at E18.5, with histograms showing the percentage of NeuroD1$^+$ cells co-expressing Ki67 at E18.5 and E16.5, and, the numbers of NeuroD1$^+$BrdU$^+$ and NeuroD1$^+$PH3$^+$ double positive cells per section at E16.5. White arrows point to double-labeled cells. Scale bar = 50 μm. Histograms are presented as mean ± SEM and were analyzed by a Student's t test. For Figure 2A-2B, n = 3 animals per genotype. For Figure 2C, n = 3-4 animals per genotype. *, $p < 0.05$; **, $p < 0.005$; ***, $p < 0.001$.

Figure 4. *In vitro* analysis of the properties of RB deficient DG NPCs. (A) Histograms representing the number of neurospheres obtained from DG NPCs isolated from Foxg1-Cre RB Ctrl and Foxg1-Cre RB KO embryos at E14.5 (B) Neuronal differentiation assays performed using DG NPCs isolated from Foxg1-Cre RB Ctrl and Foxg1-Cre RB KO embryos at E14.5. NPCs cells were plated as monolayers, then differentiated for 7 days and BrdU added to different plates at 0, 1, 3, 5 and 7 days of differentiation. Tuj1 staining was used to identify immature neurons present

in culture. Percentages of $BrdU^+/Tuj1^+$ cells at day 1,3,5, and 7 are expressed relative to the percentage of $BrdU^+/Tuj1^+$ at day 0 in the corresponding genotype. (C) Representative pictures of RB Ctrl and RB KO $Tuj1^+$ neurons at day 3 after differentiation, illustrating the presence of BrdU in $Tuj1^+$ neurons. Scale bar = 100 μm. Data are presented as mean ± SEM and were analyzed by Student's t test for (A) and one-way ANOVA for (B). N = 4 animals per genotype in (A), n = 3 and n = 4 animals for Foxg1-Cre RB Ctrl and RB KO, respectively, in (B). **, $p < 0.005$.

Figure 5. Loss of RB affects cell proliferation and impairs neurogenesis in the adult hippocampus. (A) Schematic representation of the experimental design used in tamoxifen treatment, and, Western blot analysis of protein extracts from iNes-Ctrl and RB iNes-KO YFP^+ neurospheres showing loss of RB protein. (B, C) Representative single-plane confocal images of YFP/Sox2/Ki67 (B) and YFP/DCX/Ki67 (C) triple staining in the adult hippocampus of NestinCreERT2/YFP mice at 10 days and 35 days after TAM treatment, respectively. Histograms in (B, C) are showing the percentage of $YFP^+/Sox2^+$ cells co-expressing Ki67 (B) and the total number of $YFP^+/DCX^+/Ki67^+$ per DG (C) in iNes-Ctrl and RB iNes-KO mice. (D) Single-plane confocal images of YFP/NeuroD1/NeuN triple staining in the adult hippocampus of iNes-Ctrl and RB iNes-KO mice at 35 days after TAM treatment. (E-F) Histograms showing the percentages of YFP^+ cells expressing NeuN but not NeuroD1 (E) and the density of $NeuroD1^+/YFP^+$ cells per μm^3 (F) 35 days after TAM treatment. White arrows and white asterisks point to YFP^+ cells expressing NeuN only. Scale bars = 50 μm. Histograms are presented as mean ± SEM and were analyzed by a Student's t test for. N = 3 animals per genotype. *, $p < 0.05$; **, $p < 0.005$.

Figure 6. RB is essential for the survival of newborn DGCs in the adult hippocampus. (A) Schematic representation of the experimental design used in tamoxifen and BrdU treatments. (B) Representative images of BrdU staining in the DG of iNes-Ctrl and RB iNes-KO mice, with histograms showing the number of $BrdU^+$ and $AC3^+$ cells per DG in both genotypes. Nuclei were counterstained with DAPI (Red). (C) Schematic representation of the experimental design used for retroviral injections. (D) Representative single-plane confocal images of GFP/Ki67 double staining in the adult DG 7 days after viral injection, with histograms showing the percentages of GFP^+ cells co-expressing Ki67 at 7 and 14dpi. (E) Representative single-plane confocal image of GFP/RFP double staining in the adult DG 28 days after viral injection, with histograms showing the percentages of RFP^+ cells co-expressing GFP at the different time points in both genotypes. The yellow arrow points to a cell expressing RFP only whereas the white arrows point to cells co-expressing RFP and GFP. Scale bars = 50 μm. Histograms are presented as mean ± SEM and were analyzed by a Student's t test for (B) and (D), and a one-way ANOVA for (E). N = 3 animals per genotype. *, $p < 0.05$; ***, $p < 0.001$. Abbreviations: gcl, granule cell layer.

Figure 7. E2F1 KO partially rescues the survival of RB-deficient newborn DGCs in the adult hippocampus. (A) Schematic representation of the experimental design used for retroviral injections. $Rb^{lox/+}$ (RB Ctrl), $Rb^{lox/lox}$ (RB KO), $Rb^{lox/lox}$; $E2f1^{-/-}$ (RB-E2f1 DKO) and $Rb^{lox/lox}$; $E2f3^{lox/lox}$ (RB-E2f3 DKO) were strereotaxically injected with a mixture of CAG-Cre:GFP and CAG-RFP and euthanized 28 days later. (B) Histograms showing the percentages of RFP^+ cells co-expressing GFP at 28 days post injection detected in animals carrying the four distinct genotypes. Histograms are presented as mean ± SEM and were analyzed by a one-way ANOVA. N = 3 animals per genotype. *, $p < 0.05$; ***, $p < 0.001$

Figure 1

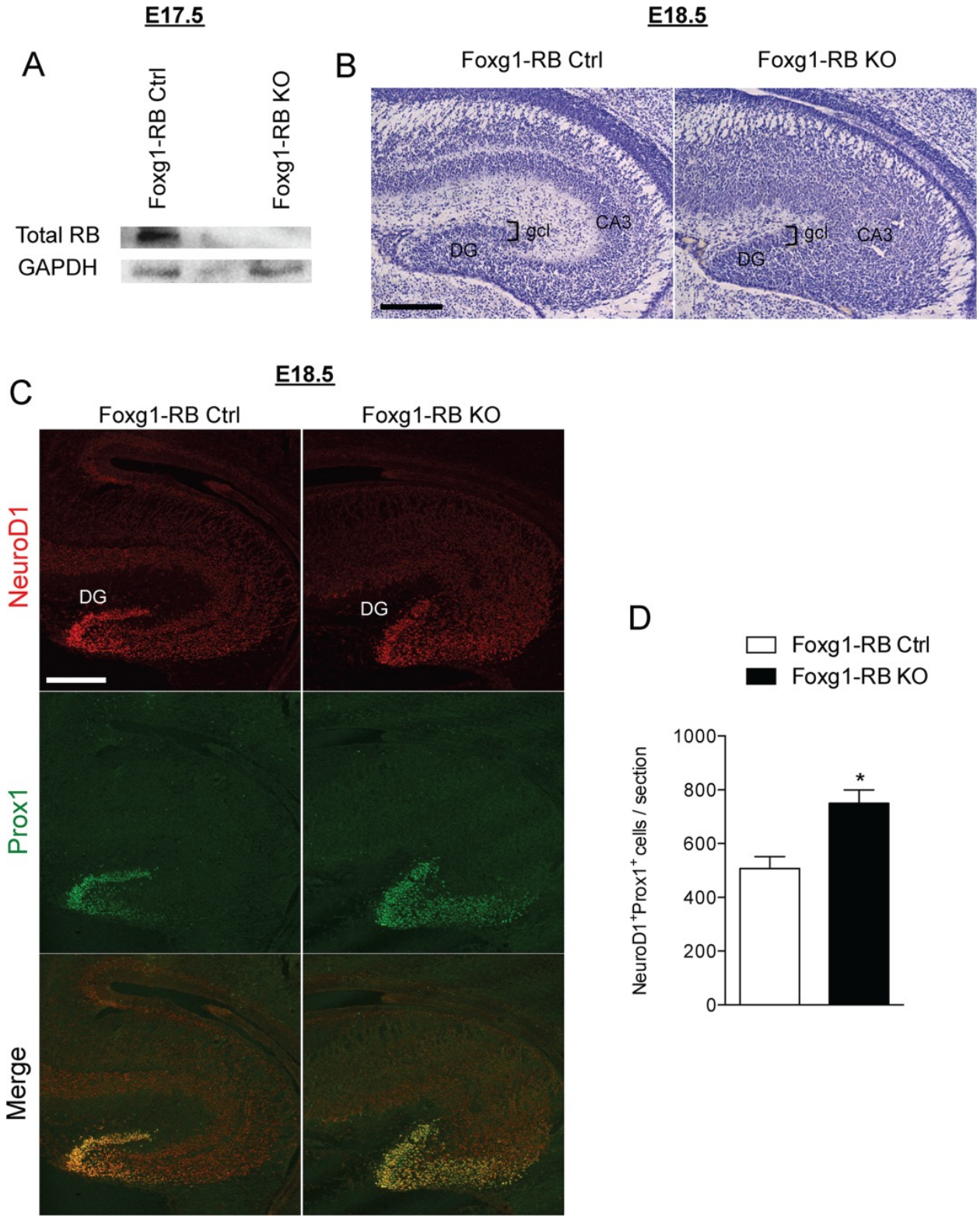
E17.5
A
Foxg1-RB Ctrl
Foxg1-RB KO
Total RB
GAPDH
E18.5
B
Foxg1-RB Ctrl
Foxg1-RB KO
gcl
CA3
DG
C
E18.5
Foxg1-RB Ctrl
Foxg1-RB KO
NeuroD1
Prox1
Merge
DG
D
Foxg1-RB Ctrl
Foxg1-RB KO
NeuroD1+Prox1+ cells / section
1000
800
600
400
200
0
*

Figure 2

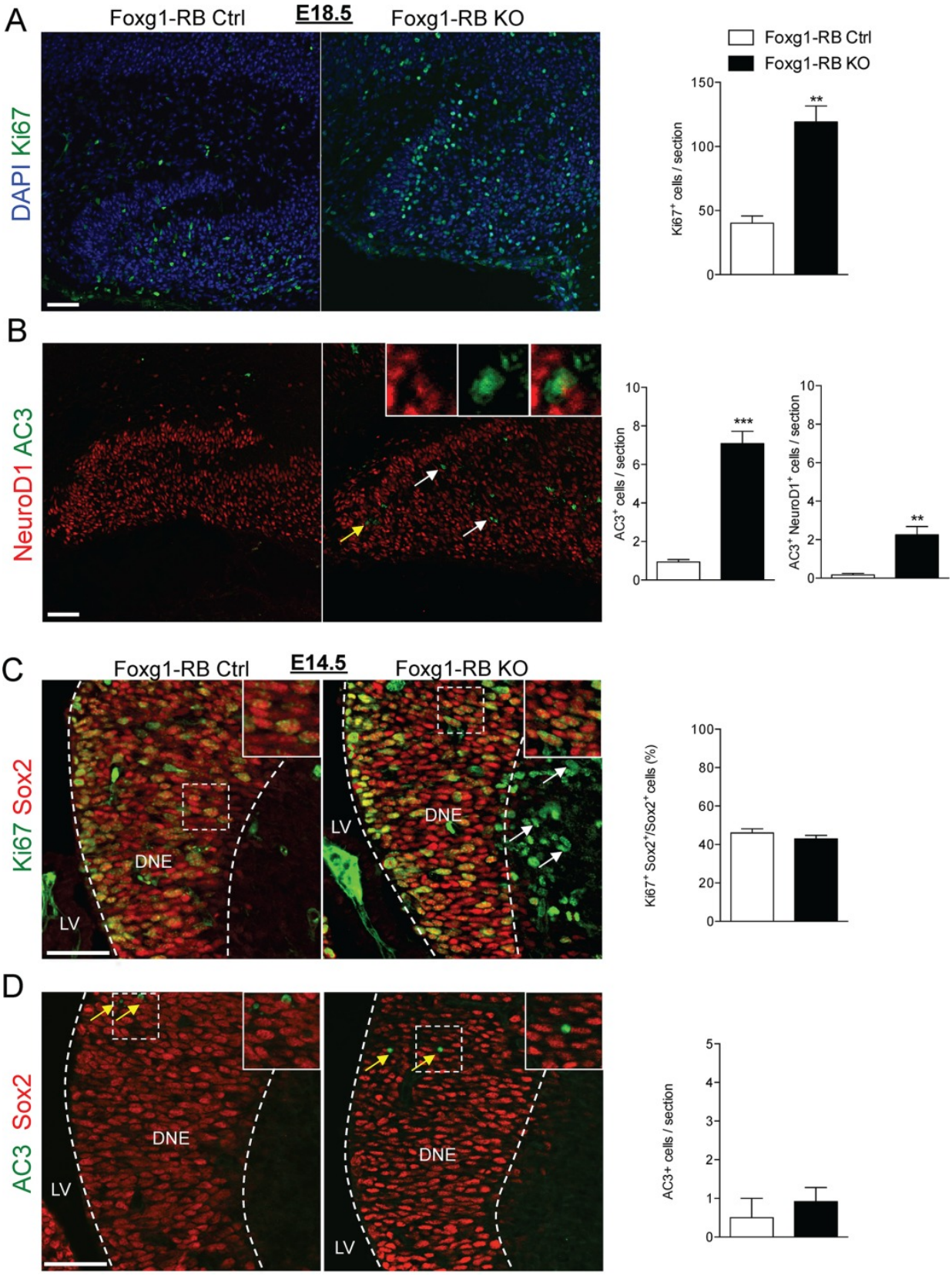
A
Foxg1-RB Ctrl
E18.5
Foxg1-RB KO
DAPI Ki67
Foxg1-RB Ctrl
Foxg1-RB KO
Ki67+ cells / section
150
100
50
0
**
B
NeuroD1 AC3
AC3+ cells / section
10
8
6
4
2
0
***
AC3+ NeuroD1+ cells / section
10
8
6
4
2
0
**
C
Foxg1-RB Ctrl
E14.5
Foxg1-RB KO
Ki67 Sox2
DNE
LV
DNE
LV
Ki67+ Sox2+/Sox2+ cells (%)
100
80
60
40
20
0
D
AC3 Sox2
DNE
LV
DNE
LV
AC3+ cells / section
5
4
3
2
1
0

Figure 3

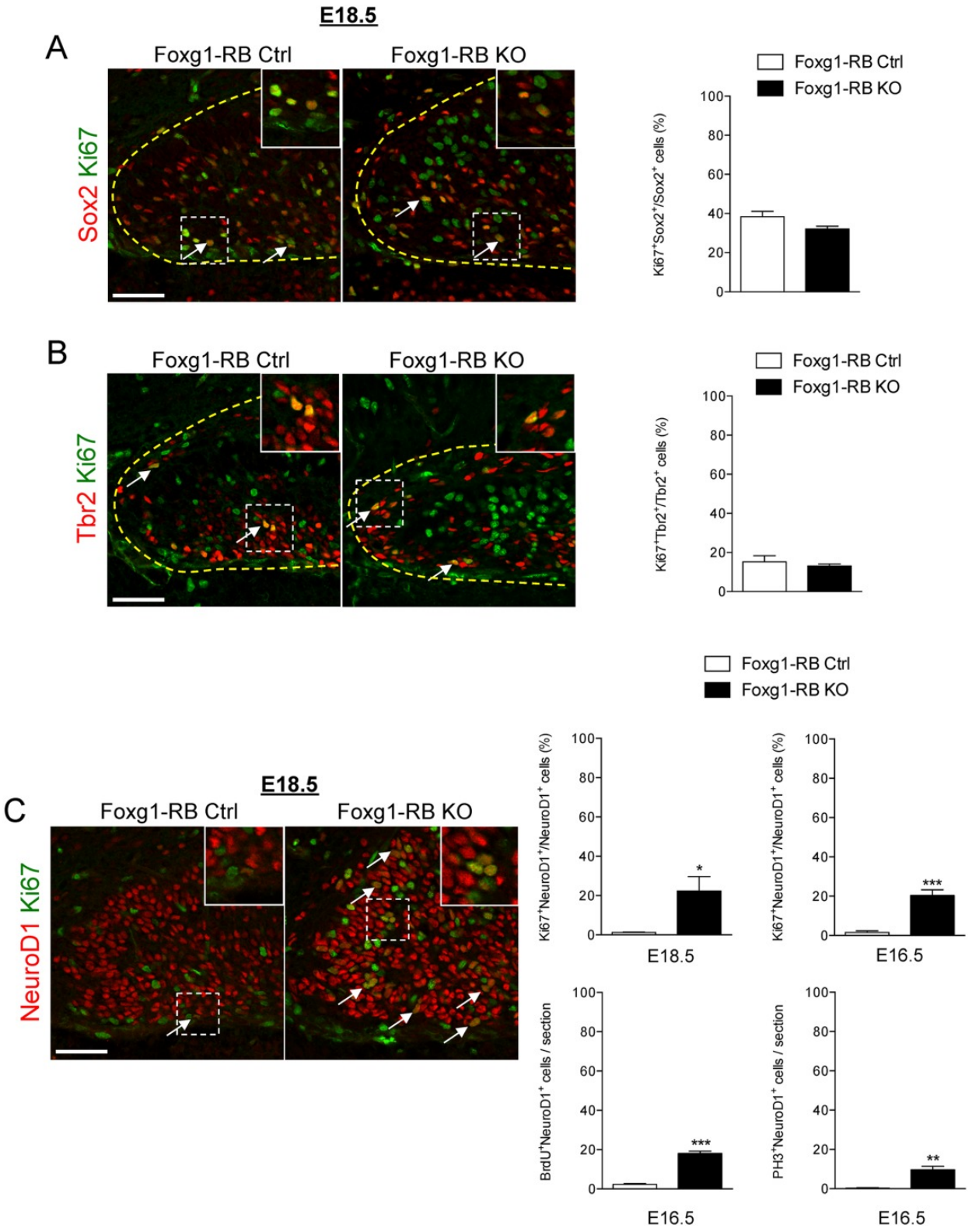
E18.5
A
Foxg1-RB Ctrl
Foxg1-RB KO
Sox2 Ki67
Foxg1-RB Ctrl
Foxg1-RB KO
Ki67+Sox2+/Sox2+ cells (%)
B
Foxg1-RB Ctrl
Foxg1-RB KO
Tbr2 Ki67
Foxg1-RB Ctrl
Foxg1-RB KO
Ki67+Tbr2+/Tbr2+ cells (%)
Foxg1-RB Ctrl
Foxg1-RB KO
C
E18.5
Foxg1-RB Ctrl
Foxg1-RB KO
NeuroD1 Ki67
Ki67+NeuroD1+/NeuroD1+ cells (%)
E18.5
Ki67+NeuroD1+/NeuroD1+ cells (%)
E16.5
BrdU+NeuroD1+ cells / section
E16.5
PH3+NeuroD1+ cells / section
E16.5

Figure 4

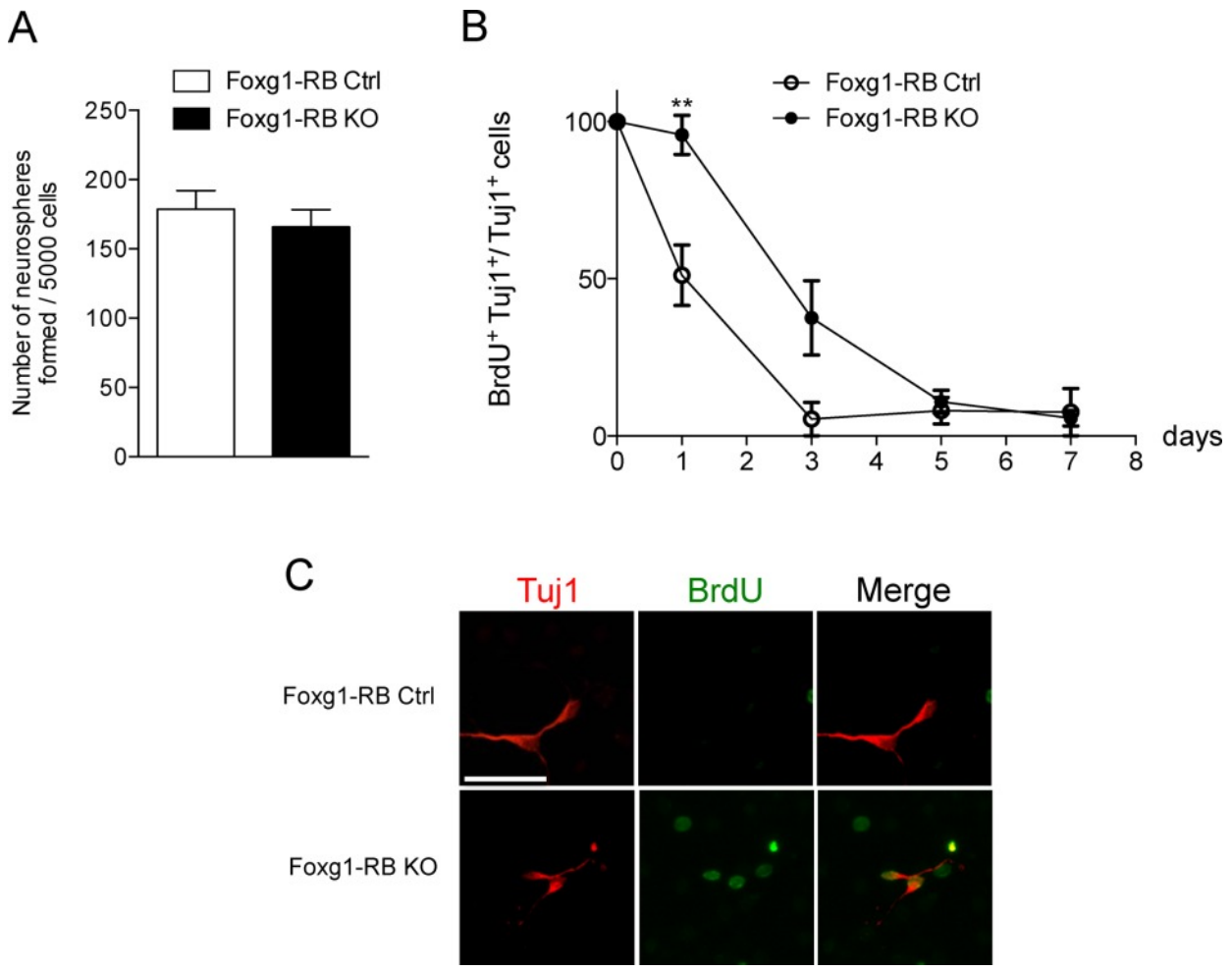
A
Foxg1-RB Ctrl
Foxg1-RB KO
Number of neurospheres formed / 5000 cells
250
200
150
100
50
0
B
Foxg1-RB Ctrl
Foxg1-RB KO
**
BrdU+ Tuj1+/ Tuj1+ cells
100
50
0
0 1 2 3 4 5 6 7 8
days
C
Tuj1
BrdU
Merge
Foxg1-RB Ctrl
Foxg1-RB KO

Figure 5

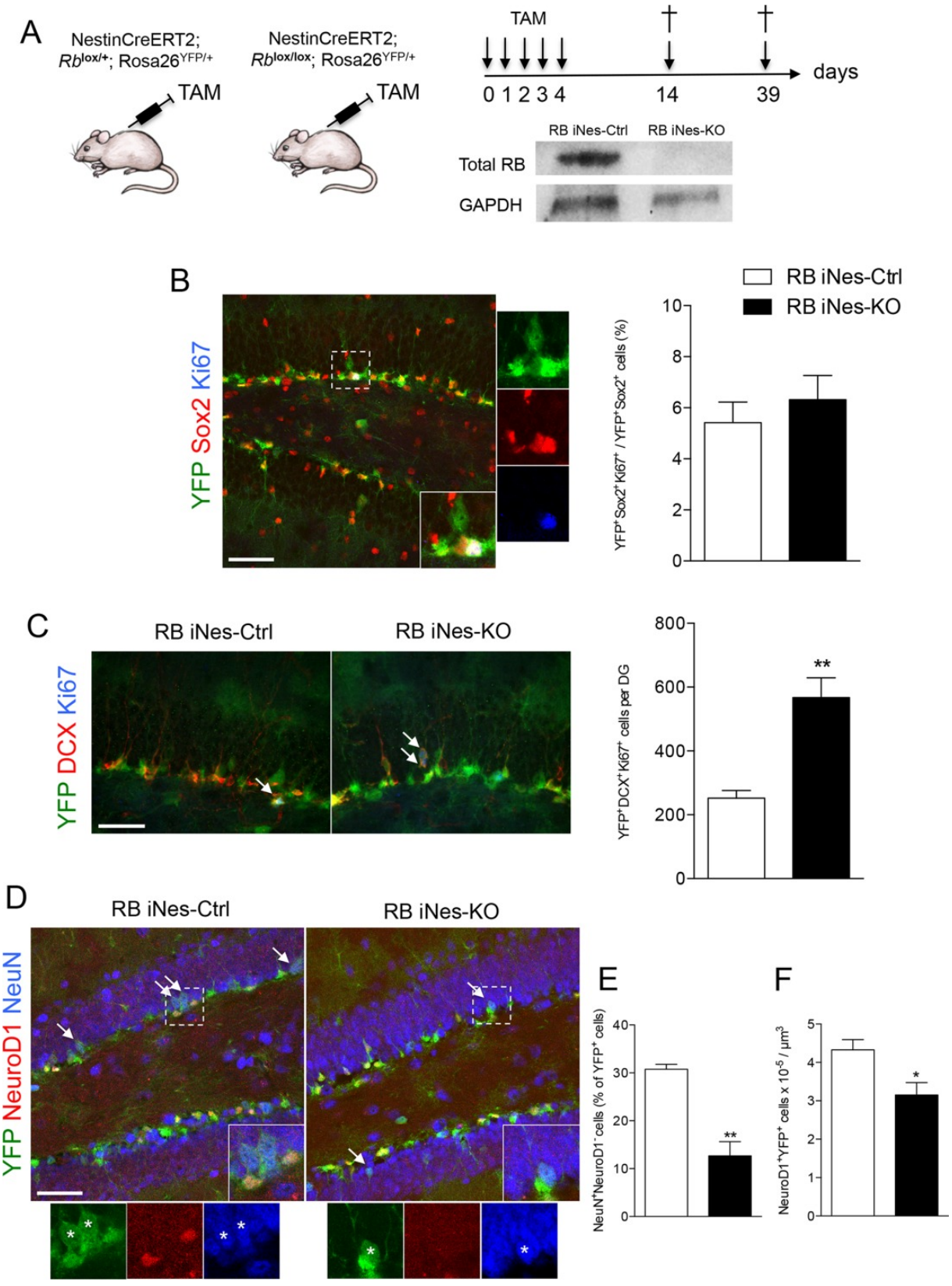
A
NestinCreERT2; Rb lox/+; Rosa26 YFP/+
NestinCreERT2; Rb lox/lox; Rosa26 YFP/+
TAM
TAM
TAM
0 1 2 3 4
14
39
days
RB iNes-Ctrl
RB iNes-KO
Total RB
GAPDH
B
YFP Sox2 Ki67
RB iNes-Ctrl
RB iNes-KO
YFP+Sox2+Ki67+ / YFP+Sox2+ cells (%)
C
RB iNes-Ctrl
RB iNes-KO
YFP DCX Ki67
YFP+DCX+Ki67+ cells per DG
D
RB iNes-Ctrl
RB iNes-KO
YFP NeuroD1 NeuN
E
NeuN+NeuroD1- cells (% of YFP+ cells)
F
NeuroD1+YFP+ cells x 10-5 / µm3

Figure 6

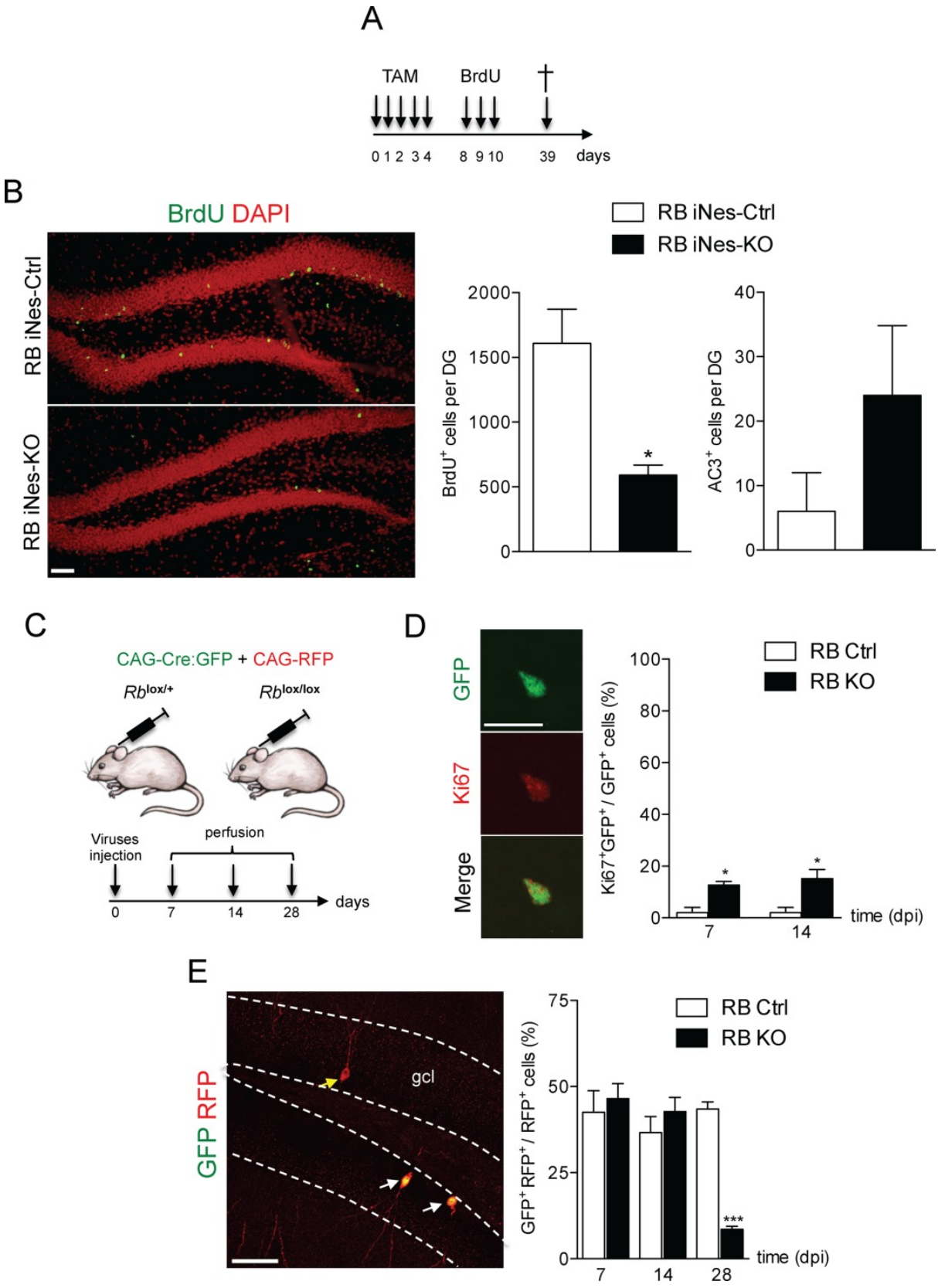
A
TAM
BrdU
†
0 1 2 3 4
8 9 10
39
days
B
BrdU DAPI
RB iNes-Ctrl
RB iNes-KO
RB iNes-Ctrl
RB iNes-KO
BrdU+ cells per DG
2000
1500
1000
500
0
*
AC3+ cells per DG
40
30
20
10
0
C
CAG-Cre:GFP + CAG-RFP
Rblox/+
Rblox/lox
Viruses injection
perfusion
0
7
14
28
days
D
GFP
Ki67
Merge
RB Ctrl
RB KO
Ki67+GFP+ / GFP+ cells (%)
100
80
60
40
20
0
*
*
7
14
time (dpi)
E
GFP RFP
gcl
RB Ctrl
RB KO
GFP+ RFP+ / RFP+ cells (%)
75
50
25
0
***
7
14
28
time (dpi)

Figure 7

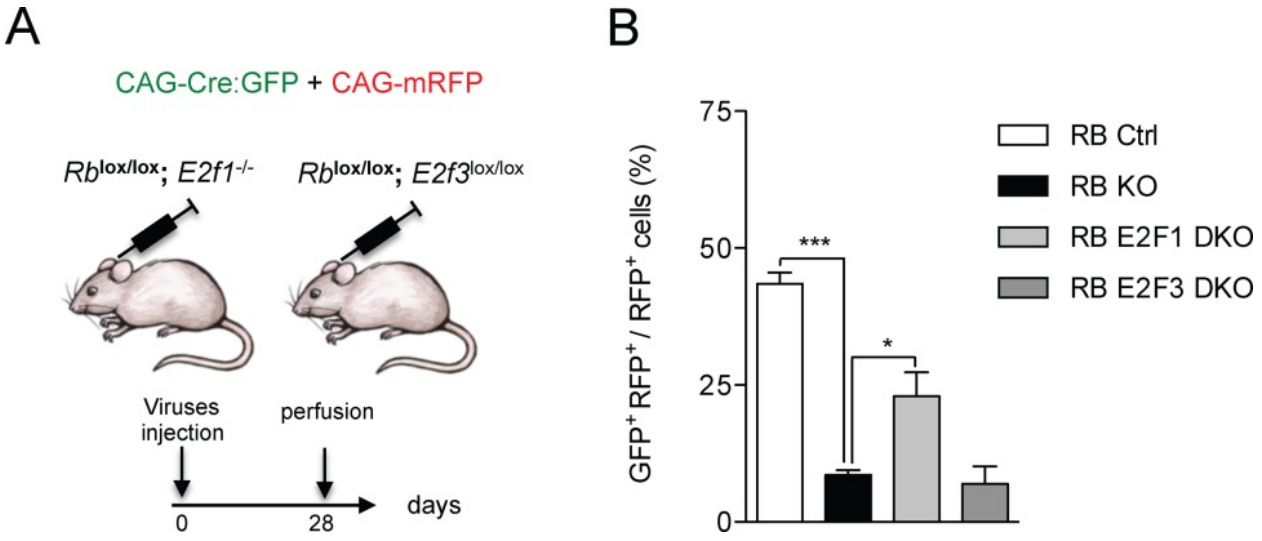
A
CAG-Cre:GFP + CAG-mRFP
Rb^lox/lox; E2f1^-/-
Rb^lox/lox; E2f3^lox/lox
Viruses injection
perfusion
0
28
days
B
GFP+ RFP+ / RFP+ cells (%)
75
50
25
0
***
*
RB Ctrl
RB KO
RB E2F1 DKO
RB E2F3 DKO

Supporting information

Table 1: List of primary antibodies used for immunostainings

Antigen	Origin/Reference	Species
NeuroD1	Santa Cruz Biotechnology, sc-1084	goat
Prox1	Merck Millipore, AB5475	rabbit
Ki67	BD Biosciences, 550609 Cell Marque, 275R	mouse rabbit
Cleaved Caspase3	Cell Signaling, 9661	rabbit
Sox2	Santa Cruz Biotechnology, sc-17320	goat
Tbr2	Abcam, ab23345	rabbit
βIII-Tubulin (Tuj1)	Covance (now Biolegend), 801202	mouse
BrdU	Accurate, OBT0030	rat
YFP (GFP)	Abcam, ab13970	chicken
NeuN	Merck Millipore, MAB377 Encor Biotechnology, RPCA-FOX3	mouse rabbit
Doublecortin	Santa Cruz Biotechnology, sc-8066	goat
RFP	Abcam, ab62341	rabbit

Supplemental Figure 1

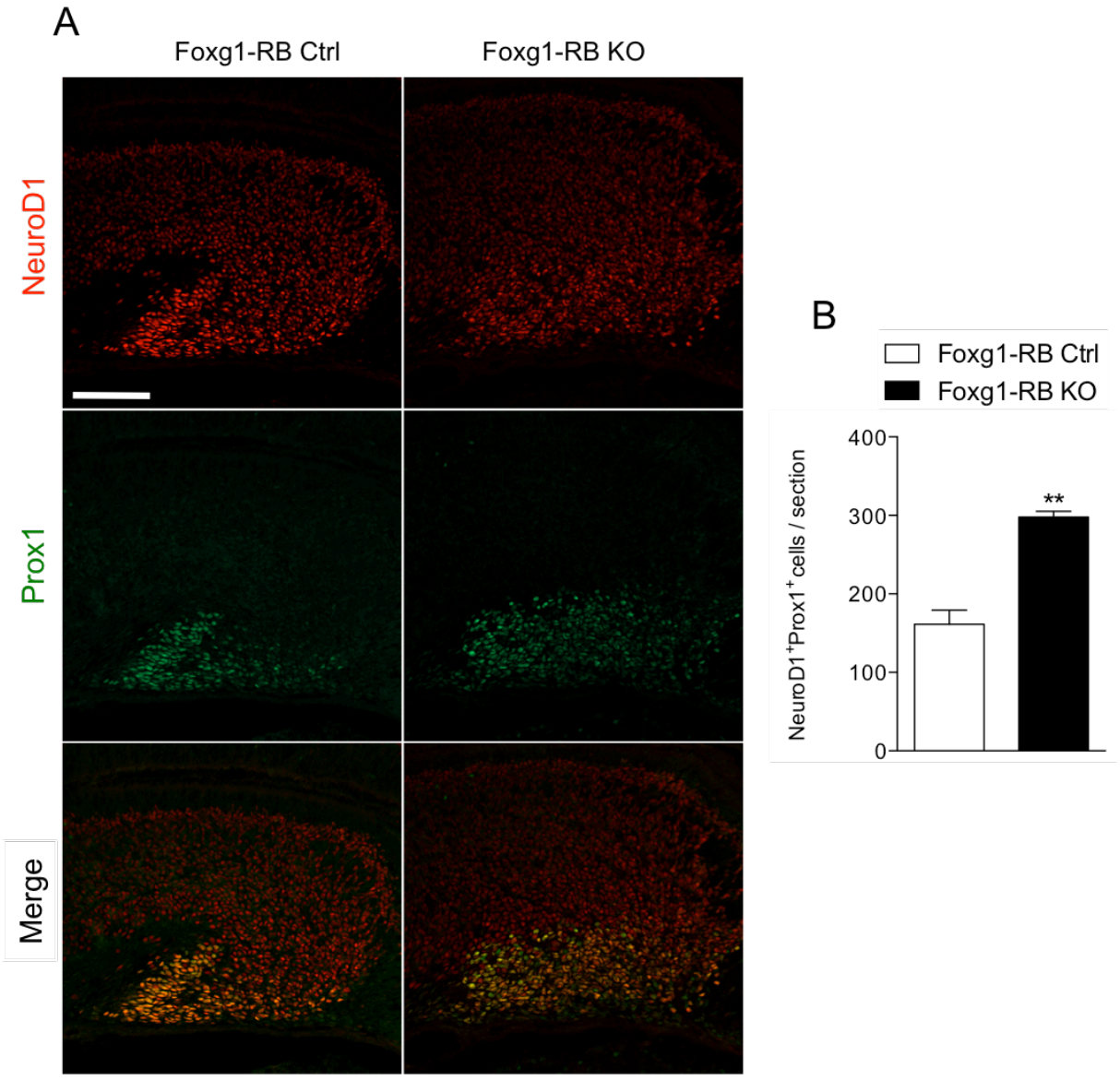

Figure S1. Deletion of RB leads to an expansion of the number of DGCs at E16.5
(A) Single-plane confocal images of NeuroD1 (red), Prox1 (green) and merged NeuroD1/Prox1 (yellow) staining in the DG at E16.5, illustrating the increased number of DGCs in the absence of RB. (B) Histogram showing number of NeuroD1+Prox1+ cells per section in Foxg1-Cre RB Ctrl and Foxg1-Cre RB KO. Scale bar = 100 µm. Data in (B) are presented as mean ± SEM and were analyzed by a Student's t test. N = 3 animals for FoxG1-Cre RB Ctrl and n = 3 animals for FoxG1-Cre RB KO. **, $p < 0.005$.

Supplemental Figure 2

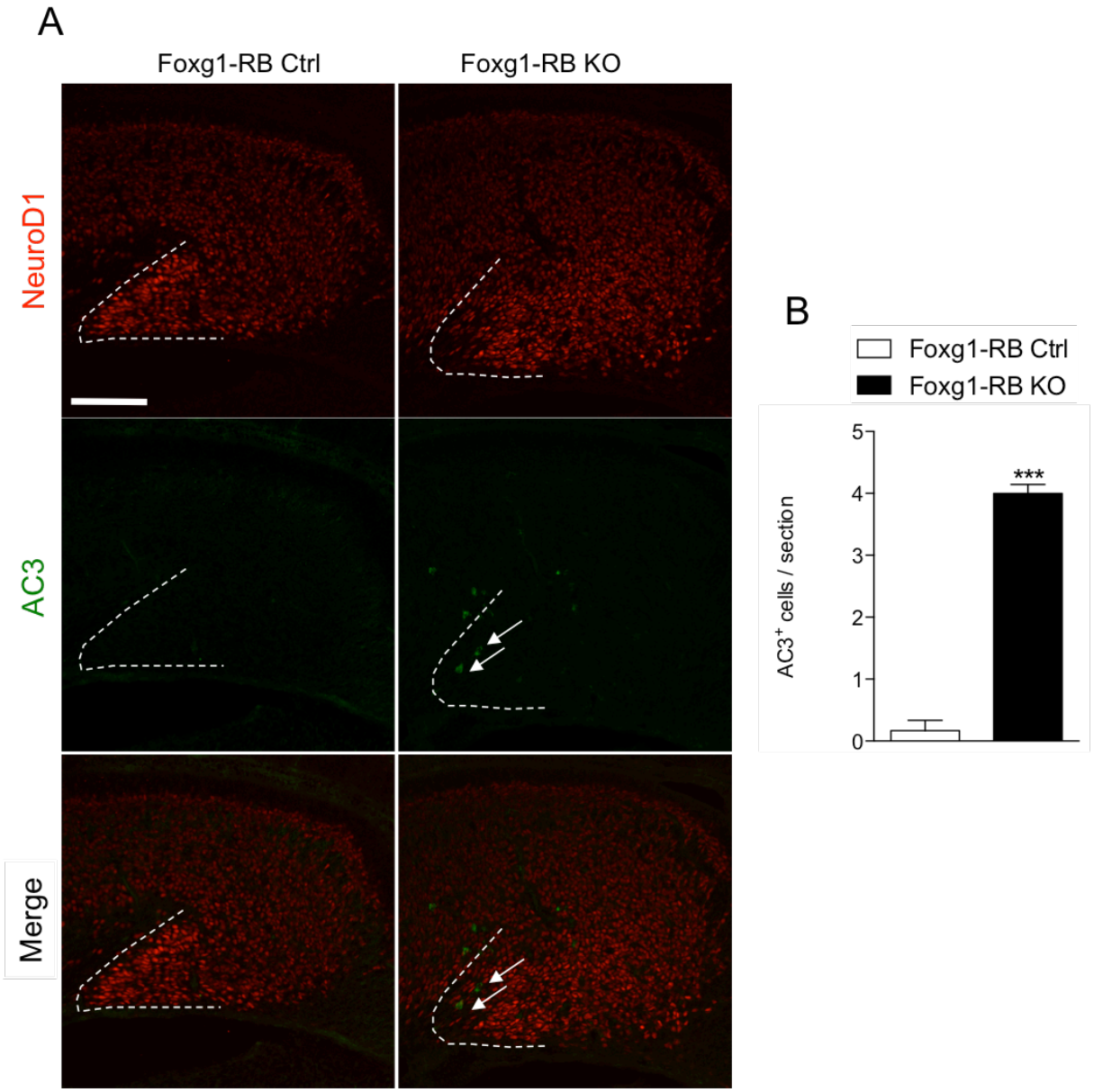

Figure S2. Deletion of RB increases cell death in the DG at E16.5
(A) Single-plane confocal images of NeuroD1 (red), AC3 (green) and merged NeuroD1/AC3 staining in the DG at E16.5, illustrating the increased number of apoptotic cells in the absence of RB in the DG. (B) Histogram showing number of $AC3^{+}$ cells per section in Foxg1-Cre RB Ctrl and Foxg1-Cre RB KO. Scale bar = 100 µm. Data in (B) are presented as mean ± SEM and were analyzed by a Student's t test. N = 3 animals for FoxG1-Cre RB Ctrl and n = 3 animals for FoxG1-Cre RB KO. ***, $p < 0.001$.

Supplemental Figure 3

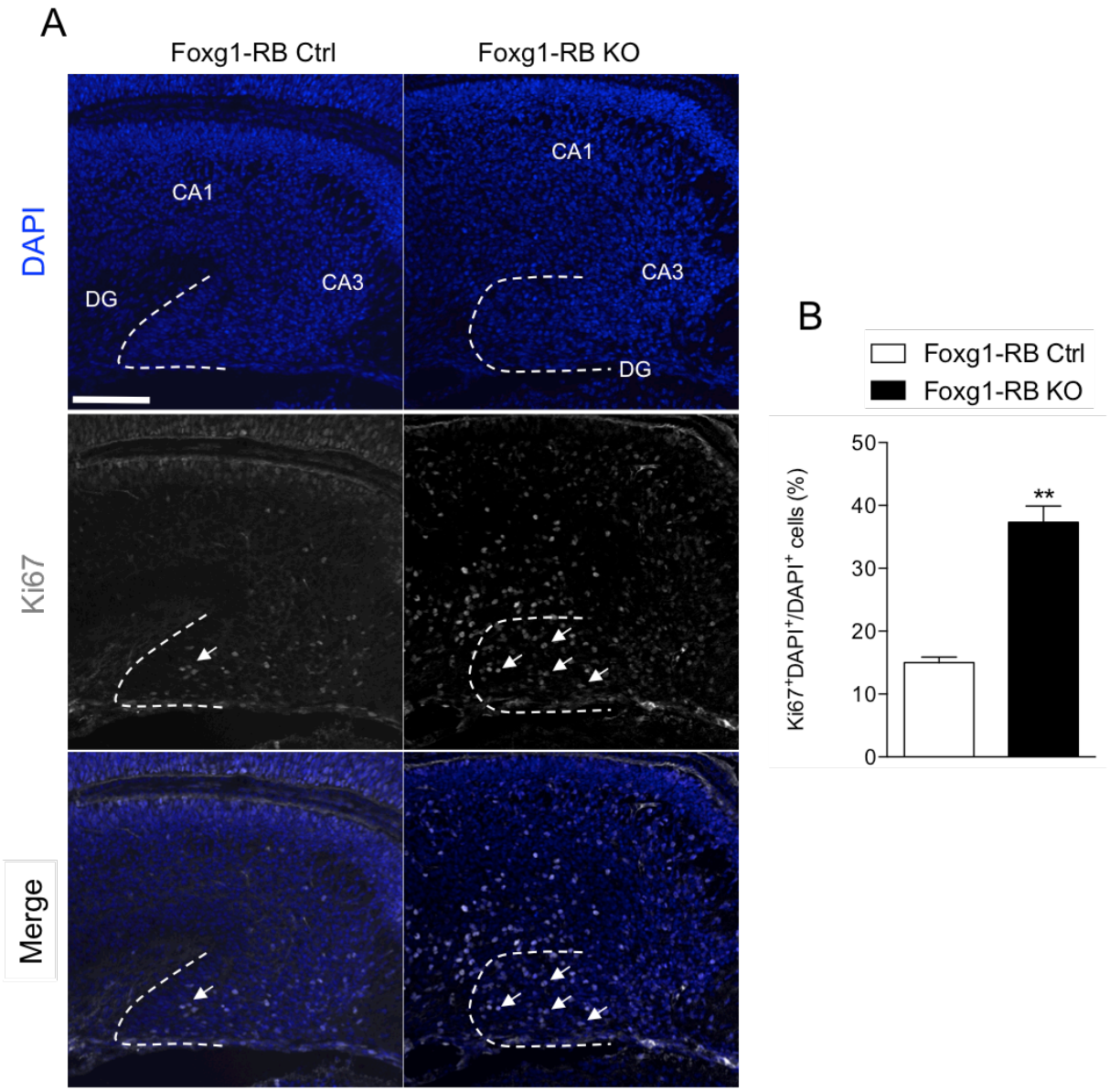

Figure S3. Deletion of RB increases cell proliferation in the DG at E16.5
(A) Single-plane confocal images of DAPI (blue), Ki67 (grey) and merged DAPI/Ki67 staining in the DG at E16.5, illustrating the increased proliferation in the absence of RB in the DG. (B) Histogram showing the percentage of $DAPI^{+}$ expressing Ki67 in Foxg1-Cre RB Ctrl and Foxg1-Cre RB KO. Scale bar = 100 µm. Data in (B) are presented as mean ± SEM and were analyzed by a Student's t test. N = 3 animals for FoxG1-Cre RB Ctrl and n = 3 animals for FoxG1-Cre RB KO. **, $p < 0.005$. Abbreviation: DG, Dentate Gyrus.

Supplemental Figure 4

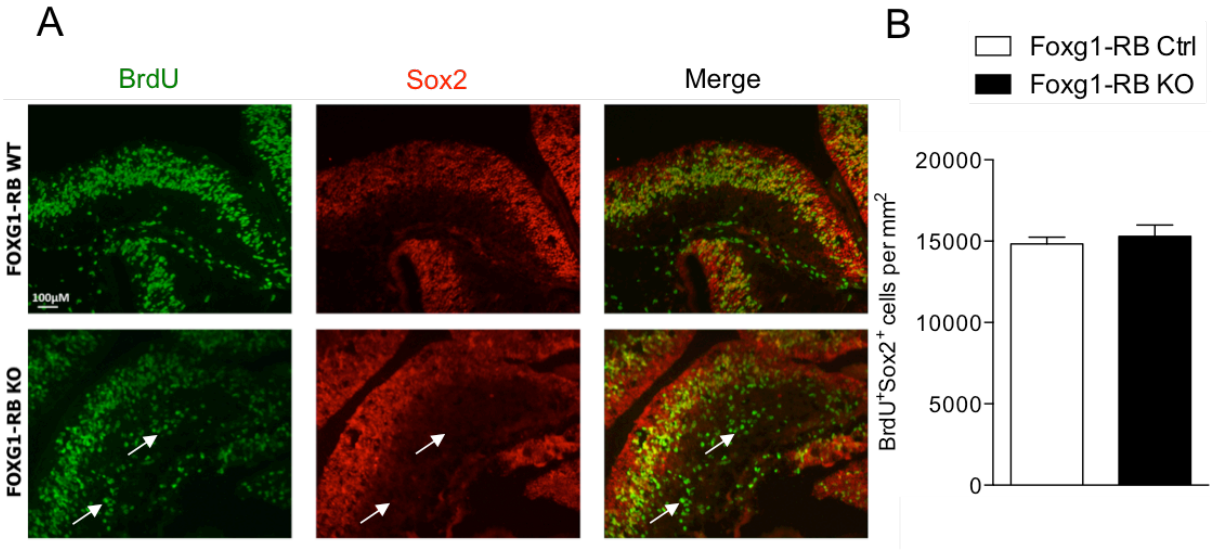

Figure S4. RB loss does not affect proliferation of Sox2$^+$ cells in the primordial hippocampus at E14.5.

(A) Immunostaining performed on coronal sections at medial levels in Foxg1-Cre RB Ctrl and Foxg1-Cre RB KO animals at E14.5. A 30 min BrdU pulse was performed before animals were sacrificed. BrdU is shown in green and Sox2 in red. Scale bar = 100uM. White arrows point to ectopic BrdU$^+$ cells in future CA1-CA3 area. Data in (B) are presented as mean ± SEM and were analyzed by a Student's t test. N = 3 animals for FoxG1-Cre RB Ctrl and n = 3 animals for FoxG1-Cre RB KO.

Supplemental Figure 5

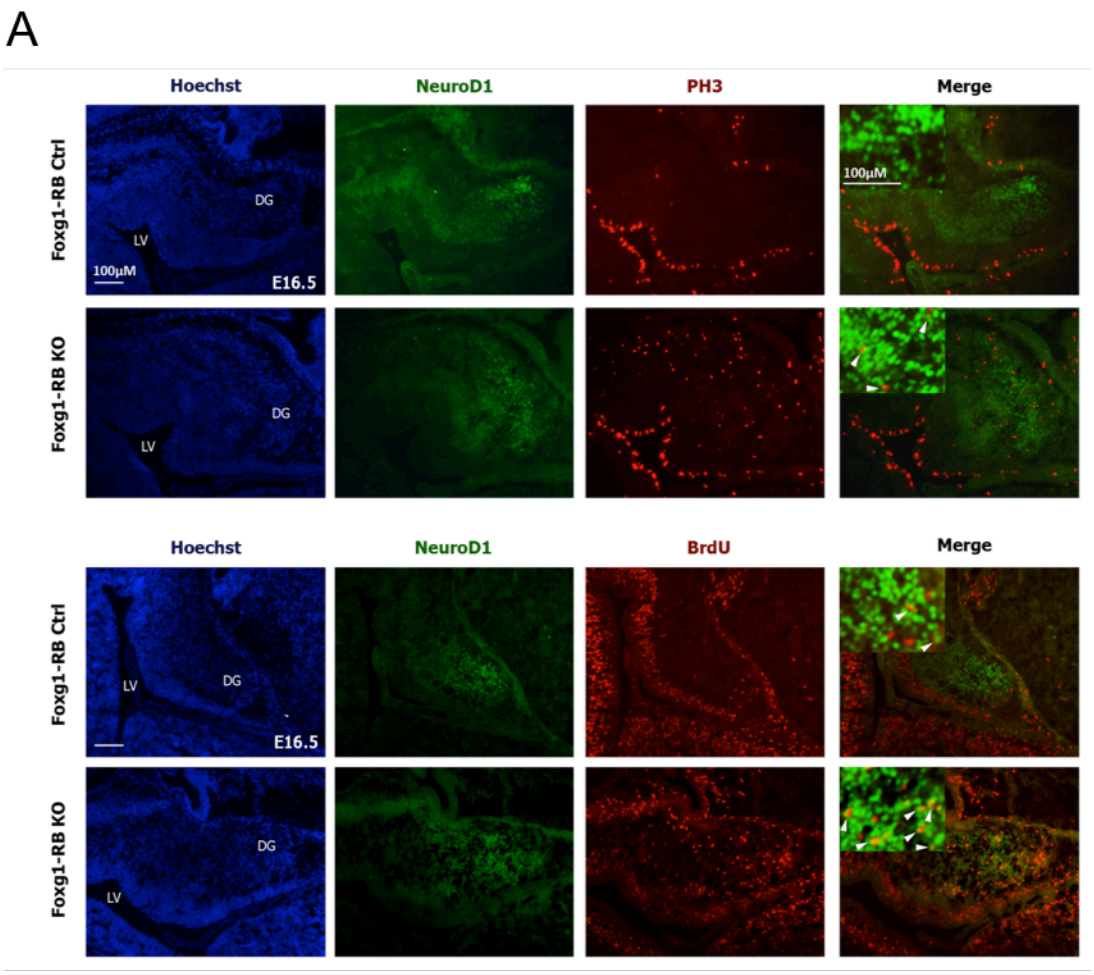

Figure S5. Deletion of RB increases the number of BrdU^{+}NeuroD1^{+} and PH3^{+}NeuroD1^{+} cells in the DG at E16.5.

(A) Immunostaining performed on sagital sections at medial levels in Foxg1-Cre RB Ctrl and Foxg1-Cre RB Ctrl animals at E16.5. 1h BrdU pulse was performed before animals were sacrificed. Top panels: NeuroD1 is shown in green and PH3 in red. Lower panels: NeuroD1 in green and BrdU in red. Scale bar= 100uM. Abbreviation: DG, Dentate Gyrus; LV, lateral ventricle.

CHAPTER 3

Bensun C. Fong, Imane Chakroun, Smitha Paul, Joseph Bastasic, Daniel O'Neil, Edward Yakubovich, Nastaran Ahmadi, Anthony Carter, Mohamed Ariff Iqbal, Alysen Clark, Gustavo Leone[2], David S. Park[3], Renaud Vandenbosch[4]* & Ruth S. Slack*. The Rb/E2F axis is a master regulator of the molecular signatures instructing the quiescent and activated adult neural stem cell state. In press, 2022.

University of Ottawa Brain and Mind Research Institute, Department of Cellular and Molecular Medicine, University of Ottawa, Canada K1H 8M5; 2 - MCW Cancer Centre, Medical College of Wisconsin; 3 - Departments of Clinical Neurosciences, Cell Biology and Anatomy, University of Calgary, Calgary, AB, T2N 4N1; 4 - Université de Liège, Laboratoire de Neurobiologie du Développement, 4000 Liège, Belgique.

Corresponding Authors*:

Ruth S. Slack: rslack@uottawa.ca

Renaud Vandenbosch: rvandenbosch@uliege.be

The experiments were performed by BCF, except for Supplementary Figure S3G. Western blots and chromatin immunoprecipitation were performed in collaboration with IC, while cell culture was performed in collaboration with IC and SP. Immunohistochemical staining and quantification of the 8-week timepoint and V-SVZ sections were performed in collaboration with JB. Bioinformatic analysis and qPCR validation of the E2F1/3-DKO phenotype was performed in collaboration with DO. Immunohistochemical staining and quantification of the E2F1/3-DKO phenotype was performed in collaboration with NA and RV.

EY provided further quantification of proliferation in the E2F1/3-DKO phenotype, included as Supplementary Figure S3G.

Experiments were conceptualized by BCF, RSS and RV. SP, AC, MA and AC provided technical assistance. The manuscript was written by BCF and RSS, and all authors contributed to critical review of the manuscript.

The Rb/E2F axis is a master regulator of the molecular signatures instructing the quiescent and activated adult neural stem cell state

Bensun C. Fong, Imane Chakroun, Smitha Paul, Joseph Bastasic, Daniel O'Neil, Edward Yakubovich, Nastaran Ahmadi, Anthony Carter, Mohamed Ariff Iqbal, Alysen Clark, Gustavo Leone[2], David S. Park[3], Renaud Vandenbosch[4*] & Ruth S. Slack*

University of Ottawa Brain and Mind Research Institute, Department of Cellular and Molecular Medicine, University of Ottawa, Canada K1H 8M5; 2 - MCW Cancer Centre, Medical College of Wisconsin; 3 - Departments of Clinical Neurosciences, Cell Biology and Anatomy, University of Calgary, Calgary, AB, T2N 4N1; 4 - Université de Liège, Laboratoire de Neurobiologie du Développement, 4000 Liège, Belgique.

*Corresponding Authors:

Ruth S. Slack: rslack@uottawa.ca

Renaud Vandenbosch: rvandenbosch@uliege.be

Abstract

The long-term maintenance of the adult neurogenic niche and neurogenesis is dependent on the proper regulation of entry and exit from quiescence. The dynamic transition from quiescence to activation is a complex process requiring not only precise cell cycle control, but also a co-ordinated phenotypic transition involving transcriptional and morphological changes. Presently, the mechanisms by which such a complex repertoire of factors interact and co-ordinate with the core cell cycle machinery to mediate these critical NSC fate transitions remains unknown. Here we show that the Rb/E2F axis functions as an on-off switch for NSC quiescence and activation, by linking the cell cycle machinery to pivotal regulators of NSC fate. Compound deletion of Rb family proteins results in massive activation and expansion of NSCs, and induces a global transcriptomic transition towards NSC activation followed by niche depletion. Deletion of their target activator E2Fs1/3 results in the failure of NSCs to become activated and the acquisition of a global transcriptome associated with intractable NSC quiescence and the cessation of adult neurogenesis. We further show that the Rb/E2F axis orchestrates these fate transitions through the direct regulation of factors essential to NSC function, including REST and ASCL1. This places the Rb/E2F axis as a master regulator of NSC fate, coordinating cell cycle control with NSC activation and quiescence fate transitions.

Introduction

Compelling evidence reveals that neurogenesis, which occurs in the adult mammalian brain, plays an important role in memory and cognition, and has significant therapeutic potential for endogenous repair (Gonçalves et al., 2016). The generation of neurons throughout life depends on the long-term maintenance of a population of quiescent neural stem cells (NSCs), which reside in defined niches. Critical to this process is the ability to maintain and effectively regulate NSC entry and exit from quiescence. The dynamic transition from quiescence to activation is a complex process requiring not only precise cell cycle control, but also a co-ordinated phenotypic transition involving transcriptional and morphological changes (Urbán et al., 2019a). Single-cell transcriptomic studies have shown that NSCs progressing between states of quiescence and activation possess distinct gene expression profiles, essential for NSCs to maintain both a quiescent state as well as competence to respond to niche environmental cues. Quiescent NSCs are enriched in cell signaling, communication and adhesion genes, unlike activated NSCs, which express a repertoire of genes necessary for activation, including ribosomal and RNA synthesis as well as DNA replication and repair (Basak et al., 2018; Codega et al., 2014). Presently, it remains elusive how such a complex repertoire of factors interact and function in a co-ordinated manner with the core cell cycle machinery to mediate these critical NSC fate transitions.

The Retinoblastoma gene Rb was the first tumor suppressor gene to be cloned (Friend et al., 1986; Lee et al., 1987) and its function has been intensively studied in the field of oncogenesis. While Rb family proteins have been shown to interact with multiple cellular

factors, the best-established binding partners are the E2F family of transcription factors through which the Rb family regulates G1-S transition. Three Rb family proteins share overlapping functions: pRb, p107 and p130, and interact with E2Fs to regulate proliferation, self-renewal and the onset of differentiation. We and others have shown that the Rb family and their regulatory targets control the expression of pluripotency factors such as Sox2 (Julian et al., 2013; Kareta et al., 2015), while studies have identified an essential role for the Rb family in regulating haematopoetic stem cell homeostasis by repressing tissue-specific E2F targets (Kim et al., 2017; Viatour et al., 2008).

Here we show that the Rb/E2F pathway serves as a master regulator of adult NSC fate, by co-ordinating the regulation of the transcriptional program that controls quiescence and activation. We show that the Rb/E2F axis functions as an on-off switch for NSC quiescence and activation, by linking the cell cycle machinery to pivotal regulators of NSC fate. Compound deletion of Rb family proteins results in massive activation and expansion of NSCs, and induces a global transcriptomic transition towards NSC activation followed by niche depletion. By contrast, deletion of activator E2Fs, E2F1 and E2F3 results in the failure of NSCs to undergo activation, and the acquisition of a global transcriptome associated with intractable NSC quiescence. We further show that the Rb/E2F axis orchestrates these fate transitions through the direct regulation of factors essential to NSC function, including REST and ASCL1. This places the Rb/E2F axis as a master regulator of NSC fate, coordinating cell cycle control with NSC activation and quiescence fate transitions.

Results

Our previous results revealed that Rb is required to regulate proliferation and survival of committed neuroblasts in the adult brain (Naser et al., 2016; Vandenbosch et al., 2016), however, Rb itself was dispensable in regulating the function of the adult NSC population. Given that cell cycle regulation is a crucial requirement to control NSC quiescence and long-term maintenance, we asked whether there was redundancy in Rb family protein function, and whether these pocket proteins played a critical role in the regulation of the NSC population. To test this, we used tamoxifen (Tam)-inducible NestinCreER^{T2};EYFP mice to conditionally delete Rb and p130 in adult NSCs, together with a germline deletion of p107 (Rb-TKO). Mice triple-heterozygous for Rb family (Rb-THC), which exhibited a phenotype similar to wild type animals (Fig.S1A), were used as littermate controls.

In the subgranular zone (SGZ) of the hippocampal dentate gyrus, Rb family loss resulted in a dramatic 6.3-fold expansion of the total YFP+ recombined cell population, 4 weeks post-Tam (Fig.1A). This population, 75% labelled with proliferation marker Ki67, was comprised of over 80% Sox2-expressing cells, suggesting that Rb family proteins are essential to maintain NSC quiescence in the dentate gyrus. This massive increase in YFP+ cell proliferation could be rescued with the replacement of a single allele of Rb (Fig.S1B-C).

To define the phenotype of YFP+ cells generated in Rb-TKO mice, we co-stained for NeuroD1 neuroblasts and Prox1, a marker for commitment to a granule cell neuron fate. While the proportion of recombined cells expressing NeuroD1 was similar to controls

(Fig.1B), Rb-TKO cells exhibited a 2.5-fold impairment in the induction of Prox1 (Fig.1C), and absence of terminal neuronal differentiation (NeuN). Consistent with the inability to complete neuronal differentiation, Rb-TKO cells underwent cell death, evident by increased active Caspase-3 (AC3) (Fig.1D). By 8 weeks post-Tam, the entire adult NSC niche was depleted, exhibiting a 5.7-fold depletion of the Sox2+ population, and an 8.4-fold reduction of Dcx+ neuroblasts (Fig.1E). These results demonstrate that Rb family proteins are essential for the control of SGZ NSC quiescence and long-term niche maintenance.

As the subventricular zone (SVZ) represents another adult NSC niche, we asked if the Rb family requirement was similar between niches. As in the SGZ, there was a striking loss of quiescence, with a maximal expansion of the YFP+ population at 4 weeks post-Tam where Rb-TKO cells exhibited a 7.1-fold expansion of the Sox2+ Dcx+ co-localized population (Fig.1F). By 8 weeks post-Tam this population began to decline, exhibiting an increase in cell death (Fig.1G, S2A). Consistent with an impairment in differentiation, the Rb-TKO SVZ generated periventricular heterotopias (Fig.S2B), characterized by an accumulation of Sox2+/Dcx+ co-expressing cells which developed as a mass within the lateral ventricle, a structure observed in human disease (Ferland et al., 2009). In summary, our results show that Rb family proteins play a critical role in the control of NSC quiescence as well as the long-term maintenance of NSCs in both adult neurogenic niches.

To interrogate the mechanisms by which Rb family proteins control NSC fate, we FACS-isolated the recombined YFP+ cell population directly from the SVZ niche of adult Rb-THC and Rb-TKO mice, to define transcriptomic profiles 10 days post-Tam. We used bulk RNA-Seq to ensure the necessary sequencing depth for differential expression analyses. Proportionally, the YFP+ fraction of Rb-TKO cells was 3-fold greater than Rb-THC (Fig.2A, Quadrant Q2), in line with SVZ characterization (Fig.1F). Efficient knock-down of Rb family proteins was established (Fig.S3A-C) and validated by qPCR (Fig.2B). Transcriptomic analysis identified 4817 significantly differentially expressed genes (DEGs) with DESeq2-adjusted p-value <0.05 (Fig.2C). The differentially expressed genes were broken down into signature themes including cell cycle, genes associated with NSC quiescence, activation, differentiation and signaling (Fig.2D). Consistent with Rb family classical function, compound loss of pRb/p107/p130 resulted in activation of cell cycle genes (Cyclins A2, E2, Cdks1/2, Thymidine kinase, Cdc6). There was a dramatic change in the NSC phenotype from downregulation of genes associated both with deep NSC quiescence including Aqp4, Id3, Pdgfrb and Aldoc, and with shallow NSC quiescence including Fgfr3 and Dbi (Delgado et al., 2021; Urbán et al., 2019b). By contrast, genes and signaling pathways associated with NSC activation were significantly induced, including Ezh2, Suz12, Pcna, together with upregulation of activated NSC markers including Nestin, Pax6, as well as Shh, Wnt, and Jak2 pathways (Kim 2017). Taken together, Rb family proteins are not only required for cell cycle control, but also for the control of genes required to regulate the phenotypic signature of quiescent NSCs.

As Rb family proteins function by regulating transcription through several factors, we next pursued the E2F family, their best known regulatory targets. RNA-seq reveals that activator E2Fs1/2/3, repressor E2Fs5/6, and atypical E2Fs7/8 were significantly upregulated in the absence of the Rb family (Fig.2E,F), consistent with previous studies showing that E2Fs require Rb family proteins for their regulation (Chong et al., 2009). Given that the expression of activator E2Fs is significantly induced in the NSCs of Rb-TKO animals, and our previous results have shown that E2F1 and E2F3 are highly expressed in this population (Callaghan et al., 1999), we asked if Rb family proteins mediate their function through activator E2Fs1 and 3. To determine if E2F1 and E2F3 play an important role in regulating NSC fate, we generated Tam-inducible NestinCreER^{T2};EYFP mice to conditionally delete E2F3, together with germline deletion of E2F1 (E2F1/3-DKO); with mice double-heterozygous (E2F1/3-HET) used as littermate controls.

We FACS-isolated the recombined YFP+ cell population directly from the SVZ niche of adult E2F1/3-HET and E2F1/3-DKO mice to define transcriptomic profiles 10 days post-Tam. Transcriptomic analyses identified 4514 significant DEGs with DESeq2-adjusted p-value < 0.05 (Fig.3A). Efficient knock-down of activator E2Fs1/3 was established (Fig.S3D-F) and validated by qPCR (Fig.3B). In contrast to the massive exit from quiescence exhibited in Rb-TKO mice, E2F1/3-DKO mice exhibited the opposite phenotype, as NSCs failed to undergo activation, leading to a cessation of adult neurogenesis (Fig.3C). In line with classical activator E2F function, cell cycle genes were significantly downregulated. Genes associated with NSC quiescence (Aqp4, Id3, Pdgfrb,

Apoe, Fgfr3, Dbi) were now highly induced, while genes associated with NSC activation were significantly downregulated. Consistent with persistent NSC quiescence, the induction of genes associated with quiescent NSCs (Tgfbr3, Bmp6, and S100β) was validated by qPCR (Fig.3D). In summary, the loss of activator E2Fs1/3 resulted in a transcriptomic profile reflecting deep NSC quiescence – the opposite of that found with Rb-TKO deficiency.

To confirm this phenotype of deep quiescence, immunohistochemical analyses of the SGZ NSC niche was performed on E2F1/3-DKO and littermate E2F1/3 HET controls, 4 weeks post-Tam (Fig.3E). Our results revealed a dramatic impairment in NSC activation and a complete cessation of adult neurogenesis, quantified as a 15.2-fold decrease in Ki67-labelled cell proliferation and an 11.8-fold decrease in Dcx-expressing neuroblasts (Fig.3F). Loss of activator E2Fs resulted in a dramatic reduction in proliferation among Sox2-expressing cells in both the SVZ and SGZ (Fig.S3G). Taken together, these data suggest a critical requirement for activator E2Fs, E2F1 and E2F3, to execute NSC activation, and ultimately neurogenesis.

We find that Rb-TKO and E2F1/3-DKO populations exhibit opposing regulation of gene transcripts associated with quiescence and activation signatures (Fig.4A, S4A-B), the co-ordinated function of which is critical to maintain both the NSC niche and adult neurogenesis. To more rigorously characterize this role for the Rb/E2F axis, we examined each of our transcriptomic profiles against published datasets. We first compared the transcriptomes against a single-cell RNASeq dataset, with distinct clusters spanning all

stages of adult SVZ neurogenesis (Basak et al., 2018). In Rb-TKO populations, we find a striking upregulation of genes specific to active NSC and early progenitor cells, accompanied by simultaneous downregulation of quiescence-specific genes (Fig.4B). By contrast, the loss of activator E2Fs1/3 resulted in upregulation of genes specific to quiescent and primed NSCs, and downregulation of genes associated with NSC activation (Fig.4D). We next compared the transcriptomes against datasets specifically focused on the distinct molecular characterization of activated and quiescent NSC populations (Codega et al., 2014). In our Rb-TKO signature, 611 significant and majority-downregulated DEGs overlap with the quiescent NSC signature, while 478 significantly and majority-upreglated DEGs overlap with the activated NSC signature (Fig.4C). In the E2F1/3-DKO signature, 512 significant and vastly-upregulated DEGs overlap with the quiescent NSC signature, while 553 significant and vastly-downregulated DEGs overlap with the activated NSC signature (Fig.4E). In summary, alignment of our transcriptomic signatures with published datasets revealed critical roles for Rb family proteins and activator E2Fs1/3 in the regulation of the molecular signatures associated with the quiescence and activation of adult NSCs.

To uncover the mechanisms underlying Rb/E2F-mediated regulation of NSC fate, we searched for master transcriptional regulators and key pathways controlled by the Rb/E2F axis (Fig. 5A). On both datasets, we used iRegulon to establish the enrichment of transcription factor motifs surrounding the transcriptional start sites of significantly downregulated genes. We found consistent evidence in both Rb-TKO and E2F1/3-DKO supporting a role for the Rb/E2F axis as an upstream regulator of REST, the RE1-

Silencing Transcription factor, along with its downstream transcriptional network. As an established transcriptional repressor (Chong et al., 1995; Schoenherr and Anderson, 1995) known to control the activity of neuron-specific gene promoters (Mu et al., 2012), recent studies have demonstrated a requirement for REST in maintaining adult NSC quiescence in the SVZ and SGZ (Gao et al., 2011; Mukherjee et al., 2016; Soldati et al., 2015). The Rb-TKO dataset revealed REST-regulated RE1 motifs on 738 gene targets (31% of input), as well as motifs corresponding to known REST target Sox11 (Bergsland et al., 2006) on 151 gene targets (6% of input). Similarly, the E2F1/3-DKO dataset revealed RE1 and Sox11 motifs on 76 and 603 gene targets (representing 3% and 28% of input), respectively. To further corroborate this finding, we next used Network Analyst to construct a molecular network surrounding each dataset, and compare significant DEG targets against the ENCODE transcription factor-gene interactions database. For both datasets, REST cofactors SIN3A and CoREST (Rcor1) were significantly interconnected with the DEGs. This is supported by the significant upregulation of REST in either dataset, accompanied by the significant downregulation of REST targets Sox4 and Sox11, and validated by qPCR (Fig.5B). The dysregulation of REST, REST cofactors and downstream regulatory targets together suggest that the Rb/E2F axis is a key regulator of REST function. Given that REST is a master regulator of NSC fate, not only in the control of NSC quiescence, but also NSC differentiation, we hypothesize that REST represents a novel mechanism through which Rb family proteins and their activator E2F targets regulate NSC activation, quiescence, and long-term maintenance.

To determine whether REST is a direct regulatory target for the Rb/E2F axis, we performed molecular and cellular manipulations to define the underlying mechanism. We first asked whether endogenous REST protein was altered in the absence of Rb family proteins. FACS-isolated SVZ NSCs from Rb-THC and Rb-TKO mice, 10 days post-Tam, were cultured and early differentiation was evaluated over a time course of 3 days. In Rb-THC NSCs, Western blots revealed that REST expression decreases within 1 day of differentiation, consistent with previous findings (Ballas et al., 2005; McGann et al., 2020). By contrast, REST remains highly-expressed in Rb-TKO NSCs induced to differentiation (Fig.6A). To ask if the Rb family proteins and activator E2Fs can directly regulate REST expression, we first searched for E2F consensus sites at REST regulatory regions and identified 5 motifs within REST introns/exons (Fig.6B). Using Chromatin Immunoprecipitation (ChIP), we found significant binding by p107, p130, E2F3 and E2F4 at motifs in close proximity: 1 (bs1), 2 and 3 (bs2/3) (Fig.6C). Significant E2F1 binding was found at bs2/3 (Fig.6D). The identified binding at REST was significant compared to both IgG and negative locus control Cacng1 (Fig.6C,D). p107, p130, E2F3 and E2F binding was further confirmed with p107-deficient and Rb-TKO NSCs (Fig.6C,D, S5A,B). Binding at Ccna2 (Fig.S5C) was used as positive target of Rb family proteins and E2Fs (Julian et al., 2016; Litovchick et al., 2007). These results identify direct binding of Rb/E2F proteins within REST regulatory regions, and suggest a requirement for Rb family proteins in the endogenous regulation of REST in adult NSCs.

To ask if dysregulation of REST contributed to the phenotype observed in Rb-TKO NSCs, we examined the expression of neuronal differentiation markers by Western blot

(Fig.6E). In Rb-TKO NSCs, we observed impaired expression of neuroblast markers NeuroD1, Dcx and βIII-tubulin, while expression of pro-activation factor ASCL1 was elevated (Fig.6E,F). To ask if blocking REST function could rescue the phenotype of Rb-TKO NSCs, NSC cultures were transduced with lentivectors expressing either a dominant-negative truncated REST, dnREST-V5-mCherry (Chong et al., 1995), or an mCherry control. While dnREST-V5 was not able to rescue expression of differentiation markers in Rb-TKO NSCs, it increased the expression of known REST target Sox11 (Bergsland et al., 2006), and resulted in an even more striking increase in the expression of ASCL1 (Fig.6E,F). Together, these results suggest a requirement for the Rb/E2F pathway in repressing REST activity and maintaining expression of REST target genes, including the pivotal regulator of NSC fate, ASCL1.

Recent studies have defined a dynamic role for ASCL1 in the regulation of activation and quiescence, as ASCL1 is localized to activated NSCs in both the SVZ and SGZ, becoming induced upon activation (Andersen et al., 2014), and is eliminated upon re-entry into quiescence through HUWE1-mediated degradation (Urban et al., 2016). Using immunohistochemistry in the SGZ, we observed strong upregulation of ASCL1 in response to Rb-TKO (Fig.7A), reflecting a 2.1-fold increase in the proportion of recombined cells expressing ASCL1. Performing ChIP against a E2F site at the ASCL1 promoter that we previously reported in embryonic NSCs (Julian et al., 2016), we reveal E2F3, E2F4, p107 and p130 binding in wild-type adult NSCs differentiated for 0 or 1 days (Fig.7B), with binding at Ccna2 promoter used as a positive target (Fig.S5C). Taken

together, these reflect consistent elevated ASCL1 expression in response to loss of Rb Family proteins, and a requirement for the Rb/E2F axis in the regulation of ASCL1.

Given the increase in ASCL1 protein expression in response to dnREST-V5 (Fig.6E,F), we next asked if Rb/E2F regulation of ASCL1 may be influenced by REST. Although previous studies suggested regulation via a RE-1 site 49kb upstream of ASCL1 (Ballas et al., 2005; Jørgensen et al., 2009), we uncovered REST binding at a distinct peak, 94kb upstream of ASCL1 (Fig.S6A-C); with REST being the closest regulated gene to this peak (Fig.S6D,E). ChIP in wild-type adult NSCs differentiated for up to 3 days confirms significant binding of REST at the 94 kb peak alone, increasing with differentiation time; with Snap25 used as a positive REST target (Fig.7C). Together, these results show that the Rb/E2F axis directly regulates master regulators REST and ASCL1, with additional functional interaction on ASCL1 by REST.

As REST and its regulatory network play a critical role in the control of adult NSC quiescence, onset of differentiation, as well as tumor suppression, we examined the functional consequence of REST dysregulation by performing rescue experiments in the SGZ niche. Two weeks post-Tam, we performed dual stereotaxic injections of lentivectors into both hemispheres, respectively carrying dnREST-V5-mCherry or mCherry control, targeting the dentate gyrus of Rb-THC and Rb-TKO mice. We first asked if dnREST could rescue the expression of the REST target gene, ASCL1, by measuring the proportion of ASCL1 expression in mCherry-transduced cells at 4 days and 14 days post injection (Fig.7D, S7A,B). At 4 days post injection in Rb-THC controls and Rb-TKO, there was a 2-

fold and 2.8-fold increase in the proportion of ASCL1-expressing cells in response to dnREST-V5, suggesting that REST loss of function results in an early increase in ASCL1 expression in NSCs. This increase in ASCL1 expression was also maintained at 14 days post injection in Rb-TKO mice. This suggests that blocking REST function, in particular aberrant REST expression following Rb-TKO, increases the expression of ASCL1 in NSCs, with both Rb-THC and Rb-TKO animals revealing a role for REST in the regulation of ASCL1.

To ask whether dysregulated REST contributes to the exhaustion of adult NSCs in Rb-TKO animals, we tested whether blocking REST function with dnREST could rescue NSC depletion 14 days following injection (Fig.7E). Transduction of Rb-THC littermate controls with either mCherry or dnREST-V5 had no effect on the maintenance of the NSC population after 14 days (Fig S7B). By contrast, REST loss of function in Rb-TKO results in a partial rescue of mCherry-expressing cells. While double labelled cells were readily detected at 4 days in Rb-TKO animals (Fig S7A), by 14 days there was a drastic 14.6-fold depletion of LV-mCherry-transduced cells. Transduction of NSCs with dnREST-V5 resulted in a partial rescue (only a 3.8-fold depletion) of Rb-TKO cells representing a partial rescue of double labelled cells, that were strikingly visible at 14 days (Fig. 7E, S7C,D). This shows that blocking REST function by transduction of dnREST can partially rescue NSC depletion in Rb family-deficient adult NSCs. Taken together, we show that that REST is an important regulatory target for Rb/E2F axis, that plays an important role in the long-term maintenance of the adult NSC population.

In conclusion, the Rb/E2F axis regulates NSC function through the coordination of cell cycle control with the transcriptional networks instructing phenotypes of adult NSC quiescence and activation, which are essential for the long term maintenance of NSC and neurogenesis throughout life.

Discussion

The results of these studies support a number of conclusions: First, we show that Rb family proteins are required for the long-term maintenance of the adult neural stem cell pool, by playing an essential role in maintaining quiescence and preventing niche depletion. Second, we show that activator E2Fs1/3 are critical Rb family regulatory targets that are essential for NSC activation as, in their absence, adult NSCs fail to become activated and neurogenesis cannot proceed. Third, we show that the Rb/E2F axis is not only important for cell cycle control, but more importantly, is crucial for the induction of genes associated with the activation and quiescence molecular signature. Fourth, Rb/E2F controls entry and exit from quiescence through direct control of key regulatory factors, including REST and ASCL1. Taken together, the Rb/E2F axis serves as a master regulator, which coordinates cell cycle control with the regulation of the molecular signature associated with the activation/quiescence phenotype, a function that is essential in the long-term maintenance of adult NSCs and neurogenesis.

Rb family proteins are essential for adult NSC maintenance

Earlier studies by our group and others have shown that Rb is dispensable for adult NSC function in the SVZ and SGZ (Jaafar et al., 2016; Vandenbosch et al., 2016), while p107 is required for balancing self-renewal versus differentiation mediated through Hes1 (Vanderluit et al., 2004, 2007). Here, we show that loss of all Rb family proteins results in a complete loss of quiescence and massive activation of the entire adult NSC pool. These results show that Rb family proteins play a crucial role in regulating the function of adult NSCs, by maintaining the quiescence essential for the maintenance of this cell population

in both neurogenic niches. While studies in other systems have established ectopic proliferation following Rb family deletion (Jiang et al., 2010; Sage, 2000; Viatour et al., 2008, 2011b), functional compensation between Rb family proteins (Ajioka et al., 2007; Burkhart et al., 2010; Sage et al., 2003) and the promotion of reprogramming following Rb inactivation (Kareta et al., 2015), the impact on the adult NSC population is dramatic, as Rb family proteins regulate not only cell cycle control but the molecular signature associated with NSC quiescence and activation. Thus, the global changes identified in Rb-TKO signify a novel role for Rb family proteins as broad transcriptional regulators of NSC fate, representing a previously unknown function.

Activator E2Fs E2F1 and E2F3 are essential for NSC activation

Rb family proteins are known to associate with at least 110 regulatory targets that modulate transcription (Morris and Dyson, 2001), with the best-characterized being E2F family transcription factors: activators E2F1-3a and repressors E2F3b-6. Here we show that E2F1 and E2F3 are critical for NSC function, as absence of both of these factors results in a complete cessation of NSC activation and neurogenesis. Previous studies have demonstrated a moderate decrease in adult NSC proliferation (Cooper-Kuhn et al., 2002), while we have shown that loss of E2F3 or individual isoforms, E2F3a or E2F3b, result in imbalances in self-renewal/commitment decisions (Julian et al., 2013; McClellan et al., 2007). None of the phenotypes previously reported with individual E2Fs have resulted in the dramatic phenotypes generated by the loss of E2Fs1/3, where adult NSCs are unable to exit quiescence. Interestingly, earlier studies revealed that retinal progenitors and muller glia could proliferate in the absence of all activator E2Fs1/2/3,

unlike that seen in the adult neurogenic niches described here (Chen et al., 2009a). Thus, our results demonstrate that activator E2Fs 1/3 are essential for adult NSC activation and for the generation of the molecular signature required for NSC activation and neurogenesis.

The Rb/E2F axis regulates phenotypes of adult NSC quiescence and activation

These results highlight a previously unknown and novel function for the Rb/E2F axis altogether, revealing a critical requirement not only for cell cycle control but for the acquisition of the cell and transcriptomic phenotypes associated with quiescence and activation. Recent studies have demonstrated that quiescence is an active, dynamic process, wherein NSCs progressing between states of quiescence and activation possess distinct gene expression profiles, which allow quiescent NSCs to respond to environmental cues ultimately culminating in NSC activation (Basak et al., 2018; Codega et al., 2014) Alignment of our transcriptomic profiles with published population-specific signatures reveals a striking alignment, in which loss of Rb family proteins aligns with an activated state, and loss of E2Fs1/3 aligns with the molecular signature of the quiescent state. The depth of cell quiescence and reduced sensitivity to growth signals reflected in these signatures has yet to be evaluated; previous studies coupling modeling and cell culture have suggested that quiescence depth may be associated with incresased threshold required to activate a Rb/E2F bistable switch (Kwon et al., 2017). Taken together, the Rb/E2F axis not only controls the cell cycle in NSCs, but also plays an essential role to generate the molecular signature of quiescent and activated cells, a novel and crucial role for Rb family proteins in the control of adult NSC function.

The Rb/E2F axis directly regulates NSC fate via REST

Our transcriptomic profiles suggest an Rb/E2F-dependent mechanism regulating the molecular signatures of NSC quiescence and activation. Following loss of Rb family proteins or activator E2Fs, we observe dysregulation of the REST gene regulatory network, with elevated REST and downregulation of numerous proneural targets containing RE-1 sites, including Dcx, L1cam and SoxC proteins Sox4/Sox11 (Bergsland et al., 2006; Lepagnol-Bestel et al., 2009; Mu et al., 2012). REST has been recently shown to maintain both NSC quiescence as well as progenitor proliferation and number, to prevent precocious differentiation (Mukherjee et al., 2016). Given that Rb-TKO and E2F1/3-DKO generate opposing phenotypes in the regulation of NSC quiescence and activation, the common induction of REST and its targets may appear contradictory. While activator E2Fs can function as transcriptional activators in proliferating cells, they have also been shown to serve as transcriptional repressors to silence E2F target genes in differentiating cells, such that activating E2Fs serve as a tether to recruit Rb family proteins to target genes (Chong et al., 2009). In the context of the adult neurogenic niche, our data suggest that activator E2Fs1/3 are essential for Rb family-mediated repression of REST. Analysis of both transcriptomic and ChIP data demonstrate direct binding by p107/p130 and E2F3/E2F4 at the REST regulatory regions, consistent with a model whereby E2Fs1/3 recruit Rb family proteins to repress REST in adult NSCs. The increased magnitude of REST target gene repression in response to E2F1/3 deficiency is consistent with activator E2Fs mediating Rb family protein function regulating REST. In response to E2F1/3-DKO, the lack of REST cofactor (CoREST and Sin3A) upregulation suggests that activator E2Fs are required to recruit REST cofactors. This may link

activator E2Fs with a reported requirement for CoREST in modulating REST target expression despite REST dissociation (Ballas et al., 2005). Based on this model, we show that Rb-family proteins and activator E2Fs1/3 together are required for REST regulation.

The Rb/E2F axis and REST regulate ASCL1

In response to loss of Rb family proteins, we observe that the massive transcriptional shift towards activation is accompanied by an increased number of ASCL1-expressing activated NSCs. Together with ChIP data demonstrating direct ASCL1 binding by p107/p130 and E2F3/E2F4, our data suggest a role for the Rb/E2F axis in repressing ASCL1 expression to maintain NSC quiescence. While ASCL1 regulation occurs at multiple levels, most notably at the level of protein degradation mediated by E3 ubiquitin ligase Huwei1 (Urban et al., 2016), we also demonstrate that blocking REST function through dnREST transduction results in increased induction of ASCL1 expression, consistent with ASCL1 being a regulatory target for REST (Gao et al., 2011). Distinct from a previously described site (Ballas et al., 2005; Jørgensen et al., 2009), in the context of adult NSCs, we have identified REST binding at a distinct peak 94kb upstream of ASCL1. REST regulation of ASCL1 is also supported by our findings in vivo, as dnREST transduction results in an increased percentage of ASCL1-expressing cells in the adult SGZ. Interestingly, dnREST partially rescued the depletion of adult NSCs following loss of Rb family proteins, as dnREST transduction resulted in a significant increase in activated, Ascl1-expressing cells after 14 days. This suggests that the Rb/E2F regulatory axis is required for proper REST regulation, which is important for the maintenance of the NSC niche in the adult SGZ.

Establishing the regulatory network dependent on the Rb/E2F axis is critical in the context of stem cell regulation, differentiation, and oncogenesis, as Rb is functionally inactivated in a wide range of paediatric and adult cancers (Burkhart and Sage, 2008). Rb family proteins are crucial to the complex regulatory framework governing the canonical cell cycle (Dick and Rubin, 2013), and further integrate upstream mechanisms including organ size control, mediated through YAP (Ehmer et al., 2014). In contrast with its function in the adult mouse SVZ and SGZ, loss of Rb in human cerebral organoids results in increased NSC proliferation (Matsui et al., 2017), suggesting a lower degree of functional compensation in humans than observed in mouse models. This work further informs our understanding of the upstream mechanisms regulating pivotal factors REST and ASCL1, and provides further functional context. REST expression is altered in multiple pathological conditions (reviewed in (Poiana et al., 2020), including multiple cancers including human medulloblastoma, where abnormal REST expression is proposed to block neuronal differentiation in an effort to maintain NSC stemness (Su et al., 2006).

In the context of regenerative medicine, the Rb/E2F axis also provides biological targets for pharmacological interventions targeting NSC fate. Small molecule inhibitors of E2F have been used to inhibit tumorigenesis following Rb family inactivation in adult mice (Sangwan et al., 2012). The drug harmine has been employed to recapitulate the phenotype associated with compound p107/p130 loss through phosphorylation of DYRK1A (Forristal et al., 2014; Göckler et al., 2009), a component of the large repressive complex DREAM recruited by p107 and p130. In line with our study, DYRK1A is believed

to mediate the cognitive defects that characterize Down syndrome, including the deregulation of multiple genes including L1cam, through binding with a REST-interacting SWI/SNF complex (Lepagnol-Bestel et al., 2009).

In conclusion, we describe a novel, previously unknown function for Rb family proteins and their target activator E2Fs1/3, in the regulation of NSC activation and quiescence. We demonstrate how transcriptional signatures of quiescence and activation among adult NSCs are co-ordinated with cell cycle control, and show that the Rb/E2F axis serves as a master regulator of the molecular program instructing adult NSC exit from and re-entry into quiescence, essential for niche maintenance and ultimately adult neurogenesis.

Accession Numbers

Data have been deposited in GEO under accession number GEO: GSE190766.

Acknowledgments

This work was supported by core facilities at the University of Ottawa including Surgical Core; Dr. Vera Tang, Flow Cytometry Core; Cell Biology and Image Acquisition Core, facilities at the Ottawa Hospital Research Institute, including the Flow Cytometry and Cell Sorting Facility and StemCore Laboratories, and The Centre for Applied Genomics, at The Hospital for Sick Children, Toronto. This work was funded by CIHR grants to RSS and by an Ontario Graduate Scholarship to BCF.

Figure Legends and Figures

Figure 1: Rb family are essential to maintain NSC quiescence in adult DG and SVZ

(A) IHC of YFP+ recombined and Sox2+ self-renewing cells in the DG of indicated mice. Quantification (N=3) of total counts of YFP+ recombined and YFP+Sox2+ self-renewing recombined cells, per DG, as well as Sox2+ self-renewing cells and Ki67+ cycling cells expressed as a percentage of YFP+ recombined cells, per DG.
(B) IHC of NeuroD1+ neuroblasts, Sox2+ self-renewing and YFP+ recombined cells in the DG of indicated mice. Quantification (N=3) of Sox2+ self-renewing cells as a percentage of YFP+NeuroD1+ recombined neuroblasts, as well as NeuroD1+ neuroblasts as a percentage of YFP+ recombined cells, per DG.
(C) IHC of Prox1+ committed neurons, Sox2+ self-renewing and YFP+ recombined cells in the DG of indicated mice. Quantification (N=3) of Prox1+ committed neurons as a percentage of YFP+ recombined cells, as a comparison between Sox2+ and Prox1+ cell populations, per DG.
(D) IHC of NeuN+ post-mitotic neurons and YFP+ recombined cells in the DG of indicated mice. Quantification (N=3) of NeuN+ post-mitotic neurons as a percentage of YFP+ recombined cells, as well as total counts of YFP+AC3+ apoptotic recombined cells, per DG.
(E) IHC of YFP+ recombined, Sox2+ self-renewing and Dcx+ neuroblasts in the DG of indicated mice. Quantifications (N=3) of total counts of YFP+ recombined cells in DG of indicated mice, as well as total counts of YFP+ recombined, YFP+Sox2+ self-renewing recombined cells, YFP+Dcx+ recombined neuroblasts and YFP+Sox2+Dcx+ recombined cell type, per DG.
(F) IHC of YFP+ recombined, Sox2+ self-renewing and Dcx+ neuroblasts in the SVZ of indicated mice at 4wpi. Quantification (N=3) of total counts of YFP+ recombined, YFP+Sox2+ total self-renewing recombined, YFP+Sox2+Dcx+ recombined cell type, and YFP+Sox2+Dcx- total non-differentiating self-renewing recombined cells, per SVZ.
(G) Quantification of total counts of YFP+AC3+ apoptotic recombined cells, per SVZ.

Scale bars, 100μm. Error bars, mean ± STD. Statistical significance was measured using unpaired Student's t-tests, *p< 0.05, **p < 0.01, ***p < 0.001, ****p < 0.0001.

Figure 2: Transcriptomic analysis of Rb Family function in Adult Neurogenic Niche

(A) Representative 488FL-Log Height vs SSC-Log Height FACS plots demonstrating gating strategy. The YFP+ enriched population is clearly defined in Q2.
(B) qPCR analysis of Rb, p107 and p130 mRNA levels in response to indicated induced knockout (N=3). Values were normalized to GAPDH.
(C) MA-plot for the shrunken $\log_2$ fold changes. Significantly differentially expressed genes ($p<0.05$) are indicated in red.
(D) Relative transcriptomic expression of significantly differentially expressed genes, grouped by curated functional category.
(E) Relative transcriptomic expression of E2F family transcription factors.
(F) qPCR analysis of Atypical E2Fs, E2F7 and E2F8, in response to indicated induced knockout (N=3). Values were normalized to GAPDH.

Error bars, mean ± STD. Statistics: qPCR analysis (B,F) employs unpaired Student's t-tests; Relative expression plots (D,E) employ DESeq2-adjusted p-values. * p< 0.05, **p < 0.01, ***p < 0.001, ****p < 0.0001

Figure 3: Activator E2Fs 1 and 3 are essential for adult NSC activation and neurogenesis

(A) MA-plot for the shrunken log2 fold changes. Significantly differentially expressed genes ($p<0.05$) are indicated in red.
(B) qPCR analysis of E2F1 and E2F3 mRNA levels in response to indicated induced knockout (N=3-5). For E2F1, values were GAPDH-normalized to 1 following $2^{-\Delta\Delta Ct}$ method.
(C) Relative transcriptomic expression of significantly differentially expressed genes, grouped by curated functional category.
(D) qPCR analysis of quiescence-associated genes Tgfbr3, Bmp6, S100β, as well as differentiation-associated genes Dcx and Dlx1. E2Fs, E2F7 and E2F8, in response to indicated induced knockout (N=3). Values were GAPDH-normalized to 1 following $2^{-\Delta\Delta Ct}$ method.
(E) IHC staining of YFP+ recombined cells and Dcx+ neuroblasts in DG of indicated mice. Scale bar, 100μm.
(F) IHC staining from (F), inset, as well as staining of YFP+ recombined and Ki67+ cycling cells in DG of indicated mice. Scale bar, 50μm. Quantification (N=3) of total counts of Ki67+ cycling cells and Dcx+ neuroblasts, per DG.

Error bars, mean ± STD. Statistics: IHC and qPCR analysis (B,D,F) employs unpaired Student's t-tests; Relative expression plot (C) employs DESeq2-adjusted p-values. * p< 0.05, **p < 0.01, ***p < 0.001, ****p < 0.0001

Figure 4: Rb/E2F pathway transcriptomic regulation of NSC activation and quiescence

(A) Relative transcriptomic expression of significantly differentially expressed qNSC-associated and aNSC-associated genes, across both datasets.
(B) Genes differentially expressed in response to Rb-TKO, including direction and significance, overlapped with Basak et al., 2018 signature.
(C) Significantly differentially expressed genes in response to Rb-TKO, overlapped with qNSC and aNSC signatures from Codega et al., 2011, and proportional directionality of overlap.
(D) Genes differentially expressed in response to E2F1/3-DKO, including direction and significance, overlapped with Basak et al., 2018 signature.
(E) Significantly differentially expressed genes in response to E2F1/3-DKO, overlapped with qNSC and aNSC signatures from Codega et al., 2011, and proportional directionality of overlap.

Statistics: Relative expression plot employs DESeq2-adjusted p-values. Genes with DESeq2-adjusted p-value < 0.05 were used as input for respective signatures in (B,D) and (C,E). * p< 0.05, **p < 0.01, ***p < 0.001, ****p < 0.0001

Figure 5: The Rb/E2F pathway regulates NSC fate via REST

(A) Medial: Curated significant GO:BP gene sets using genes downregulated (in response to indicated knockout) as input. iRegulon transcription factor enrichment results, using significantly downregulated genes (in response to indicated knockout) as input. REST and Sox11 are highlighted in each. Lateral: Network Analyst TF-Protein enrichment results, using all significant genes (in response to indicated knockout) as input. REST cofactors SIN3A and CoREST are highlighted in each.
(B) Lateral: Summary of significant differential gene expression affecting the REST/SoxC pathway, in response to indicated knockout. Medial: qPCR analysis of REST and SoxC proteins Sox4 and Sox11, in response to indicated induced knockout (N=3). Values were normalized to GAPDH. Error bars, mean ± STD.

Statistics: qPCR analysis (B) employs unpaired Student's t-tests; summary table employs DESeq2-adjusted p-values. Genes with DESeq2-adjusted p-value < 0.05 were considered significant for analysis using iRegulon and Network Analyst in (A). *p< 0.05, **p < 0.01, ***p < 0.001, ****p < 0.0001

Figure 6: Rb family proteins regulate REST expression

(A) Western blot on total protein extracts from adult NSCs expressing indicated knockout, differentiated for 0, 1, or 3 days. β-actin is used as a loading control.
(B) A schematic representation of REST gene indicating the presence of 5 E2F motifs within its introns and exons.
(C) ChIP on adult NSC chromatin harvested from wild-type +/+ and p107-null -/- mice (N=3-7). Error bars, mean ± SEM.
(D) ChIP on chromatin from adult p107-null -/- NSCs and adult Rb-TKO NSCs (N=3-7). Error bars, mean ± SEM.
(E) Western blot on total protein extracts from adult NSCs infected with lentivector expressing mCherry or dnREST-V5 at P2, and differentiated at P3 for 0, 1, or 3 days.
(F) Quantification of Western blot in (E) using Image J. Statistical significance was measured using a paired, 2-tailed Student's t-test. n=3, ** $p < 0.05$.

Statistics: Statistical significance was measured using an unpaired, 2-tailed Student's t-test. * $p < 0.05$ vs IgG and Cacng1, *** $p < 0.05$ in wt vs p107 null (C) or p107 null vs Rb-TKO mice (D).

Figure 7. The Rb/E2F pathway regulates NSC activation and quiescence through REST and ASCL1

(A) IHC staining of ASCL1+ activated NSCs, YFP+ recombined and Sox2+ self-renewing cells in the DG of indicated mice. Scale bar, 50μm. Quantification (N=3) of ASCL1+ activated NSCs as a percentage of YFP+ recombined cells, per DG.
(B) Schematic representation of ASCL1 gene indicating an E2F3/4 peak at its promoter (Julian et al, 2016). ChIP on adult NSC chromatin harvested from wild-type +/+ mice, differentiated for 0, 1, or 3 days (N=3), targeting this peak.
(C) ChIP on adult NSC chromatin harvested from wild-type +/+ mice, differentiated for 0, 1, or 3 days (N=3), targeting the specified peak.
(D) IHC staining of YFP+ recombined cells and ASCL1+ activated NSCs in the DG of indicated mice, 4 days and 14 days after injection with indicated mCherry+ expression lentivector. Scale bar, 50μm. Quantification (N=3) of ASCL1+ activated NSCs expressed as a percentage of total mCherry+ labelled cells, in indicated mice at same timepoints.
(E) IHC staining of YFP+mCherry+ colocalization, 14 days after injection with indicated mCherry+ expression lentivector. Quantification (N=3) of YFP+ recombined cells expressed as a percentage of total mCherry+ labelled cells, in indicated mice at same timepoint. Scale bar, 100μm.

Error bars, mean ± STD. Statistics: Statistical significance for ChIP (B,C) was measured using an unpaired, 2-tailed Student's t-test, * $p < 0.05$ vs IgG. Statistical significance for IHC (A,D,E) employs unpaired Student's t-tests, *$p< 0.05$, **$p < 0.01$, ***$p < 0.001$, ****$p < 0.0001$.

Supplementary Figure 1**:** Validation and rescue of the Rb-TKO phenotype

(A) Quantification (N=3) of total YFP+ recombined cells, per DG, in indicated mice, 4 weeks post-Tam.
(B) IHC of YFP+ recombined, Ki67+ proliferating and Sox2+ self-renewing cells in the DG of indicated mice, 4 weeks post-Tam. Quantification (N=3) of proliferation markers Ki67 and BrdU expression, expressed as a percentage of YFP+Sox2+ self-renewing recombined cells, per DG. Scale bar, 50μm.
(C) IHC of YFP+ recombined cells, Sox2+ self-renewing cells and NeuN+ post-mitotic neurons in the DG of indicated mice at indicated timepoints. Quantification (N=3) of YFP+Sox2+ self-renewing recombined cells, normalized to granule cell layer area, per DG. Scale bar, 100μm.

Error bars, mean ± STD. Statistical significance was measured using unpaired Student's t-tests, *p< 0.05, **p < 0.01, ***p < 0.001, ****p < 0.0001.

Supplementary Figure 2**:** Extended and gross phenotype of Rb-TKO in the V-SVZ

(A) Representative IHC of YFP+ recombined, Sox2+ self-renewing and Dcx+ neuroblasts in the SVZ of indicated mice at 8wpi. Scale bar, 50μm.
(B) Representative full-structure IHC of YFP+ recombined, Sox2+ self-renewing and Dcx+ neuroblasts in the SVZ of indicated mice at indicated timepoints. Scale bar, 100μm.

Supplementary Figure 3**:** Bioinformatic validation of Rb-TKO and E2F1/3-DKO

(A) Sashimi plots of exon-level gene expression of indicated Rb Family protein. For induced deletion (Rb, p130) floxed exon is centred; for germline deletion (p107) whole gene is shown.
(B) Principal component plot of sequenced Rb-THC and Rb-TKO samples.
(C) Heatmap of sample-to-sample distances between sequenced Rb-THC and Rb-TKO samples.
(D) Sashimi plots of exon-level gene expression of indicated Activator E2F. For induced deletion (E2F3) focus shows exon-level knockdown; for germline deletion (E2F1) whole gene is shown.
(E) Principal component plot of sequenced E2F1/3-HET and E2F1/3-DKO samples.
(F) Heatmap of sample-to-sample distances between sequenced E2F1/3-HET and E2F1/3-DKO samples.
(G) Quantification (N=3) of Ki67+Sox2+ proliferating self-renewing cells expressed as a percentage of total Sox2+ self-renewing cells, per SVZ or DG. Error bars, mean ± STD.

Supplementary Figure 4: Broad transcriptional signatures of Rb-TKO and E2F1/3-DKO

(A) Enrichment maps of GO:BP gene set terms enriched in Rb-TKO or E2F1/3-DKO relative to respective controls. Grey circles annotate clusters of gene sets with strong overlap along annotated theme.
(B) Lateral: Indicated direction and significance of differential regulation of curated GO:BP terms characteristic of "Cell Cycle" or "Neurogenesis", in response to indicated induced knockout. Medial: Relative transcriptomic expression of characteristic significantly differentially expressed genes, across both datasets.

Statistics: Relative expression plot employs DESeq2-adjusted p-values. * $p < 0.05$, ** $p < 0.01$, *** $p < 0.001$, **** $p < 0.0001$

Supplementary Figure 5: Validation of molecular analysis, Rb-TKO and $p107^{-/-}$

A. Western blot on chromatin used in ChIP. β-actin and β-tubulin are used as loading controls.
B. ChIP on adult NSCs chromatin harvested from wt, p107 null and Rb-TKO mice, n= 3-7, * $p < 0.05$ vs IgG and Cacng1, *** $p < 0.05$ in wt vs p107 null or p107 null vs Rb-TKO mice.
C. ChIP on wt type adult NSCs differentiated for 0, 1 or 3 days. n=3, * $p < 0.05$ vs IgG.

Statistical significance was measured using unpaired, 2-tailed Student's t-test.

Supplementary Figure 6: Confirmation of 94kb upstream peak

A. ChIP-seq on Rest in C2C12 myocytes (Caltech TFBS Track, ENCODE) showing a peak at 94 Kb upstream of Ascl1.
B. ChIP-seq on Rest showing binding at 94 Kb upstream of Ascl1 in both QNP and TAP and a peak in QNP at 49 Kb downstream of Rest (Mukherjee et al, 2016).
C. ChIP-seq on Rest showing a peak at 94 Kb upstream of Ascl1 in all human cell lines tested.
D. Expression of Pah in different organs and cell lines from gene expression profiling data by GeneAtlas. The dataset is available online at the BioGPS website.
E. A heatmap of the expression of Pah, Rest, Ascl1 and Sox11 in adult NSCs (Rb-THC/ TKO), eNS, and CN cultured for or 4, 9, or 11 days. iQNP and TAP RNA-seq datasets are from Mukherjee et al, 2016.

Supplementary Figure 7: Control and gross phenotypes following dnREST transduction

(A) IHC of YFP+ recombined cells and ASCL1+ activated NSCs in the DG of control Rb-THC mice, 4 days after injection with indicated mCherry+ expression lentivector. Quantification (N=3) of YFP+ recombined cells expressed as a percentage of total mCherry+ labelled cells, in indicated mice at same timepoint. Scale bar, 50μm.
(B) IHC of YFP+ recombined cells and ASCL1+ activated NSCs in the DG of control Rb-THC mice, 14 days after injection with indicated mCherry+ expression lentivector. Scale bar, 100μm.
(C) Representative IHC of YFP+ recombined cells and ASCL1+ activated NSCs in the DG of Rb-TKO mice, 14 days after injection with indicated mCherry+ expression lentivector. Scale bar, 100μm.
(D) Representative IHC of YFP+ recombined and Ki67+ proliferating cells in the DG of Rb-TKO mice, 14 days after injection with indicated mCherry+ expression lentivector. Scale bar, 100μm.

Error bars, mean ± STD.

Figure 1

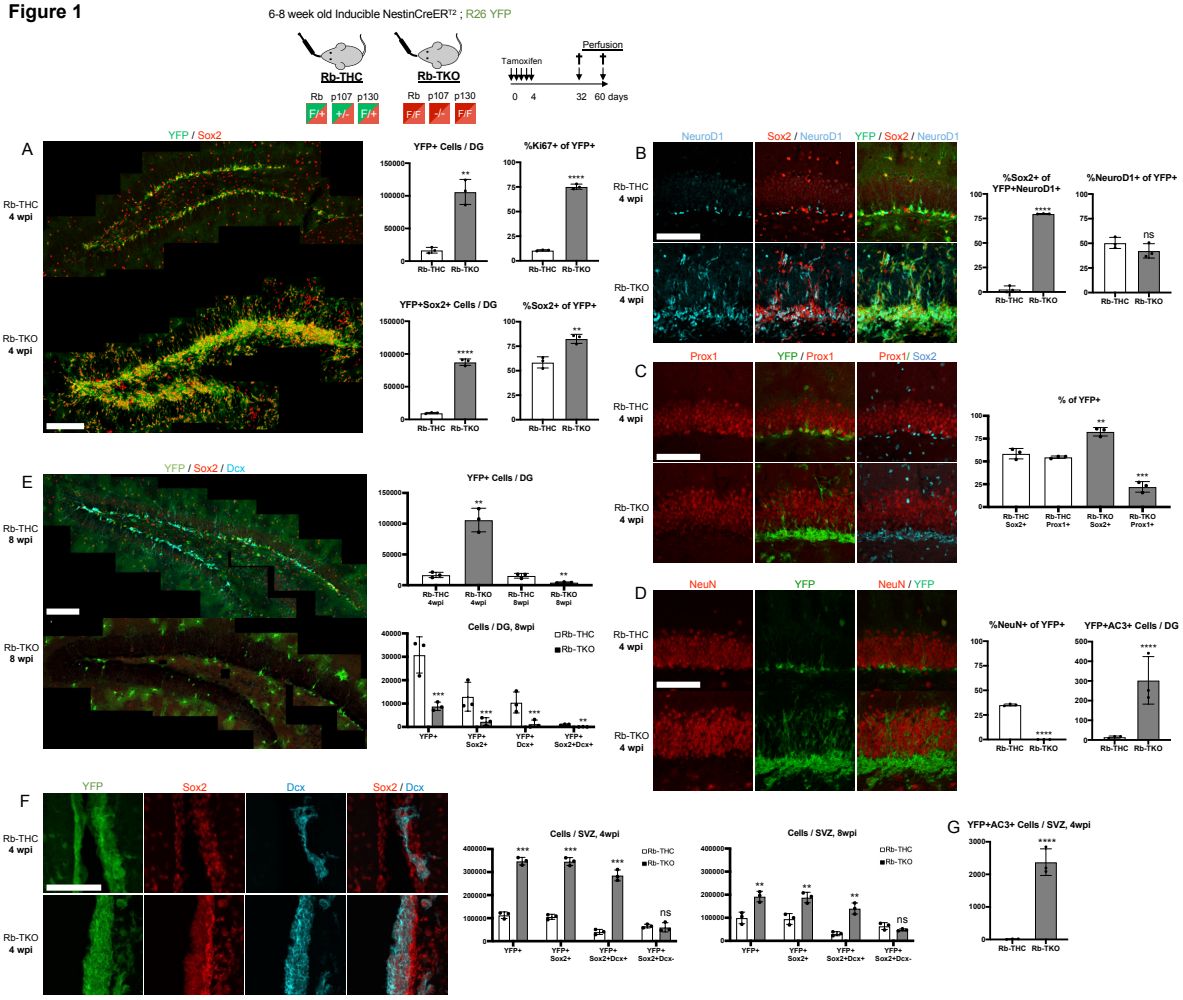
6-8 week old Inducible NestinCreER^T2 ; R26 YFP
Rb-THC
Rb-TKO
Rb p107 p130
F/+ +/- F/F
Rb p107 p130
F/F -/- F/F
Tamoxifen
Perfusion
0 4 32 60 days
A
YFP / Sox2
Rb-THC 4 wpi
Rb-TKO 4 wpi
YFP+ Cells / DG
%Ki67+ of YFP+
YFP+Sox2+ Cells / DG
%Sox2+ of YFP+
B
NeuroD1
Sox2 / NeuroD1
YFP / Sox2 / NeuroD1
%Sox2+ of YFP+NeuroD1+
%NeuroD1+ of YFP+
C
Prox1
YFP / Prox1
Prox1/ Sox2
% of YFP+
D
NeuN
YFP
NeuN / YFP
%NeuN+ of YFP+
YFP+AC3+ Cells / DG
E
YFP / Sox2 / Dcx
Rb-THC 8 wpi
Rb-TKO 8 wpi
YFP+ Cells / DG
Cells / DG, 8wpi
F
YFP
Sox2
Dcx
Sox2 / Dcx
Cells / SVZ, 4wpi
Cells / SVZ, 8wpi
G
YFP+AC3+ Cells / SVZ, 4wpi

Figure 2

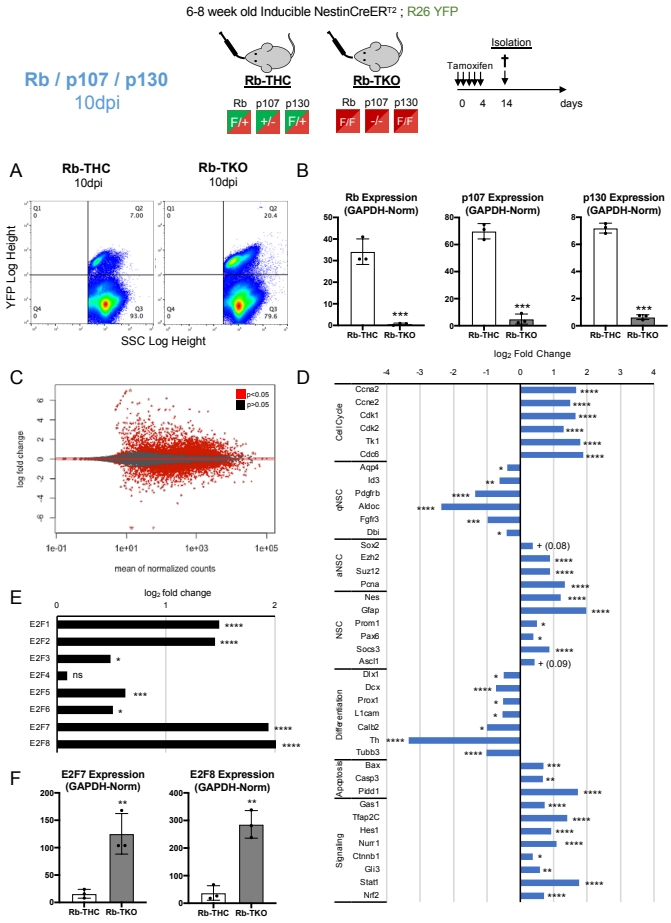
6-8 week old Inducible NestinCreER^{T2} ; R26 YFP
Rb / p107 / p130
10dpi
Rb-THC
Rb-TKO
Rb p107 p130
F/+ +/- F/+
Rb p107 p130
F/F -/- F/F
Isolation
Tamoxifen
0 4 14
days
A
Rb-THC 10dpi
Rb-TKO 10dpi
YFP Log Height
SSC Log Height
B
Rb Expression (GAPDH-Norm)
p107 Expression (GAPDH-Norm)
p130 Expression (GAPDH-Norm)
Rb-THC Rb-TKO
log2 Fold Change
C
p<0.05
p>0.05
log fold change
mean of normalized counts
D
Cell Cycle
qNSC
aNSC
NSC
Differentiation
Apoptosis
Signaling
E
log2 fold change
E2F1 E2F2 E2F3 E2F4 E2F5 E2F6 E2F7 E2F8
ns
F
E2F7 Expression (GAPDH-Norm)
E2F8 Expression (GAPDH-Norm)

Figure 3

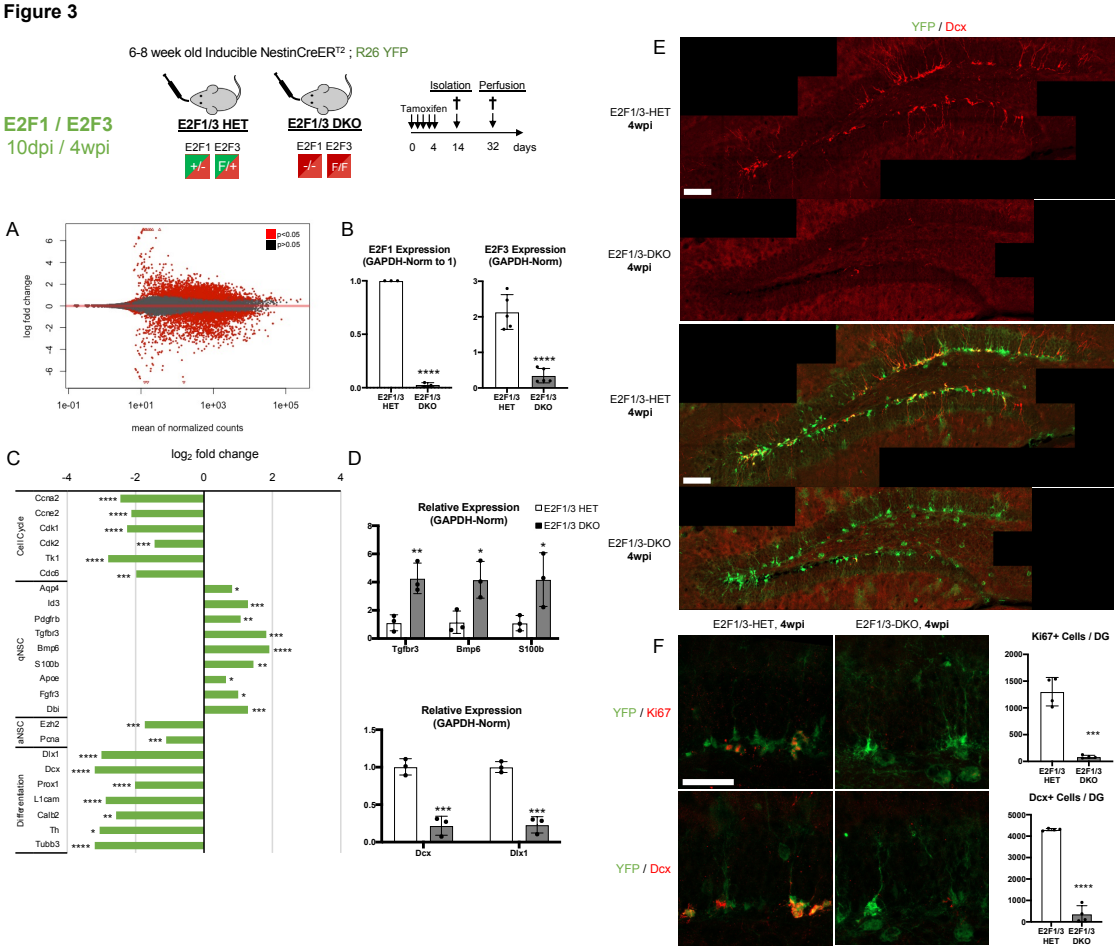
6-8 week old Inducible NestinCreER^{T2} ; R26 YFP
E2F1 / E2F3
10dpi / 4wpi
E2F1/3 HET
E2F1 E2F3
+/- F/+
E2F1/3 DKO
E2F1 E2F3
-/- F/F
Tamoxifen
Isolation
Perfusion
0 4 14 32 days
A
log fold change
mean of normalized counts
B
E2F1 Expression (GAPDH-Norm to 1)
E2F3 Expression (GAPDH-Norm)
E2F1/3 HET
E2F1/3 DKO
C
log$_2$ fold change
Cell Cycle
qNSC
aNSC
Differentiation
Ccne2
Ccne2
Cdk1
Cdk2
Tk1
Cdc6
Aqp4
Id3
Pdgfrb
Tgfbr3
Bmp6
S100b
Apoe
Fgfr3
Dbi
Ezh2
Pcna
Dlx1
Dcx
Prox1
L1cam
Calb2
Th
Tubb3
D
Relative Expression (GAPDH-Norm)
E2F1/3 HET
E2F1/3 DKO
Tgfbr3
Bmp6
S100b
Relative Expression (GAPDH-Norm)
Dcx
Dlx1
E
YFP / Dcx
E2F1/3-HET 4wpi
E2F1/3-DKO 4wpi
E2F1/3-HET 4wpi
E2F1/3-DKO 4wpi
F
E2F1/3-HET, 4wpi
E2F1/3-DKO, 4wpi
YFP / Ki67
YFP / Dcx
Ki67+ Cells / DG
Dcx+ Cells / DG
E2F1/3 HET
E2F1/3 DKO

Figure 4

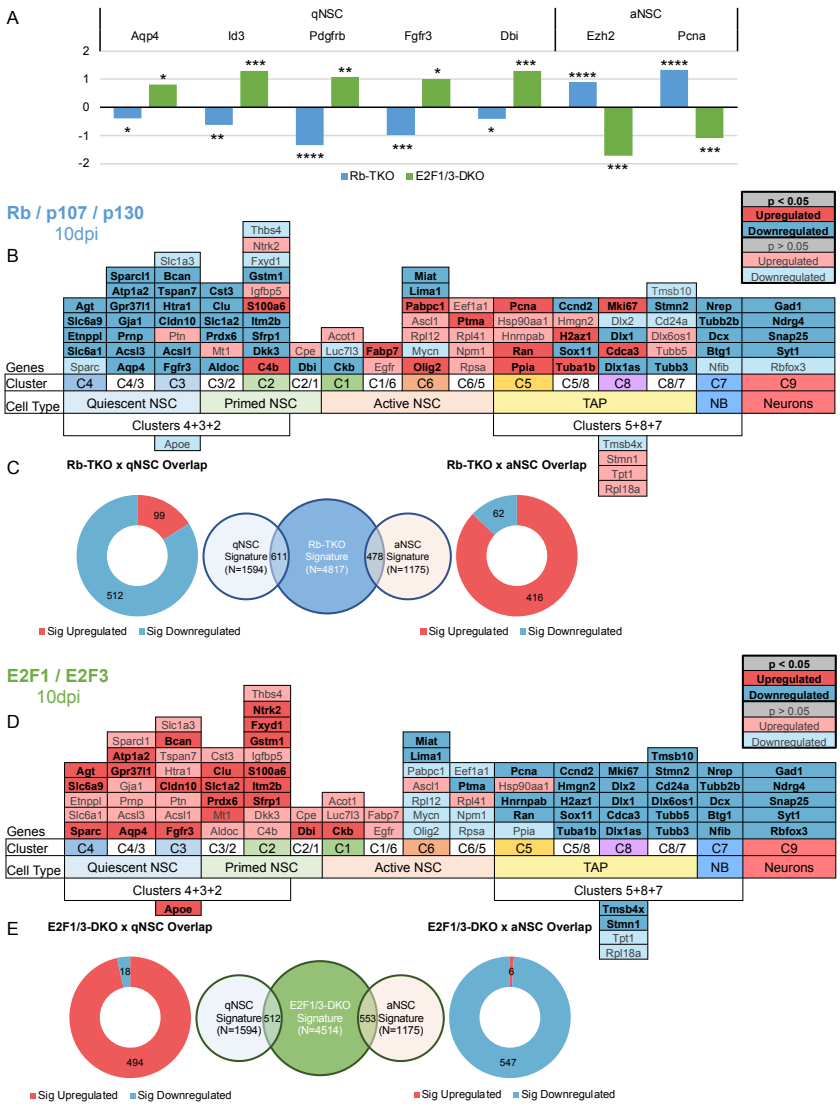
A
qNSC
aNSC
Aqp4
Id3
Pdgfrb
Fgfr3
Dbi
Ezh2
Pcna
Rb-TKO
E2F1/3-DKO
Rb / p107 / p130
10dpi
B
p < 0.05
Upregulated
Downregulated
p > 0.05
Upregulated
Downregulated
Genes
Cluster
Cell Type
Quiescent NSC
Primed NSC
Active NSC
TAP
NB
Neurons
Clusters 4+3+2
Clusters 5+8+7
C
Rb-TKO x qNSC Overlap
Rb-TKO x aNSC Overlap
qNSC Signature (N=1594)
Rb-TKO Signature (N=4817)
aNSC Signature (N=1175)
Sig Upregulated
Sig Downregulated
E2F1 / E2F3
10dpi
D
E
E2F1/3-DKO x qNSC Overlap
E2F1/3-DKO x aNSC Overlap
E2F1/3-DKO Signature (N=4514)

Figure 5

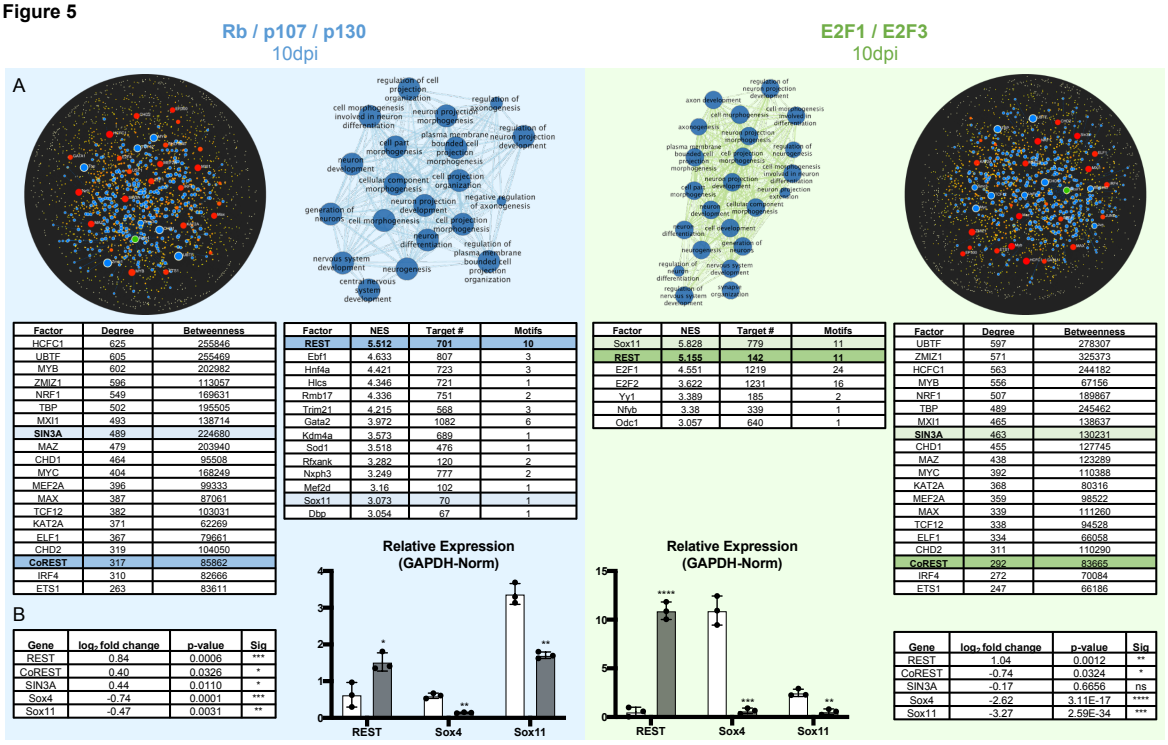

Factor	Degree	Betweenness
HCFC1	625	255846
UBTF	605	255469
MYB	602	202982
ZMIZ1	596	113057
NRF1	549	169631
TBP	502	195505
MXI1	493	138714
SIN3A	489	224680
MAZ	479	203940
CHD1	464	95508
MYC	404	168249
MEF2A	396	99333
MAX	387	87061
TCF12	382	103031
KAT2A	371	62269
ELF1	367	79861
CHD2	319	104050
CoREST	317	85862
IRF4	310	82666
ETS1	263	83611

Factor	NES	Target #	Motifs
REST	**5.512**	**701**	**10**
Ebf1	4.633	807	3
Hnf4a	4.421	723	3
Hlcs	4.346	721	1
Rmb17	4.336	751	2
Trim21	4.215	568	3
Gata2	3.972	1082	6
Kdm4a	3.573	689	1
Sod1	3.518	476	1
Rfxank	3.282	120	2
Nxph3	3.249	777	2
Mef2d	3.16	102	1
Sox11	3.073	70	1
Dbp	3.054	67	1

Gene	$\log_2$ fold change	p-value	Sig
REST	0.84	0.0006	***
CoREST	0.40	0.0326	*
SIN3A	0.44	0.0110	*
Sox4	-0.74	0.0001	***
Sox11	-0.47	0.0031	**

Factor	NES	Target #	Motifs
Sox11	5.828	779	11
REST	**5.155**	**142**	**11**
E2F1	4.551	1219	24
E2F2	3.622	1231	16
Yy1	3.389	185	2
Nfyb	3.38	339	1
Odc1	3.057	640	1

Factor	Degree	Betweenness
UBTF	597	278307
ZMIZ1	571	325373
HCFC1	563	244182
MYB	556	67156
NRF1	507	189867
TBP	489	245462
MXI1	465	138637
SIN3A	463	130231
CHD1	455	127745
MAZ	438	123289
MYC	392	110388
KAT2A	368	80316
MEF2A	359	98522
MAX	339	111260
TCF12	338	94528
ELF1	334	66058
CHD2	311	110290
CoREST	292	83865
IRF4	272	70084
ETS1	247	66186

Gene	$\log_2$ fold change	p-value	Sig
REST	1.04	0.0012	**
CoREST	-0.74	0.0324	*
SIN3A	-0.17	0.6656	ns
Sox4	-2.62	3.11E-17	****
Sox11	-3.27	2.59E-34	***

Figure 6

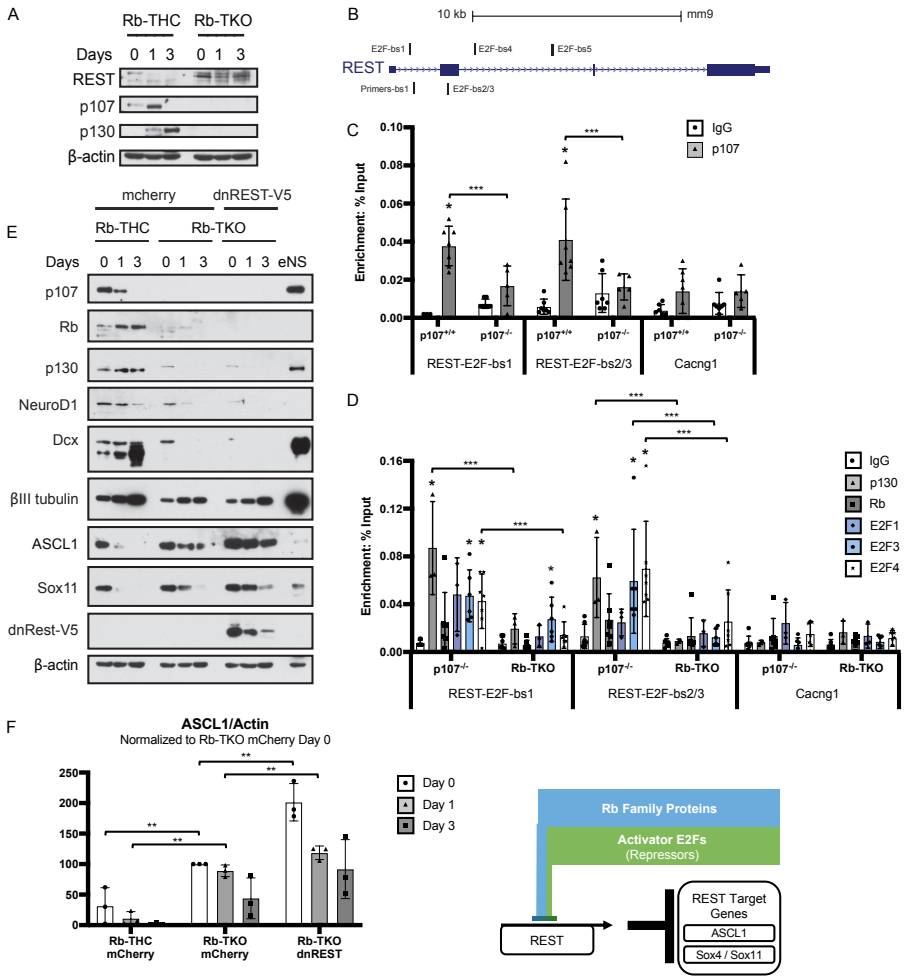
A
Rb-THC
Rb-TKO
Days 0 1 3 0 1 3
REST
p107
p130
β-actin
B
10 kb
mm9
E2F-bs1
E2F-bs4
E2F-bs5
REST
Primers-bs1
E2F-bs2/3
C
IgG
p107
Enrichment: % Input
REST-E2F-bs1
REST-E2F-bs2/3
Cacng1
D
IgG
p130
Rb
E2F1
E2F3
E2F4
Enrichment: % Input
REST-E2F-bs1
REST-E2F-bs2/3
Cacng1
E
mcherry
dnREST-V5
Rb-THC
Rb-TKO
Days 0 1 3 0 1 3 0 1 3 eNS
p107
Rb
p130
NeuroD1
Dcx
βIII tubulin
ASCL1
Sox11
dnRest-V5
β-actin
F
ASCL1/Actin
Normalized to Rb-TKO mCherry Day 0
Rb-THC mCherry
Rb-TKO mCherry
Rb-TKO dnREST
Day 0
Day 1
Day 3
Rb Family Proteins
Activator E2Fs
(Repressors)
REST
REST Target Genes
ASCL1
Sox4 / Sox11

Figure 7

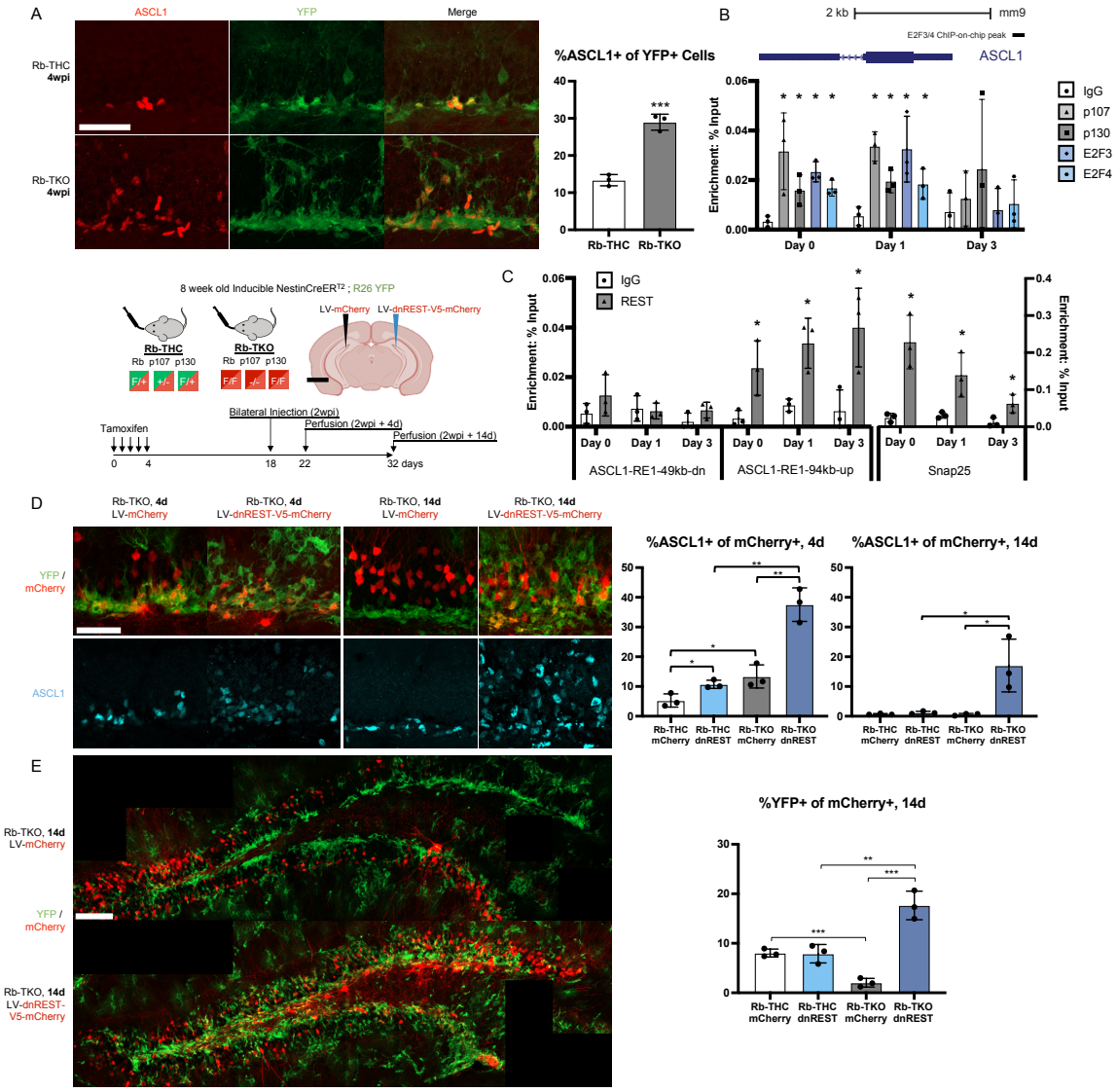
A
ASCL1
YFP
Merge
Rb-THC 4wpi
Rb-TKO 4wpi
8 week old Inducible NestinCreER^T2 ; R26 YFP
Rb-THC
Rb p107 p130
Rb-TKO
Rb p107 p130
LV-mCherry
LV-dnREST-V5-mCherry
Tamoxifen
Bilateral Injection (2wpi)
Perfusion (2wpi + 4d)
Perfusion (2wpi + 14d)
0
4
18
22
32 days
B
2 kb
mm9
E2F3/4 ChIP-on-chip peak
ASCL1
%ASCL1+ of YFP+ Cells
Rb-THC
Rb-TKO
Enrichment: % Input
Day 0
Day 1
Day 3
IgG
p107
p130
E2F3
E2F4
C
IgG
REST
Enrichment: % Input
ASCL1-RE1-49kb-dn
ASCL1-RE1-94kb-up
Snap25
D
Rb-TKO, 4d LV-mCherry
Rb-TKO, 4d LV-dnREST-V5-mCherry
Rb-TKO, 14d LV-mCherry
Rb-TKO, 14d LV-dnREST-V5-mCherry
YFP / mCherry
ASCL1
%ASCL1+ of mCherry+, 4d
%ASCL1+ of mCherry+, 14d
Rb-THC mCherry
Rb-THC dnREST
Rb-TKO mCherry
Rb-TKO dnREST
E
Rb-TKO, 14d LV-mCherry
YFP / mCherry
Rb-TKO, 14d LV-dnREST-V5-mCherry
%YFP+ of mCherry+, 14d

S1; Supplementary Figure 1

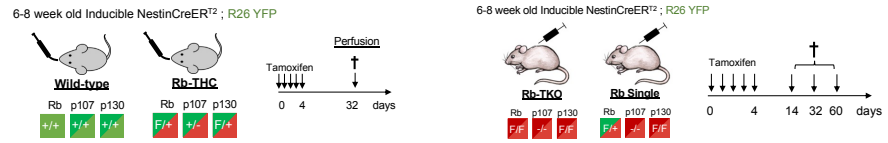

S1A

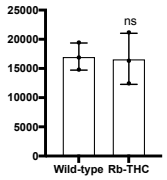

S1B

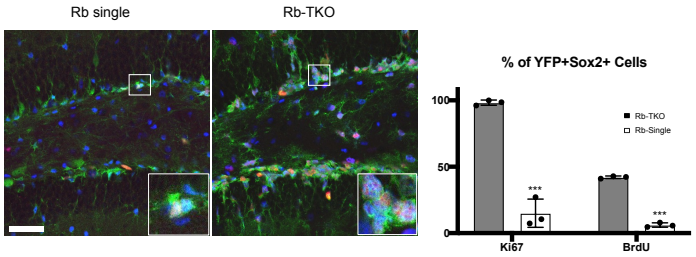

S1C

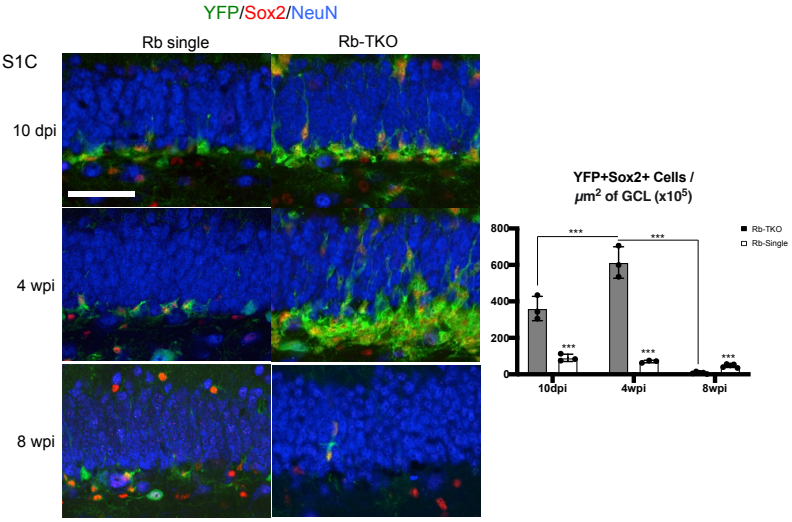

S2; Supplementary Figure 2

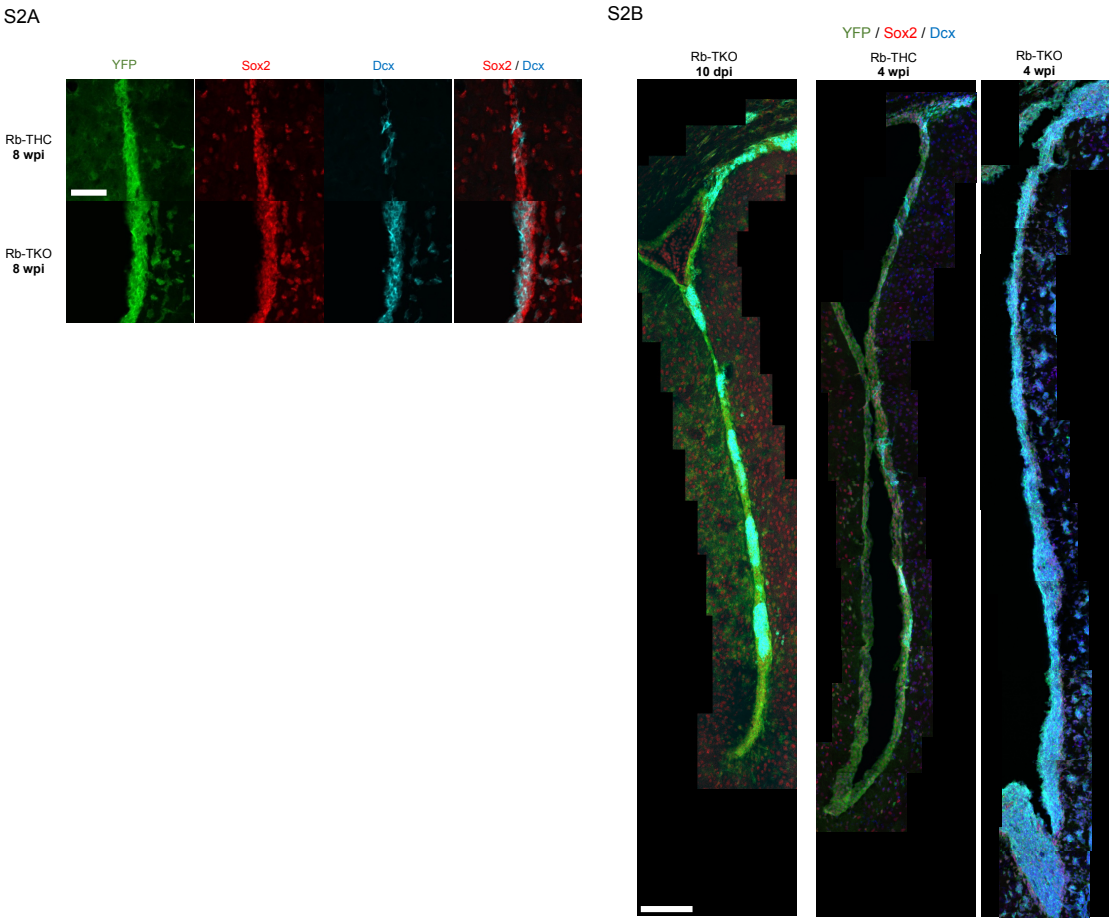

S3; Supplementary Figure 3

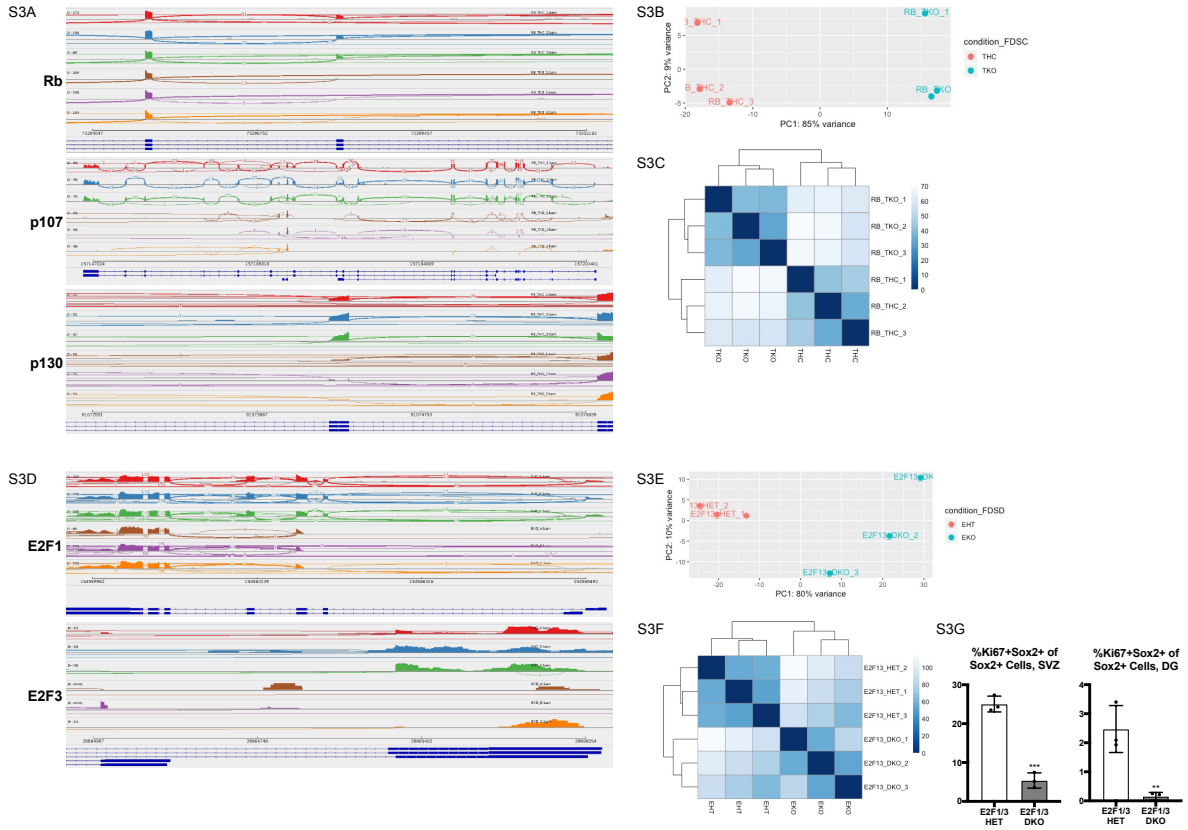

S4; Supplementary Figure 4

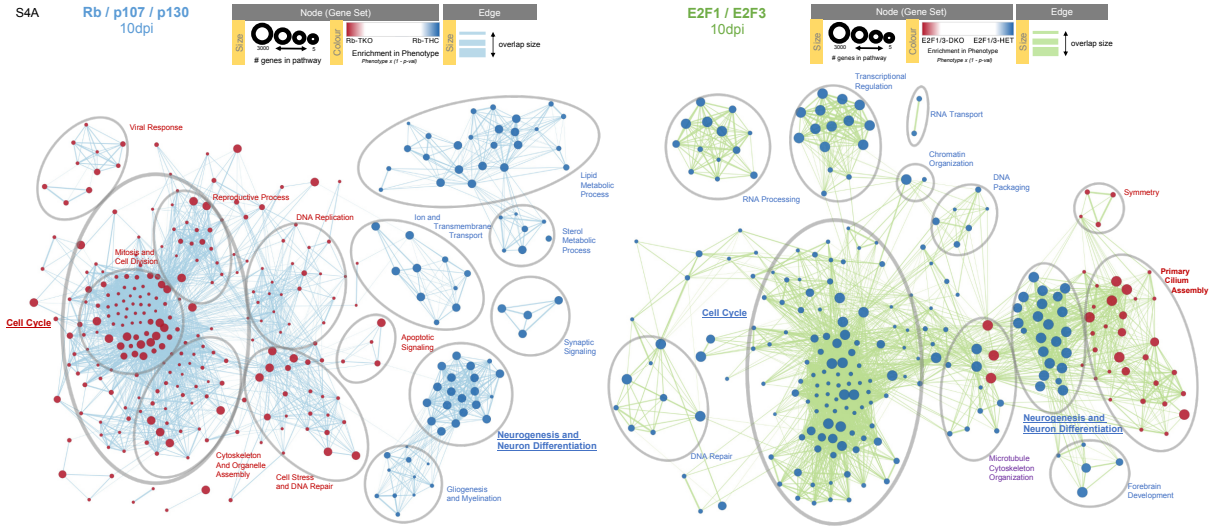

S4B

Curated Significant GO:BP Terms, Rb-TKO

	Upregulated	p-value
Cell Cycle	cell cycle process	2.04E-86
	cell cycle	2.43E-75
	mitotic cell cycle process	1.54E-73
	mitotic cell cycle	1.92E-71
	regulation of cell cycle	1.12E-37
	regulation of cell cycle process	3.88E-37

	Downregulated	p-value
Neurogenesis	nervous system development	5.13E-11
	neurogenesis	1.18E-10
	ensheathment of neurons	1.35E-09
	axon ensheathment	1.35E-09
	myelination	2.24E-08
	generation of neurons	1.42E-07
	neuron development	1.56E-07
	neuron differentiation	1.73E-07
	neuron projection development	6.80E-07

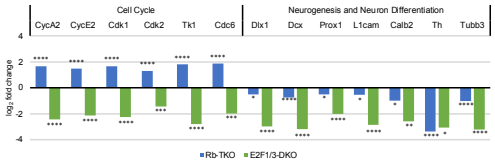

Curated Significant GO:BP Terms, E2F1/3-DKO

	Downregulated	p-value
Cell Cycle	mitotic cell cycle	1.41E-48
	cell cycle process	1.17E-46
	mitotic cell cycle process	3.87E-46
	cell cycle	1.88E-40
	regulation of cell cycle process	1.38E-20
	regulation of cell cycle	1.33E-19

		p-value
Neurogenesis	neuron projection development	1.74E-14
	neuron differentiation	4.64E-14
	neuron development	6.24E-14
	generation of neurons	7.09E-13
	neurogenesis	1.76E-12
	neuron projection morphogenesis	2.03E-12

S5; Supplementary Figure 5

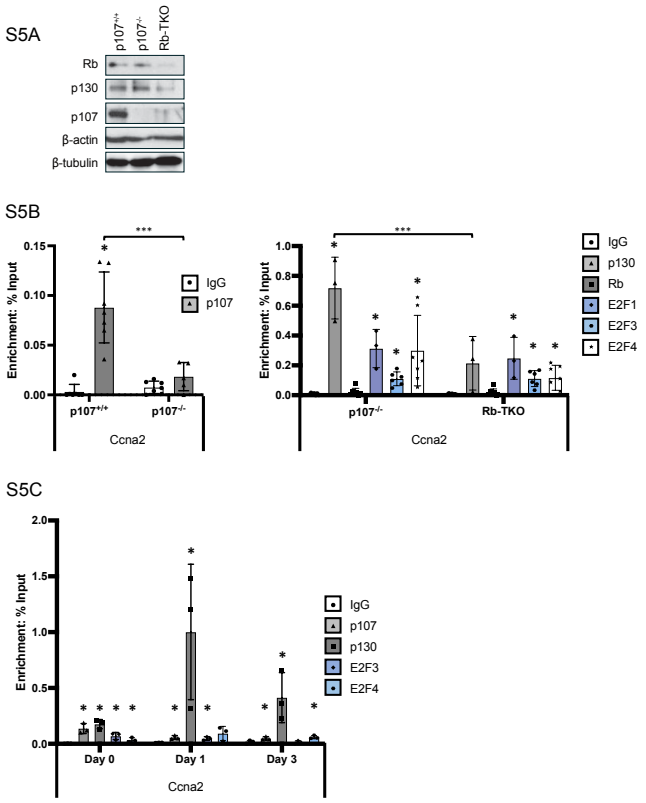

S6; Supplementary Figure 6

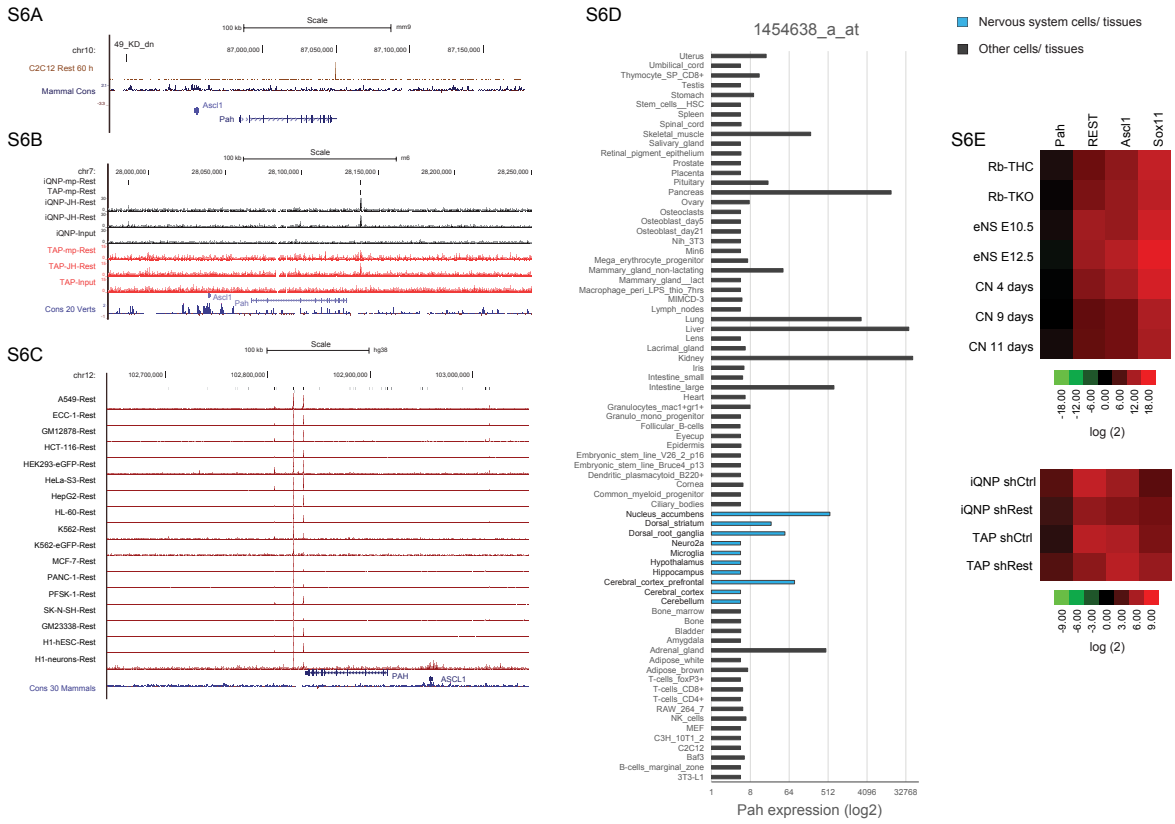

S7; Supplementary Figure 7

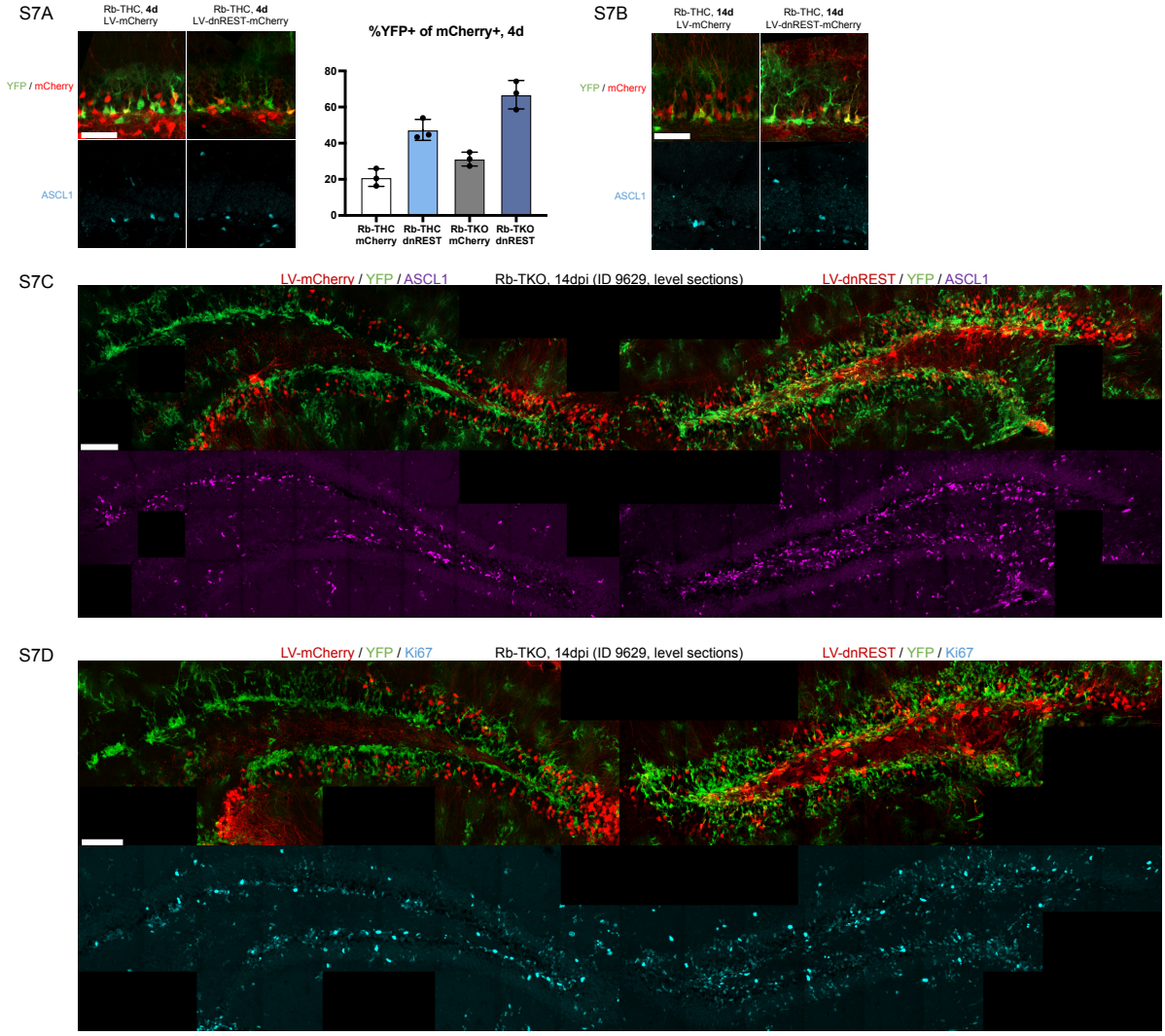

Supplementary Tables

Table 1: Antibodies

Antibody	Host	Supplier	Cat #	IHC Conc.	Usage
E2F1	Rabbit	Santa Cruz	sc-193		ChIP
E2F3	Rabbit	Abcam	ab-50917		ChIP
E2F4	Rabbit	Santa Cruz	sc-1082		ChIP
E2F4	Rabbit	NovusBio	NBP1-21374		ChIP
IgG	Rabbit	Signa-Aldrich	I8140		ChIP
p130	Rabbit	Santa Cruz	sc-317		ChIP
Rest	Rabbit	Millipore	07-579		ChIP
p107	Rabbit	Santa Cruz	sc-318		WB, ChIP
p130	Mouse	BD Biosciences	610262		WB, ChIP
Rb	Rabbit	Santa Cruz	sc-50		WB, ChIP
β-actin-HRP	Mouse	Santa Cruz	sc-47778		WB
βIII tubulin	Rabbit	Covance	PRB 435P		WB
Dcx	Rabbit	Cell signaling	4604		WB
Mash1	Mouse	BD Biosciences	556604		WB
NeuroD1	Goat	Santa Cruz	sc-1084		WB
Rest	Rabbit	Abcam	ab-21635		WB
Sox11	Rabbit	Abcam	ab-134107		WB
V5-tag	Rabbit	Bethyl	A190-120A		WB
YFP	Chicken	Abcam	ab13970	1:5000	IHC
Nestin	Goat	R&D Systems	AF2736	1:1000	IHC
GFAP	Mouse	Millipore	MAB3402	1:1000	IHC
Sox2	Goat	SCBT	sc-17320	1:500	IHC
Sox2	Goat	Neuromics	GT15098	1:500	IHC
Ascl1	Rabbit	Abcam	ab211327	1:500	IHC
Ki67	Rabbit	Cell Marque	275R	1:500	IHC
Tbr2	Rat	Invitrogen	14-4875-82	1:500	IHC
Dcx	Goat	SCBT	SC-8066	1:500	IHC
Dcx	Guinea Pig	Millipore	AB2253	1:1000	IHC
Dcx	Rabbit	Cell Signaling	4604S	1:500	IHC
NeuroD1	Goat	SCBT	sc-1084	1:500	IHC
Prox1	Rabbit	Millipore	AB5475	1:1000	IHC
NeuN	Rabbit	Millipore	MAB377	1:1000	IHC
Sox11	Rabbit	Abcam	ab134107	1:500	IHC
mCherry	Rat	ThermoFisher	M11217	1:2000	IHC
Active Caspase 3	Rabbit	Cell Signaling	9664S	1:250	IHC
S100-β	Rabbit	Dako	Z0311	1:400	IHC

Table 2: Genotyping Primers

	Primer A (5')	Primer B (3')	Primer C
Rb	CTC TAG ATC CTC TCA TTC TTC CC	CCT TGA CCA TAG CCC AGC AC	
p107	CAT GAA CAG ACT TGT CAT TCC AC	GC ACG AGA CTA GTG AGA CGT GC	TCG CTG GCA GTC TGA GTC AG AG
p130	GTG TTG TAA CAT TCT CGT GGG	GAC TGC TGG TAT TAG AAC CC	
E2F1	GGATATGATTCTTGGACTT CTTGG	CTAAATCTGACCACCAA ACGC	CAAGTGCCAGCGGGGC TGCTA
E2F3	GTGGCTGGAAGGGTGCCA AG	TGAATCATGGACAGAGC CAGG	GATTGATTCTGGGTTGT CAGG
ROSA26-GFP	GCGAAGAGTTTGTCCTCA ACC	GGAGCGGGAGAAATGG ATATG	AAAGTCGCTCTGAGTTG TTAT
Con-Cre (Cre)	GAACC TGATG GACAT GTTCA GG	AGTGC GTTCG AACGC TAGAG CCTGT	
Con-Cre (Control)	TTACG TCCAT CGTGG ACAGC	TGGGC TGGGT GTTAG CCTTA	

Table 3: qPCR Primers

	Forward (5')	Reverse (3')
Rb	TGCATCTTTATCGCAGCAGTT	GTTCACACGTCCGTTCTAATTTG
p107	CAAGAGTCAAGGAAGTTCGCA	TCGAAGGAGCAATTTTCAGCTTT
p130	AAGGCACATGCTAACCAATGAA	GAGCAGTTACCGCAGCATGA
E2F1	CTGCAGCAACTGCAGGAGAG	CTCCGAAAGCAGTTGCAGC
E2F3	GGTCCTGGATCTGAACAAGGC	CCTTCCAGCACGTTGGTGAT
E2F7	GCCAAGCAGGAAACAGAAGA	ACCGTGCCAACCATACTGAT
E2F8	GAGAAATCCCAGCCGAGTC	CATAAATCCGCCGACGTT
REST	GGCAGATGGCCGAATTGATG	CTTTGAGGTCAGCCGACTCT
Sox4	GAACGCCTTTATGGTGTGGT	GAACGGAATCTTGTCGCTGT
Sox11	CCCTGTCGCTGGTGGATAAG	GGTCGGAGAAGTTCGCCTC
Prox1	AGAAGGGTTGACATTGGAGTGA	TGCGTGTTGCACCACAGAATA
Tgfbr3	GTCCCTGTGTTTGTCCTGATG	AGCCAGACAGAACGGTGAAG
Bmp6	CAAGTCTTGCAGGAGCATCA	ATGTCAAATTCCAGCCAACC
S100b	GGTGACAAGCACAAGCIGAA	TCCATCACTTTGTCCACCAC
Dcx	ACACCCTTGATGGAAAGCAG	TTCAGGACCACAAGCAATGA
Dlx1	GAACCGGAGGTTCCAACAA	TGACCTGCGTCTGTGTGAGT
GAPDH	GGTGAAGGTCGGTGTGAACG	CTCGCTCCTGGAAGATGGTG

Table 4: ChIP Primers

Cyclin A2	TGT AAG ATT CCC GTC GGG CCT TC	AGG CGG GAG GAG CGT AGA GCC
Cacng1	GAC TTC TAT TAA TGC TTG TCA CTA GGC	GGG TAT TTC TAG CCC TCA GAT G
mREST	CTT TGA GGC TGG AGG TTG AG	GCT TGA CTT GGC CTA CTT GC
Ezh2	GCA AAT AGC TCA CCC CAT GT	GGG ATT TTG CCA TTC AGA TG
Sox4	TGCAATGAGAAGCTCCAAATC	GGAAAGAGGCAGCAGAAATC
Sox11	AGGGTTTTGTCCCGTCTCTC	TCCGAAGACCGTTACTCCAG
mRps26	CGA TAG TTC CAG AGC GGA AG	CAT GGC GTC TTA AGG TGG TT
Cdc6	TTC CTC CGA GGT CTC AAA AG	CGG CAG CCA ATA GGA CAG
Mybl2	CTC CCC TCT TCC CCA TGC	AAG GGG CGA AGC GTA CAA G

Tables 5 and 6 contain RNASeq information not enclosed in this thesis, but have been deposited as processed data tables in GEO under accession number GEO: GSE190766.

Methods

Animals

All experiments were approved by the Animal Care Ethics Committee of the University of Ottawa and adhered to the Guidelines of the Canadian Council on Animal Care. Animals were genotyped according to published protocols: primers are listed in Supplementary Table 2.

Rb-TKO (Rb conditional mutant; p107 -/-; p130 conditional mutant) mice were provided by J. Sage (Viatour et al., 2008), and crossed with Nestin-CreER^{T2} (Cicero et al., 2009); R26-stop-enhanced yellow fluorescent protein (YFP) (Srinivas et al., 2001) mice, a gift from S. Baker. All Rb-TKO mice were maintained on a mixed 129Sv/J X C57/BL6 background; Rb-THC mice were generated by crossing Rb-TKO mice with wild-type 129Sv/J X C57/BL6 mice from Charles River to generate a triple-heterozygous control.

E2F1/3-DKO (E2F1 -/- (Field et al., 1996); E2F3 conditional mutant (Wu et al., 2001)) mice were provided by G. Leone, and crossed with Nestin-CreER^{T2};R26EYFP mice described above. All E2F1/3-DKO mice were maintained on a mixed FVB/N X 129Sv/J X C57/BL6 background; E2F1/3-HET mice were generated by crossing E2F1/3-DKO mice with wild-type FVB/N X 129Sv/J X C57/BL6 mice from Charles River to generate a double-heterozygous control. All Nestin-CreER^{T2} animals used were heterozygotes for Cre expression. In all experiments, both females and males were used; all animals were 6-10 weeks old upon initial intervention.

For Cre induction in adult NestinCreERT2 animals, mice were administered tamoxifen (TAM) at 200 mg/kg/d for 5d (gavage; dissolved in 10% EtOH/90% corn oil), with initial weight used for dose calculation; weight after final injection was monitored, and semi-weekly wellness checks were performed until euthanization. Tamoxifen administration in Figures S1B-C was 150 mg/kg/d for 5d (ip; dissolved in 10% EtOH/90% sunflower oil). To analyze cell proliferation, NestinCreERT2 mice were given a single injection of EdU (50mg/kg, i.p) 2 hours before euthanization and perfusion.

Histology

Tissue perfusion and fixation was performed as previously described (McClellan et al., 2007). Briefly, animals were perfused transcardially with 4% paraformaldehyde, immersed in PFA overnight, and immersed in 20% sucrose for long-term storage. After removing the cerebellum to establish a flat coronal edge, fixed brains were frozen between -30 and -40 ºC prior to sectioning.

Brains were serially sectioned into 30 µm coronal sections, maintaining temperature between -18 and -20ºC, and collecting the SVZ and hippocampal formation. Wells containing free-floating 1:9 serial sections were stored long-term at 4ºC.

Imunohistochemistry and Imaging, Cell Quantification, Statistical Analysis

Immunohistochemistry was performed as previously described (Vandenbosch et al., 2016). Antibodies are listed in Supplementary Table 1.

Sections for quantifications of colocalized cells were imaged using Zeiss LSM510, and later Zeiss LSM800 confocal microscopes, employing a 40x objective. Z-stacks spanned 10 µm of post-processing section width, with 2.0 µm spacing between Z-positions. Sections quantifying single labelling were quantified on an Olympus BX-51 microscope. Images were analyzed using Fiji (Schindelin et al., 2012).

For cell quantification in the adult SGZ, every ninth section throughout the DG was quantified and counts were summed and multiplied by 9 to generate an estimate of the total number of cells in the DG. For cell quantification in the adult SVZ, given the larger structure, every eighteenth section throughout the SVZ was quantified and counts were summed and multiplied by 18 to generate an estimate of the total number of cells in the SVZ.

All statistical comparisons in this study were performed using an unpaired two-tailed t test. Differences were considered significant with a p value of < 0.05 (*), $^{**}p< 0.01$, $^{***}p < 0.001$, $^{****}p<0.0001$. Unless otherwise stated, all data is presented as the arithmetic mean, plus or minus the standard deviation of the mean (mean ± STD). For each experiment, biological replicates of 3-5 animals per genotype were used.

FACS and RNA isolation

Isolation of YFP+ cell population was performed as previously described (Iqbal, Fong, Slack, in press), employing tissue micro-dissected from mice 10 days post-tamoxifen injection. The YFP+ cell population was FACS-isolated using a cutoff of 488-FL-Log-Height ≥ 10^2. For RNA-Seq input, cell pellets containing minimum 200,000 YFP+ cells were frozen, and RNA isolated using the Arcturus® PicoPure® RNA Isolation Kit (ThermoFisher). Cell pellets were divided into four: I was sent for fragment analysis at OHRI StemCore Facility; II was used for qPCR validation of knockout or differential gene expression; III was sent for sequencing; IV was reserved as a backup.

qRT-PCR and RNASeq

Samples for RNA quantification were prepared using the Rotor-Gene SYBR® Green PCR Kit (Qiagen) and quantified on a Qiagen Rotor-Gene Q Real-Time PCR Machine. RNA concentrations for each primer set were normalized using standard curves prepared from wild-type adult NSCs as standard. Primers used are listed in Supplementary Table 3, and RNA quantifications are expressed relative to GAPDH (normalized to 1).

For RNA-seq RNA input for NGS was only considered sufficient if three criteria were met: 1) concentration ≥7 ng/uL, for submission of minimum 35ng of RNA, 2) 260/280 ≥ 2 and RQN ≥ 8.0. RNASeq was performed at TCAG at the Hospital for Sick Children, following internal QC. Samples were run in sets of 6, reflecting 3 biological replicates. cDNA conversion used the SMART-Seq® v4 Ultra® Low Input RNA Kit for Sequencing (Clontech, now Takara), while Library Preparation used the Nextera XT DNA Library Preparation Kit (Illumina). Sequencing was performed on an Illumina HiSeq 2500, using a multiplexed PE126bp high output flow cell.

Bioinformatic Analysis
Raw reads as FastQ files were first validated as downloads using md5sum and subjected to FastQC (Andrews et al., 2012) to ensure run quality and suitability for the standard protocol of analysis without trimming or phred scores. For alignment, FastQ files were aligned to Hisat2 GRCm38 index using HiSat2 (Kim et al., 2019) to generate BAM files. Aligned reads were visualized in IGV (Robinson et al., 2011). For read assignment, BAM files were converted to feature counts using featureCounts, part of the subread package (Liao et al., 2014), as well as the Ensembl GRCm38.101 GTF file, build dated August 2020.

Differential expression analysis of feature counts was established in R 3.5.3 (Team, 2021) using DESeq2 (Love et al., 2014), and employed Independent Hypothesis Weighting using the IHW package (Ignatiadis et al., 2016). For the Rb-TKO dataset, batch correction was employed to account for batch effects distinguishing samples RB_THC_1 and RB_TKO_1, stemming from sample preparation; effects are visible in Fig.S3C. Ensembl Stable IDs were converted to MGI symbols using biomaRt (Durinck et al., 2009).

The data discussed in this publication have been deposited in NCBI's Gene Expression Omnibus (Edgar et al., 2002) and are accessible through GEO Series accession number GSE190766 (https://www.ncbi.nlm.nih.gov/geo/query/acc.cgi?acc= GSE190766).

Network Analysis
Pathway and network enrichment analysis generally followed a published protocol (Reimand et al., 2019). Enrichment analysis with Gene Ontology: Biological Process was performed using g:GOSt and g:Convert as part of the g:Profiler toolset (Raudvere et al., 2019; Reimand et al., 2007), and visualized in Cytoscape 3.8.2 (Shannon et al., 2003) using Enrichment Map (Merico et al., 2010).

Gene regulatory network analysis was performed using iRegulon (Janky et al., 2014), analyzing a putative regulatory region spanning 20kb centred around the TSS, using a motif rankings database from 10 species; significant genes ($p<0.05$) were used as input. ENCODE TF-gene interactions were assessed using NetworkAnalyst (Zhou et al., 2019); all genes were used as input.

In Vitro Culture
Cells were isolated as previously described (Iqbal, Fong, Slack, in press), either as FACS-sorted YFP+ cells at 10dpi or microdissected from wild-type, Rb-THC or Rb-TKO mice. For the latter, to compensate for the absence of FACS, a separate rinse in DMEM:F12 was required to remove excess Percoll from the cell surface. Cells were plated at a concentration of 10 cells/µL in stem cell media as previously described (Reynolds and Weiss, 1992). Briefly, DMEM/F12 (Gibco 11330-032) is supplemented with B27 without Vitamin A (Gibco 12587010), EGF (Sigma E-1257), bFGF (Sigma F-0291), heparin (Sigma H-3149) and Penicillin/Streptomycin (Gibco 1570-063) to

encourage neurosphere growth. Neurospheres were passaged after 6-7 days, up to three times, plated at a concentration of 4 cells/µL.
For Differentiation Assay, plates were coated with 10% Matrigel (VWR CACB356230) in serum-free media. Cells were plated as neurospheres, and grown in differentiation media; DMEM/F12 supplemented with B27 with Vitamin A (Gibco 17504044), N2 (Gibco 17502048), 2% HI-FBS (Wisent 080-150) and Penicillin/Streptomycin. Cells were differentiated for 0, 1 and 3 days, with a media change on Day 2.

Lentiviral Vector Transduction
A pLVX-EF1a-IRES-mCherry lentiviral expression vector construct was commercially obtained (Clontech 631987) and used as control. A truncated, dominant-negative REST (Bergsland et al., 2006; Chen et al., 1998) with a V5 tag was cloned into the expression vector to generate a PLVX-E2F1a-dnREST-V5-IRES-mCherry. Lentiviruses were produced in 293T cells using PEI and ultracentrifugation, following established protocols (TANG et al., 2015), and was resuspended in PBS into small aliquots. Live titre using 293T cells confirmed achieving a minimum concentration of 1.2E+09 TU/mL. For use *in vitro*, passaged cells (Passage P2) were infected with lentiviral particles at a multiplicity of infection (MOI) of 30, before neurosphere differentiation after 5-7 days.

Stereotaxic Injections
Bilateral injections of lentivirus were performed at the uOttawa Surgery Core by Dr. Anthony Carter. In order to target the SGZ, lentiviruses were bilaterally injected into the dentate gyrus following published co-ordinates (Xi et al., 2016): -1.7mm anterior/posterior, ±1.2 mediolateral, -2.4mm dorsoventral from Bregma. The injection volume was 1.0 µL, at a rate of 0.2 µL/min.

Western Blot
Cell pellets of cultured adult NSCs were solubilized in a lysis buffer containing 20 mM Tris pH 6.8, 6M urea and 0.1% SDS as previously described (Liu et al., 2010). 20 mg of proteins were separated on 10% SDS-PAGE following standard protocols. After transfer and blocking, membranes were incubated with primary antibodies overnight at 4° C, washed 3 times with TTTBS buffer (Tris-buffered saline, TBS with 0.05% TritonX-100 and 0.05% Tween 20), incubated with HRP-tagged secondary antibody for 1 hour, and washed at room temperature. Alternatively, β-actin blot was incubated for 1 hour at room temperature. Finally, signal was developed using Clarity Enhanced chemiluminescence Western Blotting Substrate (BioRad). Antibodies used in Western Blot are listed in Supplementary Table 2. Western blot bands were quantified using ImageJ (Schneider et al., 2012).

ChIP
ChIP assays followed by quantitative real-time PCR (qPCR) were performed as previously described (Julian et al., 2016; Liu et al., 2010). 10 µg of 30 min cross-linked chromatin and 0.8 µg of antibodies were used in ChIP assays. Antibodies are listed in Supplementary Table 1, and qPCR primers are listed in Supplementary Table 4.

ChIP-seq analysis

ChIP-seq data on REST in C2C12 myocytes was performed by Barbara Wold lab at Caltech (Davis et al., 2018; Dunham et al., 2012) under the ENCODE accession number ENCSR000AIS. ChIP-seq data on REST in rat cells (QNP and TAP) were performed by (Mukherjee et al., 2016) and obtained from NCBI as Short Reads Archive under accession number SRP060618. ChIP-seq data on REST in human cells were released by the ENCODE project (Davis et al., 2018; Dunham et al., 2012) and performed by the Michael Snyder's laboratory at Stanford (HEK293 eGFP-REST, ENCSR896UBV; K562, ENCSR137ZMQ; K562 eGFP-REST, ENCSR054JMQ), Bradley Bernstein's laboratory at Broad Institute (A549, ENCSR892DRK; H1-hESC, ENCSR663WAR) or Richard Myers' laboratory at HAIB (GM23338, ENCSR871KYB; HCT-116, ENCSR000BVI; MCF-7, ENCSR000BSP; PFSK-1, ENCSR000BOX; HeLa-S3, ENCSR000BMN; H1-hESC, ENCSR000BHM; GM12878, ENCSR000BQS; HL-60, ENCSR000BTF; PANC-1, ENCSR000BUP; k562, ENCSR000BMW; SK-N-SH, ENCSR000BJJ; HepG2, ENCSR000BJL; H1-neurons, ENCSR000BTV; ECC-1, ENCSR000BUU). The data were obtained from NCBI under accession numbers SRP008797 (ECC-1, GM12878, H1-hESC, H1-neurons, HCT-116, HeLa-S3, HepG2, HL-60, k562, MCF-7, PANC-1, PFSK-1, SK-N-SH) and SRP012412 (A549, GM23338, H1-hESC, HEK293 eGFP-REST, K562, K562 eGFP-REST). Sequencing read data were analyzed following ENCODE pipeline. Conditions with more than one technical or biological replicates were combined into single FastQ files. Human data were aligned to the GRCh38 (hg38) version of the human genome, while rat data were aligned to the Rnor_6.0 (rn6) version of the rat genome.

References

Abderrahmani, A., Niederhauser, G., Lenain, V., Regazzi, R., and Waeber, G. (2005). The hairy and enhancer of split 1 is a negative regulator of the repressor element silencer transcription factor. Febs Lett *579*, 6199–6204. https://doi.org/10.1016/j.febslet.2005.09.093.

Adams, M.R., Sears, R., Nuckolls, F., Leone, G., and Nevins, J.R. (2000). Complex Transcriptional Regulatory Mechanisms Control Expression of the E2F3 Locus. Mol Cell Biol *20*, 3633–3639. https://doi.org/10.1128/mcb.20.10.3633-3639.2000.

Ajioka, I., Martins, R.A.P., Bayazitov, I.T., Donovan, S., Johnson, D.A., Frase, S., Cicero, S.A., Boyd, K., Zakharenko, S.S., and Dyer, M.A. (2007). Differentiated horizontal interneurons clonally expand to form metastatic retinoblastoma in mice. Cell *131*, 378–390. https://doi.org/10.1016/j.cell.2007.09.036.

Altman, J. (1962). Are New Neurons Formed in the Brains of Adult Mammals? Science *135*, 1127–1128. https://doi.org/10.1126/science.135.3509.1127.

ALTMAN, J., and DAS, G.D. (1965). Post-Natal Origin of Microneurones in the Rat Brain. Nature *207*, 953–956. https://doi.org/10.1038/207953a0.

Alvarez-Buylla, A., and Nottebohm, F. (1988). Migration of young neurons in adult avian brain. Nature *335*, 353–354. https://doi.org/10.1038/335353a0.

Andersen, J., Urban, N., Achimastou, A., Ito, A., Simic, M., Ullom, K., Martynoga, B., Lebel, M., Göritz, C., Frisén, J., et al. (2014). A transcriptional mechanism integrating inputs from extracellular signals to activate hippocampal stem cells. Neuron *83*, 1085–1097. https://doi.org/10.1016/j.neuron.2014.08.004.

Andrés, M.E., Burger, C., Peral-Rubio, M.J., Battaglioli, E., Anderson, M.E., Grimes, J., Dallman, J., Ballas, N., and Mandel, G. (1999). CoREST: A functional corepressor required for regulation of neural-specific gene expression. Proc National Acad Sci *96*, 9873–9878. https://doi.org/10.1073/pnas.96.17.9873.

Andreu, Z., Khan, M.A., González-Gómez, P., Negueruela, S., Hortigüela, R., Emeterio, J.S., Ferrón, S.R., Martínez, G., Vidal, A., Fariñas, I., et al. (2015). The cyclin-dependent kinase inhibitor p27 kip1 regulates radial stem cell quiescence and neurogenesis in the adult hippocampus. Stem Cells *33*, 219–229. https://doi.org/10.1002/stem.1832.

Andrews, S., Krueger, F., Segonds-Pichon, A., Biggins, L., Krueger, C., and Wingett, S. (2012). FastQC.

Andrusiak, M.G., Vandenbosch, R., Park, D.S., and Slack, R.S. (2012). The retinoblastoma protein is essential for survival of postmitotic neurons. J Neurosci *32*, 14809–14814. https://doi.org/10.1523/jneurosci.1912-12.2012.

Andrusiak, M.G., Vandenbosch, R., Dick, F.A., Park, D.S., and Slack, R.S. (2014). LXCXE-independent chromatin remodeling by Rb/E2f mediates neuronal quiescence. Cell Cycle *12*, 1416–1423. https://doi.org/10.4161/cc.24527.

Artegiani, B., Lindemann, D., and Calegari, F. (2011). Overexpression of cdk4 and cyclinD1 triggers greater expansion of neural stem cells in the adult mouse brain. The Journal of Experimental Medicine *208*, 937–948. https://doi.org/10.1084/jem.20102167.

Artegiani, B., Lyubimova, A., Muraro, M., Es, J.H. van, Oudenaarden, A. van, and Clevers, H. (2017). A Single-Cell RNA Sequencing Study Reveals Cellular and Molecular Dynamics of the Hippocampal Neurogenic Niche. Cell Reports *21*, 3271–3284. https://doi.org/10.1016/j.celrep.2017.11.050.

Bagchi, S., Weinmann, R., and Raychaudhuri, P. (1991). The retinoblastoma protein copurifies with E2F-I, an E1A-regulated inhibitor of the transcription factor E2F. Cell *65*, 1063–1072. https://doi.org/10.1016/0092-8674(91)90558-g.

Ballas, N., Grunseich, C., Lu, D.D., Speh, J.C., and Mandel, G. (2005). REST and Its Corepressors Mediate Plasticity of Neuronal Gene Chromatin throughout Neurogenesis. Cell *121*, 645–657. https://doi.org/10.1016/j.cell.2005.03.013.

Basak, O., Krieger, T.G., Muraro, M.J., Wiebrands, K., Stange, D.E., Frias-Aldeguer, J., Rivron, N.C., Wetering, M. van de, Es, J.H. van, Oudenaarden, A. van, et al. (2018). Troy+ brain stem cells cycle through quiescence and regulate their number by sensing niche occupancy. Proc National Acad Sci *115*, E610–E619. https://doi.org/10.1073/pnas.1715911114.

Baur, K., Abdullah, Y., Mandl, C., Hölzl-Wenig, G., Shi, Y., Edelkraut, U., Khatri, P., and Ciccolini, F. (2020). Basal neural stem cells in the subventricular zone drive postnatal neurogenesis with apical stem cells acting as proliferation gate-keepers. Biorxiv 2020.11.20.391102. https://doi.org/10.1101/2020.11.20.391102.

Beckervordersandforth, R., and Rolando, C. (2020). Untangling human neurogenesis to understand and counteract brain disorders. Curr Opin Pharmacol *50*, 67–73. https://doi.org/10.1016/j.coph.2019.12.002.

Belyaev, N.D., Wood, I.C., Bruce, A.W., Street, M., Trinh, J.-B., and Buckley, N.J. (2004). Distinct RE-1 Silencing Transcription Factor-containing Complexes Interact with Different Target Genes*. J Biol Chem *279*, 556–561. https://doi.org/10.1074/jbc.m310353200.

Berg, D.A., Su, Y., Jimenez-Cyrus, D., Patel, A., Huang, N., Morizet, D., Lee, S., Shah, R., Ringeling, F.R., Jain, R., et al. (2019). A Common Embryonic Origin of Stem Cells Drives

Developmental and Adult Neurogenesis. Cell *177*, 654-668.e15. https://doi.org/10.1016/j.cell.2019.02.010.

Berge, S.A. van den, Strien, M.E. van, Korecka, J.A., Dijkstra, A.A., Sluijs, J.A., Kooijman, L., Eggers, R., Filippis, L.D., Vescovi, A.L., Verhaagen, J., et al. (2011). The proliferative capacity of the subventricular zone is maintained in the parkinsonian brain. Brain *134*, 3249–3263. https://doi.org/10.1093/brain/awr256.

Bergmann, O., Liebl, J., Bernard, S., Alkass, K., Yeung, M.S.Y., Steier, P., Kutschera, W., Johnson, L., Landén, M., Druid, H., et al. (2012). The Age of Olfactory Bulb Neurons in Humans. Neuron *74*, 634–639. https://doi.org/10.1016/j.neuron.2012.03.030.

Bergsland, M., Werme, M., Malewicz, M., Perlmann, T., and Muhr, J. (2006). The establishment of neuronal properties is controlled by Sox4 and Sox11. Genes Dev *20*, 3475–3486. https://doi.org/10.1101/gad.403406.

Bertoli, C., and Bruin, R.A.M. de (2014). Turning cell cycle entry on its head. Elife *3*, e03475. https://doi.org/10.7554/elife.03475.

Beukelaers, P., Vandenbosch, R., Caron, N., Nguyen, L., Belachew, S., Moonen, G., Kiyokawa, H., Barbacid, M., Santamaria, D., and Malgrange, B. (2011). Cdk6-dependent regulation of G(1) length controls adult neurogenesis. Stem Cells *29*, 713–724. https://doi.org/10.1002/stem.616.

Blais, A., Oevelen, C.J.C. van, Margueron, R., Acosta-Alvear, D., and Dynlacht, B.D. (2007). Retinoblastoma tumor suppressor protein–dependent methylation of histone H3 lysine 27 is associated with irreversible cell cycle exit. J Cell Biology *179*, 1399–1412. https://doi.org/10.1083/jcb.200705051.

Blanchet, E., Annicotte, J.-S., Lagarrigue, S., Aguilar, V., Clapé, C., Chavey, C., Fritz, V., Casas, F., Apparailly, F., Auwerx, J., et al. (2011). E2F transcription factor-1 regulates oxidative metabolism. Nat Cell Biol *13*, 1146–1152. https://doi.org/10.1038/ncb2309.

Boldrini, M., Fulmore, C.A., Tartt, A.N., Simeon, L.R., Pavlova, I., Poposka, V., Rosoklija, G.B., Stankov, A., Arango, V., Dwork, A.J., et al. (2018). Human Hippocampal Neurogenesis Persists throughout Aging. Cell Stem Cell *22*, 589-599.e5. https://doi.org/10.1016/j.stem.2018.03.015.

Bonaguidi, M.A., Wheeler, M.A., Shapiro, J.S., Stadel, R.P., Sun, G.J., Ming, G., and Song, H. (2011). In Vivo Clonal Analysis Reveals Self-Renewing and Multipotent Adult Neural Stem Cell Characteristics. Cell *145*, 1142–1155. https://doi.org/10.1016/j.cell.2011.05.024.

Bonaguidi, M.A., Stadel, R.P., Berg, D.A., Sun, J., Ming, G.-L., and Song, H. (2016). Diversity of Neural Precursors in the Adult Mammalian Brain. Cold Spring Harbor Perspectives in Biology *8*, a018838-20. https://doi.org/10.1101/cshperspect.a018838.

Bond, A.M., Ming, G., and Song, H. (2015). Adult Mammalian Neural Stem Cells and Neurogenesis: Five Decades Later. Cell Stem Cell *17*, 385–395. https://doi.org/10.1016/j.stem.2015.09.003.

Borrett, M.J., Innes, B.T., Jeong, D., Tahmasian, N., Storer, M.A., Bader, G.D., Kaplan, D.R., and Miller, F.D. (2020). Single-Cell Profiling Shows Murine Forebrain Neural Stem Cells Reacquire a Developmental State when Activated for Adult Neurogenesis. Cell Reports *32*, 108022. https://doi.org/10.1016/j.celrep.2020.108022.

Brehm, A., and Kouzarides, T. (1999). Retinoblastoma protein meets chromatin. Trends Biochem Sci *24*, 142–145. https://doi.org/10.1016/s0968-0004(99)01368-7.

Brehm, A., Miska, E.A., McCance, D.J., Reid, J.L., Bannister, A.J., and Kouzarides, T. (1998). Retinoblastoma protein recruits histone deacetylase to repress transcription. Nature *391*, 597–601. https://doi.org/10.1038/35404.

Bruce, A.W., Donaldson, I.J., Wood, I.C., Yerbury, S.A., Sadowski, M.I., Chapman, M., Göttgens, B., and Buckley, N.J. (2004). Genome-wide analysis of repressor element 1 silencing transcription factor/neuron-restrictive silencing factor (REST/NRSF) target genes. P Natl Acad Sci Usa *101*, 10458–10463. https://doi.org/10.1073/pnas.0401827101.

Bruin, A. de, Maiti, B., Jakoi, L., Timmers, C., Buerki, R., and Leone, G. (2003). Identification and Characterization of E2F7, a Novel Mammalian E2F Family Member Capable of Blocking Cellular Proliferation*. J Biol Chem *278*, 42041–42049. https://doi.org/10.1074/jbc.m308105200.

Burke, J.R., Hura, G.L., and Rubin, S.M. (2012). Structures of inactive retinoblastoma protein reveal multiple mechanisms for cell cycle control. Gene Dev *26*, 1156–1166. https://doi.org/10.1101/gad.189837.112.

Burkhart, D.L., and Sage, J. (2008). Cellular mechanisms of tumour suppression by the retinoblastoma gene. Nat Rev Cancer *8*, 671–682. https://doi.org/10.1038/nrc2399.

Burkhart, D.L., Ngai, L.K., Roake, C.M., Viatour, P., Thangavel, C., Ho, V.M., Knudsen, E.S., and Sage, J. (2010). Regulation of RB Transcription In Vivo by RB Family Members. Molecular and Cellular Biology *30*, 1729–1745. https://doi.org/10.1128/mcb.00952-09.

Cajal, S.R. (1913). Sobre la degeneración y regeneracíon del sistema nervioso. Imprenta de Hijos de Nicolás Moya, Madrid *2*. .

Calderone, A., Jover, T., Noh, K., Tanaka, H., Yokota, H., Lin, Y., Grooms, S.Y., Regis, R., Bennett, M.V.L., and Zukin, R.S. (2003). Ischemic Insults Derepress the Gene Silencer REST in Neurons Destined to Die. J Neurosci *23*, 2112–2121. https://doi.org/10.1523/jneurosci.23-06-02112.2003.

Callaghan, D.A., Dong, L., Callaghan, S.M., Hou, Y.X., Dagnino, L., and Slack, R.S. (1999). Neural precursor cells differentiating in the absence of Rb exhibit delayed terminal mitosis and deregulated E2F 1 and 3 activity. Dev Biol *207*, 257–270. https://doi.org/10.1006/dbio.1998.9162.

Cam, H., Balciunaite, E., Blais, A., Spektor, A., Scarpulla, R.C., Young, R., Kluger, Y., and Dynlacht, B.D. (2004). A Common Set of Gene Regulatory Networks Links Metabolism and Growth Inhibition. Mol Cell *16*, 399–411. https://doi.org/10.1016/j.molcel.2004.09.037.

Carabalona, A., Beguin, S., Pallesi-Pocachard, E., Buhler, E., Pellegrino, C., Arnaud, K., Hubert, P., Oualha, M., Siffroi, J.P., Khantane, S., et al. (2012). A glial origin for periventricular nodular heterotopia caused by impaired expression of Filamin-A. Hum Mol Genet *21*, 1004–1017. https://doi.org/10.1093/hmg/ddr531.

Carleton, A., Petreanu, L.T., Lansford, R., Alvarez-Buylla, A., and Lledo, P.-M. (2003). Becoming a new neuron in the adult olfactory bulb. Nat Neurosci *6*, 507–518. https://doi.org/10.1038/nn1048.

Cartwright, P., Müller, H., Wagener, C., Holm, K., and Helin, K. (1998). E2F-6: a novel member of the E2F family is an inhibitor of E2F-dependent transcription. Oncogene *17*, 611–623. https://doi.org/10.1038/sj.onc.1201975.

Ceanga, M., Dahab, M., Witte, O.W., and Keiner, S. (2021). Adult Neurogenesis and Stroke: A Tale of Two Neurogenic Niches. Front Neurosci-Switz *15*, 700297. https://doi.org/10.3389/fnins.2021.700297.

Cebrian-Silla, A., Nascimento, M.A., Redmond, S.A., Mansky, B., Wu, D., Obernier, K., Rodriguez, R.R., Gonzalez-Granero, S., García-Verdugo, J.M., Lim, D.A., et al. (2021). Single-cell analysis of the ventricular-subventricular zone reveals signatures of dorsal and ventral adult neurogenesis. Elife *10*, e67436. https://doi.org/10.7554/elife.67436.

Chapouton, P., Skupien, P., Hesl, B., Coolen, M., Moore, J.C., Madelaine, R., Kremmer, E., Faus-Kessler, T., Blader, P., Lawson, N.D., et al. (2010). Notch activity levels control the balance between quiescence and recruitment of adult neural stem cells. J Neurosci *30*, 7961–7974. https://doi.org/10.1523/jneurosci.6170-09.2010.

Chellappan, S.P., Hiebert, S., Mudryj, M., Horowitz, J.M., and Nevins, J.R. (1991). The E2F transcription factor is a cellular target for the RB protein. Cell *65*, 1053–1061. https://doi.org/10.1016/0092-8674(91)90557-f.

Chen, D., Pacal, M., Wenzel, P., Knoepfler, P.S., Leone, G., and Bremner, R. (2009a). Division and apoptosis of E2f-deficient retinal progenitors. Nature *462*, 925–929. https://doi.org/10.1038/nature08544.

Chen, H.-Z., Tsai, S.-Y., and Leone, G. (2009b). Emerging roles of E2Fs in cancer: an exit from cell cycle control. Nat Rev Cancer *9*, 785–797. https://doi.org/10.1038/nrc2696.

Chen, Q., Liang, D., and Overbeek, P.A. (2008). Overexpression of E2F5/p130, but not E2F5 alone, can inhibit E2F-induced cell cycle entry in transgenic mice. Mol Vis *14*, 602–614. .

Chen, Z.-F., Paquette, A.J., and Anderson, D.J. (1998). NRSF/REST is required in vivo for repression of multiple neuronal target genes during embryogenesis. Nat Genet *20*, 136–142. https://doi.org/10.1038/2431.

Cheung, T.H., and Rando, T.A. (2013). Molecular regulation of stem cell quiescence. Nat Rev Mol Cell Biol *14*, 329–340. https://doi.org/10.1038/nrm3591.

Chiasson, B.J., Tropepe, V., Morshead, C.M., and Kooy, D. van der (1999). Adult Mammalian Forebrain Ependymal and Subependymal Cells Demonstrate Proliferative Potential, but only Subependymal Cells Have Neural Stem Cell Characteristics. J Neurosci *19*, 4462–4471. https://doi.org/10.1523/jneurosci.19-11-04462.1999.

Chkheidze, R., Raisanen, J., Gagan, J., Richardson, T.E., Pinho, M.C., Raj, K., Achilleos, M., Slepicka, C., White, C.L., Evers, B.M., et al. (2021). Alterations in the RB Pathway With Inactivation of RB1 Characterize Glioblastomas With a Primitive Neuronal Component. J Neuropath Exp Neur https://doi.org/10.1093/jnen/nlab109.

Chong, J.A., Tapia-Ramirez, J., Kim, S., Toledo-Aral, J.J., Zheng, Y., Boutros, M.C., Altshuller, Y.M., Frohman, M.A., Kraner, S.D., and Mandel, G. (1995). REST: A mammalian silencer protein that restricts sodium channel gene expression to neurons. Cell *80*, 949–957. https://doi.org/10.1016/0092-8674(95)90298-8.

Chong, J.-L., Wenzel, P.L., Sáenz-Robles, M.T., Nair, V., Ferrey, A., Hagan, J.P., Gomez, Y.M., Sharma, N., Chen, H.-Z., Ouseph, M., et al. (2009). E2f1-3 switch from activators in progenitor cells to repressors in differentiating cells. Nature *462*, 930–934. https://doi.org/10.1038/nature08677.

Christensen, J., Cloos, P., Toftegaard, U., Klinkenberg, D., Bracken, A.P., Trinh, E., Heeran, M., Stefano, L.D., and Helin, K. (2005). Characterization of E2F8, a novel E2F-like cell-cycle regulated repressor of E2F-activated transcription. Nucleic Acids Res *33*, 5458–5470. https://doi.org/10.1093/nar/gki855.

Cicero, S.A., Johnson, D., Reyntjens, S., Frase, S., Connell, S., Chow, L.M.L., Baker, S.J., Sorrentino, B.P., and Dyer, M.A. (2009). Cells previously identified as retinal stem cells are pigmented ciliary epithelial cells. Proceedings of the National Academy of Sciences *106*, 6685–6690. https://doi.org/10.1073/pnas.0901596106.

Classon, M., Salama, S., Gorka, C., Mulloy, R., Braun, P., and Harlow, E. (2000). Combinatorial roles for pRB, p107, and p130 in E2F-mediated cell cycle control. Proceedings of the National Academy of Sciences *97*, 10820–10825. https://doi.org/10.1073/pnas.190343497.

Cobrinik, D., Lee, M.H., Hannon, G., Mulligan, G., Bronson, R.T., Dyson, N., Harlow, E., Beach, D., Weinberg, R.A., and Jacks, T. (1996). Shared role of the pRB-related p130 and p107

proteins in limb development. Genes Dev *10*, 1633–1644. https://doi.org/10.1101/gad.10.13.1633.

Codega, P., Silva-Vargas, V., Paul, A., Maldonado-Soto, A.R., Deleo, A.M., Pastrana, E., and Doetsch, F. (2014). Prospective identification and purification of quiescent adult neural stem cells from their in vivo niche. Neuron *82*, 545–559. https://doi.org/10.1016/j.neuron.2014.02.039.

Cooper-Kuhn, C.M., Vroemen, M., Brown, J., Ye, H., Thompson, M.A., Winkler, J., and Kuhn, H.G. (2002). Impaired Adult Neurogenesis in Mice Lacking the Transcription Factor E2F1. Mol Cell Neurosci *21*, 312–323. https://doi.org/10.1006/mcne.2002.1176.

Coupé, P., Manjón, J.V., Lanuza, E., and Catheline, G. (2019). Lifespan Changes of the Human Brain In Alzheimer's Disease. Sci Rep-Uk *9*, 3998. https://doi.org/10.1038/s41598-019-39809-8.

Cuitiño, M.C., Pécot, T., Sun, D., Kladney, R., Okano-Uchida, T., Shinde, N., Saeed, R., Perez-Castro, A.J., Webb, A., Liu, T., et al. (2019). Two Distinct E2F Transcriptional Modules Drive Cell Cycles and Differentiation. Cell Reports *27*, 3547-3560.e5. https://doi.org/10.1016/j.celrep.2019.05.004.

Curtis, M.A., Penney, E.B., Pearson, A.G., Roon-Mom, W.M.C. van, Butterworth, N.J., Dragunow, M., Connor, B., and Faull, R.L.M. (2003). Increased cell proliferation and neurogenesis in the adult human Huntington's disease brain. Proc National Acad Sci *100*, 9023–9027. https://doi.org/10.1073/pnas.1532244100.

Dadwal, P., Mahmud, N., Sinai, L., Azimi, A., Fatt, M., Wondisford, F.E., Miller, F.D., and Morshead, C.M. (2015). Activating Endogenous Neural Precursor Cells Using Metformin Leads to Neural Repair and Functional Recovery in a Model of Childhood Brain Injury. Stem Cell Rep *5*, 166–173. https://doi.org/10.1016/j.stemcr.2015.06.011.

Dahiya, A., Gavin, M.R., Luo, R.X., and Dean, D.C. (2000). Role of the LXCXE Binding Site in Rb Function. Mol Cell Biol *20*, 6799–6805. https://doi.org/10.1128/mcb.20.18.6799-6805.2000.

Davis, C.A., Hitz, B.C., Sloan, C.A., Chan, E.T., Davidson, J.M., Gabdank, I., Hilton, J.A., Jain, K., Baymuradov, U.K., Narayanan, A.K., et al. (2018). The Encyclopedia of DNA elements (ENCODE): data portal update. Nucleic Acids Res *46*, D794–D801. https://doi.org/10.1093/nar/gkx1081.

DeGregori, J., and Johnson, D. (2006). Distinct and Overlapping Roles for E2F Family Members in Transcription, Proliferation and Apoptosis. Curr Mol Med *6*, 739–748. https://doi.org/10.2174/1566524010606070739.

Delgado, A.C., Maldonado-Soto, A.R., Silva-Vargas, V., Mizrak, D., Känel, T. von, Tan, K.R., Paul, A., Madar, A., Cuervo, H., Kitajewski, J., et al. (2021). Release of stem cells from quiescence reveals gliogenic domains in the adult mouse brain. Science *372*, 1205–1209. https://doi.org/10.1126/science.abg8467.

Denoth-Lippuner, A., and Jessberger, S. (2021). Formation and integration of new neurons in the adult hippocampus. Nat Rev Neurosci *22*, 223–236. https://doi.org/10.1038/s41583-021-00433-z.

Dick, F.A., and Rubin, S.M. (2013). Molecular mechanisms underlying RB protein function. Nat Rev Mol Cell Biol *14*, 297–306. https://doi.org/10.1038/nrm3567.

Doetsch, F., Verdugo, J.M.-G., Caille, I., Alvarez-Buylla, A., Chao, M.V., and Casaccia-Bonnefil, P. (2002). Lack of the Cell-Cycle Inhibitor p27Kip1 Results in Selective Increase of Transit-Amplifying Cells for Adult Neurogenesis. J Neurosci *22*, 2255–2264. https://doi.org/10.1523/jneurosci.22-06-02255.2002.

Donega, V., Burm, S.M., Strien, M.E. van, Bodegraven, E.J. van, Paliukhovich, I., Geut, H., Berg, W.D.J. van de, Li, K.W., Smit, A.B., Basak, O., et al. (2019). Transcriptome and proteome profiling of neural stem cells from the human subventricular zone in Parkinson's disease. Acta Neuropathologica Commun *7*, 84. https://doi.org/10.1186/s40478-019-0736-0.

Dunaief, J.L., Strober, B.E., Guha, S., Khavari, P.A., Ålin, K., Luban, J., Begemann, M., Crabtree, G.R., and Goff, S.P. (1994). The retinoblastoma protein and BRG1 form a complex and cooperate to induce cell cycle arrest. Cell *79*, 119–130. https://doi.org/10.1016/0092-8674(94)90405-7.

Dunham, I., Kundaje, A., Aldred, S.F., Collins, P.J., Davis, C.A., Doyle, F., Epstein, C.B., Frietze, S., Harrow, J., Kaul, R., et al. (2012). An Integrated Encyclopedia of DNA Elements in the Human Genome. Nature *489*, 57–74. https://doi.org/10.1038/nature11247.

Duque, A., and Spector, R. (2019). A balanced evaluation of the evidence for adult neurogenesis in humans: implication for neuropsychiatric disorders. Brain Struct Funct *224*, 2281–2295. https://doi.org/10.1007/s00429-019-01917-6.

Durinck, S., Spellman, P.T., Birney, E., and Huber, W. (2009). Mapping identifiers for the integration of genomic datasets with the R/Bioconductor package biomaRt. Nat Protoc *4*, 1184–1191. https://doi.org/10.1038/nprot.2009.97.

Dyson, N. (1998). The regulation of E2F by pRB-family proteins. Genes Dev *12*, 2245–2262. https://doi.org/10.1101/gad.12.15.2245.

Dyson, N., Howley, P.M., Münger, K., and Harlow, E. (1989). The Human Papilloma Virus-16 E7 Oncoprotein Is Able to Bind to the Retinoblastoma Gene Product. Science *243*, 934–937. https://doi.org/10.1126/science.2537532.

Edgar, R., Domrachev, M., and Lash, A.E. (2002). Gene Expression Omnibus: NCBI gene expression and hybridization array data repository. Nucleic Acids Res *30*, 207–210. https://doi.org/10.1093/nar/30.1.207.

Ehmer, U., Zmoos, A.-F., Auerbach, R.K., Vaka, D., Butte, A.J., Kay, M.A., and Sage, J. (2014). Organ Size Control Is Dominant over Rb Family Inactivation to Restrict Proliferation In Vivo. Cell Reports *8*, 371–381. https://doi.org/10.1016/j.celrep.2014.06.025.

Eriksson, P.S., Perfilieva, E., Björk-Eriksson, T., Alborn, A.-M., Nordborg, C., Peterson, D.A., and Gage, F.H. (1998). Neurogenesis in the adult human hippocampus. Nat Med *4*, 1313–1317. https://doi.org/10.1038/3305.

Ertaylan, G., Okawa, S., Schwamborn, J.C., and Sol, A. del (2014). Gene regulatory network analysis reveals differences in site-specific cell fate determination in mammalian brain. Front Cell Neurosci *8*, 437. https://doi.org/10.3389/fncel.2014.00437.

Esteves, M., Serra-Almeida, C., Saraiva, C., and Bernardino, L. (2020). New insights into the regulatory roles of microRNAs in adult neurogenesis. Curr Opin Pharmacol *50*, 38–45. https://doi.org/10.1016/j.coph.2019.11.003.

Favaro, R., Valotta, M., Ferri, A.L.M., Latorre, E., Mariani, J., Giachino, C., Lancini, C., Tosetti, V., Ottolenghi, S., Taylor, V., et al. (2009). Hippocampal development and neural stem cell maintenance require Sox2-dependent regulation of Shh. Nat Neurosci *12*, 1248–1256. https://doi.org/10.1038/nn.2397.

Felsani, A., Mileo, A.M., and Paggi, M.G. (2006). Retinoblastoma family proteins as key targets of the small DNA virus oncoproteins. Oncogene *25*, 5277–5285. https://doi.org/10.1038/sj.onc.1209621.

Ferguson, K.L., Vanderluit, J.L., Hébert, J.M., McIntosh, W.C., Tibbo, E., MacLaurin, J.G., Park, D.S., Wallace, V.A., Vooijs, M., McConnell, S.K., et al. (2002). Telencephalon-specific Rb knockouts reveal enhanced neurogenesis, survival and abnormal cortical development. The EMBO Journal *21*, 3337–3346. https://doi.org/10.1093/emboj/cdf338.

Ferland, R.J., Batiz, L.F., Neal, J., Lian, G., Bundock, E., Lu, J., Hsiao, Y.-C., Diamond, R., Mei, D., Banham, A.H., et al. (2009). Disruption of neural progenitors along the ventricular and subventricular zones in periventricular heterotopia. Hum Mol Genet *18*, 497–516. https://doi.org/10.1093/hmg/ddn377.

Field, S.J., Tsai, F.-Y., Kuo, F., Zubiaga, A.M., Kaelin, W.G., Livingston, D.M., Orkin, S.H., and Greenberg, M.E. (1996). E2F-1 Functions in Mice to Promote Apoptosis and Suppress Proliferation. Cell *85*, 549–561. https://doi.org/10.1016/s0092-8674(00)81255-6.

Fong, B.C., and Slack, R.S. (2017). RB: An essential player in adult neurogenesis. Neurogenesis *4*, e1270382–e1270382. https://doi.org/10.1080/23262133.2016.1270382.

Forristal, C., Henley, S.A., MacDonald, J.I., Bush, J.R., Ort, C., Passos, D.T., Talluri, S., Ishak, C.A., Thwaites, M.J., Norley, C.J., et al. (2014). Loss of the Mammalian DREAM Complex Deregulates Chondrocyte Proliferation. Molecular and Cellular Biology *34*, 2221–2234. https://doi.org/10.1128/mcb.01523-13.

Francke, U., and Kung, F. (1976). Sporadic bilateral retinoblastoma and 13q-chromosomal deletion. Med Pediatr Oncol *2*, 379–385. https://doi.org/10.1002/mpo.2950020404.

Franjic, D., Skarica, M., Ma, S., Arellano, J.I., Tebbenkamp, A.T.N., Choi, J., Xu, C., Li, Q., Morozov, Y.M., Andrijevic, D., et al. (2022). Transcriptomic taxonomy and neurogenic trajectories of adult human, macaque, and pig hippocampal and entorhinal cells. Neuron *110*, 452-469.e14. https://doi.org/10.1016/j.neuron.2021.10.036.

Friend, S.H., Bernards, R., Rogelj, S., Weinberg, R.A., Rapaport, J.M., Albert, D.M., and Dryja, T.P. (1986). A human DNA segment with properties of the gene that predisposes to retinoblastoma and osteosarcoma. Nature *323*, 643–646. https://doi.org/10.1038/323643a0.

Fuentealba, L.C., Rompani, S.B., Parraguez, J.I., Obernier, K., Romero, R., Cepko, C.L., and Alvarez-Buylla, A. (2015). Embryonic Origin of Postnatal Neural Stem Cells. Cell *161*, 1644–1655. https://doi.org/10.1016/j.cell.2015.05.041.

Furutachi, S., Matsumoto, A., Nakayama, K.I., and Gotoh, Y. (2013). p57 controls adult neural stem cell quiescence and modulates the pace of lifelong neurogenesis. The EMBO Journal *32*, 970–981. https://doi.org/10.1038/emboj.2013.50.

Furutachi, S., Miya, H., Watanabe, T., Kawai, H., Yamasaki, N., Harada, Y., Imayoshi, I., Nelson, M., Nakayama, K.I., Hirabayashi, Y., et al. (2015). Slowly dividing neural progenitors are an embryonic origin of adult neural stem cells. Nat Neurosci *18*, 657–665. https://doi.org/10.1038/nn.3989.

Gao, Z., Ure, K., Ding, P., Nashaat, M., Yuan, L., Ma, J., Hammer, R.E., and Hsieh, J. (2011). The Master Negative Regulator REST/NRSF Controls Adult Neurogenesis by Restraining the Neurogenic Program in Quiescent Stem Cells. The Journal of Neuroscience *31*, 9772–9786. https://doi.org/10.1523/jneurosci.1604-11.2011.

Gaubatz, S., Lindeman, G.J., Ishida, S., Jakoi, L., Nevins, J.R., Livingston, D.M., and Rempel, R.E. (2000). E2F4 and E2F5 Play an Essential Role in Pocket Protein–Mediated G1 Control. Mol Cell *6*, 729–735. https://doi.org/10.1016/s1097-2765(00)00071-x.

Gaubatz, S., Lees, J.A., Lindeman, G.J., and Livingston, D.M. (2001). E2F4 Is Exported from the Nucleus in a CRM1-Dependent Manner. Mol Cell Biol *21*, 1384–1392. https://doi.org/10.1128/mcb.21.4.1384-1392.2001.

Girling, R., Partridge, J.F., Bandara, L.R., Burden, N., Totty, N.F., Hsuan, J.J., and Thangue, N.B.L. (1993). A new component of the transcription factor DRTF1/E2F. Nature *362*, 83–87. https://doi.org/10.1038/362083a0.

Göckler, N., Jofre, G., Papadopoulos, C., Soppa, U., Tejedor, F.J., and Becker, W. (2009). Harmine specifically inhibits protein kinase DYRK1A and interferes with neurite formation. FEBS Journal *276*, 6324–6337. https://doi.org/10.1111/j.1742-4658.2009.07346.x.

Goldman, S.A., and Nottebohm, F. (1983). Neuronal production, migration, and differentiation in a vocal control nucleus of the adult female canary brain. Proc National Acad Sci *80*, 2390–2394. https://doi.org/10.1073/pnas.80.8.2390.

Gonçalves, J.T., Schafer, S.T., and Gage, F.H. (2016). Adult Neurogenesis in the Hippocampus: From Stem Cells to Behavior. Cell *167*, 897–914. https://doi.org/10.1016/j.cell.2016.10.021.

Götz, M., and Huttner, W.B. (2005). The cell biology of neurogenesis. Nat Rev Mol Cell Biol *6*, 777–788. https://doi.org/10.1038/nrm1739.

Gould, E., McEwen, B.S., Tanapat, P., Galea, L.A.M., and Fuchs, E. (1997). Neurogenesis in the Dentate Gyrus of the Adult Tree Shrew Is Regulated by Psychosocial Stress and NMDA Receptor Activation. J Neurosci *17*, 2492–2498. https://doi.org/10.1523/jneurosci.17-07-02492.1997.

Gould, E., Reeves, A.J., Fallah, M., Tanapat, P., Gross, C.G., and Fuchs, E. (1999). Hippocampal neurogenesis in adult Old World primates. Proc National Acad Sci *96*, 5263–5267. https://doi.org/10.1073/pnas.96.9.5263.

Gu, Y., Arruda-Carvalho, M., Wang, J., Janoschka, S.R., Josselyn, S.A., Frankland, P.W., and Ge, S. (2012). Optical controlling reveals time-dependent roles for adult-born dentate granule cells. Nat Neurosci *15*, 1700–1706. https://doi.org/10.1038/nn.3260.

Guemez-Gamboa, A., Coufal, N.G., and Gleeson, J.G. (2014). Primary Cilia in the Developing and Mature Brain. Neuron *82*, 511–521. https://doi.org/10.1016/j.neuron.2014.04.024.

Guiley, K.Z., Liban, T.J., Felthousen, J.G., Ramanan, P., Litovchick, L., and Rubin, S.M. (2015). Structural mechanisms of DREAM complex assembly and regulation. Genes Dev *29*, 961–974. https://doi.org/10.1101/gad.257568.114.

Hamilton, L.K., Dufresne, M., Joppé, S.E., Petryszyn, S., Aumont, A., Calon, F., Barnabé-Heider, F., Furtos, A., Parent, M., Chaurand, P., et al. (2015). Aberrant Lipid Metabolism in the Forebrain Niche Suppresses Adult Neural Stem Cell Proliferation in an Animal Model of Alzheimer's Disease. Cell Stem Cell *17*, 397–411. https://doi.org/10.1016/j.stem.2015.08.001.

Harada, Y., Yamada, M., Imayoshi, I., Kageyama, R., Suzuki, Y., Kuniya, T., Furutachi, S., Kawaguchi, D., and Gotoh, Y. (2021). Cell cycle arrest determines adult neural stem cell ontogeny by an embryonic Notch-nonoscillatory Hey1 module. Nat Commun *12*, 6562. https://doi.org/10.1038/s41467-021-26605-0.

Harris, L., Rigo, P., Stiehl, T., Gaber, Z.B., Austin, S.H.L., Masdeu, M. del M., Edwards, A., Urbán, N., Marciniak-Czochra, A., and Guillemot, F. (2021). Coordinated changes in cellular behavior ensure the lifelong maintenance of the hippocampal stem cell population. Cell Stem Cell *28*, 863-876.e6. https://doi.org/10.1016/j.stem.2021.01.003.

Helin, K., Harlow, E., and Fattaey, A. (1993a). Inhibition of E2F-1 transactivation by direct binding of the retinoblastoma protein. Mol Cell Biol *13*, 6501–6508. https://doi.org/10.1128/mcb.13.10.6501.

Helin, K., Wu, C.L., Fattaey, A.R., Lees, J.A., Dynlacht, B.D., Ngwu, C., and Harlow, E. (1993b). Heterodimerization of the transcription factors E2F-1 and DP-1 leads to cooperative trans-activation. Gene Dev *7*, 1850–1861. https://doi.org/10.1101/gad.7.10.1850.

Hochgerner, H., Zeisel, A., Lönnerberg, P., and Linnarsson, S. (2018). Conserved properties of dentate gyrus neurogenesis across postnatal development revealed by single-cell RNA sequencing. Nat Neurosci *21*, 1–15. https://doi.org/10.1038/s41593-017-0056-2.

Hsiao, K.M., McMahon, S.L., and Farnham, P.J. (1994). Multiple DNA elements are required for the growth regulation of the mouse E2F1 promoter. Gene Dev *8*, 1526–1537. https://doi.org/10.1101/gad.8.13.1526.

Hsieh, J. (2012). Orchestrating transcriptional control of adult neurogenesis. Genes Dev *26*, 1010–1021. https://doi.org/10.1101/gad.187336.112.

Hsu, J., Arand, J., Chaikovsky, A., Mooney, N.A., Demeter, J., Brison, C.M., Oliverio, R., Vogel, H., Rubin, S.M., Jackson, P.K., et al. (2019). E2F4 regulates transcriptional activation in mouse embryonic stem cells independently of the RB family. Nat Commun *10*, 2939. https://doi.org/10.1038/s41467-019-10901-x.

Hurford, R.K., Cobrinik, D., Lee, M.H., and Dyson, N. (1997). pRB and p107/p130 are required for the regulated expression of different sets of E2F responsive genes. Genes Dev *11*, 1447–1463. https://doi.org/10.1101/gad.11.11.1447.

Hwang, J.-Y., and Zukin, R.S. (2018). REST, a master transcriptional regulator in neurodegenerative disease. Current Opinion in Neurobiology *48*, 193–200. https://doi.org/10.1016/j.conb.2017.12.008.

Ignatiadis, N., Klaus, B., Zaugg, J.B., and Huber, W. (2016). Data-driven hypothesis weighting increases detection power in genome-scale multiple testing. Nature Methods *13*, 577–580. https://doi.org/10.1038/nmeth.3885.

Imayoshi, I., Sakamoto, M., Ohtsuka, T., Takao, K., Miyakawa, T., Yamaguchi, M., Mori, K., Ikeda, T., Itohara, S., and Kageyama, R. (2008). Roles of continuous neurogenesis in the structural and functional integrity of the adult forebrain. Nat Neurosci *11*, 1153–1161. https://doi.org/10.1038/nn.2185.

Jaafar, C., Omais, S., Lafi, S.A., Jamal, N.E., Noubani, M., Skaf, L., and Ghanem, N. (2016). Role of Rb during Neurogenesis and Axonal Guidance in the Developing Olfactory System. Frontiers in Molecular Neuroscience *9*, 171–15. https://doi.org/10.3389/fnmol.2016.00081.

Jacks, T., Fazeli, A., Schmitt, E.M., Bronson, R.T., Goodell, M.A., and Weinberg, R.A. (1992). Effects of an Rb mutation in the mouse. Nature *359*, 295–300. https://doi.org/10.1038/359295a0.

James, R., Kim, Y., Hockberger, P.E., and Szele, F.G. (2011). Subventricular Zone Cell Migration: Lessons from Quantitative Two-Photon Microscopy. Front Neurosci-Switz *5*, 30. https://doi.org/10.3389/fnins.2011.00030.

Janky, R., Verfaillie, A., Imrichová, H., Sande, B.V. de, Standaert, L., Christiaens, V., Hulselmans, G., Herten, K., Sanchez, M.N., Potier, D., et al. (2014). iRegulon: From a Gene List to a Gene Regulatory Network Using Large Motif and Track Collections. PLoS Computational Biology *10*, e1003731-19. https://doi.org/10.1371/journal.pcbi.1003731.

Jiang, Z., Deng, T., Jones, R., Li, H., Herschkowitz, J.I., Liu, J.C., Weigman, V.J., Tsao, M.-S., Lane, T.F., Perou, C.M., et al. (2010). Rb deletion in mouse mammary progenitors induces luminal-B or basal-like/EMT tumor subtypes depending on p53 status. J Clin Invest *120*, 3296–3309. https://doi.org/10.1172/jci41490.

Johnson, R., Teh, C.H., Kunarso, G., Wong, K.Y., Srinivasan, G., Cooper, M.L., Volta, M., Chan, S.S., Lipovich, L., Pollard, S.M., et al. (2008). REST Regulates Distinct Transcriptional Networks in Embryonic and Neural Stem Cells. PLoS Biol *6*, e256-15. https://doi.org/10.1371/journal.pbio.0060256.

Jørgensen, H.F., Terry, A., Beretta, C., Pereira, C.F., Leleu, M., Chen, Z.-F., Kelly, C., Merkenschlager, M., and Fisher, A.G. (2009). REST selectively represses a subset of RE1-containing neuronal genes in mouse embryonic stem cells. Development *136*, 715–721. https://doi.org/10.1242/dev.028548.

Julian, L.M., and Blais, A. (2015). Transcriptional control of stem cell fate by E2Fs and pocket proteins. Frontiers in Genetics *6*, 161. https://doi.org/10.3389/fgene.2015.00161.

Julian, L.M., Vandenbosch, R., Pakenham, C.A., Andrusiak, M.G., Nguyen, A.P., McClellan, K.A., Svoboda, D.S., Lagace, D.C., Park, D.S., Leone, G., et al. (2013). Opposing regulation of Sox2 by cell-cycle effectors E2f3a and E2f3b in neural stem cells. Cell Stem Cell *12*, 440–452. https://doi.org/10.1016/j.stem.2013.02.001.

Julian, L.M., Liu, Y., Pakenham, C.A., Dugal-Tessier, D., Ruzhynsky, V., Bae, S., Tsai, S.-Y., Leone, G., Slack, R.S., and Blais, A. (2016). Tissue-specific targeting of cell fate regulatory genes by E2f factors. Cell Death and Differentiation *23*, 565–575. https://doi.org/10.1038/cdd.2015.36.

Kalamakis, G., Brüne, D., Ravichandran, S., Bolz, J., Fan, W., Ziebell, F., Stiehl, T., Catalá-Martinez, F., Kupke, J., Zhao, S., et al. (2019). Quiescence Modulates Stem Cell Maintenance and Regenerative Capacity in the Aging Brain. Cell *176*, 1407-1419.e14. https://doi.org/10.1016/j.cell.2019.01.040.

Kaplan, M.S., and Hinds, J.W. (1977). Neurogenesis in the Adult Rat: Electron Microscopic Analysis of Light Radioautographs. Science *197*, 1092–1094. https://doi.org/10.1126/science.887941.

Kareta, M.S., Gorges, L.L., Hafeez, S., Benayoun, B.A., Marro, S., Zmoos, A.-F., Cecchini, M.J., Spacek, D., Batista, L.F.Z., O'Brien, M., et al. (2015). Inhibition of pluripotency networks by the Rb tumor suppressor restricts reprogramming and tumorigenesis. Cell Stem Cell *16*, 39–50. https://doi.org/10.1016/j.stem.2014.10.019.

Kawamura, M., Sato, S., Matsumoto, G., Fukuda, T., Shiba-Fukushima, K., Noda, S., Takanashi, M., Mori, N., and Hattori, N. (2019). Loss of nuclear REST/NRSF in aged-dopaminergic neurons in Parkinson's disease patients. Neurosci Lett *699*, 59–63. https://doi.org/10.1016/j.neulet.2019.01.042.

Kim, D., Paggi, J.M., Park, C., Bennett, C., and Salzberg, S.L. (2019). Graph-based genome alignment and genotyping with HISAT2 and HISAT-genotype. Nat Biotechnol *37*, 907–915. https://doi.org/10.1038/s41587-019-0201-4.

Kim, E., Cheng, Y., Bolton-Gillespie, E., Cai, X., Ma, C., Tarangelo, A., Le, L., Jambhekar, M., Raman, P., Hayer, K.E., et al. (2017). Rb family proteins enforce the homeostasis of quiescent hematopoietic stem cells by repressing Socs3 expression. The Journal of Experimental Medicine *214*, 1901–1912. https://doi.org/10.1084/jem.20160719.

Kim, E.J., Ables, J.L., Dickel, L.K., Eisch, A.J., and Johnson, J.E. (2011). Ascl1 (Mash1) Defines Cells with Long-Term Neurogenic Potential in Subgranular and Subventricular Zones in Adult Mouse Brain. Plos One *6*, e18472. https://doi.org/10.1371/journal.pone.0018472.

Kim, Y., Comte, I., Szabo, G., Hockberger, P., and Szele, F.G. (2009). Adult Mouse Subventricular Zone Stem and Progenitor Cells Are Sessile and Epidermal Growth Factor Receptor Negatively Regulates Neuroblast Migration. Plos One *4*, e8122. https://doi.org/10.1371/journal.pone.0008122.

Kippin, T.E., Martens, D.J., and Kooy, D. van der (2005). p21 loss compromises the relative quiescence of forebrain stem cell proliferation leading to exhaustion of their proliferation capacity. Genes Dev *19*, 756–767. https://doi.org/10.1101/gad.1272305.

Knopman, D.S., Amieva, H., Petersen, R.C., Chételat, G., Holtzman, D.M., Hyman, B.T., Nixon, R.A., and Jones, D.T. (2021). Alzheimer disease. Nat Rev Dis Primers *7*, 33. https://doi.org/10.1038/s41572-021-00269-y.

Knudsen, E.S., and Knudsen, K.E. (2008). Tailoring to RB: tumour suppressor status and therapeutic response. Nat Rev Cancer *8*, 714–724. https://doi.org/10.1038/nrc2401.

Kohyama, J., Sanosaka, T., Tokunaga, A., Takatsuka, E., Tsujimura, K., Okano, H., and Nakashima, K. (2010). BMP-induced REST regulates the establishment and maintenance of astrocytic identity. J Cell Biology *189*, 159–170. https://doi.org/10.1083/jcb.200908048.

Komori, H., Goto, Y., Kurayoshi, K., Ozono, E., Iwanaga, R., Bradford, A.P., Araki, K., and Ohtani, K. (2018). Differential requirement for dimerization partner DP between E2F-dependent activation of tumor suppressor and growth-related genes. Sci Rep-Uk *8*, 8438. https://doi.org/10.1038/s41598-018-26860-0.

Kooy, D. van der, and Weiss, and S. (2000). Why Stem Cells? Science *287*, 1439–1441. https://doi.org/10.1126/science.287.5457.1439.

Kornack, D.R., and Rakic, P. (1999). Continuation of neurogenesis in the hippocampus of the adult macaque monkey. Proc National Acad Sci *96*, 5768–5773. https://doi.org/10.1073/pnas.96.10.5768.

Kovesdi, I., Reichel, R., and Nevins, J.R. (1986). Identification of a cellular transcription factor involved in E1A trans-activation. Cell *45*, 219–228. https://doi.org/10.1016/0092-8674(86)90386-7.

Kowalczyk, A., Filipkowski, R.K., Rylski, M., Wilczynski, G.M., Konopacki, F.A., Jaworski, J., Ciemerych, M.A., Sicinski, P., and Kaczmarek, L. (2004). The critical role of cyclin D2 in adult neurogenesis. J Cell Biol *167*, 209–213. https://doi.org/10.1083/jcb.200404181.

Krek, W., Xu, G., and Livingston, D.M. (1995). Cyclin A-kinase regulation of E2F-1 DNA binding function underlies suppression of an S phase checkpoint. Cell *83*, 1149–1158. https://doi.org/10.1016/0092-8674(95)90141-8.

Kuhn, H., Dickinson-Anson, H., and Gage, F. (1996). Neurogenesis in the dentate gyrus of the adult rat: age-related decrease of neuronal progenitor proliferation. J Neurosci *16*, 2027–2033. https://doi.org/10.1523/jneurosci.16-06-02027.1996.

Kwon, J.S., Everetts, N.J., Wang, X., Wang, W., Croce, K.D., Xing, J., and Yao, G. (2017). Controlling Depth of Cellular Quiescence by an Rb-E2F Network Switch. Cell Reports *20*, 3223–3235. https://doi.org/10.1016/j.celrep.2017.09.007.

Lavado, A., Lagutin, O.V., Chow, L.M.L., Baker, S.J., and Oliver, G. (2010). Prox1 Is Required for Granule Cell Maturation and Intermediate Progenitor Maintenance During Brain Neurogenesis. PLoS Biol *8*, e1000460. https://doi.org/10.1371/journal.pbio.1000460.

LeCouter, J.E., Kablar, B., Whyte, P.F., Ying, C., and Rudnicki, M.A. (1998a). Strain-dependent embryonic lethality in mice lacking the retinoblastoma-related p130 gene. Development *125*, 4669–4679. .

LeCouter, J.E., Kablar, B., Hardy, W.R., Ying, C., Megeney, L.A., May, L.L., and Rudnicki, M.A. (1998b). Strain-dependent myeloid hyperplasia, growth deficiency, and accelerated cell cycle in mice lacking the Rb-related p107 gene. Mol Cell Biol *18*, 7455–7465. https://doi.org/10.1128/mcb.18.12.7455.

Lee, C., Chang, J.H., Lee, H.S., and Cho, Y. (2002a). Structural basis for the recognition of the E2F transactivation domain by the retinoblastoma tumor suppressor. Gene Dev *16*, 3199–3212. https://doi.org/10.1101/gad.1046102.

Lee, E.Y., Hu, N., Yuan, S.S., Cox, L.A., Bradley, A., Lee, W.H., and Herrup, K. (1994). Dual roles of the retinoblastoma protein in cell cycle regulation and neuron differentiation. Gene Dev *8*, 2008–2021. https://doi.org/10.1101/gad.8.17.2008.

Lee, E.Y., Cam, H., Ziebold, U., Rayman, J.B., Lees, J.A., and Dynlacht, B.D. (2002b). E2F4 loss suppresses tumorigenesis in Rb mutant mice. Cancer Cell *2*, 463–472. https://doi.org/10.1016/s1535-6108(02)00207-6.

Lee, J.-O., Russo, A.A., and Pavletich, N.P. (1998). Structure of the retinoblastoma tumour-suppressor pocket domain bound to a peptide from HPV E7. Nature *391*, 859–865. https://doi.org/10.1038/36038.

Lee, M.H., Williams, B.O., Mulligan, G., Mukai, S., Bronson, R.T., Dyson, N., Harlow, E., and Jacks, T. (1996). Targeted disruption of p107: functional overlap between p107 and Rb. Genes Dev *10*, 1621–1632. https://doi.org/10.1101/gad.10.13.1621.

Lee, N., Park, S.J., Haddad, G., Kim, D.-K., Park, S.-M., Park, S.K., and Choi, K.Y. (2016). Interactomic analysis of REST/ NRSF and implications of its functional links with the transcription suppressor TRIM28 during neuronal differentiation. Scientific Reports *6*, 1–14. https://doi.org/10.1038/srep39049.

Lee, W.-H., Shew, J.-Y., Hong, F.D., Sery, T.W., Donoso, L.A., Young, L.-J., Bookstein, R., and Lee, E.Y.H.P. (1987). The retinoblastoma susceptibility gene encodes a nuclear phosphoprotein associated with DNA binding activity. Nature *329*, 642–645. https://doi.org/10.1038/329642a0.

Lees, J.A., Saito, M., Vidal, M., Valentine, M., Look, T., Harlow, E., Dyson, N., and Helin, K. (1993). The retinoblastoma protein binds to a family of E2F transcription factors. Mol Cell Biol *13*, 7813–7825. https://doi.org/10.1128/mcb.13.12.7813.

Leone, G., DeGregori, J., Yan, Z., Jakoi, L., Ishida, S., Williams, R.S., and Nevins, J.R. (1998). E2F3 activity is regulated during the cell cycle and is required for the induction of S phase. Gene Dev *12*, 2120–2130. https://doi.org/10.1101/gad.12.14.2120.

Leone, G., Nuckolls, F., Ishida, S., Adams, M., Sears, R., Jakoi, L., Miron, A., and Nevins, J.R. (2000). Identification of a Novel E2F3 Product Suggests a Mechanism for Determining Specificity of Repression by Rb Proteins. Mol Cell Biol *20*, 3626–3632. https://doi.org/10.1128/mcb.20.10.3626-3632.2000.

Lepagnol-Bestel, A.-M., Zvara, A., Maussion, G., Quignon, F., Ngimbous, B., Ramoz, N., Imbeaud, S., Loe-Mie, Y., Benihoud, K., Agier, N., et al. (2009). DYRK1A interacts with the REST/NRSF-SWI/SNF chromatin remodelling complex to deregulate gene clusters involved in

the neuronal phenotypic traits of Down syndrome. Hum Mol Genet *18*, 1405–1414. https://doi.org/10.1093/hmg/ddp047.

Li, H., Collado, M., Villasante, A., Matheu, A., Lynch, C.J., Cañamero, M., Rizzoti, K., Carneiro, C., Martínez, G., Vidal, A., et al. (2012). p27(Kip1) directly represses Sox2 during embryonic stem cell differentiation. Cell Stem Cell *11*, 845–852. https://doi.org/10.1016/j.stem.2012.09.014.

Li, J., Ran, C., Li, E., Gordon, F., Comstock, G., Siddiqui, H., Cleghorn, W., Chen, H.-Z., Kornacker, K., Liu, C.-G., et al. (2008). Synergistic function of E2F7 and E2F8 is essential for cell survival and embryonic development. Developmental Cell *14*, 62–75. https://doi.org/10.1016/j.devcel.2007.10.017.

Liao, Y., Smyth, G.K., and Shi, W. (2014). featureCounts: an efficient general purpose program for assigning sequence reads to genomic features. Bioinformatics *30*, 923–930. https://doi.org/10.1093/bioinformatics/btt656.

Liban, T.J., Thwaites, M.J., Dick, F.A., and Rubin, S.M. (2016). Structural Conservation and E2F Binding Specificity within the Retinoblastoma Pocket Protein Family. Journal of Molecular Biology *428*, 1–25. https://doi.org/10.1016/j.jmb.2016.08.017.

Lindeman, G.J., Dagnino, L., Gaubatz, S., Xu, Y., Bronson, R.T., Warren, H.B., and Livingston, D.M. (1998). A specific, nonproliferative role for E2F-5 in choroid plexus function revealed by gene targeting. Gene Dev *12*, 1092–1098. https://doi.org/10.1101/gad.12.8.1092.

Litovchick, L., Sadasivam, S., Florens, L., Zhu, X., Swanson, S.K., Velmurugan, S., Chen, R., Washburn, M.P., Liu, X.S., and DeCaprio, J.A. (2007). Evolutionarily Conserved Multisubunit RBL2/p130 and E2F4 Protein Complex Represses Human Cell Cycle-Dependent Genes in Quiescence. Mol Cell *26*, 539–551. https://doi.org/10.1016/j.molcel.2007.04.015.

Liu, D.X., Nath, N., Chellappan, S.P., and Greene, L.A. (2005). Regulation of neuron survival and death by p130 and associated chromatin modifiers. Genes Dev *19*, 719–732. https://doi.org/10.1101/gad.1296405.

Liu, Y., Chu, A., Chakroun, I., Islam, U., and Blais, A. (2010). Cooperation between myogenic regulatory factors and SIX family transcription factors is important for myoblast differentiation. Nucleic Acids Res *38*, 6857–6871. https://doi.org/10.1093/nar/gkq585.

Lledo, P.-M., and Valley, M. (2016). Adult Olfactory Bulb Neurogenesis. Csh Perspect Biol *8*, a018945. https://doi.org/10.1101/cshperspect.a018945.

Llorens-Bobadilla, E., Zhao, S., Baser, A., Saiz-Castro, G., Zwadlo, K., and Martin-Villalba, A. (2015). Single-Cell Transcriptomics Reveals a Population of Dormant Neural Stem Cells that Become Activated upon Brain Injury. Cell Stem Cell *17*, 329–340. https://doi.org/10.1016/j.stem.2015.07.002.

Loh, Y.-H., Wu, Q., Chew, J.-L., Vega, V.B., Zhang, W., Chen, X., Bourque, G., George, J., Leong, B., Liu, J., et al. (2006). The Oct4 and Nanog transcription network regulates pluripotency in mouse embryonic stem cells. Nat Genet *38*, 431–440. https://doi.org/10.1038/ng1760.

Lois, C., and Alvarez-Buylla, A. (1994). Long-Distance Neuronal Migration in the Adult Mammalian Brain. Science *264*, 1145–1148. https://doi.org/10.1126/science.8178174.

Lois, C., García-Verdugo, J.-M., and Alvarez-Buylla, A. (1996). Chain Migration of Neuronal Precursors. Science *271*, 978–981. https://doi.org/10.1126/science.271.5251.978.

López-Sánchez, N., Garrido-García, A., Ramón-Landreau, M., Cano-Daganzo, V., and Frade, J.M. (2021). E2F4-Based Gene Therapy Mitigates the Phenotype of the Alzheimer's Disease Mouse Model 5xFAD. Neurotherapeutics 1–20. https://doi.org/10.1007/s13311-021-01151-1.

Love, M.I., Huber, W., and Anders, S. (2014). Moderated estimation of fold change and dispersion for RNA-seq data with DESeq2. Genome Biology *15*, 31–48. https://doi.org/10.1186/s13059-014-0550-8.

Lundberg, A.S., and Weinberg, R.A. (1998). Functional Inactivation of the Retinoblastoma Protein Requires Sequential Modification by at Least Two Distinct Cyclin-cdk Complexes. Mol Cell Biol *18*, 753–761. https://doi.org/10.1128/mcb.18.2.753.

MacPherson, D., Sage, J., Crowley, D., Trumpp, A., Bronson, R.T., and Jacks, T. (2003). Conditional Mutation of Rb Causes Cell Cycle Defects without Apoptosis in the Central Nervous System. Molecular and Cellular Biology *23*, 1044–1053. https://doi.org/10.1128/mcb.23.3.1044-1053.2003.

Mampay, M., and Sheridan, G.K. (2019). REST: An epigenetic regulator of neuronal stress responses in the young and ageing brain. Front Neuroendocrin *53*, 100744. https://doi.org/10.1016/j.yfrne.2019.04.001.

Marqués-Torrejón, M.Á., Porlan, E., Banito, A., Gómez-Ibarlucea, E., Lopez-Contreras, A.J., Fernández-Capetillo, Ó., Vidal, A., Gil, J., Torres, J., and Fariñas, I. (2013). Cyclin-dependent kinase inhibitor p21 controls adult neural stem cell expansion by regulating Sox2 gene expression. Cell Stem Cell *12*, 88–100. https://doi.org/10.1016/j.stem.2012.12.001.

Matsui, T., Nieto-Estévez, V., Kyrychenko, S., Schneider, J.W., and Hsieh, J. (2017). Retinoblastoma protein controls growth, survival and neuronal migration in human cerebral organoids. Development *144*, 1025–1034. https://doi.org/10.1242/dev.143636.

McClellan, K.A., and Slack, R.S. (2006). Novel functions for cell cycle genes in nervous system development. Cell Cycle (Georgetown, Tex.) *5*, 1506–1513. https://doi.org/10.4161/cc.5.14.2980.

McClellan, K.A., Ruzhynsky, V.A., Douda, D.N., Vanderluit, J.L., Ferguson, K.L., Chen, D., Bremner, R., Park, D.S., Leone, G., and Slack, R.S. (2007). Unique Requirement for Rb/E2F3 in Neuronal Migration: Evidence for Cell Cycle-Independent Functions. Molecular and Cellular Biology *27*, 4825–4843. https://doi.org/10.1128/mcb.02100-06.

McClellan, K.A., Vanderluit, J.L., Julian, L.M., Andrusiak, M.G., Dugal-Tessier, D., Park, D.S., and Slack, R.S. (2009). The p107/E2F Pathway Regulates Fibroblast Growth Factor 2 Responsiveness in Neural Precursor Cells. Molecular and Cellular Biology *29*, 4701–4713. https://doi.org/10.1128/mcb.01767-08.

McClelland, S., Brennan, G.P., Dubé, C., Rajpara, S., Iyer, S., Richichi, C., Bernard, C., and Baram, T.Z. (2014). The transcription factor NRSF contributes to epileptogenesis by selective repression of a subset of target genes. Elife *3*, e01267. https://doi.org/10.7554/elife.01267.

McGann, J.C., Spinner, M., Garg, S.K., Mullendorf, K., Woltjer, R.L., and Mandel, G. (2020). Genome-wide assessment of REST binding profiles reveals distinctions between human and mouse hippocampus. Biorxiv 2020.07.07.192229. https://doi.org/10.1101/2020.07.07.192229.

Merico, D., Isserlin, R., Stueker, O., Emili, A., and Bader, G.D. (2010). Enrichment Map: A Network-Based Method for Gene-Set Enrichment Visualization and Interpretation. Plos One *5*, e13984. https://doi.org/10.1371/journal.pone.0013984.

Meyer, K., Feldman, H.M., Lu, T., Drake, D., Lim, E.T., Ling, K.-H., Bishop, N.A., Pan, Y., Seo, J., Lin, Y.-T., et al. (2019). REST and Neural Gene Network Dysregulation in iPSC Models of Alzheimer's Disease. Cell Reports *26*, 1112-1127.e9. https://doi.org/10.1016/j.celrep.2019.01.023.

Mich, J.K., Signer, R.A., Nakada, D., Pineda, A., Burgess, R.J., Vue, T.Y., Johnson, J.E., and Morrison, S.J. (2014). Prospective identification of functionally distinct stem cells and neurosphere-initiating cells in adult mouse forebrain. Elife *3*, e02669. https://doi.org/10.7554/elife.02669.

Ming, G.-L., and Song, H. (2011). Adult neurogenesis in the mammalian brain: significant answers and significant questions. Neuron *70*, 687–702. https://doi.org/10.1016/j.neuron.2011.05.001.

Mirzadeh, Z., Merkle, F.T., Soriano-Navarro, M., Garcia-Verdugo, J.M., and Alvarez-Buylla, A. (2008). Neural Stem Cells Confer Unique Pinwheel Architecture to the Ventricular Surface in Neurogenic Regions of the Adult Brain. Cell Stem Cell *3*, 265–278. https://doi.org/10.1016/j.stem.2008.07.004.

Moberg, K., Starz, M.A., and Lees, J.A. (1996). E2F-4 switches from p130 to p107 and pRB in response to cell cycle reentry. Mol Cell Biol *16*, 1436–1449. https://doi.org/10.1128/mcb.16.4.1436.

Moreno, E., Pandit, S.K., Toussaint, M.J.M., Bongiovanni, L., Harkema, L., Essen, S.C. van, Liere, E.A. van, Westendorp, B., and Bruin, A. de (2021). Atypical E2Fs either Counteract or Cooperate with RB during Tumorigenesis Depending on Tissue Context. Cancers *13*, 2033. https://doi.org/10.3390/cancers13092033.

Moreno-Jiménez, E.P., Flor-García, M., Terreros-Roncal, J., Rábano, A., Cafini, F., Pallas-Bazarra, N., Ávila, J., and Llorens-Martín, M. (2019). Adult hippocampal neurogenesis is abundant in neurologically healthy subjects and drops sharply in patients with Alzheimer's disease. Nat Med *25*, 554–560. https://doi.org/10.1038/s41591-019-0375-9.

Morris, E.J., and Dyson, N.J. (2001). Retinoblastoma protein partners. Adv Cancer Res *82*, 1–54. https://doi.org/10.1016/s0065-230x(01)82001-7.

Morshead, C., and Kooy, D. van der (1992). Postmitotic death is the fate of constitutively proliferating cells in the subependymal layer of the adult mouse brain. J Neurosci *12*, 249–256. https://doi.org/10.1523/jneurosci.12-01-00249.1992.

Morshead, C.M., Reynolds, B.A., Craig, C.G., McBurney, M.W., Staines, W.A., Morassutti, D., Weiss, S., and Kooy, D. van der (1994). Neural stem cells in the adult mammalian forebrain: A relatively quiescent subpopulation of subependymal cells. Neuron *13*, 1071–1082. https://doi.org/10.1016/0896-6273(94)90046-9.

Morshead, C.M., Craig, C.G., and Kooy, D. van der (1998). In vivo clonal analyses reveal the properties of endogenous neural stem cell proliferation in the adult mammalian forebrain. Development *125*, 2251–2261. https://doi.org/10.1242/dev.125.12.2251.

Mortazavi, A., Thompson, E.C.L., Garcia, S.T., Myers, R.M., and Wold, B. (2006). Comparative genomics modeling of the NRSF/REST repressor network: From single conserved sites to genome-wide repertoire. Genome Research *16*, 1208–1221. https://doi.org/10.1101/gr.4997306.

Mu, Y., and Gage, F.H. (2011). Adult hippocampal neurogenesis and its role in Alzheimer's disease. Molecular Neurodegeneration *6*, 85. https://doi.org/10.1186/1750-1326-6-85.

Mu, L., Berti, L., Masserdotti, G., Covic, M., Michaelidis, T.M., Doberauer, K., Merz, K., Rehfeld, F., Haslinger, A., Wegner, M., et al. (2012). SoxC Transcription Factors Are Required for Neuronal Differentiation in Adult Hippocampal Neurogenesis. J Neurosci *32*, 3067–3080. https://doi.org/10.1523/jneurosci.4679-11.2012.

Mukherjee, S., Brulet, R., Zhang, L., and Hsieh, J. (2016). REST regulation of gene networks in adult neural stem cells. Nature Communications *7*, 1–14. https://doi.org/10.1038/ncomms13360.

Müller, H., Moroni, M.C., Vigo, E., Petersen, B.O., Bartek, J., and Helin, K. (1997). Induction of S-phase entry by E2F transcription factors depends on their nuclear localization. Mol Cell Biol *17*, 5508–5520. https://doi.org/10.1128/mcb.17.9.5508.

Mulligan, G., and Jacks, T. (1998). The retinoblastoma gene family: cousins with overlapping interests. Trends Genet *14*, 223–229. https://doi.org/10.1016/s0168-9525(98)01470-x.

Nam, S.C., Kim, Y., Dryanovski, D., Walker, A., Goings, G., Woolfrey, K., Kang, S.S., Chu, C., Chenn, A., Erdelyi, F., et al. (2007). Dynamic features of postnatal subventricular zone cell motility: A two-photon time-lapse study. J Comp Neurol *505*, 190–208. https://doi.org/10.1002/cne.21473.

Narasimha, A.M., Kaulich, M., Shapiro, G.S., Choi, Y.J., Sicinski, P., and Dowdy, S.F. (2014). Cyclin D activates the Rb tumor suppressor by mono-phosphorylation. Elife *3*, e02872. https://doi.org/10.7554/elife.02872.

Naser, R., Vandenbosch, R., Omais, S., Hayek, D., Jaafar, C., Lafi, S.A., Saliba, A., Baghdadi, M., Skaf, L., and Ghanem, N. (2016). Role of the Retinoblastoma protein, Rb, during adult neurogenesis in the olfactory bulb. Scientific Reports *6*, 20230. https://doi.org/10.1038/srep20230.

Nechiporuk, T., McGann, J., Mullendorff, K., Hsieh, J., Wurst, W., Floss, T., and Mandel, G. (2016). The REST remodeling complex protects genomic integrity during embryonic neurogenesis. Elife *5*, e09584. https://doi.org/10.7554/elife.09584.

Nesti, E., Corson, G.M., McCleskey, M., Oyer, J.A., and Mandel, G. (2014). C-terminal domain small phosphatase 1 and MAP kinase reciprocally control REST stability and neuronal differentiation. Proc National Acad Sci *111*, E3929–E3936. https://doi.org/10.1073/pnas.1414770111.

Nishihara, S., Tsuda, L., and Ogura, T. (2003). The canonical Wnt pathway directly regulates NRSF/REST expression in chick spinal cord. Biochem Bioph Res Co *311*, 55–63. https://doi.org/10.1016/j.bbrc.2003.09.158.

Obernier, K., Cebrian-Silla, A., Thomson, M., Parraguez, J.I., Anderson, R., Guinto, C., Rodriguez, J.R., García-Verdugo, J.M., and Alvarez-Buylla, A. (2018). Adult Neurogenesis Is Sustained by Symmetric Self- Renewal and Differentiation. Stem Cell *22*, 221-234.e8. https://doi.org/10.1016/j.stem.2018.01.003.

Ohm, T.G. (2007). The dentate gyrus in Alzheimer's disease. Prog Brain Res *163*, 723–740. https://doi.org/10.1016/s0079-6123(07)63039-8.

O'Leary, T.P., Askari, B., Lee, B., Darby, K., Knudson, C., Ash, A.M., Seib, D.R., Espinueva, D.F., and Snyder, J.S. (2021). Inhibiting adult neurogenesis differentially affects spatial learning in females and males. Biorxiv 2021.10.27.466135. https://doi.org/10.1101/2021.10.27.466135.

Opavsky, R., Tsai, S.-Y., Guimond, M., Arora, A., Opavska, J., Becknell, B., Kaufmann, M., Walton, N.A., Stephens, J.A., Fernandez, S.A., et al. (2007). Specific tumor suppressor function for E2F2 in Myc-induced T cell lymphomagenesis. Proc National Acad Sci *104*, 15400–15405. https://doi.org/10.1073/pnas.0706307104.

Oshikawa, M., Okada, K., Nakajima, K., and Ajioka, I. (2013). Cortical excitatory neurons become protected from cell division during neurogenesis in an Rb family-dependent manner. Development *140*, 2310–2320. https://doi.org/10.1242/dev.095653.

Otsuki, L., and Brand, A.H. (2018). Cell cycle heterogeneity directs the timing of neural stem cell activation from quiescence. Science (New York, N.Y.) *360*, 99–102. https://doi.org/10.1126/science.aan8795.

Pajcini, K.V., Corbel, S.Y., Sage, J., Pomerantz, J.H., and Blau, H.M. (2010). Transient inactivation of Rb and ARF yields regenerative cells from postmitotic mammalian muscle. Cell Stem Cell *7*, 198–213. https://doi.org/10.1016/j.stem.2010.05.022.

Palm, K., Belluardo, N., Metsis, M., and Timmusk, T. õnis (1998). Neuronal Expression of Zinc Finger Transcription Factor REST/NRSF/XBR Gene. J Neurosci *18*, 1280–1296. https://doi.org/10.1523/jneurosci.18-04-01280.1998.

Pan, H., Yin, C., Dyson, N.J., Harlow, E., Yamasaki, L., and Dyke, T.V. (1998). Key Roles for E2F1 in Signaling p53-Dependent Apoptosis and in Cell Division within Developing Tumors. Mol Cell *2*, 283–292. https://doi.org/10.1016/s1097-2765(00)80273-7.

Paredes, M.F., Sorrells, S.F., Cebrian-Silla, A., Sandoval, K., Qi, D., Kelley, K.W., James, D., Mayer, S., Chang, J., Auguste, K.I., et al. (2018). Does Adult Neurogenesis Persist in the Human Hippocampus? Cell Stem Cell *23*, 780–781. https://doi.org/10.1016/j.stem.2018.11.006.

Pechnick, R.N., Zonis, S., Wawrowsky, K., Pourmorady, J., and Chesnokova, V. (2008). p21Cip1 restricts neuronal proliferation in the subgranular zone of the dentate gyrus of the hippocampus. Proceedings of the National Academy of Sciences of the United States of America *105*, 1358–1363. https://doi.org/10.1073/pnas.0711030105.

Pilz, G.-A., Bottes, S., Betizeau, M., Jörg, D.J., Carta, S., Simons, B.D., Helmchen, F., and Jessberger, S. (2018). Live imaging of neurogenesis in the adult mouse hippocampus. Science (New York, N.Y.) *359*, 658–662. https://doi.org/10.1126/science.aao5056.

Poiana, G., Gioia, R., Sineri, S., Cardarelli, S., Lupo, G., and Cacci, E. (2020). Transcriptional regulation of adult neural stem/progenitor cells: tales from the subventricular zone. Neural Regen Res *15*, 1773–1783. https://doi.org/10.4103/1673-5374.280301.

Porlan, E., Morante-Redolat, J.M., Marqués-Torrejón, M.Á., Andreu-Agulló, C., Carneiro, C., Gómez-Ibarlucea, E., Soto, A., Vidal, A., Ferrón, S.R., and Fariñas, I. (2013). Transcriptional repression of Bmp2 by p21(Waf1/Cip1) links quiescence to neural stem cell maintenance. Nat Neurosci *16*, 1567–1575. https://doi.org/10.1038/nn.3545.

Praag, H. van, Schinder, A.F., Christie, B.R., Toni, N., Palmer, T.D., and Gage, F.H. (2002). Functional neurogenesis in the adult hippocampus. Nature *415*, 1030–1034. https://doi.org/10.1038/4151030a.

Previll, L.A., Crosby, M.E., Castellani, R.J., Bowser, R., Perry, G., Smith, M.A., and Zhu, X. (2007). Increased Expression of p130 in Alzheimer Disease. Neurochem Res *32*, 639–644. https://doi.org/10.1007/s11064-006-9146-3.

Qiu, J., Takagi, Y., Harada, J., Topalkara, K., Wang, Y., Sims, J.R., Zheng, G., Huang, P., Ling, Y., Scadden, D.T., et al. (2009). p27 Kip1Constrains Proliferation of Neural Progenitor Cells in Adult Brain Under Homeostatic and Ischemic Conditions. Stem Cells *27*, 920–927. https://doi.org/10.1002/stem.1.

Raudvere, U., Kolberg, L., Kuzmin, I., Arak, T., Adler, P., Peterson, H., and Vilo, J. (2019). g:Profiler: a web server for functional enrichment analysis and conversions of gene lists (2019 update). Nucleic Acids Res *47*, W191–W198. https://doi.org/10.1093/nar/gkz369.

Reimand, J., Kull, M., Peterson, H., Hansen, J., and Vilo, J. (2007). g:Profiler—a web-based toolset for functional profiling of gene lists from large-scale experiments. Nucleic Acids Res *35*, W193–W200. https://doi.org/10.1093/nar/gkm226.

Reimand, J., Isserlin, R., Voisin, V., Kucera, M., Tannus-Lopes, C., Rostamianfar, A., Wadi, L., Meyer, M., Wong, J., Xu, C., et al. (2019). Pathway enrichment analysis and visualization of omics data using g:Profiler, GSEA, Cytoscape and EnrichmentMap. Nat Protoc *14*, 482–517. https://doi.org/10.1038/s41596-018-0103-9.

Rempel, R.E., Saenz-Robles, M.T., Storms, R., Morham, S., Ishida, S., Engel, A., Jakoi, L., Melhem, M.F., Pipas, J.M., Smith, C., et al. (2000). Loss of E2F4 Activity Leads to Abnormal Development of Multiple Cellular Lineages. Mol Cell *6*, 293–306. https://doi.org/10.1016/s1097-2765(00)00030-7.

Ren, B., Cam, H., Takahashi, Y., Volkert, T., Terragni, J., Young, R.A., and Dynlacht, B.D. (2002). E2F integrates cell cycle progression with DNA repair, replication, and G2/M checkpoints. Gene Dev *16*, 245–256. https://doi.org/10.1101/gad.949802.

Reynolds, B., and Weiss, S. (1992). Generation of neurons and astrocytes from isolated cells of the adult mammalian central nervous system. Science (New York, N.Y.) *255*, 1707–1710. https://doi.org/10.1126/science.1553558.

Richards, B.A., and Frankland, P.W. (2017). The Persistence and Transience of Memory. Neuron *94*, 1071–1084. https://doi.org/10.1016/j.neuron.2017.04.037.

Robertson, K.D., Ait-Si-Ali, S., Yokochi, T., Wade, P.A., Jones, P.L., and Wolffe, A.P. (2000). DNMT1 forms a complex with Rb, E2F1 and HDAC1 and represses transcription from E2F-responsive promoters. Nat Genet *25*, 338–342. https://doi.org/10.1038/77124.

Robinson, J.T., Thorvaldsdóttir, H., Winckler, W., Guttman, M., Lander, E.S., Getz, G., and Mesirov, J.P. (2011). Integrative Genomics Viewer. Nat Biotechnol *29*, 24–26. https://doi.org/10.1038/nbt.1754.

Roopra, A., Sharling, L., Wood, I.C., Briggs, T., Bachfischer, U., Paquette, A.J., and Buckley, N.J. (2000). Transcriptional Repression by Neuron-Restrictive Silencer Factor Is Mediated via the Sin3-Histone Deacetylase Complex. Mol Cell Biol *20*, 2147–2157. https://doi.org/10.1128/mcb.20.6.2147-2157.2000.

Rotgers, E., Rivero-Müller, A., Nurmio, M., Parvinen, M., Guillou, F., Huhtaniemi, I., Kotaja, N., Bourguiba-Hachemi, S., and Toppari, J. (2014). Retinoblastoma protein (RB) interacts with E2F3 to control terminal differentiation of Sertoli cells. Cell Death Dis *5*, e1274. https://doi.org/10.1038/cddis.2014.232.

Saavedra, H.I., Wu, L., Bruin, A. de, Timmers, C., Rosol, T.J., Weinstein, M., Robinson, M.L., and Leone, G. (2002). Specificity of E2F1, E2F2, and E2F3 in mediating phenotypes induced by loss of Rb. Cell Growth & Differentiation : The Molecular Biology Journal of the American Association for Cancer Research *13*, 215–225. .

Sage, J. (2000). Targeted disruption of the three Rb-related genes leads to loss of G1 control and immortalization. Genes Dev *14*, 3037–3050. https://doi.org/10.1101/gad.843200.

Sage, J. (2012). The retinoblastoma tumor suppressor and stem cell biology. Genes Dev *26*, 1409–1420. https://doi.org/10.1101/gad.193730.112.

Sage, J., Miller, A.L., Pérez-Mancera, P.A., Wysocki, J.M., and Jacks, T. (2003). Acute mutation of retinoblastoma gene function is sufficient for cell cycle re-entry. Nature *424*, 223–228. https://doi.org/10.1038/nature01764.

Sahay, A., Scobie, K.N., Hill, A.S., O'Carroll, C.M., Kheirbek, M.A., Burghardt, N.S., Fenton, A.A., Dranovsky, A., and Hen, R. (2011). Increasing adult hippocampal neurogenesis is sufficient to improve pattern separation. Nature *472*, 466–470. https://doi.org/10.1038/nature09817.

Sangwan, M., McCurdy, S.R., Livne-bar, I., Ahmad, M., Wrana, J.L., Chen, D., and Bremner, R. (2012). Established and New Mouse Models Reveal E2f1 and Cdk2 Dependency of Retinoblastoma and Expose Strategies to Block Tumor Initiation. Oncogene *31*, 5019–5028. https://doi.org/10.1038/onc.2011.654.

Schade, A.E., Fischer, M., and DeCaprio, J.A. (2019). RB, p130 and p107 differentially repress G1/S and G2/M genes after p53 activation. Nucleic Acids Res https://doi.org/10.1093/nar/gkz961.

Schindelin, J., Arganda-Carreras, I., Frise, E., Kaynig, V., Longair, M., Pietzsch, T., Preibisch, S., Rueden, C., Saalfeld, S., Schmid, B., et al. (2012). Fiji: an open-source platform for biological-image analysis. Nat Methods *9*, 676–682. https://doi.org/10.1038/nmeth.2019.

Schneider, C.A., Rasband, W.S., and Eliceiri, K.W. (2012). NIH Image to ImageJ: 25 years of image analysis. Nat Methods *9*, 671–675. https://doi.org/10.1038/nmeth.2089.

Schoenherr, C.J., and Anderson, D.J. (1995). The Neuron-Restrictive Silencer Factor (NRSF): A Coordinate Repressor of Multiple Neuron-Specific Genes. Science *267*, 1360–1363. https://doi.org/10.1126/science.7871435.

Shannon, P., Markiel, A., Ozier, O., Baliga, N.S., Wang, J.T., Ramage, D., Amin, N., Schwikowski, B., and Ideker, T. (2003). Cytoscape: A Software Environment for Integrated Models of Biomolecular Interaction Networks. Genome Res *13*, 2498–2504. https://doi.org/10.1101/gr.1239303.

Sheehy, R.N., Quintanilla, L.J., and Song, J. (2021). Epigenetic Regulation in the Neurogenic Niche of the Adult Dentate Gyrus. Neurosci Lett 136343. https://doi.org/10.1016/j.neulet.2021.136343.

Shimojo, H., Ohtsuka, T., and Kageyama, R. (2008). Oscillations in Notch Signaling Regulate Maintenance of Neural Progenitors. Neuron *58*, 52–64. https://doi.org/10.1016/j.neuron.2008.02.014.

Shirodkar, S., Ewen, M., DeCaprio, J.A., Morgan, J., Livingston, D.M., and Chittenden, T. (1992). The transcription factor E2F interacts with the retinoblastoma product and a p107-cyclin A complex in a cell cycle-regulated manner. Cell *68*, 157–166. https://doi.org/10.1016/0092-8674(92)90214-w.

Smart, I. (1961). The subependymal layer of the mouse brain and its cell production as shown by radioautography after thymidine-H3 injection. J Comp Neurol *116*, 325–347. https://doi.org/10.1002/cne.901160306.

Smith, E.J., Leone, G., DeGregori, J., Jakoi, L., and Nevins, J.R. (1996). The accumulation of an E2F-p130 transcriptional repressor distinguishes a G0 cell state from a G1 cell state. Molecular and Cellular Biology *16*, 6965–6976. https://doi.org/10.1128/mcb.16.12.6965.

Snyder, J.S. (2019). Recalibrating the Relevance of Adult Neurogenesis. Trends Neurosci *42*, 164–178. https://doi.org/10.1016/j.tins.2018.12.001.

Soldati, C., Caramanica, P., Burney, M.J., Toselli, C., Bithell, A., Augusti-Tocco, G., Stanton, L.W., Biagioni, S., Buckley, N.J., and Cacci, E. (2015). RE1 silencing transcription factor/neuron-restrictive silencing factor regulates expansion of adult mouse subventricular zone-derived neural stem/progenitor cells in vitro. J Neurosci Res *93*, 1203–1214. https://doi.org/10.1002/jnr.23572.

Song, J., Sun, J., Moss, J., Wen, Z., Sun, G.J., Hsu, D., Zhong, C., Davoudi, H., Christian, K.M., Toni, N., et al. (2013). Parvalbumin interneurons mediate neuronal circuitry–neurogenesis coupling in the adult hippocampus. Nat Neurosci *16*, 1728–1730. https://doi.org/10.1038/nn.3572.

Sorrells, S.F., Paredes, M.F., Cebrian-Silla, A., Sandoval, K., Qi, D., Kelley, K.W., James, D., Mayer, S., Chang, J., Auguste, K.I., et al. (2018). Human hippocampal neurogenesis drops

sharply in children to undetectable levels in adults. Nature *124*, 319–381. https://doi.org/10.1038/nature25975.

Spalding, K.L., Bergmann, O., Alkass, K., Bernard, S., Salehpour, M., Huttner, H.B., Boström, E., Westerlund, I., Vial, C., Buchholz, B.A., et al. (2013). Dynamics of Hippocampal Neurogenesis in Adult Humans. Cell *153*, 1219–1227. https://doi.org/10.1016/j.cell.2013.05.002.

Srinivas, S., Watanabe, T., Lin, C.-S., William, C.M., Tanabe, Y., Jessell, T.M., and Costantini, F. (2001). Cre reporter strains produced by targeted insertion of EYFP and ECFP into the ROSA26 locus. BMC Developmental Biology *1*, 4. https://doi.org/10.1186/1471-213x-1-4.

Stefano, L.D. (2003). E2F7, a novel E2F featuring DP-independent repression of a subset of E2F-regulated genes. The EMBO Journal *22*, 6289–6298. https://doi.org/10.1093/emboj/cdg613.

Stengel, K.R., Thangavel, C., Solomon, D.A., Angus, S.P., Zheng, Y., and Knudsen, E.S. (2009). Retinoblastoma/p107/p130 Pocket Proteins: PROTEIN DYNAMICS AND INTERACTIONS WITH TARGET GENE PROMOTERS. Journal of Biological Chemistry *284*, 19265–19271. https://doi.org/10.1074/jbc.m808740200.

Stoub, T.R., deToledo-Morrell, L., Stebbins, G.T., Leurgans, S., Bennett, D.A., and Shah, R.C. (2006). Hippocampal disconnection contributes to memory dysfunction in individuals at risk for Alzheimer's disease. Proc National Acad Sci *103*, 10041–10045. https://doi.org/10.1073/pnas.0603414103.

Su, X., Gopalakrishnan, V., Stearns, D., Aldape, K., Lang, F.F., Fuller, G., Snyder, E., Eberhart, C.G., and Majumder, S. (2006). Abnormal Expression of REST/NRSF and Myc in Neural Stem/Progenitor Cells Causes Cerebellar Tumors by Blocking Neuronal Differentiation. Mol Cell Biol *26*, 1666–1678. https://doi.org/10.1128/mcb.26.5.1666-1678.2006.

Sueda, R., Imayoshi, I., Harima, Y., and Kageyama, R. (2019). High Hes1 expression and resultant Ascl1 suppression regulate quiescent vs. active neural stem cells in the adult mouse brain. Genes Dev 1–14. https://doi.org/10.1101/gad.323196.118.

Suh, H., Consiglio, A., Ray, J., Sawai, T., D'Amour, K.A., and Gage, F.H. (2007). In Vivo Fate Analysis Reveals the Multipotent and Self-Renewal Capacities of Sox2+ Neural Stem Cells in the Adult Hippocampus. Cell Stem Cell *1*, 515–528. https://doi.org/10.1016/j.stem.2007.09.002.

Sun, Y.-M., Greenway, D.J., Johnson, R., Street, M., Belyaev, N.D., Deuchars, J., Bee, T., Wilde, S., and Buckley, N.J. (2005). Distinct profiles of REST interactions with its target genes at different stages of neuronal development. Molecular Biology of the Cell *16*, 5630–5638. https://doi.org/10.1091/mbc.e05-07-0687.

TANG, Y., GARSON, K., LI, L., and VANDERHYDEN, B.C. (2015). Optimization of lentiviral vector production using polyethylenimine-mediated transfection. Oncol Lett *9*, 55–62. https://doi.org/10.3892/ol.2014.2684.

Team, R.C. (2021). R: A Language and Environment for Statistical Computing.

Thored, P., Arvidsson, A., Cacci, E., Ahlenius, H., Kallur, T., Darsalia, V., Ekdahl, C.T., Kokaia, Z., and Lindvall, O. (2006). Persistent Production of Neurons from Adult Brain Stem Cells During Recovery after Stroke. Stem Cells *24*, 739–747. https://doi.org/10.1634/stemcells.2005-0281.

Tirosh, I., Izar, B., Prakadan, S.M., II, M.H.W., Treacy, D., Trombetta, J.J., Rotem, A., Rodman, C., Lian, C., Murphy, G., et al. (2016). Dissecting the multicellular ecosystem of metastatic melanoma by single-cell RNA-seq. Science *352*, 189–196. https://doi.org/10.1126/science.aad0501.

Tobin, M.K., Musaraca, K., Disouky, A., Shetti, A., Bheri, A., Honer, W.G., Kim, N., Dawe, R.J., Bennett, D.A., Arfanakis, K., et al. (2019). Human Hippocampal Neurogenesis Persists in Aged Adults and Alzheimer's Disease Patients. Stem Cell *24*, 1–13. https://doi.org/10.1016/j.stem.2019.05.003.

Toda, T., and Gage, F.H. (2017). Review: adult neurogenesis contributes to hippocampal plasticity. Cell and Tissue Research *12*, 1–17. https://doi.org/10.1007/s00441-017-2735-4.

Tsai, K.Y., Hu, Y., Macleod, K.F., Crowley, D., Yamasaki, L., and Jacks, T. (1998). Mutation of E2f-1 Suppresses Apoptosis and Inappropriate S Phase Entry and Extends Survival of Rb-Deficient Mouse Embryos. Mol Cell *2*, 293–304. https://doi.org/10.1016/s1097-2765(00)80274-9.

Urbach, A. (2019). Divide or Commit – Revisiting the Role of Cell Cycle Regulators in Adult Hippocampal Neurogenesis. Fcell-07-00055.Tex *7*, 1–22. https://doi.org/10.3389/fcell.2019.00055.

Urban, N., Berg, D.L.C. van den, Forget, A., Andersen, J., Demmers, J.A.A., Hunt, C., Ayrault, O., and Guillemot, F. (2016). Return to quiescence of mouse neural stem cells by degradation of a proactivation protein. Science (New York, N.Y.) *353*, 292–295. https://doi.org/10.1126/science.aaf4802.

Urbán, N., Blomfield, I.M., and Guillemot, F. (2019a). Quiescence of Adult Mammalian Neural Stem Cells: A Highly Regulated Rest. Neuron *104*, 834–848. https://doi.org/10.1016/j.neuron.2019.09.026.

Urbán, N., Blomfield, I.M., and Guillemot, F. (2019b). Quiescence of Adult Mammalian Neural Stem Cells: A Highly Regulated Rest. Neuron *104*, 834–848. https://doi.org/10.1016/j.neuron.2019.09.026.

Vandenbosch, R., Clark, A., Fong, B.C., Omais, S., Jaafar, C., Dugal-Tessier, D., Dhaliwal, J., Lagace, D.C., Park, D.S., Ghanem, N., et al. (2016). RB regulates the production and the survival of newborn neurons in the embryonic and adult dentate gyrus. Hippocampus *26*, 1379–1392. https://doi.org/10.1002/hipo.22613.

Vanderluit, J.L., Ferguson, K.L., Nikoletopoulou, V., Parker, M., Ruzhynsky, V., Alexson, T., McNamara, S.M., Park, D.S., Rudnicki, M., and Slack, R.S. (2004). p107 regulates neural precursor cells in the mammalian brain. J Cell Biol *166*, 853–863. https://doi.org/10.1083/jcb.200403156.

Vanderluit, J.L., Wylie, C.A., McClellan, K.A., Ghanem, N., Fortin, A., Callaghan, S., MacLaurin, J.G., Park, D.S., and Slack, R.S. (2007). The Retinoblastoma family member p107 regulates the rate of progenitor commitment to a neuronal fate. J Cell Biol *178*, 129–139. https://doi.org/10.1083/jcb.200703176.

Venugopal, N., Ghosh, A., Gala, H., Aloysius, A., Vyas, N., and Dhawan, J. (2020). The primary cilium dampens proliferative signaling and represses a G2/M transcriptional network in quiescent myoblasts. Bmc Mol Cell Biology *21*, 25. https://doi.org/10.1186/s12860-020-00266-1.

Verdugo-Sivianes, E.M., and Carnero, A. (2021). Role of the Holoenzyme PP1-SPN in the Dephosphorylation of the RB Family of Tumor Suppressors During Cell Cycle. Cancers *13*, 2226. https://doi.org/10.3390/cancers13092226.

Verona, R., Moberg, K., Estes, S., Starz, M., Vernon, J.P., and Lees, J.A. (1997). E2F activity is regulated by cell cycle-dependent changes in subcellular localization. Mol Cell Biol *17*, 7268–7282. https://doi.org/10.1128/mcb.17.12.7268.

Viatour, P., Somervaille, T.C., Venkatasubrahmanyam, S., Kogan, S., McLaughlin, M.E., Weissman, I.L., Butte, A.J., Passegué, E., and Sage, J. (2008). Hematopoietic stem cell quiescence is maintained by compound contributions of the retinoblastoma gene family. Cell Stem Cell *3*, 416–428. https://doi.org/10.1016/j.stem.2008.07.009.

Viatour, P., Ehmer, U., Saddic, L.A., Dorrell, C., Andersen, J.B., Lin, C., Zmoos, A.-F., Mazur, P.K., Schaffer, B.E., Ostermeier, A., et al. (2011a). Notch signaling inhibits hepatocellular carcinoma following inactivation of the RB pathway. The Journal of Experimental Medicine *208*, 1963–1976. https://doi.org/10.1084/jem.20110198.

Viatour, P., Ehmer, U., Saddic, L.A., Dorrell, C., Andersen, J.B., Lin, C., Zmoos, A.-F., Mazur, P.K., Schaffer, B.E., Ostermeier, A., et al. (2011b). Notch signaling inhibits hepatocellular carcinoma following inactivation of the RB pathway. J Exp Medicine *208*, 1963–1976. https://doi.org/10.1084/jem.20110198.

Vicidomini, C., Guo, N., and Sahay, A. (2020). Communication, Cross Talk, and Signal Integration in the Adult Hippocampal Neurogenic Niche. Neuron *105*, 220–235. https://doi.org/10.1016/j.neuron.2019.11.029.

Walker, T.L., Overall, R.W., Vogler, S., Sykes, A.M., Ruhwald, S., Lasse, D., Ichwan, M., Fabel, K., and Kempermann, G. (2016). Lysophosphatidic Acid Receptor Is a Functional Marker of Adult Hippocampal Precursor Cells. Stem Cell Rep *6*, 552–565. https://doi.org/10.1016/j.stemcr.2016.03.002.

Walkley, C.R., and Orkin, S.H. (2006). Rb is dispensable for self-renewal and multilineage differentiation of adult hematopoietic stem cells. Proceedings of the National Academy of Sciences *103*, 9057–9062. https://doi.org/10.1073/pnas.0603389103.

Wander, C.M., and Song, J. (2021). The Neurogenic Niche in Alzheimer's disease. Neurosci Lett 136109. https://doi.org/10.1016/j.neulet.2021.136109.

Wang, D., Russell, J.L., and Johnson, D.G. (2000). E2F4 and E2F1 Have Similar Proliferative Properties but Different Apoptotic and Oncogenic Properties In Vivo. Mol Cell Biol *20*, 3417–3424. https://doi.org/10.1128/mcb.20.10.3417-3424.2000.

Winner, B., and Winkler, J. (2015). Adult Neurogenesis in Neurodegenerative Diseases: Figure 1. Cold Spring Harbor Perspectives in Biology *7*, a021287. https://doi.org/10.1101/cshperspect.a021287.

Wirt, S.E., and Sage, J. (2010). p107 in the public eye: an Rb understudy and more. Cell Div *5*, 9–9. https://doi.org/10.1186/1747-1028-5-9.

Wirt, S.E., Adler, A.S., Gebala, V., Weimann, J.M., Schaffer, B.E., Saddic, L.A., Viatour, P., Vogel, H., Chang, H.Y., Meissner, A., et al. (2010). G1 arrest and differentiation can occur independently of Rb family function. J Cell Biol *191*, 809–825. https://doi.org/10.1083/jcb.201003048.

Wu, L., Timmers, C., Maiti, B., Saavedra, H.I., Sang, L., Chong, G.T., Nuckolls, F., Giangrande, P., Wright, F.A., Field, S.J., et al. (2001). The E2F1–3 transcription factors are essential for cellular proliferation. Nature *414*, 457–462. https://doi.org/10.1038/35106593.

Xi, Y., Dhaliwal, J.S., Ceizar, M., Vaculik, M., Kumar, K.L., and Lagace, D.C. (2016). Knockout of Atg5 delays the maturation and reduces the survival of adult-generated neurons in the hippocampus. Cell Death Dis *7*, e2127. https://doi.org/10.1038/cddis.2015.406.

Yagi, S., and Galea, L.A.M. (2019). Sex differences in hippocampal cognition and neurogenesis. Neuropsychopharmacol *44*, 200–213. https://doi.org/10.1038/s41386-018-0208-4.

Ye, F., Kang, E., Yu, C., Qian, X., Jacob, F., Yu, C., Mao, M., Poon, R.Y.C., Kim, J., Song, H., et al. (2017). DISC1 Regulates Neurogenesis via Modulating Kinetochore Attachment of Ndel1/Nde1 during Mitosis. Neuron *96*, 1–20. https://doi.org/10.1016/j.neuron.2017.10.010.

Yeh, C.-Y., Asrican, B., Moss, J., Quintanilla, L.J., He, T., Mao, X., Cassé, F., Gebara, E., Bao, H., Lu, W., et al. (2018). Mossy Cells Control Adult Neural Stem Cell Quiescence and Maintenance through a Dynamic Balance between Direct and Indirect Pathways. Neuron https://doi.org/10.1016/j.neuron.2018.07.010.

Yu, R.Q., Cooke, M., Seib, D.R., Zhao, J., and Snyder, J.S. (2019). Adult neurogenesis promotes efficient, nonspecific search strategies in a spatial alternation water maze task. Behav Brain Res *376*, 112151. https://doi.org/10.1016/j.bbr.2019.112151.

Yun, S., Tran, F., Soler, I., Reynolds, R., Suarez, M., and Eisch, A. (2019). GABAergic entorhinal cortex control of hippocampal function in stress-related disorder: Cellular and circuitry mechanisms. Ibro Reports *6*, S504–S505. https://doi.org/10.1016/j.ibror.2019.07.1577.

Zacksenhaus, E., Jiang, Z., Chung, D., Marth, J.D., Phillips, R.A., and Gallie, B.L. (1996). pRb controls proliferation, differentiation, and death of skeletal muscle cells and other lineages during embryogenesis. Genes Dev *10*, 3051–3064. https://doi.org/10.1101/gad.10.23.3051.

Zhao, C. (2006). Distinct Morphological Stages of Dentate Granule Neuron Maturation in the Adult Mouse Hippocampus. J Neurosci *26*, 3–11. https://doi.org/10.1523/jneurosci.3648-05.2006.

Zheng, W., ZhuGe, Q., Zhong, M., Chen, G., Shao, B., Wang, H., Mao, X., Xie, L., and Jin, K. (2013). Neurogenesis in Adult Human Brain after Traumatic Brain Injury. J Neurotraum *30*, 1872–1880. https://doi.org/10.1089/neu.2010.1579.

Zhou, G., Soufan, O., Ewald, J., Hancock, R.E.W., Basu, N., and Xia, J. (2019). NetworkAnalyst 3.0: a visual analytics platform for comprehensive gene expression profiling and meta-analysis. Nucleic Acids Res *47*, gkz240-. https://doi.org/10.1093/nar/gkz240.

Ziebold, U., Lee, E.Y., Bronson, R.T., and Lees, J.A. (2003). E2F3 Loss Has Opposing Effects on Different pRB-Deficient Tumors, Resulting in Suppression of Pituitary Tumors but Metastasis of Medullary Thyroid Carcinomas. Mol Cell Biol *23*, 6542–6552. https://doi.org/10.1128/mcb.23.18.6542-6552.2003.

Zini, N., Trimarchi, C., Claudio, P.P., Stiegler, P., Marinelli, F., Maltarello, M.C., Sala, D.L., Falco, G.D., Russo, G., Ammirati, G., et al. (2001). pRb2/p130 and p107 control cell growth by multiple strategies and in association with different compartments within the nucleus*. J Cell Physiol *189*, 34–44. https://doi.org/10.1002/jcp.1135.

CHAPTER 4

Yubing Liu[†], **Bensun C. Fong**[†], Richard M. Harris, Marie-Michelle McNicoll, Amaal A. Abdi, David Cook[2], Daniel Figeys[3], Jing Wang[2], Barbara Vanderhyden[2], and Ruth S. Slack*. Impaired NSC activation in the 3xTG-AD model of Alzheimer's Disease. In press, January 2022.

University of Ottawa Brain and Mind Research Institute, Department of Cellular and Molecular Medicine, University of Ottawa, Canada K1H 8M5; 2 – Ottawa Hospital Research Institute, Ottawa, Canada K1H 8L6; 3 - Department of Biochemistry, Microbiology and Immunology, University of Ottawa, Canada K1H 8M5

Corresponding Author*:

Ruth S. Slack: rslack@uottawa.ca

[†]*Authors contributed equally*

The experiments were performed by BCF in collaboration with YL. Immunohistochemical staining and quantification was performed by BCF in collaboration with RMH, MMM and AAA.

Experiments were conceptualized by BCF, YL, RMH, and RSS. DC provided technical assistance for bioinformatic analysis. The manuscript was written by YL, BCF, and RSS, and all authors contributed to critical review of the manuscript.

Alterations in NSC quiescence and activation in the 3xTG-AD model of Alzheimer's Disease

Yubing Liu†, Bensun C. Fong†, Richard M. Harris, Marie-Michelle McNicoll, Amaal A. Abdi, David Cook[2], Daniel Figeys[3], Jing Wang[2], Barbara Vanderhyden[2], and Ruth S. Slack*

University of Ottawa Brain and Mind Research Institute, Department of Cellular and Molecular Medicine, University of Ottawa, Canada K1H 8M5; 2 – Ottawa Hospital Research Institute, Ottawa, Canada K1H 8L6; 3 - Department of Biochemistry, Microbiology and Immunology, University of Ottawa, Canada K1H 8M5

† Equal contribution

Corresponding Author:

Ruth S. Slack: rslack@uottawa.ca

Introduction

Alzheimer's Disease (AD), the most common form of dementia, is a progressive neurodegenerative disorder associated with cognitive deficits and mood disorders (Knopman et al., 2021). It is characterized most commonly by distinct neuropathological features including accumulation of β-amyloid (Aβ) plaques followed by deposition of microtubule associated protein tau (tau, also MAPT) as neurofibrillary tangles (NFTs), resulting in synaptic dysfunction, neuroinflammation and neuronal loss (Wander and Song, 2021).

Recent studies have associated AD pathology with the impairment of adult neurogenesis – the process by which a quiescent pool of neural stem cells (NSCs) give rise to adult-born neurons throughout life (Bond et al., 2015). This intricately-regulated process follows a stage-wise progression through NSC activation, differentiation into neuroblasts, neuronal commitment and post-mitotic terminal differentiation as well as subsequent integration into surrounding circuitry (Bonaguidi et al., 2016). NSCs are localized to well-established neuronal niches in the mammalian brain, including the ventricular-subventricular zone (V-SVZ) of the lateral ventricles, as well as the subgranular zone (SGZ) of the hippocampal dentate gyrus (DG) (Gonçalves et al., 2016). SGZ NSCs generate granule cell neurons (GCNs), which modify existing neural circuits by inducing neural plasticity: the process of structural reorganization that plays a role in hippocampal cognitive function, including learning, memory encoding and consolidation, and spatial navigation (Sahay et al., 2011; Toda and Gage, 2017).

In humans, the hippocampus represents one of the brain regions most damaged by AD (Coupé et al., 2019). While the DG is able to withstand the effects of Aβ and tau

accumulation until later stages, it ultimately suffers from loss of entorhinal input (Ohm, 2007; Stoub et al., 2006). Analysis of GCNs in the DG of AD patients reveals alterations in both dendritic tree morphology and post-synaptic densities, which is similar to those observed following overexpression of tau-inducer GSK-3β (Llorens-Martín et al., 2013). Recent work has further associated AD progression with a decline in the number and maturation of adult-born DG neurons, distinct from typical age-related decline (Moreno-Jiménez et al., 2019). Together, this suggests a clear impact of AD on the survival and integration of adult-born neurons.

Recent work has demonstrated that AD pathology impacts adult NSC fate (Mu and Gage, 2011), including studies employing the triple-transgenic 3xTG-AD mouse model, generated by co-injecting hAPP (hAPPSwe) and hTau (hTauP301L) transgenes, under control of the Thy1.2 promoter, into PS1M146V knock-in mouse embryos. 3xTG-AD mice distinctly accumulate Aβ plaques and NFTs with age (Oddo et al., 2003), and multiple groups have demonstrated further impairments to NSC and progenitor proliferation, as well as neurogenesis, in 3xTG-AD mice as early as 2 months of age. Notably, these effects predate the onset of Aβ plaques and NFTs, yet are sustained through life as late as 18 months of age (Hamilton et al., 2010, 2015; Rodríguez et al., 2008, 2009). Sex differences were observed in proliferating cells in the 3xTG-AD SGZ, as females exhibited a relatively earlier decrease at 4 months, compared to a similar decrease in males at 9 months (Rodríguez et al., 2008). Though this decrease was associated with AD-induced deregulation of oleic acid synthesis (Hamilton et al., 2015), the regulatory mechanisms underlying the functional impairment of adult NSCs remain to be resolved.

Transcriptomic analyses have been useful to distinguish differential gene regulation in FACS-isolated populations obtained from the adult SVZ and SGZ (Codega et al., 2014; Than-Trong et al., 2018). Recently, single-cell transcriptomic approaches (single-cell RNASeq) have been able to provide a broad overview of the transcriptome throughout the stages of adult neurogenesis (Basak et al., 2018; Shin et al., 2015), and to define the mechanisms underlying the transition between, and subtype acquisition of, distinct NSC populations (Borrett et al., 2020).

To identify the deficits underlying the impairment of neurogenesis in the 3xTG-AD model of Alzheimer's disease, here, we employ single-cell RNASeq to establish population-specific defects caused by AD during the course of adult SGZ neurogenesis. Relative to non-transgenic (NTG) mice used as control, we observe a dramatic AD-induced decrease in the activated NSC population, that results in a progressive loss of cells committed to neurogenesis. RNA velocity measurements suggest that the transcriptional program within 3xTG-AD NSCs promotes return to quiescence, consistent with an impairment in the activation program. This suggests a previously-unknown phenotype for AD pathology, affecting adult neurogenesis during NSC activation ahead of subsequent impairments to neuronal differentiation.

Our work explores, at a stage-specific resolution, changes in the regulatory networks guiding adult neurogenesis, and identifies niche disturbances in the regulation of NSC quiescence and activation as a key deficit of AD, potentially underlying impaired hippocampal function.

Results

Reduced NSC and Progenitor Populations in the 3xTG-AD Brain

The 3xTG-AD mouse model of Alzheimer's Disease demonstrates profound deficits in adult neurogenesis together with progressive cognitive decline (Belfiore et al., 2019; Hamilton et al., 2010). Prior reports have observed impairments to the NSC pool in AD patients, consistent with those observed in the mouse model of 3xTG-AD (Hamilton et al., 2015; Moreno-Jiménez et al., 2019; Tobin et al., 2019). HOPX, encoded by HOP homeobox (Hopx), is an atypical homeodomain protein that is incapable of DNA binding, while lysophosphatidic acid receptor 1 (Lpar1) is a receptor of lysophosphatidic acid, a natural bioactive lipid mediator; both Hopx and Lpar1 are expressed in SGZ NSCs, with Hopx expression defining the quiescent SGZ NSC population originating during development (Berg et al., 2019; Walker et al., 2016; Zhong et al., 2018). In the absence of Lpar1 or Hopx, cell proliferation in the dentate gyrus is reduced (Li et al., 2015; Matas-Rico et al., 2008). Here, we examined the expression of Hopx and Lpar1 in the SGZ of both control (NTG) and 3xTG-AD mice through immunohistochemistry *in vivo* at 3 months of age. Both Hopx and Lpar1 showed enriched expression in Sox2-expressing SGZ NSCs (**Figs. 1A, 1E, 1H**). Relative to NTG control, fewer cells in the 3xTG-AD model express Hopx and Lpar1 (**Figs. 1C, 1G**), indicating a declined NSC population in response to AD. Taken together, our initial characterization confirms the presence of deficits in the NSC population in 3xTG-AD mice (Hamilton et al., 2015). To understand the mechanisms underlying this deficit, we next used a single-cell transcriptomic approach to characterize the transcriptional program within distinct cell populations.

Single Cell Transcriptome of the Nestin-expressing population in the SGZ

To examine these deficits at the molecular level, we used adult 3xTG-AD mice or NTG control mice carrying a tamoxifen (Tam)-inducible NestinCreER^{T2};EYFP Cre-reporter (Cicero et al., 2009; Zhu et al., 2012), targeting the adult-born NSC and their progeny. Four weeks post-Tam, we isolated YFP+ recombined cell populations using fluorescence-activated cell sorting (FACS), which were then sequenced using single cell RNA-seq (**Fig. 2A**). The transcriptomes of 11154 NTG and 8646 3xTG-AD cells were independently analyzed using the 10X Genomics platform, from which 6105 NTG and 5160 3xTG-AD cells were kept for downstream analysis, following quality control and detection of YFP expression (**Figs. S1A-C**). While there were many similarities in the transcriptomes, we also noted an increased proportion of mitochondrial genes in the 3xTG-AD cell population, relative to NTG (**Figs. S1B-C**).

Ten Clusters from Nestin-expressing cells in the SGZ

The NTG and 3xTG-AD transcriptomes were integrated using Seurat, and UMAP was used for unsupervised clustering based on gene expression. Ten major tissue-resident cell types were identified: the neurogenic lineage consisted of five cell populations including astrocyte-enriched NSCs, quiescent NSCs (qNSCs), activated NSCs (aNSCs), transiently-amplifying progenitors (TAPs) and neurons; as well as mural cells, endothelial cells, ependymal cells, oligodendrocytes, and oligodendrocyte progenitor cells (**Fig. 2B**). A heatmap demonstrating both distinct and continuous expression of the top ten over-represented genes in each cluster (**Fig. 2C**) was used for clustering validation. For non-neurogenic clusters, Mog, Mobp and Mag are markers of

oligodendrocytes, while Gpr17, Tnr and C1ql1 are representative genes in oligodendrocyte progenitor cells (Marques et al., 2019); mural cells and endothelial cells share a cluster of markers, including Myl9, Hspb1 and Myo1b, while endothelial cells have unique marker genes Flt1, Ly6c1 and Cldn5 (He et al., 2016; Zhao et al., 2018); ependymal cells are characterized by enriched expression of Ccdc153, Rsph1 and Meig1 (Mizrak et al., 2019).

Nestin-CreER^{T2} labels Nestin-expressing cells in the DG, including NSCs and their progeny (Bernal & Arranz, 2018, Youssef et al., 2018), from which the adult-born NSC, progenitor and neuronal populations originate, reflected in five cell clusters expressing characteristic neurogenic and neuronal markers (**Figs. 2C and 2D**). The majority of cells possessed stem cell characteristics, represented in three clusters: astrocyte-enriched NSCs, quiescent NSCs (qNSCs) and activated NSCs (aNSCs). The astrocyte-enriched NSC cluster shows enriched expression of astrocyte markers, including Slc7a10 and Fbxo2 (Y. Zhang et al., 2016). Quiescence markers Aqp4, and Id4 were highly expressed in the qNSC cluster, and downregulated in the aNSC and differentiating populations in line with prior characterization (Artegiani et al., 2017; Blomfield et al., 2019; Shin et al., 2015; R. Zhang et al., 2019) (**Figs. 2C and S2**). Using gene ontology, relative to the astrocyte-enriched NSC cluster, the qNSC population was enriched in genes for “nervous system development” and “cell population proliferation” (**Fig. S3**). The expression of NSC activation hallmarks, including Hopx and Fabp7, was dramatically induced in the aNSC cluster (Li et al., 2015; Matsumata et al., 2012) (**Figs. 2C-D**). Relative to the qNSC population, genes involved in “translation” and “cell population proliferation” were enriched in the aNSC cluster (**Fig. S3**). These findings

support the heterogeneity of NSCs in the hippocampus and identify a list of novel markers for the progressive NSC transition between stages of quiescence and activation.

The expression of Ascl1 and Eomes further demonstrates the gradual transition from activated NSCs to transiently-amplifying progenitors (TAPs); a fraction of TAPs are in M-phase, demonstrating expression of cell cycle-related genes including Cdk6, Mki67 and Top2a (**Figs. 2C, 2D**). Finally, the expression of differentiation markers Dcx, Tubb3 and Stmn2 is induced in the neuron cluster, suggesting acquisition of the immature neuronal phenotype (**Figs. 2C, 2D**). In line with a Nestin-CreER^{T2}-labeled population four weeks post-Tam, these integrated clusters demonstrate a continuous progression towards differentiation, and represent a stage-specific transcriptome during adult neurogenesis consistent with prior reports (Shin et al., 2015).

Defects in NSC Activation in the 3xTG-AD SGZ

To better characterize cluster-specific differences in response to 3xTG-AD pathology, we examined our samples within the integrated UMAP projection (**Fig. 3A**). Although each transcriptome reflected a similar-sized cell population (6105 NTG, 5160 3xTG-AD), examination of the five neurogenic clusters in the 3xTG-AD cell population demonstrated a greater relative proportion of astrocyte-enriched NSC and qNSC cell population and a decreased relative proportion of aNSCs, TAP and neuronal cell populations, as compared with NTG controls (**Figs. 3B-C, S4**). Cluster-specific differential gene expression was established between NTG and 3xTG-AD samples. While many important developmental genes were consistent between NTG and 3xTG-

AD samples, a number of important gene pathways displayed aberrant expression (**Fig. S5**), and demonstrated enrichment in genes associated with translation and mitochondrial function (**Fig. 3D**). Of the significantly differentially-expressed genes, those upregulated in response to 3xTG-AD were induced in the aNSC and TAP clusters, including mt-Co2, mt-Nd1 and multiple ribosomal genes (**Figs. 3D-E, S5**), reflecting a general increase in energy demand associated with proliferation. This suggests the compensatory upregulation of translation machinery and mitochondrial biogenesis, both of which are tightly controlled to maintain cell homeostasis (Gabut et al., 2020; Khacho et al., 2019; Tahmasebi et al., 2019). Genes downregulated in the 3xTG-AD model included Hopx and Lpar1 (**Fig. 3E**). In the NTG transcriptome, Lpar1 expression is low in the astrocyte-enriched NSC and qNSC populations, becoming upregulated in the aNSC population, consistent with a role for Lpar1 as a marker of NSC activation (Walker et al., 2016). In contrast, we do not observe Lpar1 upregulation, and further observe significant downregulation of Hopx, in the aNSC population of 3xTG-AD mice. Together with IHC characterization from Figure 1, these results suggest transcriptional changes consistent with a defect NSC activation, in response to AD pathology.

RNA Velocity Reveals Defects in Quiescence and Activation in 3xTG-AD NSCs

To better characterize a potential defect in NSC activation, we used RNA velocity to predict the transcriptional fate of cell populations based on RNA processing. RNA velocity measures relative differences in splicing kinetics (La Manno et al., 2018; Bergen et al., 2020), to predict the fate transitions of 3xTG-AD and NTG cells during the

course of adult neurogenesis. Here, we focused on the aNSC population, and subsequent TAP and neuron progeny, to establish a linear trend (**Fig. 4A**). The NTG velocity stream suggests the continuous progression of aNSCs through activation, proliferation and differentiation. Consistent with the dynamic transition between aNSC and TAPs, a relatively small portion of cells in the TAP cluster appeared destined to return to the aNSC cluster, with the majority predicted to progress toward differentiation into neurons (**Fig. 4B**). While the differentiation program appeared consistent between TAP and neuronal clusters in both NTG and 3xTG, we observed a dramatic shift in the fate of aNSC cells in the 3xTG-AD transcriptome, as aNSCs appeared to transition away from the expected TAP cluster and instead appear destined to an opposite fate, towards the qNSC/aNSC transition. Together with velocity pseudotime analysis predicting that aNSCs in the 3xTG-AD sample originate from the aNSC/TAP transition rather than the qNSC/aNSC transition, this suggests that aNSCs in the 3xTG-AD model demonstrate a return to quiescence. This suggests that in addition to impaired NSC activation, AD pathology may drive activated NSCs to re-enter quiescence. This could be considered an adaptive response to survive the adverse environment in the AD brain.

We asked whether characteristic genes regulating this transition may be differentially impacted in the aNSC cluster of the 3xTG-AD transcriptome. Examining the RNA velocity in individual genes, reflecting their instantaneous up- and down-regulation, we observe significant differences in hallmarks genes of quiescence and activation, in response to 3xTG-AD (**Fig. 4C**). In the aNSC cluster of NTG mice, quiescence genes Aqp4 and Apoe demonstrate down-regulation, while activation gene

Egfr demonstrates up-regulation, consistent with NSC activation (Urbán et al., 2019a). We observe the opposite in the 3xTG aNSC cluster, reflecting up-regulation of Aqp4 and Apoe, together with down-regulation of Egfr. These findings further support a return to the quiescent transcriptional program for 3xTG-AD aNSCs.

We finally sought to examine candidate genes that demonstrate differential expression and differential RNA velocity in response to 3xTG-AD. As a securin, Pttg1 is a cell cycle regulator and has been shown to be over-expressed in various tumors (Quereda and Malumbres, 2009). Here, we observe altered dynamics in Pttg1 expression in multiple clusters of the 3xTG-AD cell population, downregulated in NSC clusters but aberrantly upregulated in the TAP cluster (**Figs. 3F and 4C**). Though both Hopx and Lpar1 demonstrate enrichment in the NTG aNSC cluster, their expression was reduced in 3xTG-AD aNSCs (**Fig. 3F**), and Lpar1 appears to be downregulated in a subset of aNSC cells proximal to the aNSC/TAP transition (**Fig. 4C**). Taken together, Pttg1, Hopx and Lpar1 represent novel candidates in the AD-affected transcriptome, and may warrant future study as effectors of AD-induced defects in NSC quiescence and activation.

Discussion

This study provides several important insights. First, using single cell RNA-seq on the adult Nestin-expressing cell population, as well as their progeny over one month, allowed us to observe the effects of 3xTG-AD pathology spanning the whole course of adult neurogenesis beginning with quiescent NSCs. Previous work characterized compromised neurogenesis in response to 3xTG-AD (Hamilton et al., 2015), but focused on GFAP-expressing NSCs, as well as markers of proliferation and differentiation. Here we report imbalanced quiescence and activation of NSCs in the cell population obtained from 3xTG-AD mice, four weeks post-Tam. Compared with NTG controls, we observed that 3xTG-AD mice possess a proportionally greater qNSC population (**Fig. 3A-C**). In contrast, a reduction in aNSC proportion was identified in the 3xTG-AD cell population, an observation supported by the *in vivo* immunostaining of Lpar1, a marker of NSC activation (**Fig. 1**) (Walker et al., 2016). This timepoint further allowed us to observe the additional effects on YFP-expressing progenies, including TAPs, immature and mature neurons, each of which were disproportionately reduced in 3xTG-AD relative to NTG. Together with RNA velocity measurements, we propose that this reduction is associated with impaired NSC activation and a trend for 3xTG-AD activated NSCs towards quiescence (**Fig. 4**).

Presently, the connection between AD pathology and the complex regulatory network regulating NSC quiescence and activation remains unclear. This fate transition has been previously associated with pivotal transcription factors including REST and ASCL1 (Mukherjee 2016, (Andersen et al., 2014), (Urban et al., 2016) Impaired REST function has been associated with the altered differentiation state observed in iPSC-

derived neural cells generated from patients with sporadic AD (Meyer 2019), while expression of Ascl1 mRNA and ASCL1 protein are induced by Aβ in cerebral cortical cultures (Uchida, 2010). We observed stage-specific differences affecting candidate genes Pttg1, Hopx and Ascl1. The differential effects of 3xTG-AD on RNA velocity were also primarily observed in the aNSC cluster, which possesses the highest expression of Ascl1 and Hopx. It has been previously reported that Ascl1-expressing NSCs possess limited neurogenic proliferation potential before committing to terminal differentiation, but subsequently lose self-renewal capacity and are unable to reacquire long-term quiescence (Pilz et al., 2018). The fate of these cells remains to be explored: if quiescence is not sustainable, are they destined for apoptosis, senescence, or delayed differentiation?

Second, many genes involved in mitochondrial structure or function are upregulated in the NSCs of 3xTG-AD mice (**Figs. 3A-C**). In both NTG and 3xTG-AD mice, we observe that mitochondrial gene expression is maintained at a low level in the three NSC clusters, becomes induced in the TAP population, and returns to a low level in differentiating neurons (**Fig. 3E**). As cell number correlates with strength of statistical power, we established significant differential gene expression mostly in the larger astrocyte-enriched NSC and qNSC populations. Nevertheless, we further observed dysregulated mitochondrial biogenesis in the TAP population of 3xTG-AD mice, including upregulation of mt-Co2 and mt-Nd1, important structural components of mitochondria. While the mechanisms behind this dysregulation remain to be explored, we and others have reported that mitochondrial function tightly correlates with stem cell homeostasis (Khacho et al., 2019; H. Zhang et al., 2018).

Third, we observed a set of genes associated with translation shows a similar trend in response to 3xTG-AD. For example, both Rps2, the 40S ribosomal protein S2, and Rpl41, the 60S ribosomal protein L4, are significantly upregulated in most clusters of 3xTG-AD. The difference is most dramatic in the proliferating TAP cells, where translation is in demand (**Fig. 3E**). Ribosomal biogenesis is an important player in controlling stem cell function, including activation and proliferation (Gabut et al., 2020; Saba et al., 2021; Sharifi et al., 2020). It is possible that disturbed ribosomal biogenesis is a contributing factor of adult neurogenesis deficits in 3xTG-AD mice.

Fourth, although adult NSCs were the focus of this study, additional affected cell types contribute to NSC niche homeostasis and neuron function. Increased astrocyte number has been previously reported in human frontotemporal dementia patients and 5xFAD-AD mice (Habib et al., 2020; Terreros-Roncal et al., 2021); while we did not observe proportional differences to our astrocyte-enriched NSC population, further sub-clustering may help define a glial phenotype in 3xTG-AD mice. Beyond the neurogenic lineage, we identified five further Nestin-expressing hippocampal cell types (**Figs. 2B-C**): oligodendrocytes and their progenitors are implicated in the pathogenesis of AD (Chen et al., 2020), while mural, endothelial and ependymal cells play key structural roles that may underlie AD-induced neurovascular dysfunction (Zlokovic, 2011). Ultimately, this study enriches the list of cell-specific markers and provides greater resolution to the broad, dynamic effects of AD during hippocampal neurogenesis.

Here, we report the previously-unknown finding of imbalanced quiescence and activation of adult NSCs occurring in the hippocampus of 3xTG-AD mice. Exploring the mechanisms behind this imbalance may provide new therapeutic perspectives in AD.

Figure Legends and Figures

Figure 1: Reduced activated NSC population in the SGZ of 3xTG-AD mice

(A) IHC of Sox2 self-renewing, YFP recombined and Hopx-expressing cell populations in the SGZ of NTG and 3xTG-AD brains, at three months of age. Scale bar, 25μm. Insets represent magnified views. Arrowheads point to cells with colocalization. Scale bar, 10 μm.

(B-D) Quantification of Sox2 (B), YFP (C), and Hopx (D) cells in the SGZ of NTG and 3xTG-AD brains. *$p < 0.05$. $n = 4$.

(E) Immunostaining of Sox2 self-renewing and Lpar1-expressing cell populations in the SGZ of NTG and 3xTG-AD brains, at three months of age. Scale bar, 25μm. Insets represent magnified views. Arrowheads point to cells with colocalization. Scale bar, 10 μm.

(F-H) Quantification of Sox2 (F), Lpar1 (G), and Sox2/Lpar1 co-localized (H) cells in the SGZ of NTG and 3xTG-AD brains.

*$p < 0.05$. $n = 5$ (NTG) and 6 (3xTG-AD).

Figure 2: Ten cell clusters identified in the SGZ

(A) Experimental design. Inducible NestinCreER^{T2};R26-EYFP mice were crossed with either NTG or 3xTG-AD mice. Tamoxifen induction occurred at 2 months of age and hippocampal cells were isolated at 3 months of age. YFP-positive cells were isolated using fluorescence-activated cell sorting (FACS) and subjected to single cell RNA-seq.

(B) Integrated UMAP projection of NTG and 3xTG-AD cells, separated using Seurat into ten clusters based on their expression profiles.

(C) Heatmap demonstrating genes representative of each cluster, reflecting cluster-specific expression.

(D) UMAP projections demonstrating curated genes representative of each cluster, reflecting cluster-specific expression.

Figure 3: Single-cell RNA-seq reveals intrinsic defects in 3xTG-AD NSCs

(A) UMAP projections separating NTG and 3xTG-AD samples.

(B) Cluster proportion for each sample, expressed as a percentage of total cell number within the neurogenic clusters.

(C) Proportional difference between NTG and 3xTG-AD cluster proportions from B. Positive indicates a greater proportion in the 3xTG-AD sample, negative indicates a greater proportion in the NTG sample.

(D) Gene ontology analysis reflecting the expression fold change of indicated gene sets. Yellow reflects upregulation, blue reflects downregulation in 3xTG-AD.

(E) Violin plots demonstrating expression of representative genes, separated by cluster and sample.

Figure 4: 3xTG-AD presents defects in NSC activation

(A) UMAP projections isolating aNSC, TAP and neuron clusters, by sample.

(B) RNA velocity and pseudo-time analysis of projections from A.

(C) RNA velocity plots for indicated genes.

Figure S1: Quality control of single cell RNA-seq

A) Quality of single cell RNA sequencing and removal criteria for poor quality cells unsuitable for downstream analysis
B) Distribution of RNA counts and RNA features. The expression level of mitochondria content (mt-), ribosomal proteins (Rpl- and Rps-), and YFP expression.
C) Scatter plots of RNA counts and RNA features, mitochondria content (mt-) and RNA features, ribosomal proteins (Rps-) and RNA features, YFP expression level and RNA features.

Figure S2: Gene ontology analysis of enriched genes in NSCs population

(A) Heatmap demonstrating ten genes representative of each cluster, reflecting cluster-specific expression, for NTG and 3xTG-AD samples.
(B) UMAP projections demonstrating curated genes representative of each cluster, reflecting cluster-specific expression.

Figure S3: Gene ontology analysis of enriched genes in NSCs population

(A) Gene ontology of qNSC-enriched genes relative to dNSCs.
(B) Gene ontology of aNSC-enriched genes relative to qNSCs.

Figure S4: Cluster proportion of ten clusters

(A) Cluster proportion for each sample, expressed as a percentage of total cell number from all ten clusters.
(B) Proportional difference between NTG and 3xTG-AD cluster proportions from A. Positive indicates a greater proportion in the 3xTG-AD sample, negative indicates a greater proportion in the NTG sample.

Figure S5: VInplot of selected genes

Violin plots demonstrating expression of representative genes, separated by cluster and sample.

Figure 1

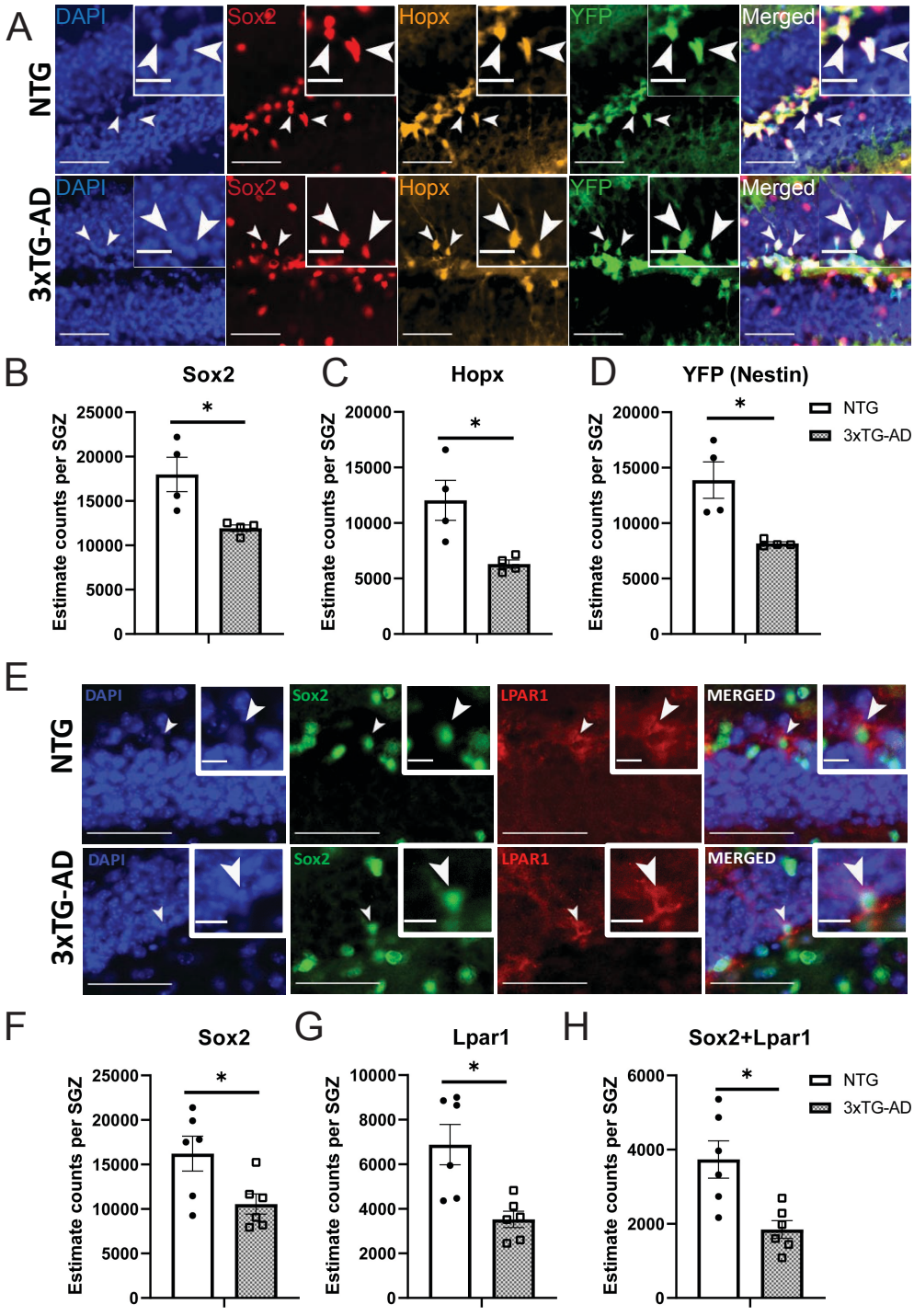
A
NTG
3xTG-AD
DAPI
Sox2
Hopx
YFP
Merged
B
Sox2
C
Hopx
D
YFP (Nestin)
Estimate counts per SGZ
NTG
3xTG-AD
E
LPAR1
MERGED
F
Sox2
G
Lpar1
H
Sox2+Lpar1

Figure 2

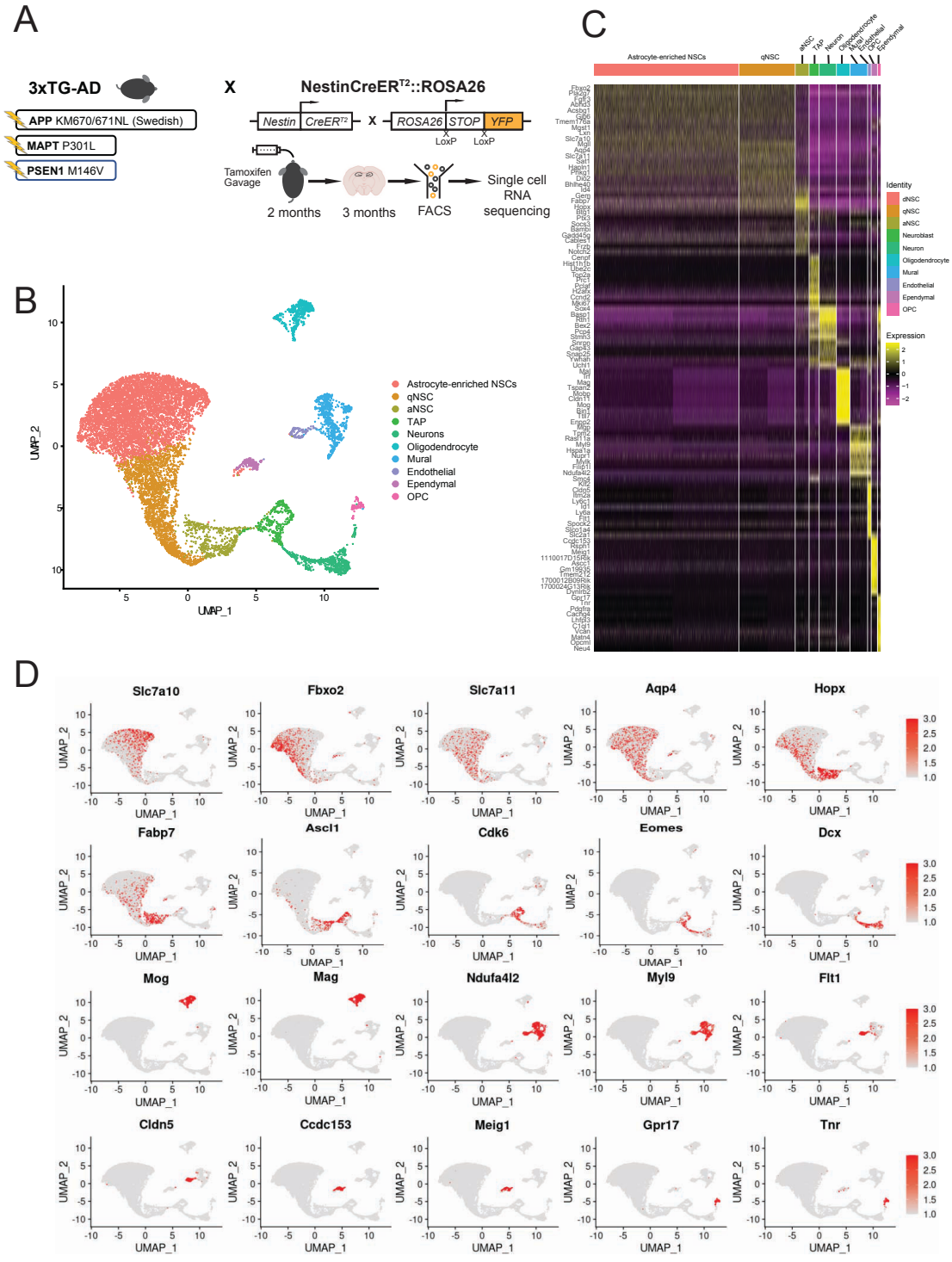
A
3xTG-AD
APP KM670/671NL (Swedish)
MAPT P301L
PSEN1 M146V
X
NestinCreER^{T2}::ROSA26
Nestin
CreER^{T2}
X
ROSA26
STOP
YFP
LoxP
LoxP
Tamoxifen Gavage
2 months
3 months
FACS
Single cell RNA sequencing
B
UMAP_1
UMAP_2
Astrocyte-enriched NSCs
qNSC
aNSC
TAP
Neurons
Oligodendrocyte
Mural
Endothelial
Ependymal
OPC
C
Astrocyte-enriched NSCs
qNSC
aNSC
TAP
Neuron
Oligodendrocyte
Mural
Endothelial
OPC
Ependymal
Identity
Expression
D
Slc7a10
Fbxo2
Slc7a11
Aqp4
Hopx
Fabp7
Ascl1
Cdk6
Eomes
Dcx
Mog
Mag
Ndufa4l2
Myl9
Flt1
Cldn5
Ccdc153
Meig1
Gpr17
Tnr
UMAP_1
UMAP_2

Figure 3

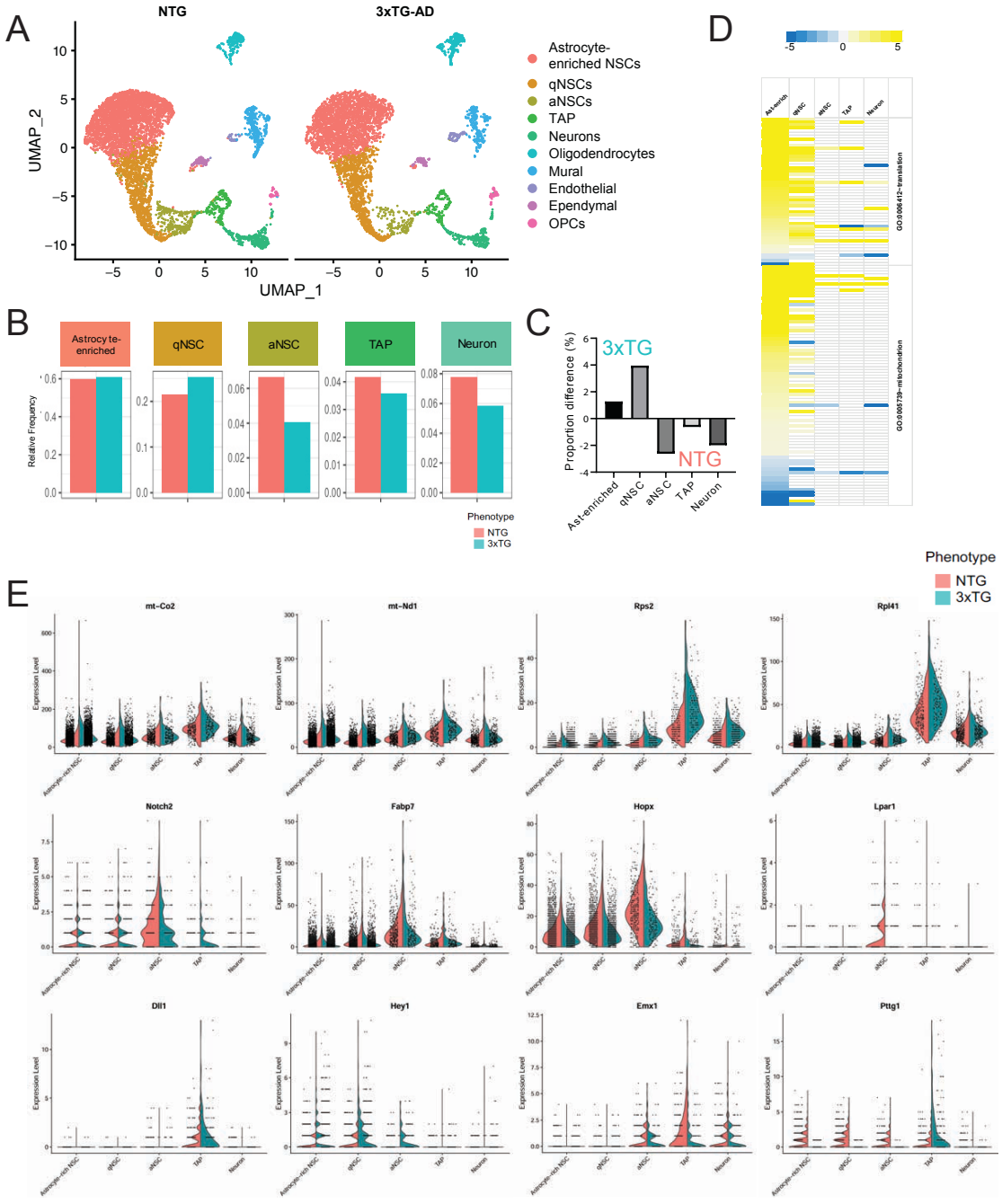
A
NTG
3xTG-AD
UMAP_2
UMAP_1
Astrocyte-enriched NSCs
qNSCs
aNSCs
TAP
Neurons
Oligodendrocytes
Mural
Endothelial
Ependymal
OPCs
B
Astrocyte-enriched
qNSC
aNSC
TAP
Neuron
Relative Frequency
Phenotype
NTG
3xTG
C
3xTG
NTG
Proportion difference (%)
Ast-enriched
qNSC
aNSC
TAP
Neuron
D
E
Phenotype
NTG
3xTG
mt-Co2
mt-Nd1
Rps2
Rpl41
Notch2
Fabp7
Hopx
Lpar1
Dll1
Hey1
Emx1
Ptg1
Expression Level

Figure 4

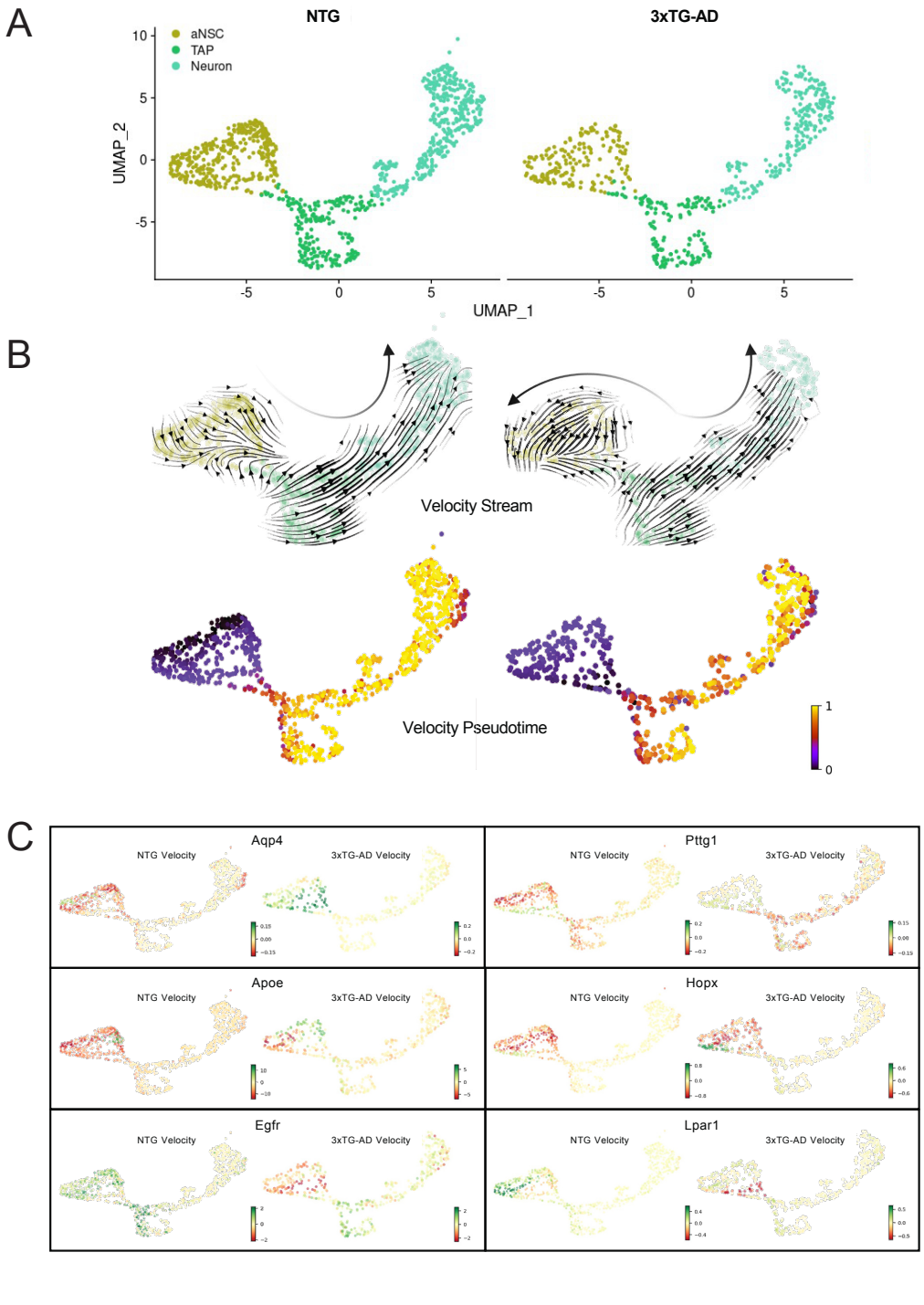
A
NTG
3xTG-AD
aNSC
TAP
Neuron
UMAP_2
UMAP_1
B
Velocity Stream
Velocity Pseudotime
C
Aqp4
Pttg1
Apoe
Hopx
Egfr
Lpar1
NTG Velocity
3xTG-AD Velocity

Figure S1

A

	NTG	3xTG-AD
Estimated Number of Cells	11,154	8,646
Fraction Reads in Cells	93.40%	93.20%
Mean Reads per Cell	43,418	53,624
Median Genes per Cell	2,344	2,367
Total Genes Detected	17,466	17,298
Median UMI Counts per Cell	5,070	5,404
Number of Cells nFeature RNA > 600 nFeature RNA < 7500 percent.yfp > 0 percent.mt < 20	6,105	5,160

B

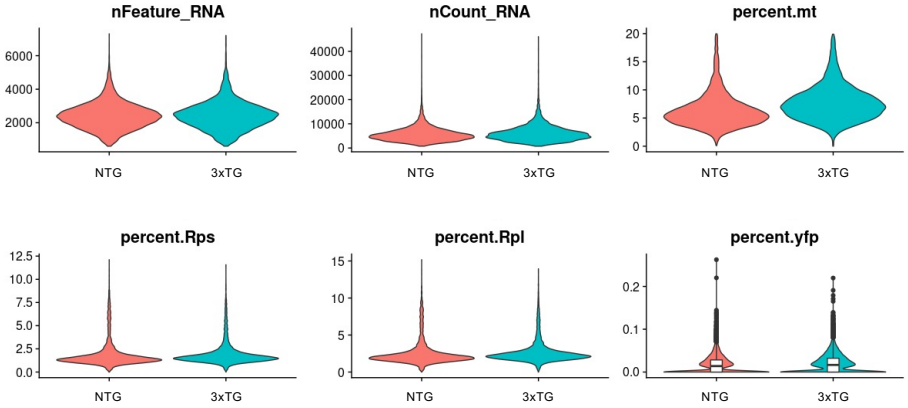

C

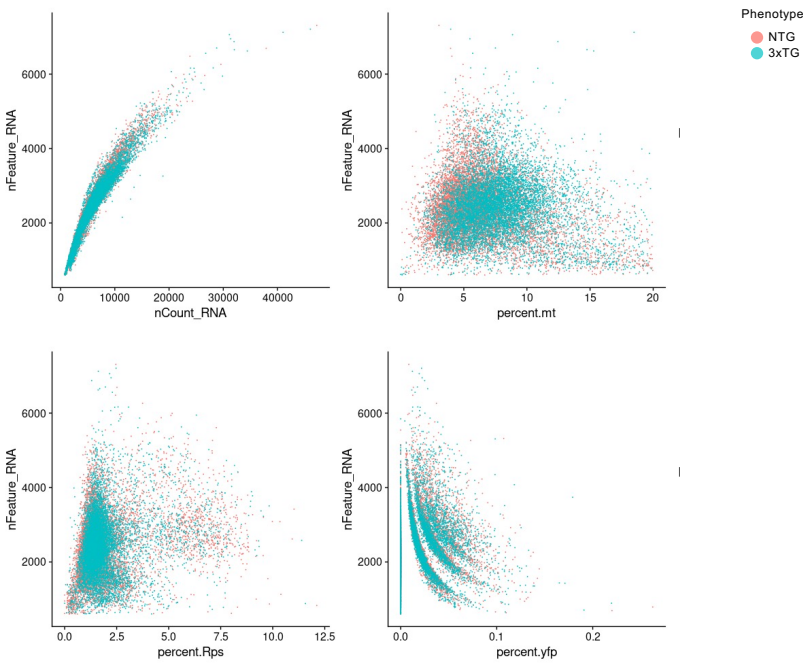

Figure S2

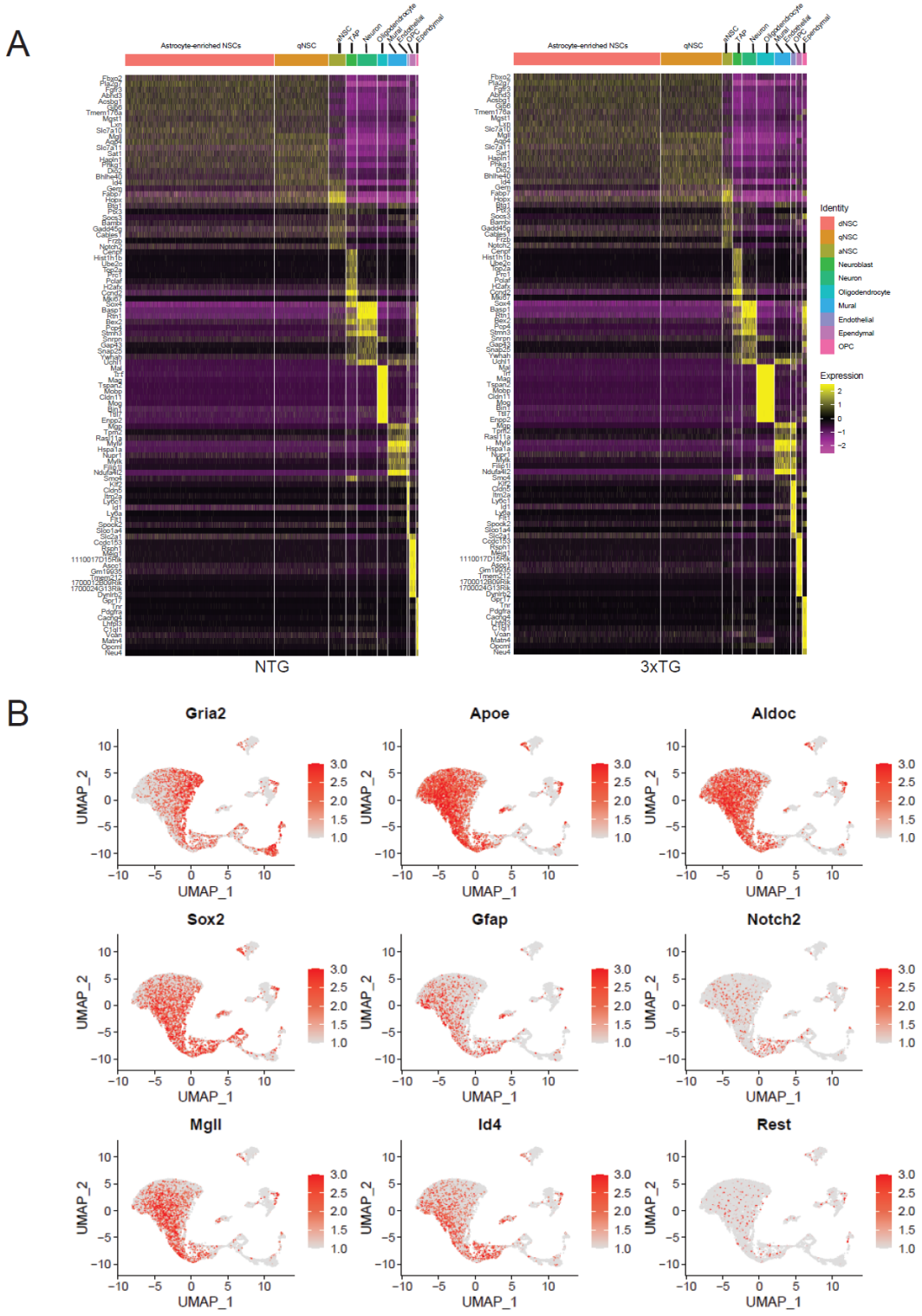
A
Astrocyte-enriched NSCs
qNSC
aNSC
TAP
Neuron
Oligodendrocyte
Mural
Endothelial
OPC
Ependymal
NTG
3xTG
Identity
qNSC
aNSC
Neuroblast
Neuron
Oligodendrocyte
Mural
Endothelial
Ependymal
OPC
Expression
B
Gria2
Apoe
Aldoc
Sox2
Gfap
Notch2
Mgll
Id4
Rest
UMAP_1
UMAP_2

Figure S3

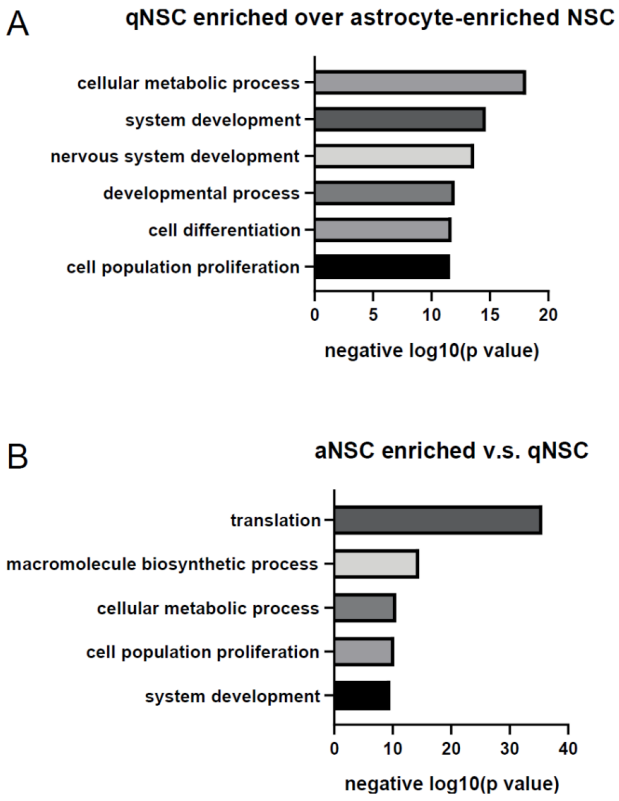
A
qNSC enriched over astrocyte-enriched NSC
cellular metabolic process
system development
nervous system development
developmental process
cell differentiation
cell population proliferation
0
5
10
15
20
negative log10(p value)
B
aNSC enriched v.s. qNSC
translation
macromolecule biosynthetic process
cellular metabolic process
cell population proliferation
system development
0
10
20
30
40
negative log10(p value)

Figure S4

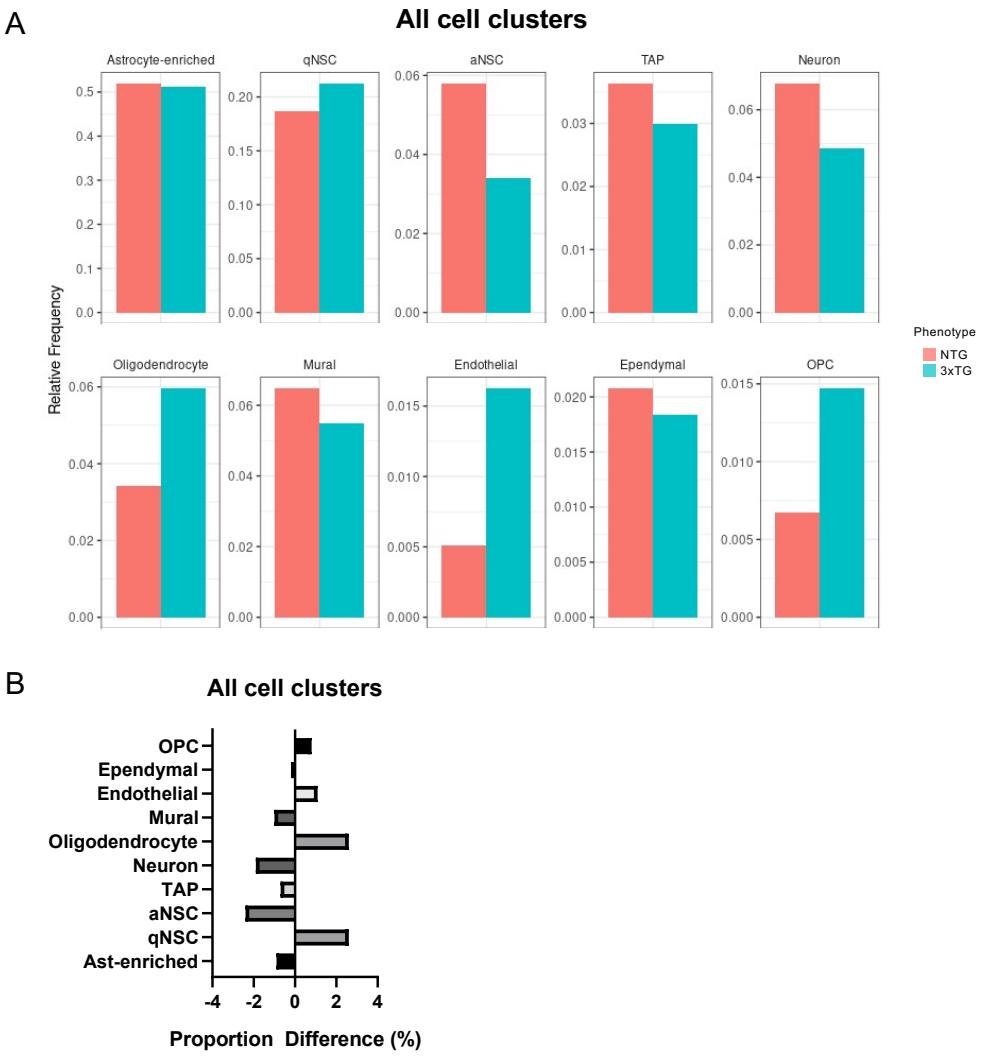
A
All cell clusters
Astrocyte-enriched
qNSC
aNSC
TAP
Neuron
Oligodendrocyte
Mural
Endothelial
Ependymal
OPC
Relative Frequency
Phenotype
NTG
3xTG
B
All cell clusters
OPC
Ependymal
Endothelial
Mural
Oligodendrocyte
Neuron
TAP
aNSC
qNSC
Ast-enriched
-4
-2
0
2
4
Proportion Difference (%)

Figure S5

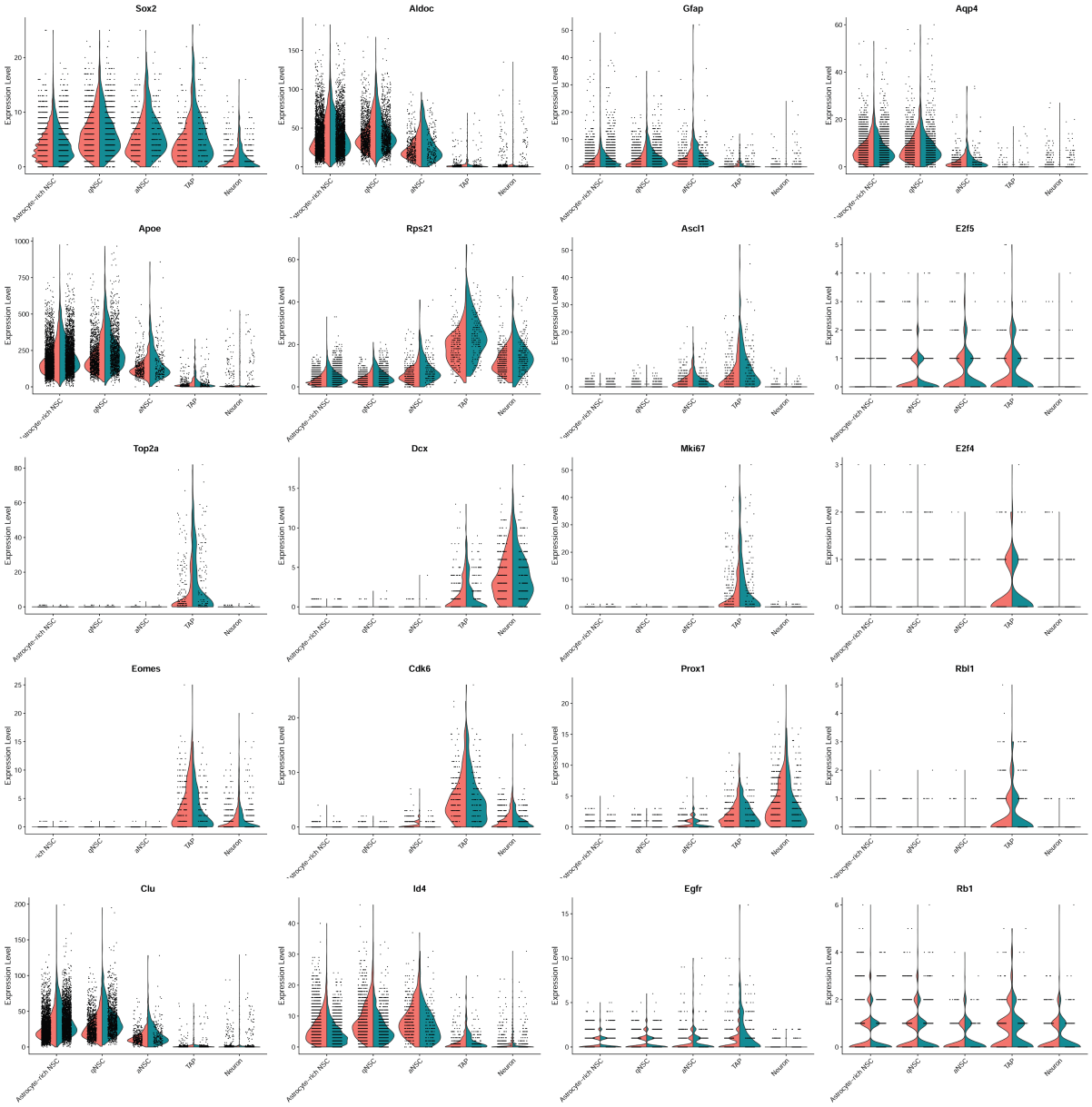
Sox2
Aldoc
Gfap
Aqp4
Apoe
Rps21
Ascl1
E2f5
Top2a
Dcx
Mki67
E2f4
Eomes
Cdk6
Prox1
Rbl1
Clu
Id4
Egfr
Rb1
Expression Level
Astrocyte-rich NSC
qNSC
aNSC
TAP
Neuron

Methods

Animals

The triple-transgenic mouse mice (3xTG-AD) were purchased from the Jackson Laboratory and previously generated at the University of California Irvine, USA (Oddo et al., 2003). Under the control of the same mouse Thy1.2 regulatory element, two transgenes carrying human familial mutations (human $APP^{/Swe}$ and human $tau^{/P301L}$) were integrated into the same locus of homozygous $PSEN1^{/M146V}$ knock-in mice (JAX stock number: 004807). Wild type mice from the same genetic background were served as non-transgenic control (NTG, JAX stock number: 101045).

The *Nestin-CreER^{T2}* mouse line (Nestin-Cre) was a gift from Dr. Suzanne J Baker at the University of Tennessee Health Science Center (Cicero et al., 2009; Zhu et al., 2012). *Nestin-CreER^{T2}* mice bear the *CreER^{T2}* transgene that is driven by the *Nestin* promoter and an enhancer in the second intron, an internal ribosomal entry size and human placental alkaline phosphatase (*hPLAP*) (Zimmerman et al., 1994). Cre-activity was mapped through cross-breeding with the *R26LSL-EYFP* mice to generate *Nestin-CreER^{T2};R26LSL-EYFP* mice (Srinivas et al., 2001). For single cell RNA-seq experiments, 3xTG-AD or NTG mice were cross-breed with *Nestin-CreER^{T2};R26LSL-EYFP* mice to generate mice with conditional YFP labeling of Nestin-positive cells for lineage tracing 3x*TG;Nestin-CreER^{T2};R26LSL-EYFP or NTG;Nestin-CreER^{T2};R26LSL-EYFP*. All experimental protocols were performed in compliance with University of Ottawa policy concerning the care and use of animals in research (protocol #ME-1765). Genotyping primer sequences are shown in Table S3.

Tamoxifen Administration

Cre recombination was induced by administration of tamoxifen (TAM) through oral gavage at a dose of 200mg/kg in *NTG;Nestin-CreER^{T2};R26LSL-EYFP* or *3xTG;Nestin-CreER^{T2};R26LSL-EYFP* mice daily at 2 months of age for five consecutive days (Khacho et al., 2016).

Animal Euthanasia

Animals were euthanized with intraperitoneal injection of Euthanyl (Sodium Pentobarbital) at 120 mg/kg. To collect brains for live cells, brains were then dissected and the SGZ or SVZ was collected for experiments. To fix the brains for immunostaining experiments, a perfusion needle was inserted into the left ventricle and the right atrium was open for systemic drainage. Mice were flushed with 20 ml of 0.9% cold saline and then perfused with 20 ml of 4% cold paraformaldehyde (PFA) (pH 7.4) to fix. Brains were dissected and post-fixed in 4% PFA at 4°C for 24 hours. Brains were then incubated and stored in 20% sucrose in PBS at 4°C with supplement of 0.3% sodium azide until processed further.

Single Cell Collection and Fluorescence-activated cell sorting (FACS)
SGZ was dissected coronally in ice-cold ACSF under a Leica M165 FC stereomicroscope from *NTG;Nestin-CreER^{T2};R26LSL-EYFP or 3xTG;Nestin-CreER^{T2};R26LSL-EYFP* mice. Tissue was collected in 1.5ml Eppendorf tube with ice-cold ACSF, transferred to pre-warmed papain solution at 20 U/ml (Worthington Cat. PAP3126), homogenized with a pestle and immediately digested for 10 mins after homogenized with a pestle (Corning, PES-15-B-SI) at 37°C on a rotator. An equal volume of resuspension medium that contains 0.5 mg/ml of DNase I (Roche Cat. # 11284932001) and 10% of fetal bovine serum (Wisent Cat. # 080150) was added to the digested tissue in papain solution. Tissue was triturated 4 to 6 times with P1000 micropipet and incubated for 5 mins at room temperature. Cell suspension was collected in 15 ml tubes and cell pellets were triturated again with another 1 ml of resuspension medium. Cell suspension from different trituration was pooled and the final volume was brought to 3.9 ml. 1.1 ml of 90% Percoll in PBS was added to 3.9 ml of cell suspension. After gentle mixing, cells were span down at 500 xg for 12.5 mins at 4°C. Cell pellet was washed with DMEM:F12 and then resuspended in sorting medium (DMEM:F12 without phenol red, Invitrogen Life Tech. Cat. # 21041-025, plus 1% BSA). YFP-positive cells from 2-3 mice of each genotype were collected after viability screening with propidium iodide staining (ThermoFisher, Cat. # P3566) on a Beckman Coulter MoFlo platform in the Flow Cytometry and Cell Sorting Facility located in the Ottawa Hospital Sprott Center (Ottawa, Canada).

Single Cell RNA Transcriptome (scRNA-seq)
Freshly collected YFP-positive cells were sent to StemCore Laboratories located in the Ottawa Hospital Sprott Center, for both *NTG;Nestin-CreER^{T2};R26LSL-EYFP and 3xTG;Nestin-CreER^{T2};R26LSL-EYFP* samples. The transcriptome of viable single cells was analyzed using the 10x Genomics Chromium Single Cell Assay platform, individually for each genotype. A single cell RNA library was created following the single cell 3' Reagent Kits v2 user guide (Cat: CG0052, 10x Genomics) on the Chromium Single Cell Instrument (10x Genomics) using Single Cell 3' Library & Gel Bead Kit v2 and Chip Kit (P/N 120236 and P/N 120237, 10x Genomics). The cDNA library was then purified with SPRIselect (Beckman Coulter). Agilent Fragment Analyzer was used to evaluate the size distribution and yield (Agilent). The sequencing was performed on Illumina NextSeq 500 instrument (Illumina) using the following parameters 28 bp Read1, 8 bp I7 Index, 0 bp I5 Index, and 98 bp Read2. Single-end reads were aligned to the reference genome, mm10, using the CellRanger pipeline (10X Genomics), after demultiplexing cell barcodes and UMI (unique molecular identifiers) barcodes. The output cell-gene matrix contains UMI counts by genes and by cell barcodes. Gene expression profiles were then mapped using Seurat v3 in R studio (Stuart et al., 2019).

Single Cell Selection and Clustering
Cells that meet the following criteria were selected for further analysis: 1) with more than 600 genes recorded; 2) with less than 7500 genes recorded; 3) with mitochondria content less than 20% of total RNA counts; and 4) with detectable YFP expression. RNA reads were normalized with the function of sctransform "SCT". Based on normalized RNA reads, cells were clustered using the following parameters: 1) dims

=1:8; and 2) resolution = 0.2. Ten cell clusters were identified based on normalized expression profiles of each cell. Based on the original RNA reads, cluster-specific markers were calculated with the function of FindAllMarkers. Differential expression between NTG and 3xTG-AD for each cluster was analyzed with the function of FindMarkers. Heatmaps of cluster-specific genes were mapped on normalized data. FeaturePlot (Umap) and VlnPlot (violin plot) of specific genes were mapped on original RNA reads.

Cell clusters with characteristics of the neurogenic lineage were sub-grouped to show differential expression of selected genes. Activated NSC, TAP and Neurons were sub-grouped and reclustered using the following parameters: 1) dims =1:13; and 2) resolution = 0.1. RNA velocity data were generated in Seurat based on normalized data, and analyzed in Python-based Spyder program using the “deterministic” mode (La Manno et al., 2018; Stuart et al., 2019).

Tissue Processing for Immunostaining

Each brain was cut into two hemispheres. One half hemisphere was frozen in -40°C isopentane (Thermo Fisher Scientific) for 60 seconds and then preserved in aluminum foil on dry ice or in -80°C freezers until cryosection. Serial coronal sectioning at 30µm thickness were performed to reveal the whole SGZ using the Leica CM1850. SGZ sections were collected sequentially from the beginning to the end of the dentate gyrus into 9 wells of a 24-well plate containing PBS and 0.01% sodium azide at 4°C.

Immunostaining

For immunofluorescence staining, sections in one of the nine wells from each brain were rinsed 3 times in wash buffer (PBS) for 5 minutes and then permeabilized 3 times with incubation buffer (0.1% Triton X-100 and 0.1% Tween-20 in PBS) for 5 minutes. Sections were incubated overnight with primary antibodies in incubation buffer at 4°C (Hopx, 1:1000, HPA030180, Atlas Antibodies; Lpar1, 1:1000, NBP1-03363, Novus Biologicals; Sox2, 1:2000, GT15098, Neuromics; YFP, 1:1000). Sections were rinsed 3 times in wash buffer for 5 minutes, and then incubated with secondary antibodies and 4',6-diamidino-2-phenylindole (DAPI) in incubation buffer for 2 hours at room temperature (anti-rabbit-Cy3, 1:1000, 711-165-152, Jackson; anti-mouse Alexa488, 1:1000, 715-165-151, Jackson; anti-goat Cy5, 1:1000, 705-165-147, Jackson; DAPI, 0.1 µg/ml, D9542, Sigma-Aldrich). Sections were mounted with Immunomount (Genetex) on FisherbrandTM SuperfrostTM Plus Microscope Slides (Thermo Fisher Scientific). Immunofluorescence images were taken with DeltaVision Elite-Olympus IX-71 or ZEISS Axioscan 7 at a 20X magnification. Images were then processed and quantified with Fiji (Image J).

Cell Counting and Statistical Analysis

Cells expressing the marker of interest were quantified along the entire SGZ of the DG. The number of all positive cells was multiplied by 9 to obtain the estimated total cell number of the whole DG (Khacho et al., 2016). Two-tailed and unpaired student's t-test was used for statistical analysis using GraphPad PRISM software (GraphPad Software, Inc).

References

Andersen, J., Urban, N., Achimastou, A., Ito, A., Simic, M., Ullom, K., Martynoga, B., Lebel, M., Göritz, C., Frisén, J., Nakafuku, M. & Guillemot, F. (2014). A transcriptional mechanism integrating inputs from extracellular signals to activate hippocampal stem cells. *Neuron*, *83*(5), 1085–1097. https://doi.org/10.1016/j.neuron.2014.08.004

Artegiani, B., Lyubimova, A., Muraro, M., van Es, J. H., van Oudenaarden, A., & Clevers, H. (2017). A Single-Cell RNA Sequencing Study Reveals Cellular and Molecular Dynamics of the Hippocampal Neurogenic Niche. *Cell Reports*, *21*(11), 3271–3284. https://doi.org/10.1016/j.celrep.2017.11.050

Basak, O., Krieger, T. G., Muraro, M. J., Wiebrands, K., Stange, D. E., Frias-Aldeguer, J., Rivron, N. C., Wetering, M. van de, Es, J. H. van, Oudenaarden, A. van, Simons, B. D., & Clevers, H. (2018). Troy+ brain stem cells cycle through quiescence and regulate their number by sensing niche occupancy. *Proceedings of the National Academy of Sciences*, *115*(4), E610–E619. https://doi.org/10.1073/pnas.1715911114

Belfiore, R., Rodin, A., Ferreira, E., Velazquez, R., Branca, C., Caccamo, A., & Oddo, S. (2019). Temporal and regional progression of Alzheimer's disease-like pathology in 3xTg-AD mice. *Aging Cell*, *18*(1), e12873. https://doi.org/10.1111/acel.12873

Berg, D. A., Su, Y., Jimenez-Cyrus, D., Patel, A., Huang, N., Morizet, D., Lee, S., Shah, R., Ringeling, F. R., Jain, R., Epstein, J. A., Wu, Q.-F., Canzar, S., Ming, G.-L., Song, H., & Bond, A. M. (2019). A Common Embryonic Origin of Stem Cells

Drives Developmental and Adult Neurogenesis. *Cell*, *177*(3), 654-668.e15. https://doi.org/10.1016/j.cell.2019.02.010

Bernal, A., & Arranz, L. (2018). Nestin-expressing progenitor cells: Function, identity and therapeutic implications. *Cellular and Molecular Life Sciences*, *75*(12), 2177–2195. https://doi.org/10.1007/s00018-018-2794-z

Blomfield, I. M., Rocamonde, B., Masdeu, M. del M., Mulugeta, E., Vaga, S., van den Berg, D. L., Huillard, E., Guillemot, F., & Urbán, N. (2019). Id4 promotes the elimination of the pro-activation factor Ascl1 to maintain quiescence of adult hippocampal stem cells. *ELife*, *8*, e48561. https://doi.org/10.7554/eLife.48561

Bonaguidi, M. A., Stadel, R. P., Berg, D. A., Sun, J., Ming, G.-L. & Song, H. (2016). Diversity of Neural Precursors in the Adult Mammalian Brain. *Cold Spring Harbor Perspectives in Biology*, *8*(4), a018838-20. https://doi.org/10.1101/cshperspect.a018838

Bond, A. M., Ming, G. & Song, H. (2015). Adult Mammalian Neural Stem Cells and Neurogenesis: Five Decades Later. *Cell Stem Cell*, *17*(4), 385–395. https://doi.org/10.1016/j.stem.2015.09.003

Borrett, M. J., Innes, B. T., Jeong, D., Tahmasian, N., Storer, M. A., Bader, G. D., Kaplan, D. R., & Miller, F. D. (2020). Single-Cell Profiling Shows Murine Forebrain Neural Stem Cells Reacquire a Developmental State when Activated for Adult Neurogenesis. *Cell Reports*, *32*(6), 108022. https://doi.org/10.1016/j.celrep.2020.108022

Chen, W.-T., Lu, A., Craessaerts, K., Pavie, B., Sala Frigerio, C., Corthout, N., Qian, X., Laláková, J., Kühnemund, M., Voytyuk, I., Wolfs, L., Mancuso, R., Salta, E.,

Balusu, S., Snellinx, A., Munck, S., Jurek, A., Fernandez Navarro, J., Saido, T. C., … De Strooper, B. (2020). Spatial Transcriptomics and In Situ Sequencing to Study Alzheimer's Disease. *Cell*, *182*(4), 976-991.e19. https://doi.org/10.1016/j.cell.2020.06.038

Cicero, S. A., Johnson, D., Reyntjens, S., Frase, S., Connell, S., Chow, L. M. L., Baker, S. J., Sorrentino, B. P., & Dyer, M. A. (2009). Cells previously identified as retinal stem cells are pigmented ciliary epithelial cells. *Proceedings of the National Academy of Sciences*, *106*(16), 6685–6690. https://doi.org/10.1073/pnas.0901596106

Codega, P., Silva-Vargas, V., Paul, A., Maldonado-Soto, A. R., Deleo, A. M., Pastrana, E., & Doetsch, F. (2014). Prospective identification and purification of quiescent adult neural stem cells from their in vivo niche. *Neuron*, *82*(3), 545–559. https://doi.org/10.1016/j.neuron.2014.02.039

Coupé, P., Manjón, J. V., Lanuza, E. & Catheline, G. (2019). Lifespan Changes of the Human Brain In Alzheimer's Disease. *Scientific Reports*, *9*(1), 3998. https://doi.org/10.1038/s41598-019-39809-8

Deng, W., Aimone, J. B., & Gage, F. H. (2010). New neurons and new memories: How does adult hippocampal neurogenesis affect learning and memory? *Nature Reviews. Neuroscience*, *11*(5), 339–350. https://doi.org/10.1038/nrn2822

Gabut, M., Bourdelais, F., & Durand, S. (2020). Ribosome and Translational Control in Stem Cells. *Cells*, *9*(2), 497. https://doi.org/10.3390/cells9020497

Gonçalves, J. T., Schafer, S. T. & Gage, F. H. (2016). Adult Neurogenesis in the Hippocampus: From Stem Cells to Behavior. *Cell*, *167*(4), 897–914. https://doi.org/10.1016/j.cell.2016.10.021

Habib, N., McCabe, C., Medina, S., Varshavsky, M., Kitsberg, D., Dvir-Szternfeld, R., Green, G., Dionne, D., Nguyen, L., Marshall, J. L., Chen, F., Zhang, F., Kaplan, T., Regev, A., & Schwartz, M. (2020). Disease-associated astrocytes in Alzheimer's disease and aging. *Nature Neuroscience*, *23*(6), 701–706. https://doi.org/10.1038/s41593-020-0624-8

Hamilton, L. K., Aumont, A., Julien, C., Vadnais, A., Calon, F., & Fernandes, K. J. L. (2010). Widespread deficits in adult neurogenesis precede plaque and tangle formation in the 3xTg mouse model of Alzheimer's disease. *The European Journal of Neuroscience*, *32*(6), 905–920. https://doi.org/10.1111/j.1460-9568.2010.07379.x

Hamilton, L. K., Dufresne, M., Joppé, S. E., Petryszyn, S., Aumont, A., Calon, F., Barnabé-Heider, F., Furtos, A., Parent, M., Chaurand, P., & Fernandes, K. J. L. (2015). Aberrant Lipid Metabolism in the Forebrain Niche Suppresses Adult Neural Stem Cell Proliferation in an Animal Model of Alzheimer's Disease. *Cell Stem Cell*, *17*(4), 397–411. https://doi.org/10.1016/j.stem.2015.08.001

He, L., Vanlandewijck, M., Raschperger, E., Andaloussi Mäe, M., Jung, B., Lebouvier, T., Ando, K., Hofmann, J., Keller, A., & Betsholtz, C. (2016). Analysis of the brain mural cell transcriptome. *Scientific Reports*, *6*(1), 35108. https://doi.org/10.1038/srep35108

Izadi, F., & Soheilifar, M. H. (2018). Exploring Potential Biomarkers Underlying Pathogenesis of Alzheimer's Disease by Differential Co-expression Analysis. *Avicenna Journal of Medical Biotechnology*, *10*(4), 233–241.

Khacho, M., Clark, A., Svoboda, D. S., Azzi, J., MacLaurin, J. G., Meghaizel, C., Sesaki, H., Lagace, D. C., Germain, M., Harper, M.-E., Park, D. S., & Slack, R. S. (2016). Mitochondrial Dynamics Impacts Stem Cell Identity and Fate Decisions by Regulating a Nuclear Transcriptional Program. *Cell Stem Cell*, *19*(2), 232–247. https://doi.org/10.1016/j.stem.2016.04.015

Khacho, M., Harris, R., & Slack, R. S. (2019). Mitochondria as central regulators of neural stem cell fate and cognitive function. *Nature Reviews. Neuroscience*, *20*(1), 34–48. https://doi.org/10.1038/s41583-018-0091-3

Kitabatake, Y., Sailor, K. A., Ming, G., & Song, H. (2007). Adult neurogenesis and hippocampal memory function: New cells, more plasticity, new memories? *Neurosurgery Clinics of North America*, *18*(1), 105–113, x. https://doi.org/10.1016/j.nec.2006.10.008

Knopman, D. S., Amieva, H., Petersen, R. C., Chételat, G., Holtzman, D. M., Hyman, B. T., Nixon, R. A. & Jones, D. T. (2021). Alzheimer disease. *Nature Reviews Disease Primers*, *7*(1), 33. https://doi.org/10.1038/s41572-021-00269-y

La Manno, G., Soldatov, R., Zeisel, A., Braun, E., Hochgerner, H., Petukhov, V., Lidschreiber, K., Kastriti, M. E., Lönnerberg, P., Furlan, A., Fan, J., Borm, L. E., Liu, Z., van Bruggen, D., Guo, J., He, X., Barker, R., Sundström, E., Castelo-Branco, G., … Kharchenko, P. V. (2018). RNA velocity of single cells. *Nature*, *560*(7719), 494–498. https://doi.org/10.1038/s41586-018-0414-6

Li, D., Takeda, N., Jain, R., Manderfield, L. J., Liu, F., Li, L., Anderson, S. A., & Epstein, J. A. (2015). Hopx distinguishes hippocampal from lateral ventricle neural stem cells. *Stem Cell Research*, *15*(3), 522–529. https://doi.org/10.1016/j.scr.2015.09.015

Liu, L., Wu, Q., Zhong, W., Chen, Y., Zhang, W., Ren, H., Sun, L., & Sun, J. (2020). Microarray Analysis of Differential Gene Expression in Alzheimer's Disease Identifies Potential Biomarkers with Diagnostic Value. *Medical Science Monitor : International Medical Journal of Experimental and Clinical Research*, *26*, e919249-1-e919249-16. https://doi.org/10.12659/MSM.919249

Llorens-Martín, M., Fuster-Matanzo, A., Teixeira, C. M., Jurado-Arjona, J., Ulloa, F., deFelipe, J., Rábano, A., Hernández, F., Soriano, E., & Ávila, J. (2013). GSK-3β overexpression causes reversible alterations on postsynaptic densities and dendritic morphology of hippocampal granule neurons in vivo. *Molecular Psychiatry*, *18*(4), 451–460. https://doi.org/10.1038/mp.2013.4

Marques, S., van Bruggen, D., & Castelo-Branco, G. (2019). Single-Cell RNA Sequencing of Oligodendrocyte Lineage Cells from the Mouse Central Nervous System. *Methods in Molecular Biology (Clifton, N.J.)*, *1936*, 1–21. https://doi.org/10.1007/978-1-4939-9072-6_1

Matas-Rico, E., García-Diaz, B., Llebrez-Zayas, P., López-Barroso, D., Santín, L., Pedraza, C., Smith-Fernández, A., Fernández-Llebrez, P., Tellez, T., Redondo, M., Chun, J., De Fonseca, F. R., & Estivill-Torrús, G. (2008). Deletion of lysophosphatidic acid receptor LPA1 reduces neurogenesis in the mouse dentate

gyrus. *Molecular and Cellular Neurosciences*, *39*(3), 342–355. https://doi.org/10.1016/j.mcn.2008.07.014

Matsumata, M., Sakayori, N., Maekawa, M., Owada, Y., Yoshikawa, T., & Osumi, N. (2012). The effects of Fabp7 and Fabp5 on postnatal hippocampal neurogenesis in the mouse. *Stem Cells (Dayton, Ohio)*, *30*(7), 1532–1543. https://doi.org/10.1002/stem.1124

Mizrak, D., Levitin, H. M., Delgado, A. C., Crotet, V., Yuan, J., Chaker, Z., Silva-Vargas, V., Sims, P. A., & Doetsch, F. (2019). Single-Cell Analysis of Regional Differences in Adult V-SVZ Neural Stem Cell Lineages. *Cell Reports*, *26*(2), 394-406.e5. https://doi.org/10.1016/j.celrep.2018.12.044

Moreno-Jiménez, E. P., Flor-García, M., Terreros-Roncal, J., Rábano, A., Cafini, F., Pallas-Bazarra, N., Ávila, J., & Llorens-Martín, M. (2019). Adult hippocampal neurogenesis is abundant in neurologically healthy subjects and drops sharply in patients with Alzheimer's disease. *Nature Medicine*, *25*(4), 554–560. https://doi.org/10.1038/s41591-019-0375-9

Mu, Y. & Gage, F. H. (2011). Adult hippocampal neurogenesis and its role in Alzheimer's disease. *Molecular Neurodegeneration*, *6*(1), 85. https://doi.org/10.1186/1750-1326-6-85

Oddo, S., Caccamo, A., Shepherd, J. D., Murphy, M. P., Golde, T. E., Kayed, R., Metherate, R., Mattson, M. P., Akbari, Y., & LaFerla, F. M. (2003). Triple-transgenic model of Alzheimer's disease with plaques and tangles: Intracellular Abeta and synaptic dysfunction. *Neuron*, *39*(3), 409–421.

Ohm, T. G. (2007). The dentate gyrus in Alzheimer's disease. *Progress in Brain Research*, *163*, 723–740. https://doi.org/10.1016/s0079-6123(07)63039-8

Pilz, G.-A., Bottes, S., Betizeau, M., Jörg, D. J., Carta, S., Simons, B. D., Helmchen, F., & Jessberger, S. (2018). Live imaging of neurogenesis in the adult mouse hippocampus. *Science*, *359*(6376), 658–662. https://doi.org/10.1126/science.aao5056

Rodríguez, J. J., Jones, V. C., Tabuchi, M., Allan, S. M., Knight, E. M., LaFerla, F. M., Oddo, S., & Verkhratsky, A. (2008). Impaired Adult Neurogenesis in the Dentate Gyrus of a Triple Transgenic Mouse Model of Alzheimer's Disease. *PLoS ONE*, *3*(8), e2935. https://doi.org/10.1371/journal.pone.0002935

Rodríguez, J. J., Jones, V. C., & Verkhratsky, A. (2009). Impaired cell proliferation in the subventricular zone in an Alzheimer's disease model. *NeuroReport*, *20*(10), 907–912. https://doi.org/10.1097/wnr.0b013e32832be77d

Saba, J. A., Liakath-Ali, K., Green, R., & Watt, F. M. (2021). Translational control of stem cell function. *Nature Reviews Molecular Cell Biology*, *22*(10), 671–690. https://doi.org/10.1038/s41580-021-00386-2

Sahay, A., Scobie, K. N., Hill, A. S., O'Carroll, C. M., Kheirbek, M. A., Burghardt, N. S., Fenton, A. A., Dranovsky, A. & Hen, R. (2011). Increasing adult hippocampal neurogenesis is sufficient to improve pattern separation. *Nature*, *472*(7344), 466–470. https://doi.org/10.1038/nature09817

Sharifi, S., da Costa, H. F. R., & Bierhoff, H. (2020). The circuitry between ribosome biogenesis and translation in stem cell function and ageing. *Mechanisms of*

Ageing and Development, *189*, 111282. https://doi.org/10.1016/j.mad.2020.111282

Shin, J., Berg, D. A., Zhu, Y., Shin, J. Y., Song, J., Bonaguidi, M. A., Enikolopov, G., Nauen, D. W., Christian, K. M., Ming, G., & Song, H. (2015). Single-Cell RNA-Seq with Waterfall Reveals Molecular Cascades underlying Adult Neurogenesis. *Cell Stem Cell*, *17*(3), 360–372. https://doi.org/10.1016/j.stem.2015.07.013

Srinivas, S., Watanabe, T., Lin, C.-S., William, C. M., Tanabe, Y., Jessell, T. M., & Costantini, F. (2001). Cre reporter strains produced by targeted insertion of EYFP and ECFP into the ROSA26 locus. *BMC Developmental Biology*, *1*(1), 4. https://doi.org/10.1186/1471-213X-1-4

Stoub, T. R., deToledo-Morrell, L., Stebbins, G. T., Leurgans, S., Bennett, D. A. & Shah, R. C. (2006). Hippocampal disconnection contributes to memory dysfunction in individuals at risk for Alzheimer's disease. *Proceedings of the National Academy of Sciences*, *103*(26), 10041–10045. https://doi.org/10.1073/pnas.0603414103

Stuart, T., Butler, A., Hoffman, P., Hafemeister, C., Papalexi, E., Mauck, W. M., Hao, Y., Stoeckius, M., Smibert, P., & Satija, R. (2019). Comprehensive Integration of Single-Cell Data. *Cell*, *177*(7), 1888-1902.e21. https://doi.org/10.1016/j.cell.2019.05.031

Tahmasebi, S., Amiri, M., & Sonenberg, N. (2019). Translational Control in Stem Cells. *Frontiers in Genetics*, *9*, 709. https://doi.org/10.3389/fgene.2018.00709

Terreros-Roncal, J., Moreno-Jiménez, E. P., Flor-García, M., Rodríguez-Moreno, C. B., Trinchero, M. F., Cafini, F., Rábano, A., & Llorens-Martín, M. (2021). Impact of

neurodegenerative diseases on human adult hippocampal neurogenesis. *Science*, *374*(6571), 1106–1113. https://doi.org/10.1126/science.abl5163

Than-Trong, E., Ortica-Gatti, S., Mella, S., Nepal, C., Alunni, A., & Bally-Cuif, L. (2018). Neural stem cell quiescence and stemness are molecularly distinct outputs of the Notch3 signaling cascade in the vertebrate adult brain. *Development*, *145*(10), dev.161034-64. https://doi.org/10.1242/dev.161034

Tobin, M. K., Musaraca, K., Disouky, A., Shetti, A., Bheri, A., Honer, W. G., Kim, N., Dawe, R. J., Bennett, D. A., Arfanakis, K., & Lazarov, O. (2019). Human Hippocampal Neurogenesis Persists in Aged Adults and Alzheimer's Disease Patients. *Cell Stem Cell*, *24*(6), 974-982.e3. https://doi.org/10.1016/j.stem.2019.05.003

Toda, T. & Gage, F. H. (2017). Review: adult neurogenesis contributes to hippocampal plasticity. *Cell and Tissue Research*, *12*(764–773), 1–17. https://doi.org/10.1007/s00441-017-2735-4

Urban, N., Berg, D. L. C. van den, Forget, A., Andersen, J., Demmers, J. A. A., Hunt, C., Ayrault, O. & Guillemot, F. (2016). Return to quiescence of mouse neural stem cells by degradation of a proactivation protein. *Science (New York, N.Y.)*, *353*(6296), 292–295. https://doi.org/10.1126/science.aaf4802

Urbán, N., Blomfield, I. M. & Guillemot, F. (2019). Quiescence of Adult Mammalian Neural Stem Cells: A Highly Regulated Rest. *Neuron*, *104*(5), 834–848. https://doi.org/10.1016/j.neuron.2019.09.026

Walker, T. L., Overall, R. W., Vogler, S., Sykes, A. M., Ruhwald, S., Lasse, D., Ichwan, M., Fabel, K., & Kempermann, G. (2016). Lysophosphatidic Acid Receptor Is a

Functional Marker of Adult Hippocampal Precursor Cells. *Stem Cell Reports*, *6*(4), 552–565. https://doi.org/10.1016/j.stemcr.2016.03.002

Wander, C. M., & Song, J. (2021). The Neurogenic Niche in Alzheimer's disease. *Neuroscience Letters*, 136109. https://doi.org/10.1016/j.neulet.2021.136109

Youssef, M., Krish, V. S., Kirshenbaum, G. S., Atsak, P., Lass, T. J., Lieberman, S. R., Leonardo, E. D., & Dranovsky, A. (2018). Ablation of proliferating neural stem cells during early life is sufficient to reduce adult hippocampal neurogenesis. *Hippocampus*, *28*(8), 586–601. https://doi.org/10.1002/hipo.22962

Yuzwa, S. A., Borrett, M. J., Innes, B. T., Voronova, A., Ketela, T., Kaplan, D. R., Bader, G. D., & Miller, F. D. (2017). Developmental Emergence of Adult Neural Stem Cells as Revealed by Single-Cell Transcriptional Profiling. *Cell Reports*, *21*(13), 3970–3986. https://doi.org/10.1016/j.celrep.2017.12.017

Zhang, H., Menzies, K. J., & Auwerx, J. (2018). The role of mitochondria in stem cell fate and aging. *Development (Cambridge, England)*, *145*(8), dev143420. https://doi.org/10.1242/dev.143420

Zhang, R., Boareto, M., Engler, A., Louvi, A., Giachino, C., Iber, D., & Taylor, V. (2019). Id4 Downstream of Notch2 Maintains Neural Stem Cell Quiescence in the Adult Hippocampus. *Cell Reports*, *28*(6), 1485-1498.e6. https://doi.org/10.1016/j.celrep.2019.07.014

Zhang, Y., Sloan, S. A., Clarke, L. E., Caneda, C., Plaza, C. A., Blumenthal, P. D., Vogel, H., Steinberg, G. K., Edwards, M. S. B., Li, G., Duncan, J. A., Cheshier, S. H., Shuer, L. M., Chang, E. F., Grant, G. A., Gephart, M. G. H., & Barres, B. A. (2016). Purification and Characterization of Progenitor and Mature Human

Astrocytes Reveals Transcriptional and Functional Differences with Mouse. *Neuron*, *89*(1), 37–53. https://doi.org/10.1016/j.neuron.2015.11.013

Zhao, Q., Eichten, A., Parveen, A., Adler, C., Huang, Y., Wang, W., Ding, Y., Adler, A., Nevins, T., Ni, M., Wei, Y., & Thurston, G. (2018). Single-Cell Transcriptome Analyses Reveal Endothelial Cell Heterogeneity in Tumors and Changes following Antiangiogenic Treatment. *Cancer Research*, *78*(9), 2370–2382. https://doi.org/10.1158/0008-5472.CAN-17-2728

Zhong, S., Zhang, S., Fan, X., Wu, Q., Yan, L., Dong, J., Zhang, H., Li, L., Sun, L., Pan, N., Xu, X., Tang, F., Zhang, J., Qiao, J., & Wang, X. (2018). A single-cell RNA-seq survey of the developmental landscape of the human prefrontal cortex. *Nature*, *555*(7697), 524–528. https://doi.org/10.1038/nature25980

Zhu, G., Chow, L. M. L., Bayazitov, I. T., Tong, Y., Gilbertson, R. J., Zakharenko, S. S., Solecki, D. J., & Baker, S. J. (2012). Pten deletion causes mTorc1-dependent ectopic neuroblast differentiation without causing uniform migration defects. *Development (Cambridge, England)*, *139*(18), 3422–3431. https://doi.org/10.1242/dev.083154

Zimmerman, L., Parr, B., Lendahl, U., Cunningham, M., McKay, R., Gavin, B., Mann, J., Vassileva, G., & McMahon, A. (1994). Independent regulatory elements in the nestin gene direct transgene expression to neural stem cells or muscle precursors. *Neuron*, *12*(1), 11–24. https://doi.org/10.1016/0896-6273(94)90148-1

Zlokovic, B. V. (2011). Neurovascular pathways to neurodegeneration in Alzheimer's disease and other disorders. *Nature Reviews. Neuroscience*, *12*(12), 723–738. https://doi.org/10.1038/nrn3114

CHAPTER 5

GENERAL DISCUSSION

Thesis Summary and Major Findings

A complex regulatory framework underlies the generation of newborn neurons in the adult mammalian brain. This reflects a dynamic process orchestrated by a vast number of intrinsic and extrinsic regulators functioning in discrete temporal windows. Within this framework, the balance between NSC quiescence and activation is crucial to maintain niche homeostasis and sustain the brain's neurogenic capacity throughout life. Investigating the contributions of cell cycle regulatory proteins to this process is important in the context of fundamental stem cell biology, but also the design of therapies seeking to treat afflictions in the CNS brought on by aging, insult, or neurodegenerative pathology.

The central topic of this thesis is to determine the relative roles of the Rb family of pocket proteins, pRb, p107 and p130, in the regulation of adult neurogenesis. Previous work from our laboratory demonstrated requirements for pRb in adult post-mitotic neuronal survival and quiescence (Andrusiak et al., 2012, 2014) and p107 in the Notch/Hes1-mediated suppression of adult NSC self-renewal (Vanderluit et al., 2004, 2007). However, interpreting their true requirements remained complicated by functional redundancy between Rb family proteins. In this dissertation, we established a central role of Rb in the production and survival of adult-born granule cell neurons in the DG, partially mediated through its interaction with E2F1. Noting that Rb was alone dispensable for the regulation of NSC quiescence, we employed inducible knock-out mouse models to establish a compound requirement for all three Rb family proteins in the regulation of adult NSC fate. We have established a role for Rb family proteins, as well as their activator E2F transcription factor targets, in the regulation of NSC quiescence and activation. Stemming further from these findings, we have identified the pivotal transcription factors REST and ASCL1 as direct regulatory targets of the Rb/E2F axis, demonstrated through ChIP on p107/p130 and E2F3/E2F4.

Along with the transcriptomic signatures following Rb-TKO and E2F1/3-DKO, our findings have revealed a function for the Rb/E2F axis as a master regulator of NSCs, able to co-ordinate cell cycle control with the regulation of the molecular signature associated with the activation/quiescence phenotype. We have also demonstrated that NSC quiescence and activation are affected in AD pathology. Using the 3xTG-AD mouse model, we observe an imbalance in quiescence and activation suggesting that AD-affected NSCs experience impaired activation and may return to quiescence. In Appendix I, unpublished RNA velocity measurements suggest that genes within the Rb/E2F axis are impacted in the activated NSC population of 3xTG-AD mice, and that the apparent dysregulation of p130 and E2F4 warrant further examination in this context. Taken together, these findings suggest that Rb family proteins are important regulators of NSC fate during adult neurogenesis, by instructing the molecular program regulating activation and quiescence, and they may serve functions relevant to the pathology of Alzheimer's Disease.

Dispensability for Rb in the regulation of adult NSC quiescence

As discussed in Chapter 2, the acute deletion of RB in adult NSCs does not disrupt their quiescence. This is a notable and unique finding, as pRb is required to prevent cell cycle re-entry in several systems, including the retina (Oshikawa et al., 2013), MEFs (Sage et al., 2003), mammalian muscle cells (Pajcini et al., 2010; Zacksenhaus et al., 1996), and adult cortical neurons (Andrusiak et al., 2012). However, it is consistent with prior findings during hematopoiesis, where deletion of RB does not affect the cell cycle of adult hematopoietic stem cells (Walkley and Orkin, 2006). In line with observations in the developing DG, we observed ectopic proliferation of immature neuroblasts following loss of RB in the adult hippocampus, which implies that some aspects of the intrinsic cell cycle machinery may be conserved between developing and adult-born

GCNs. Previous studies by our group have demonstrated an essential role for RB in the survival of adult cortical neurons (Andrusiak et al., 2012). In agreement with this, we found that adult-born GCNs do not survive in the absence of Rb, a finding mirrored by our collaborators in (Naser et al., 2016), who employed the same genetic approach to demonstrate a similar requirement for Rb in the long-term survival of adult-born OB interneurons. However, (Naser et al., 2016) also demonstrated that Rb is dispensable in the regulation of NSC quiescence in the adult V-SVZ. Taken together, these results suggest that the functional role of Rb in adult NSCs may be masked by compensation by the remaining Rb family members, p107 and p130, which has been previously reported in other systems: in MEFs, Rb loss can only partly affect quiescence, due to functional compensation by p107 (Sage et al., 2003). Moreover, the partial rescue of adult-born neuronal survival through deletion of E2F1 and not E2F3 highlights the key involvement of E2F family transcription factors – particularly activator E2Fs – in mediating the phenotype observed following inactivation of Rb family proteins.

An Expanded Requirement for Rb family proteins in NSC fate

Our investigation in Chapter 2, along with previous work from our group (Vanderluit et al., 2004, 2007), suggested that loss of individual Rb family proteins results in relatively subtle shifts in adult NSC fate. In Chapter 3, we show that compound loss of Rb family proteins induces a cell and transcriptomic phenotype resulting in loss of quiescence and massive NSC activation. This identified a crucial requirement for Rb family proteins in adult NSC function, with roles in long-term niche maintenance, maintenance of NSC quiescence and preventing niche depletion. Ectopic proliferation following Rb family deletion has been established in other systems (Jiang et al., 2010; Sage, 2000; Viatour et al., 2008, 2011b), and the rescue of proliferation with a single Rb

family allele is in line with prior work with Rb and p130 (Ajioka et al., 2007; Burkhart et al., 2010; Sage et al., 2003). Cell cycle-independent functions for Rb have been previously demonstrated, as Rb inactivation promotes the reprogramming of differentiated cells to a pluripotent state (Kareta et al., 2015). However, the significant transcriptomic effects demonstrated following Rb-TKO represent a previously unknown function and signify a novel role for Rb family proteins as broad transcriptional regulators of adult NSC fate.

The transcriptomic signature following Rb family protein deletion suggests that in addition to upregulation of cell cycle targets (including cyclin A2, cyclin E2, Cdks1/2, Thymidine kinase, and Cdc6), multiple genes and signaling pathways associated with NSC activation are upregulated, including Ezh2, Suz12, and Shh, Wnt, as well as Jak2 pathways. For the latter, we observe upregulation of Socs3 in response to Rb-TKO, an Rb family target previously reported in HSCs to maintain homeostasis through upregulation of Jak2 signaling (Kim et al., 2017). By contrast, we observe downregulation of genes associated both with deep NSC quiescence including Aqp4, Id3, Pdgfrb and Aldoc, and with shallow NSC quiescence including Fgfr3 and Dbi (Delgado et al., 2021; Urbán et al., 2019b). These represent key transcriptomic shifts in the Rb-TKO NSC phenotype and suggest an expanded requirement for Rb family proteins beyond their classical cell cycle regulatory roles.

An Expanded Requirement for E2F family transcription factors in NSC fate

In Chapter 3, we further demonstrate that of at least 110 regulatory targets with which Rb family proteins associate to modulate transcription (Morris and Dyson, 2001), the transcriptional activators E2F1 and E2F3 distinctly demonstrate an essential requirement for adult NSC activation. Compound loss of E2Fs1/3 results in the impaired induction of genes required for NSC

activation, accompanied by a complete cessation of neurogenesis. As with Rb family proteins, loss of individual activator E2Fs results in subtle phenotypes, likely the result of functional redundancy. Unpublished results from our laboratory show that loss of E2F1 alone has a negligeable effect on SGZ neurogenesis, though work by others have demonstrated a resulting decrease in V-SVZ and SGZ proliferation (Cooper-Kuhn et al., 2002). Loss of E2F3 or isoform-level deletions of activator E2F3a or repressor E2F3b result in moderate imbalances to self-renewal/commitment decisions (Julian et al., 2013; McClellan et al., 2007). By contrast, compound deletion of E2F1 and E2F3 generates a novel dramatic transcriptomic phenotype where adult NSCs are unable to exit quiescence. Notably, this may represent a tissue-specific function, as proliferation was unimpacted following deletion of E2Fs1/2/3 in retinal progenitors and muller glia (Chen et al., 2009a).

In addition to downregulation of cell cycle targets as well as activated NSC markers including Ezh2 and PCNA, the transcriptomic signature following loss of E2Fs1/3 demonstrates induction of genes associated with NSC quiescence (Aqp4, Id3, Pdgfrb, Apoe, Fgfr3, Dbi) largely opposing the signature observed following Rb family protein deletion. E2Fs1/3-DKO does broaden the induction of quiescence, as represented by further upregulation of genes including Tgfbr3, Bmp6, S100b and Apoe. Using Enrichment Maps to examining broad transcriptomic effects following loss of E2Fs1/3, we observe enrichment of gene sets associated with primary cilium assembly, a process initiated upon cell cycle exit and re-entry into quiescence (Guemez-Gamboa et al., 2014). Supporting this, IFT88, previously reported to be a key ciliary assembly protein (Venugopal et al., 2020), is significantly upregulated in response to E2F1/3-DKO. This further supports the requirement of E2F1 and E2F3 in the maintenance of NSC activation and repression of re-entry into quiescence. These findings were confirmed through IHC characterization four weeks post-Tam, demonstrating a significant deficit in Ki67-labelled

proliferation and Dcx-labelled neural differentiation, as impaired activation ultimately leads to the cessation of neurogenesis. Together, these results demonstrate that both Rb family proteins and their activator E2F targets play a critical role instructing adult NSC quiescence and activation fate.

A Collective Requirement for the RB/E2F axis in regulating REST

In Chapter 3, we align our transcriptomic profiles with published cell type-annotated signatures (Basak et al., 2018; Codega et al., 2014), to highlight a previously unknown and novel function for the Rb-E2F axis altogether, as an on-off switch for NSC quiescence and activation. Loss of Rb family proteins results in a molecular program in alignment with an activated NSC state, while loss of E2Fs1/3 results in a molecular program in alignment with a quiescent NSC state. Thus, the Rb/E2F axis not only controls the cell cycle in NSCs, but also plays an essential role to generate the molecular signature of quiescent and activated cells.

We further observe that within its requirement in the instruction of adult NSC fate, the Rb/E2F axis links the cell cycle machinery with pivotal regulators of NSC fate. The Rb/E2F axis controls the entry and exit from quiescence through the key regulator REST, a transcriptional regulator recently shown to maintain both NSC quiescence as well as progenitor proliferation and number, whose function is believed to prevent precocious differentiation (Mukherjee et al., 2016). Following loss of Rb family proteins or activator E2Fs, we observe the dysregulation of the REST gene regulatory network, with elevated REST and downregulation of numerous proneural targets containing RE1 sites: Dcx, L1cam, Sox4 and Sox11 (Bergsland et al., 2006; Lepagnol-Bestel et al., 2009; Mu et al., 2012). To explain this finding, we propose that activator E2Fs1/3 function here as transcriptional repressors – a context-dependent function in differentiating cells previously reported in other systems (Chong et al., 2009) – and that activator E2Fs1/3 are essential for Rb

family-mediated repression of REST. In line with this, we observe a greater magnitude of REST target gene repression in response to E2F1/3 deficiency, relative to Rb-TKO. Together with ChIP data demonstrating direct binding by p107/p130 and E2F3/E2F4 at REST regulatory regions, we propose a model where activator E2Fs recruit Rb family proteins to repress REST in adult NSCs.

Though not explored in the published manuscript, regulation of REST by the Rb/E2F axis may explain a phenotype observed following either loss of Rb family proteins or loss of activator E2Fs: the impairment of neurogenesis, together with increased AC3-labelled apoptosis. While this can be easily explained in the E2F1/3-DKO model as a downstream result of intractable NSC quiescence and impaired activation, it remains an unresolved phenotype following aberrant NSC activation following Rb-TKO. Through IHC of the Rb-TKO brain four weeks post-Tam, we observe the expansion of atypical Sox2/NeuroD1 and Sox2/Dcx co-expressing cell populations in both the SGZ and V-SVZ, reflecting impaired NSC commitment to the differentiation programme accompanied by continued expression of Sox2. In the V-SVZ, this appears to result in the formation of periventricular heterotopias, consistent with prior studies demonstrating impaired migration and expression of immature neuronal markers including PSA-NCAM (Carabalona et al., 2012; Ferland et al., 2009). In the SGZ, this ultimately results in the niche depletion of both Sox2- and Dcx-expressing populations at the eight-week post-Tam timepoint. In our studies *in vitro*, REST expression remained consistent in Rb-TKO NSCs even following 3 days of differentiation. Upregulation of REST may occur as a response mechanism to suppress Rb-TKO-mediated super-activation of the NSC population, and result in the repression of pro-neural genes containing RE1 sites. This may suggest a requirement for Rb family proteins in regulating neural differentiation, through the repression of the classical silencing function of REST. This mechanism has been previously observed in human medulloblastoma, where abnormal, elevated REST expression is

proposed to block neuronal differentiation, in a function believed to maintain stemness of NSCs present in the external granule layer of the cerebellum (Su et al., 2006). Ultimately, as rescue experiments blocking REST function, explored next, were performed at a relatively early timepoint following 3 days of differentiation *in vitro* or 14 days following injection *in vivo*, the mechanisms resulting in impaired neurogenesis following Rb family loss remain to be clarified.

The results of Chapter 3 extend our understanding of REST function in NSCs, including the upstream contributions of the Rb/E2F axis and characterization of a phenotype following REST overexpression. However, interpretation of REST function will have to carefully consider the very different contexts of Rb-TKO and E2F1/3-DKO. For instance, though REST is upregulated in both, a previously published signature of ribosomal REST targets (Mukherjee et al., 2016) is predicably downregulated in response to E2F1/3-DKO, but upregulated in response to Rb-TKO, where the contribution of other ribosomal regulators appears dominant over REST. A further contrast is the lack of REST cofactor CoREST and Sin3A upregulation following loss of E2Fs1/3, suggesting that activator E2Fs may be required to recruit REST cofactors. This may link activator E2Fs with a reported requirement for CoREST in modulating REST target expression despite REST dissociation (Ballas et al., 2005).

Both the Rb/E2F axis and REST regulate ASCL1

Following loss of Rb family proteins, in Chapter 3 we observe that the transcriptional shift towards activation is accompanied by an increased number of ASCL1-expressing activated NSCs, validated through ASCL1 protein expression as well as though IHC characterization of an increased ASCL1-expressing recombined cell portion. Together with ChIP data demonstrating direct ASCL1 binding by p107/p130 and E2F3/E2F4, our data suggest a role for the Rb/E2F axis

in repressing ASCL1 expression to maintain NSC quiescence. We also demonstrate that blocking REST function through transduction of a dnREST lentivector results in increased induction of ASCL1 and Sox11 expression, the latter consistent with prior studies identifying SoxB proteins including Sox11 as REST regulatory targets (Bergsland et al., 2006).

We have notably identified a novel direct molecular connection between REST and ASCL1. This connection has been previously supported by high REST expression in qNSCs and downregulation upon activation, in direct opposition to the expression pattern of ASCL1. Previous studies have also demonstrated that experimental deletion of REST in adult NSCs leads to a transient proportional increase in the ASCL1-expressing population, as well as increased ASCL1 protein *in vitro* (Gao et al., 2011). The first evidence of a molecular link between REST and ASCL1 was first proposed in ES cells by (Ballas et al., 2005), with REST binding to a putative RE1 element located 49kb downstream of the ASCL1 transcriptional start site. This direct binding would be later disputed by (Jørgensen et al., 2009), who identified no REST binding at this site. While the site would later appear in ChIP data from others (Johnson et al., 2008; Mukherjee et al., 2016) it would never be called as a peak; the observation of histone modifications on the ASCL1-RE1 site (Gao et al., 2011) offered the potential of indirect chromatin modification, and REST co-operation with additional factors. Here, we have identified REST binding at a distinct peak 94kb upstream of ASCL1, with REST being the closest regulated gene to this peak; we do not observe binding at the previously described site. Our discovery of this molecular connection may help provide additional functional context to this prior work, and its potential significance in non-neural tissues also remains to be elucidated.

REST regulation of ASCL1 is supported by our findings in vivo, as dnREST transduction results in an increased percentage of ASCL1-expressing cells in the adult SGZ. Notably, we found

that expression of dnREST partially rescued the depletion of adult NSCs observed following loss of Rb family proteins. 14 days following injection, dnREST transduction resulted in a significant increase in activated, ASCL1-expressing cells relative to a depleted mCherry-transduced control. Importantly, this suggests that not only is the Rb/E2F axis essential for the maintenance of the NSC niche in the adult SGZ, but that it mediates this requirement through the regulation of REST.

Alterations to NSC quiescence and activation in the 3xTG-AD model of AD

In Chapter 4, we investigated the effects of Alzheimer's Disease (AD) on adult neurogenesis, using the 3xTG-AD mouse model. We employed single cell RNA-seq on SGZ NSCs labelled with our inducible Cre-reporter line, one month following tamoxifen gavage. This allowed us to observe stage-specific effects of 3xTG-AD pathology in cell clusters spanning the entire neurogenic lineage. Previous studies characterized impaired neurogenesis in the 3xTG-AD model (Hamilton et al., 2015), but were limited in scope to GFAP-expressing NSCs, as well as markers of proliferation and differentiation. In this dissertation, we observed imbalanced NSC quiescence and activation within 3xTG-AD mice, reflecting a proportionally greater quiescent NSC population relative to non-transgenic (NTG) controls; this was contrasted with a reduction in the proportion of activated NSCs, supported through IHC of activation marker Lpar1 (Walker et al., 2016), and a further proportional reduction in TAP and neuron clusters.

Using measurements of RNA velocity, a means of projecting cell fate transitions within a UMAP projection of single-cell transcriptomic data, we observed that 3xTG-AD appears to induce differential cell fate in the activated NSC population. In contrast to the expected pro-neural transition towards a TAP stage, as observed in the projection of NTG cells, we observed that 3xTG-AD activated NSCs demonstrate a fate progression in the opposite direction, towards the quiescent

NSC cluster. This is supported by aberrant cluster-specific fate transitions suggesting upregulation of quiescence markers Aqp4 and Apoe, and downregulation of activation marker Egfr (Urbán et al., 2019a). Together, these results suggest that in response to 3xTG-AD, activated NSCs may attempt to re-enter a quiescent state.

Appendix I contains data withheld from the preprint, anticipating future experiments and potential novelty better suited for the final, peer-reviewed publication. Figure 1A shows altered cell cycle dynamics restricted to the activated NSC and TAP clusters of 3xTG-AD mice, as measured through the proportion of cells in G1 and S phases, with phase-specific markers originally obtained from (Tirosh et al., 2016). In response to 3xTG-AD, we observe relative shifts from G1 towards S phase in the activated NSC cluster, and from S towards G1 phase in the TAP cluster. This suggests that a block in G1/S phase progression – representing a transition between the activated NSCs largely in G1 phase and the proliferative TAPs largely in S phase – appears to be impaired in 3xTG-AD mice. Figure 1B identifies two key cell cycle regulators of G1/S progression which we propose are implicated in this impairment: the Rb family protein p130 as well as its E2F family transcription factor target E2F4. Expression of both p130 and E2F4 appear aberrantly upregulated at the activated NSC/TAP transition in 3xTG-AD mice. Strikingly, RNA velocity measurements indicate p130/E2F4 downregulation in the activated NSC population, a stark contrast with the upregulation observed in the activated NSCs of NTG mice. Taken together, these results may indicate a connection between p130/E2F4-mediated cell cycle repression in activated NSCs and their return to quiescence, as part of AD pathology. Prior work has demonstrated increased p130 expression during AD pathology, which is believed to facilitate cell cycle re-entry in postmitotic neurons (Previll et al., 2007). Recently, one research group has examined E2F4 overexpression in the 5xFAD mouse model of AD, demonstrating a reduction in

AD-associated phenotypes including hippocampal Aβ production and accumulation, following systemic administration of an adeno-associated viral vector expressing a dominant-negative E2F4 (López-Sánchez et al., 2021). Together, the results of Appendix I support our findings from Chapter 3 suggesting an essential requirement for the Rb/E2F axis in the regulation of NSC quiescence and activation, including a potential role for "dark horse" p130 and E2F4 in a pathological context.

Presently, the connection between AD pathology and the complex regulatory network regulating NSC quiescence and activation, including the Rb/E2F axis, remains unclear. Furthermore, whether the molecular connection established in Chapter 3 between the Rb/E2F axis and REST/ASCL1 may implicated in the context of AD is unknown. However, it is worth considering that previous studies have associated REST function with the altered differentiation state observed in iPSC-derived neural cells generated from patients with sporadic AD (Meyer 2019) and have demonstrated that expression of ASCL1 mRNA and protein are induced by Aβ in cerebral cortical cultures (Uchida, 2010).

Limitations and Future Studies

There are several limitations to consider while reviewing this dissertation. Chief among them is the reliance on the mouse model of adult neurogenesis, and the historical difficulties they present during translation to a human context. Some of these difficulties may be associated with the potential contribution of sex differences when interpreting experimental results, reviewed in (Yagi and Galea, 2019). Adult neurogenesis in mice has also been largely studied at a relatively early timepoint, compared with the protracted neurogenesis observed throughout life in humans, reviewed in (Snyder, 2019). Notably, the loss of Rb in human cerebral organoids results in

increased NSC proliferation (Matsui et al., 2017), in contrast with its dispensability in the regulation of NSC quiescence in the adult mouse V-SVZ and SGZ established in Chapter 2 and (Naser et al., 2016). This suggests a lower degree of functional compensation between Rb family proteins in humans than observed in mouse models. Nevertheless, so long as interpretation carefully considers these caveats and the dangers of unfounded assumptions in re: translation, mouse models continue to serve as the gold standard of experimental inquiry into mammalian adult neurogenesis, particularly in models of neurodegenerative pathologies including AD.

We acknowledge that the transcriptomic and molecular analyses in Chapter 3 were performed in cells isolated from the V-SVZ, while the majority of characterization, including rescue experiments following dnREST transduction, focused on the SGZ. While there are evident differences in the generated progeny from either – OB-destined migratory neuroblasts vs GCNs – the intrinsic similarities between adult NSCs in the SVZ and SGZ remain a focus of ongoing study, including their exposure to different signals and niche-derived factors (Ertaylan et al., 2014). Examination of NSCs isolated from the SGZ niche, likely using single-cell transcriptomic approaches as performed in Chapter 4, would help clarify the pertinence of our transcriptomic results to SGZ neurogenesis, and better define a tissue-specific requirement for the Rb/E2F axis in regulating the molecular program instructing adult SGZ NSCs. More broadly, as alterations in the Rb/E2F axis have been identified in 81% of paediatric and adult tumors in the Cancer Genome Atlas dataset (Chkheidze et al., 2021) – most commonly the functional inactivation of Rb (Burkhart and Sage, 2008) – our characterization of the Rb/E2f-regulated molecular program may be relevant in non-neural tissues and during oncogenesis, including the direct regulation of REST and ASCL1.

Finally, the timepoints used in Chapter 3 to examine rescue of the Rb-TKO phenotype with dnREST examines the contributions of the Rb/E2F axis during early stages of neurogenesis, including NSC fate, at the expense of its effects on differentiation and commitment. Investigating the effects beyond 3 days of differentiation *in vitro* or 14 days following transduction *in vivo* would help identify the eventual fate of the expanded activated, largely ASCL1-expressing, population, and establish whether apparent defects in neurogenesis following loss of Rb family proteins may also be rescued through inactivation of REST.

Conclusion

While the experimental modulation of adult neurogenesis may represent a paradigm of endogenous repair, any therapeutic potential is reliant on present efforts to define and characterize the mechanisms underlying the regulation of adult NSC fate. In this dissertation, we demonstrate a requirement for the Rb/E2F axis in the broad regulation of the molecular program instructing adult NSC quiescence and activation, with a potentially significant role within the pathology of Alzheimer's disease. The Rb/E2F axis may represent a new avenue for developing therapies for neurodegenerative diseases, and includes a known pharmacological target, as the drug harmine has been shown to phosphorylate DREAM complex component DYRK1A (Forristal et al., 2014; Göckler et al., 2009) to recapitulate the phenotype observed following loss of p107 and p130. Ultimately, this work addresses the key issue of how transcriptional signatures of quiescence and activation among adult NSCs are co-ordinated with cell cycle control, and demonstrates that the Rb/E2F axis serves as a master regulator of the molecular program instructing adult NSC exit from and re-entry into quiescence.

REFERENCES

Abderrahmani, A., Niederhauser, G., Lenain, V., Regazzi, R., and Waeber, G. (2005). The hairy and enhancer of split 1 is a negative regulator of the repressor element silencer transcription factor. Febs Lett *579*, 6199–6204.

Adams, M.R., Sears, R., Nuckolls, F., Leone, G., and Nevins, J.R. (2000). Complex Transcriptional Regulatory Mechanisms Control Expression of the E2F3 Locus. Mol Cell Biol *20*, 3633–3639.

Ajioka, I., Martins, R.A.P., Bayazitov, I.T., Donovan, S., Johnson, D.A., Frase, S., Cicero, S.A., Boyd, K., Zakharenko, S.S., and Dyer, M.A. (2007). Differentiated horizontal interneurons clonally expand to form metastatic retinoblastoma in mice. Cell *131*, 378–390.

Altman, J. (1962). Are New Neurons Formed in the Brains of Adult Mammals? Science *135*, 1127–1128.

ALTMAN, J., and DAS, G.D. (1965). Post-Natal Origin of Microneurones in the Rat Brain. Nature *207*, 953–956.

Alvarez-Buylla, A., and Nottebohm, F. (1988). Migration of young neurons in adult avian brain. Nature *335*, 353–354.

Andersen, J., Urban, N., Achimastou, A., Ito, A., Simic, M., Ullom, K., Martynoga, B., Lebel, M., Göritz, C., Frisén, J., et al. (2014). A transcriptional mechanism integrating inputs from extracellular signals to activate hippocampal stem cells. Neuron *83*, 1085–1097.

Andrés, M.E., Burger, C., Peral-Rubio, M.J., Battaglioli, E., Anderson, M.E., Grimes, J., Dallman, J., Ballas, N., and Mandel, G. (1999). CoREST: A functional corepressor required for regulation of neural-specific gene expression. Proc National Acad Sci *96*, 9873–9878.

Andrusiak, M.G., Vandenbosch, R., Park, D.S., and Slack, R.S. (2012). The retinoblastoma protein is essential for survival of postmitotic neurons. J Neurosci *32*, 14809–14814.

Andrusiak, M.G., Vandenbosch, R., Dick, F.A., Park, D.S., and Slack, R.S. (2014). LXCXE-independent chromatin remodeling by Rb/E2f mediates neuronal quiescence. Cell Cycle *12*, 1416–1423.

Artegiani, B., Lindemann, D., and Calegari, F. (2011). Overexpression of cdk4 and cyclinD1 triggers greater expansion of neural stem cells in the adult mouse brain. The Journal of Experimental Medicine *208*, 937–948.

Artegiani, B., Lyubimova, A., Muraro, M., Es, J.H. van, Oudenaarden, A. van, and Clevers, H. (2017). A Single-Cell RNA Sequencing Study Reveals Cellular and Molecular Dynamics of the Hippocampal Neurogenic Niche. Cell Reports *21*, 3271–3284.

Bagchi, S., Weinmann, R., and Raychaudhuri, P. (1991). The retinoblastoma protein copurifies with E2F-I, an E1A-regulated inhibitor of the transcription factor E2F. Cell *65*, 1063–1072.

Ballas, N., Grunseich, C., Lu, D.D., Speh, J.C., and Mandel, G. (2005). REST and Its Corepressors Mediate Plasticity of Neuronal Gene Chromatin throughout Neurogenesis. Cell *121*, 645–657.

Basak, O., Krieger, T.G., Muraro, M.J., Wiebrands, K., Stange, D.E., Frias-Aldeguer, J., Rivron, N.C., Wetering, M. van de, Es, J.H. van, Oudenaarden, A. van, et al. (2018). Troy+ brain stem cells cycle through quiescence and regulate their number by sensing niche occupancy. Proc National Acad Sci *115*, E610–E619.

Baur, K., Abdullah, Y., Mandl, C., Hölzl-Wenig, G., Shi, Y., Edelkraut, U., Khatri, P., and Ciccolini, F. (2020). Basal neural stem cells in the subventricular zone drive postnatal neurogenesis with apical stem cells acting as proliferation gate-keepers. Biorxiv 2020.11.20.391102.

Beckervordersandforth, R., and Rolando, C. (2020). Untangling human neurogenesis to understand and counteract brain disorders. Curr Opin Pharmacol *50*, 67–73.

Belyaev, N.D., Wood, I.C., Bruce, A.W., Street, M., Trinh, J.-B., and Buckley, N.J. (2004). Distinct RE-1 Silencing Transcription Factor-containing Complexes Interact with Different Target Genes*. J Biol Chem *279*, 556–561.

Berg, D.A., Su, Y., Jimenez-Cyrus, D., Patel, A., Huang, N., Morizet, D., Lee, S., Shah, R., Ringeling, F.R., Jain, R., et al. (2019). A Common Embryonic Origin of Stem Cells Drives Developmental and Adult Neurogenesis. Cell *177*, 654-668.e15.

Berge, S.A. van den, Strien, M.E. van, Korecka, J.A., Dijkstra, A.A., Sluijs, J.A., Kooijman, L., Eggers, R., Filippis, L.D., Vescovi, A.L., Verhaagen, J., et al. (2011). The proliferative capacity of the subventricular zone is maintained in the parkinsonian brain. Brain *134*, 3249–3263.

Bergmann, O., Liebl, J., Bernard, S., Alkass, K., Yeung, M.S.Y., Steier, P., Kutschera, W., Johnson, L., Landén, M., Druid, H., et al. (2012). The Age of Olfactory Bulb Neurons in Humans. Neuron *74*, 634–639.

Bergsland, M., Werme, M., Malewicz, M., Perlmann, T., and Muhr, J. (2006). The establishment of neuronal properties is controlled by Sox4 and Sox11. Genes Dev *20*, 3475–3486.

Bertoli, C., and Bruin, R.A.M. de (2014). Turning cell cycle entry on its head. Elife *3*, e03475.

Beukelaers, P., Vandenbosch, R., Caron, N., Nguyen, L., Belachew, S., Moonen, G., Kiyokawa, H., Barbacid, M., Santamaria, D., and Malgrange, B. (2011). Cdk6-dependent regulation of G(1) length controls adult neurogenesis. Stem Cells *29*, 713–724.

Blais, A., Oevelen, C.J.C. van, Margueron, R., Acosta-Alvear, D., and Dynlacht, B.D. (2007). Retinoblastoma tumor suppressor protein–dependent methylation of histone H3 lysine 27 is associated with irreversible cell cycle exit. J Cell Biology *179*, 1399–1412.

Blanchet, E., Annicotte, J.-S., Lagarrigue, S., Aguilar, V., Clapé, C., Chavey, C., Fritz, V., Casas, F., Apparailly, F., Auwerx, J., et al. (2011). E2F transcription factor-1 regulates oxidative metabolism. Nat Cell Biol *13*, 1146–1152.

Boldrini, M., Fulmore, C.A., Tartt, A.N., Simeon, L.R., Pavlova, I., Poposka, V., Rosoklija, G.B., Stankov, A., Arango, V., Dwork, A.J., et al. (2018). Human Hippocampal Neurogenesis Persists throughout Aging. Cell Stem Cell *22*, 589-599.e5.

Bonaguidi, M.A., Wheeler, M.A., Shapiro, J.S., Stadel, R.P., Sun, G.J., Ming, G., and Song, H. (2011). In Vivo Clonal Analysis Reveals Self-Renewing and Multipotent Adult Neural Stem Cell Characteristics. Cell *145*, 1142–1155.

Bonaguidi, M.A., Stadel, R.P., Berg, D.A., Sun, J., Ming, G.-L., and Song, H. (2016). Diversity of Neural Precursors in the Adult Mammalian Brain. Cold Spring Harbor Perspectives in Biology *8*, a018838-20.

Borrett, M.J., Innes, B.T., Jeong, D., Tahmasian, N., Storer, M.A., Bader, G.D., Kaplan, D.R., and Miller, F.D. (2020). Single-Cell Profiling Shows Murine Forebrain Neural Stem Cells Reacquire a Developmental State when Activated for Adult Neurogenesis. Cell Reports *32*, 108022.

Brehm, A., and Kouzarides, T. (1999). Retinoblastoma protein meets chromatin. Trends Biochem Sci *24*, 142–145.

Brehm, A., Miska, E.A., McCance, D.J., Reid, J.L., Bannister, A.J., and Kouzarides, T. (1998). Retinoblastoma protein recruits histone deacetylase to repress transcription. Nature *391*, 597–601.

Bruce, A.W., Donaldson, I.J., Wood, I.C., Yerbury, S.A., Sadowski, M.I., Chapman, M., Göttgens, B., and Buckley, N.J. (2004). Genome-wide analysis of repressor element 1 silencing transcription factor/neuron-restrictive silencing factor (REST/NRSF) target genes. P Natl Acad Sci Usa *101*, 10458–10463.

Bruin, A. de, Maiti, B., Jakoi, L., Timmers, C., Buerki, R., and Leone, G. (2003). Identification and Characterization of E2F7, a Novel Mammalian E2F Family Member Capable of Blocking Cellular Proliferation*. J Biol Chem *278*, 42041–42049.

Burke, J.R., Hura, G.L., and Rubin, S.M. (2012). Structures of inactive retinoblastoma protein reveal multiple mechanisms for cell cycle control. Gene Dev *26*, 1156–1166.

Burkhart, D.L., and Sage, J. (2008). Cellular mechanisms of tumour suppression by the retinoblastoma gene. Nat Rev Cancer *8*, 671–682.

Burkhart, D.L., Ngai, L.K., Roake, C.M., Viatour, P., Thangavel, C., Ho, V.M., Knudsen, E.S., and Sage, J. (2010). Regulation of RB Transcription In Vivo by RB Family Members. Molecular and Cellular Biology *30*, 1729–1745.

Cajal, S.R. (1913). Sobre la degeneración y regeneracíon del sistema nervioso. Imprenta de Hijos de Nicolás Moya, Madrid *2*.

Calderone, A., Jover, T., Noh, K., Tanaka, H., Yokota, H., Lin, Y., Grooms, S.Y., Regis, R., Bennett, M.V.L., and Zukin, R.S. (2003). Ischemic Insults Derepress the Gene Silencer REST in Neurons Destined to Die. J Neurosci *23*, 2112–2121.

Cam, H., Balciunaite, E., Blais, A., Spektor, A., Scarpulla, R.C., Young, R., Kluger, Y., and Dynlacht, B.D. (2004). A Common Set of Gene Regulatory Networks Links Metabolism and Growth Inhibition. Mol Cell *16*, 399–411.

Carabalona, A., Beguin, S., Pallesi-Pocachard, E., Buhler, E., Pellegrino, C., Arnaud, K., Hubert, P., Oualha, M., Siffroi, J.P., Khantane, S., et al. (2012). A glial origin for periventricular nodular heterotopia caused by impaired expression of Filamin-A. Hum Mol Genet *21*, 1004–1017.

Carleton, A., Petreanu, L.T., Lansford, R., Alvarez-Buylla, A., and Lledo, P.-M. (2003). Becoming a new neuron in the adult olfactory bulb. Nat Neurosci *6*, 507–518.

Cartwright, P., Müller, H., Wagener, C., Holm, K., and Helin, K. (1998). E2F-6: a novel member of the E2F family is an inhibitor of E2F-dependent transcription. Oncogene *17*, 611–623.

Ceanga, M., Dahab, M., Witte, O.W., and Keiner, S. (2021). Adult Neurogenesis and Stroke: A Tale of Two Neurogenic Niches. Front Neurosci-Switz *15*, 700297.

Chapouton, P., Skupien, P., Hesl, B., Coolen, M., Moore, J.C., Madelaine, R., Kremmer, E., Faus-Kessler, T., Blader, P., Lawson, N.D., et al. (2010). Notch activity levels control the balance between quiescence and recruitment of adult neural stem cells. J Neurosci *30*, 7961–7974.

Chellappan, S.P., Hiebert, S., Mudryj, M., Horowitz, J.M., and Nevins, J.R. (1991). The E2F transcription factor is a cellular target for the RB protein. Cell *65*, 1053–1061.

Chen, D., Pacal, M., Wenzel, P., Knoepfler, P.S., Leone, G., and Bremner, R. (2009a). Division and apoptosis of E2f-deficient retinal progenitors. Nature *462*, 925–929.

Chen, H.-Z., Tsai, S.-Y., and Leone, G. (2009b). Emerging roles of E2Fs in cancer: an exit from cell cycle control. Nat Rev Cancer *9*, 785–797.

Chen, Q., Liang, D., and Overbeek, P.A. (2008). Overexpression of E2F5/p130, but not E2F5 alone, can inhibit E2F-induced cell cycle entry in transgenic mice. Mol Vis *14*, 602–614.

Cheung, T.H., and Rando, T.A. (2013). Molecular regulation of stem cell quiescence. Nat Rev Mol Cell Biol *14*, 329–340.

Chiasson, B.J., Tropepe, V., Morshead, C.M., and Kooy, D. van der (1999). Adult Mammalian Forebrain Ependymal and Subependymal Cells Demonstrate Proliferative Potential, but only Subependymal Cells Have Neural Stem Cell Characteristics. J Neurosci *19*, 4462–4471.

Chong, J.A., Tapia-Ramirez, J., Kim, S., Toledo-Aral, J.J., Zheng, Y., Boutros, M.C., Altshuller, Y.M., Frohman, M.A., Kraner, S.D., and Mandel, G. (1995). REST: A mammalian silencer protein that restricts sodium channel gene expression to neurons. Cell *80*, 949–957.

Chong, J.-L., Wenzel, P.L., Sáenz-Robles, M.T., Nair, V., Ferrey, A., Hagan, J.P., Gomez, Y.M., Sharma, N., Chen, H.-Z., Ouseph, M., et al. (2009). E2f1-3 switch from activators in progenitor cells to repressors in differentiating cells. Nature *462*, 930–934.

Christensen, J., Cloos, P., Toftegaard, U., Klinkenberg, D., Bracken, A.P., Trinh, E., Heeran, M., Stefano, L.D., and Helin, K. (2005). Characterization of E2F8, a novel E2F-like cell-cycle regulated repressor of E2F-activated transcription. Nucleic Acids Res *33*, 5458–5470.

Classon, M., Salama, S., Gorka, C., Mulloy, R., Braun, P., and Harlow, E. (2000). Combinatorial roles for pRB, p107, and p130 in E2F-mediated cell cycle control. Proceedings of the National Academy of Sciences *97*, 10820–10825.

Cobrinik, D., Lee, M.H., Hannon, G., Mulligan, G., Bronson, R.T., Dyson, N., Harlow, E., Beach, D., Weinberg, R.A., and Jacks, T. (1996). Shared role of the pRB-related p130 and p107 proteins in limb development. Genes Dev *10*, 1633–1644.

Codega, P., Silva-Vargas, V., Paul, A., Maldonado-Soto, A.R., Deleo, A.M., Pastrana, E., and Doetsch, F. (2014). Prospective identification and purification of quiescent adult neural stem cells from their in vivo niche. Neuron *82*, 545–559.

Cooper-Kuhn, C.M., Vroemen, M., Brown, J., Ye, H., Thompson, M.A., Winkler, J., and Kuhn, H.G. (2002). Impaired Adult Neurogenesis in Mice Lacking the Transcription Factor E2F1. Mol Cell Neurosci *21*, 312–323.

Cuitiño, M.C., Pécot, T., Sun, D., Kladney, R., Okano-Uchida, T., Shinde, N., Saeed, R., Perez-Castro, A.J., Webb, A., Liu, T., et al. (2019). Two Distinct E2F Transcriptional Modules Drive Cell Cycles and Differentiation. Cell Reports *27*, 3547-3560.e5.

Curtis, M.A., Penney, E.B., Pearson, A.G., Roon-Mom, W.M.C. van, Butterworth, N.J., Dragunow, M., Connor, B., and Faull, R.L.M. (2003). Increased cell proliferation and neurogenesis in the adult human Huntington's disease brain. Proc National Acad Sci *100*, 9023–9027.

Dadwal, P., Mahmud, N., Sinai, L., Azimi, A., Fatt, M., Wondisford, F.E., Miller, F.D., and Morshead, C.M. (2015). Activating Endogenous Neural Precursor Cells Using Metformin Leads

to Neural Repair and Functional Recovery in a Model of Childhood Brain Injury. Stem Cell Rep *5*, 166–173.

Dahiya, A., Gavin, M.R., Luo, R.X., and Dean, D.C. (2000). Role of the LXCXE Binding Site in Rb Function. Mol Cell Biol *20*, 6799–6805.

DeGregori, J., and Johnson, D. (2006). Distinct and Overlapping Roles for E2F Family Members in Transcription, Proliferation and Apoptosis. Curr Mol Med *6*, 739–748.

Delgado, A.C., Maldonado-Soto, A.R., Silva-Vargas, V., Mizrak, D., Känel, T. von, Tan, K.R., Paul, A., Madar, A., Cuervo, H., Kitajewski, J., et al. (2021). Release of stem cells from quiescence reveals gliogenic domains in the adult mouse brain. Science *372*, 1205–1209.

Denoth-Lippuner, A., and Jessberger, S. (2021). Formation and integration of new neurons in the adult hippocampus. Nat Rev Neurosci *22*, 223–236.

Dick, F.A., and Rubin, S.M. (2013). Molecular mechanisms underlying RB protein function. Nat Rev Mol Cell Biol *14*, 297–306.

Doetsch, F., Verdugo, J.M.-G., Caille, I., Alvarez-Buylla, A., Chao, M.V., and Casaccia-Bonnefil, P. (2002). Lack of the Cell-Cycle Inhibitor p27Kip1 Results in Selective Increase of Transit-Amplifying Cells for Adult Neurogenesis. J Neurosci *22*, 2255–2264.

Donega, V., Burm, S.M., Strien, M.E. van, Bodegraven, E.J. van, Paliukhovich, I., Geut, H., Berg, W.D.J. van de, Li, K.W., Smit, A.B., Basak, O., et al. (2019). Transcriptome and proteome profiling of neural stem cells from the human subventricular zone in Parkinson's disease. Acta Neuropathologica Commun *7*, 84.

Dunaief, J.L., Strober, B.E., Guha, S., Khavari, P.A., Ålin, K., Luban, J., Begemann, M., Crabtree, G.R., and Goff, S.P. (1994). The retinoblastoma protein and BRG1 form a complex and cooperate to induce cell cycle arrest. Cell *79*, 119–130.

Duque, A., and Spector, R. (2019). A balanced evaluation of the evidence for adult neurogenesis in humans: implication for neuropsychiatric disorders. Brain Struct Funct *224*, 2281–2295.

Dyson, N. (1998). The regulation of E2F by pRB-family proteins. Genes Dev *12*, 2245–2262.

Dyson, N., Howley, P.M., Münger, K., and Harlow, E. (1989). The Human Papilloma Virus-16 E7 Oncoprotein Is Able to Bind to the Retinoblastoma Gene Product. Science *243*, 934–937.

Eriksson, P.S., Perfilieva, E., Björk-Eriksson, T., Alborn, A.-M., Nordborg, C., Peterson, D.A., and Gage, F.H. (1998). Neurogenesis in the adult human hippocampus. Nat Med *4*, 1313–1317.

Esteves, M., Serra-Almeida, C., Saraiva, C., and Bernardino, L. (2020). New insights into the regulatory roles of microRNAs in adult neurogenesis. Curr Opin Pharmacol *50*, 38–45.

Favaro, R., Valotta, M., Ferri, A.L.M., Latorre, E., Mariani, J., Giachino, C., Lancini, C., Tosetti, V., Ottolenghi, S., Taylor, V., et al. (2009). Hippocampal development and neural stem cell maintenance require Sox2-dependent regulation of Shh. Nat Neurosci *12*, 1248–1256.

Felsani, A., Mileo, A.M., and Paggi, M.G. (2006). Retinoblastoma family proteins as key targets of the small DNA virus oncoproteins. Oncogene *25*, 5277–5285.

Ferguson, K.L., Vanderluit, J.L., Hébert, J.M., McIntosh, W.C., Tibbo, E., MacLaurin, J.G., Park, D.S., Wallace, V.A., Vooijs, M., McConnell, S.K., et al. (2002). Telencephalon-specific Rb knockouts reveal enhanced neurogenesis, survival and abnormal cortical development. The EMBO Journal *21*, 3337–3346.

Ferland, R.J., Batiz, L.F., Neal, J., Lian, G., Bundock, E., Lu, J., Hsiao, Y.-C., Diamond, R., Mei, D., Banham, A.H., et al. (2009). Disruption of neural progenitors along the ventricular and subventricular zones in periventricular heterotopia. Hum Mol Genet *18*, 497–516.

Field, S.J., Tsai, F.-Y., Kuo, F., Zubiaga, A.M., Kaelin, W.G., Livingston, D.M., Orkin, S.H., and Greenberg, M.E. (1996). E2F-1 Functions in Mice to Promote Apoptosis and Suppress Proliferation. Cell *85*, 549–561.

Fong, B.C., and Slack, R.S. (2017). RB: An essential player in adult neurogenesis. Neurogenesis *4*, e1270382–e1270382.

Forristal, C., Henley, S.A., MacDonald, J.I., Bush, J.R., Ort, C., Passos, D.T., Talluri, S., Ishak, C.A., Thwaites, M.J., Norley, C.J., et al. (2014). Loss of the Mammalian DREAM Complex Deregulates Chondrocyte Proliferation. Molecular and Cellular Biology *34*, 2221–2234.

Francke, U., and Kung, F. (1976). Sporadic bilateral retinoblastoma and 13q-chromosomal deletion. Med Pediatr Oncol *2*, 379–385.

Fuentealba, L.C., Rompani, S.B., Parraguez, J.I., Obernier, K., Romero, R., Cepko, C.L., and Alvarez-Buylla, A. (2015). Embryonic Origin of Postnatal Neural Stem Cells. Cell *161*, 1644–1655.

Furutachi, S., Matsumoto, A., Nakayama, K.I., and Gotoh, Y. (2013). p57 controls adult neural stem cell quiescence and modulates the pace of lifelong neurogenesis. The EMBO Journal *32*, 970–981.

Furutachi, S., Miya, H., Watanabe, T., Kawai, H., Yamasaki, N., Harada, Y., Imayoshi, I., Nelson, M., Nakayama, K.I., Hirabayashi, Y., et al. (2015). Slowly dividing neural progenitors are an embryonic origin of adult neural stem cells. Nat Neurosci *18*, 657–665.

Gao, Z., Ure, K., Ding, P., Nashaat, M., Yuan, L., Ma, J., Hammer, R.E., and Hsieh, J. (2011). The Master Negative Regulator REST/NRSF Controls Adult Neurogenesis by Restraining the Neurogenic Program in Quiescent Stem Cells. The Journal of Neuroscience *31*, 9772–9786.

Gaubatz, S., Lindeman, G.J., Ishida, S., Jakoi, L., Nevins, J.R., Livingston, D.M., and Rempel, R.E. (2000). E2F4 and E2F5 Play an Essential Role in Pocket Protein–Mediated G1 Control. Mol Cell *6*, 729–735.

Gaubatz, S., Lees, J.A., Lindeman, G.J., and Livingston, D.M. (2001). E2F4 Is Exported from the Nucleus in a CRM1-Dependent Manner. Mol Cell Biol *21*, 1384–1392.

Girling, R., Partridge, J.F., Bandara, L.R., Burden, N., Totty, N.F., Hsuan, J.J., and Thangue, N.B.L. (1993). A new component of the transcription factor DRTF1/E2F. Nature *362*, 83–87.

Göckler, N., Jofre, G., Papadopoulos, C., Soppa, U., Tejedor, F.J., and Becker, W. (2009). Harmine specifically inhibits protein kinase DYRK1A and interferes with neurite formation. FEBS Journal *276*, 6324–6337.

Goldman, S.A., and Nottebohm, F. (1983). Neuronal production, migration, and differentiation in a vocal control nucleus of the adult female canary brain. Proc National Acad Sci *80*, 2390–2394.

Gonçalves, J.T., Schafer, S.T., and Gage, F.H. (2016). Adult Neurogenesis in the Hippocampus: From Stem Cells to Behavior. Cell *167*, 897–914.

Götz, M., and Huttner, W.B. (2005). The cell biology of neurogenesis. Nat Rev Mol Cell Biol *6*, 777–788.

Gould, E., McEwen, B.S., Tanapat, P., Galea, L.A.M., and Fuchs, E. (1997). Neurogenesis in the Dentate Gyrus of the Adult Tree Shrew Is Regulated by Psychosocial Stress and NMDA Receptor Activation. J Neurosci *17*, 2492–2498.

Gould, E., Reeves, A.J., Fallah, M., Tanapat, P., Gross, C.G., and Fuchs, E. (1999). Hippocampal neurogenesis in adult Old World primates. Proc National Acad Sci *96*, 5263–5267.

Gu, Y., Arruda-Carvalho, M., Wang, J., Janoschka, S.R., Josselyn, S.A., Frankland, P.W., and Ge, S. (2012). Optical controlling reveals time-dependent roles for adult-born dentate granule cells. Nat Neurosci *15*, 1700–1706.

Guemez-Gamboa, A., Coufal, N.G., and Gleeson, J.G. (2014). Primary Cilia in the Developing and Mature Brain. Neuron *82*, 511–521.

Guiley, K.Z., Liban, T.J., Felthousen, J.G., Ramanan, P., Litovchick, L., and Rubin, S.M. (2015). Structural mechanisms of DREAM complex assembly and regulation. Genes Dev *29*, 961–974.

Hamilton, L.K., Dufresne, M., Joppé, S.E., Petryszyn, S., Aumont, A., Calon, F., Barnabé-Heider, F., Furtos, A., Parent, M., Chaurand, P., et al. (2015). Aberrant Lipid Metabolism in the Forebrain Niche Suppresses Adult Neural Stem Cell Proliferation in an Animal Model of Alzheimer's Disease. Cell Stem Cell *17*, 397–411.

Harada, Y., Yamada, M., Imayoshi, I., Kageyama, R., Suzuki, Y., Kuniya, T., Furutachi, S., Kawaguchi, D., and Gotoh, Y. (2021). Cell cycle arrest determines adult neural stem cell ontogeny by an embryonic Notch-nonoscillatory Hey1 module. Nat Commun *12*, 6562.

Harris, L., Rigo, P., Stiehl, T., Gaber, Z.B., Austin, S.H.L., Masdeu, M. del M., Edwards, A., Urbán, N., Marciniak-Czochra, A., and Guillemot, F. (2021). Coordinated changes in cellular behavior ensure the lifelong maintenance of the hippocampal stem cell population. Cell Stem Cell *28*, 863-876.e6.

Helin, K., Harlow, E., and Fattaey, A. (1993a). Inhibition of E2F-1 transactivation by direct binding of the retinoblastoma protein. Mol Cell Biol *13*, 6501–6508.

Helin, K., Wu, C.L., Fattaey, A.R., Lees, J.A., Dynlacht, B.D., Ngwu, C., and Harlow, E. (1993b). Heterodimerization of the transcription factors E2F-1 and DP-1 leads to cooperative trans-activation. Gene Dev *7*, 1850–1861.

Hochgerner, H., Zeisel, A., Lönnerberg, P., and Linnarsson, S. (2018). Conserved properties of dentate gyrus neurogenesis across postnatal development revealed by single-cell RNA sequencing. Nat Neurosci *21*, 1–15.

Hsiao, K.M., McMahon, S.L., and Farnham, P.J. (1994). Multiple DNA elements are required for the growth regulation of the mouse E2F1 promoter. Gene Dev *8*, 1526–1537.

Hsieh, J. (2012). Orchestrating transcriptional control of adult neurogenesis. Genes Dev *26*, 1010–1021.

Hsu, J., Arand, J., Chaikovsky, A., Mooney, N.A., Demeter, J., Brison, C.M., Oliverio, R., Vogel, H., Rubin, S.M., Jackson, P.K., et al. (2019). E2F4 regulates transcriptional activation in mouse embryonic stem cells independently of the RB family. Nat Commun *10*, 2939.

Hurford, R.K., Cobrinik, D., Lee, M.H., and Dyson, N. (1997). pRB and p107/p130 are required for the regulated expression of different sets of E2F responsive genes. Genes Dev *11*, 1447–1463.

Hwang, J.-Y., and Zukin, R.S. (2018). REST, a master transcriptional regulator in neurodegenerative disease. Current Opinion in Neurobiology *48*, 193–200.

Imayoshi, I., Sakamoto, M., Ohtsuka, T., Takao, K., Miyakawa, T., Yamaguchi, M., Mori, K., Ikeda, T., Itohara, S., and Kageyama, R. (2008). Roles of continuous neurogenesis in the structural and functional integrity of the adult forebrain. Nat Neurosci *11*, 1153–1161.

Jacks, T., Fazeli, A., Schmitt, E.M., Bronson, R.T., Goodell, M.A., and Weinberg, R.A. (1992). Effects of an Rb mutation in the mouse. Nature *359*, 295–300.

Jiang, Z., Deng, T., Jones, R., Li, H., Herschkowitz, J.I., Liu, J.C., Weigman, V.J., Tsao, M.-S., Lane, T.F., Perou, C.M., et al. (2010). Rb deletion in mouse mammary progenitors induces

luminal-B or basal-like/EMT tumor subtypes depending on p53 status. J Clin Invest *120*, 3296–3309.

Johnson, R., Teh, C.H., Kunarso, G., Wong, K.Y., Srinivasan, G., Cooper, M.L., Volta, M., Chan, S.S., Lipovich, L., Pollard, S.M., et al. (2008). REST Regulates Distinct Transcriptional Networks in Embryonic and Neural Stem Cells. PLoS Biol *6*, e256-15.

Jørgensen, H.F., Terry, A., Beretta, C., Pereira, C.F., Leleu, M., Chen, Z.-F., Kelly, C., Merkenschlager, M., and Fisher, A.G. (2009). REST selectively represses a subset of RE1-containing neuronal genes in mouse embryonic stem cells. Development *136*, 715–721.

Julian, L.M., and Blais, A. (2015). Transcriptional control of stem cell fate by E2Fs and pocket proteins. Frontiers in Genetics *6*, 161.

Julian, L.M., Vandenbosch, R., Pakenham, C.A., Andrusiak, M.G., Nguyen, A.P., McClellan, K.A., Svoboda, D.S., Lagace, D.C., Park, D.S., Leone, G., et al. (2013). Opposing regulation of Sox2 by cell-cycle effectors E2f3a and E2f3b in neural stem cells. Cell Stem Cell *12*, 440–452.

Kalamakis, G., Brüne, D., Ravichandran, S., Bolz, J., Fan, W., Ziebell, F., Stiehl, T., Catalá-Martinez, F., Kupke, J., Zhao, S., et al. (2019). Quiescence Modulates Stem Cell Maintenance and Regenerative Capacity in the Aging Brain. Cell *176*, 1407-1419.e14.

Kaplan, M.S., and Hinds, J.W. (1977). Neurogenesis in the Adult Rat: Electron Microscopic Analysis of Light Radioautographs. Science *197*, 1092–1094.

Kareta, M.S., Gorges, L.L., Hafeez, S., Benayoun, B.A., Marro, S., Zmoos, A.-F., Cecchini, M.J., Spacek, D., Batista, L.F.Z., O'Brien, M., et al. (2015). Inhibition of pluripotency networks by the Rb tumor suppressor restricts reprogramming and tumorigenesis. Cell Stem Cell *16*, 39–50.

Kawamura, M., Sato, S., Matsumoto, G., Fukuda, T., Shiba-Fukushima, K., Noda, S., Takanashi, M., Mori, N., and Hattori, N. (2019). Loss of nuclear REST/NRSF in aged-dopaminergic neurons in Parkinson's disease patients. Neurosci Lett *699*, 59–63.

Kim, E., Cheng, Y., Bolton-Gillespie, E., Cai, X., Ma, C., Tarangelo, A., Le, L., Jambhekar, M., Raman, P., Hayer, K.E., et al. (2017). Rb family proteins enforce the homeostasis of quiescent hematopoietic stem cells by repressing Socs3 expression. The Journal of Experimental Medicine *214*, 1901–1912.

Kim, E.J., Ables, J.L., Dickel, L.K., Eisch, A.J., and Johnson, J.E. (2011). Ascl1 (Mash1) Defines Cells with Long-Term Neurogenic Potential in Subgranular and Subventricular Zones in Adult Mouse Brain. Plos One *6*, e18472.

Kippin, T.E., Martens, D.J., and Kooy, D. van der (2005). p21 loss compromises the relative quiescence of forebrain stem cell proliferation leading to exhaustion of their proliferation capacity. Genes Dev *19*, 756–767.

Knudsen, E.S., and Knudsen, K.E. (2008). Tailoring to RB: tumour suppressor status and therapeutic response. Nat Rev Cancer *8*, 714–724.

Kohyama, J., Sanosaka, T., Tokunaga, A., Takatsuka, E., Tsujimura, K., Okano, H., and Nakashima, K. (2010). BMP-induced REST regulates the establishment and maintenance of astrocytic identity. J Cell Biology *189*, 159–170.

Komori, H., Goto, Y., Kurayoshi, K., Ozono, E., Iwanaga, R., Bradford, A.P., Araki, K., and Ohtani, K. (2018). Differential requirement for dimerization partner DP between E2F-dependent activation of tumor suppressor and growth-related genes. Sci Rep-Uk *8*, 8438.

Kooy, D. van der, and Weiss, and S. (2000). Why Stem Cells? Science *287*, 1439–1441.

Kornack, D.R., and Rakic, P. (1999). Continuation of neurogenesis in the hippocampus of the adult macaque monkey. Proc National Acad Sci *96*, 5768–5773.

Kovesdi, I., Reichel, R., and Nevins, J.R. (1986). Identification of a cellular transcription factor involved in E1A trans-activation. Cell *45*, 219–228.

Kowalczyk, A., Filipkowski, R.K., Rylski, M., Wilczynski, G.M., Konopacki, F.A., Jaworski, J., Ciemerych, M.A., Sicinski, P., and Kaczmarek, L. (2004). The critical role of cyclin D2 in adult neurogenesis. J Cell Biol *167*, 209–213.

Krek, W., Xu, G., and Livingston, D.M. (1995). Cyclin A-kinase regulation of E2F-1 DNA binding function underlies suppression of an S phase checkpoint. Cell *83*, 1149–1158.

Kuhn, H., Dickinson-Anson, H., and Gage, F. (1996). Neurogenesis in the dentate gyrus of the adult rat: age-related decrease of neuronal progenitor proliferation. J Neurosci *16*, 2027–2033.

Lavado, A., Lagutin, O.V., Chow, L.M.L., Baker, S.J., and Oliver, G. (2010). Prox1 Is Required for Granule Cell Maturation and Intermediate Progenitor Maintenance During Brain Neurogenesis. PLoS Biol *8*, e1000460.

LeCouter, J.E., Kablar, B., Whyte, P.F., Ying, C., and Rudnicki, M.A. (1998a). Strain-dependent embryonic lethality in mice lacking the retinoblastoma-related p130 gene. Development *125*, 4669–4679.

LeCouter, J.E., Kablar, B., Hardy, W.R., Ying, C., Megeney, L.A., May, L.L., and Rudnicki, M.A. (1998b). Strain-dependent myeloid hyperplasia, growth deficiency, and accelerated cell cycle in mice lacking the Rb-related p107 gene. Mol Cell Biol *18*, 7455–7465.

Lee, C., Chang, J.H., Lee, H.S., and Cho, Y. (2002a). Structural basis for the recognition of the E2F transactivation domain by the retinoblastoma tumor suppressor. Gene Dev *16*, 3199–3212.

Lee, E.Y., Hu, N., Yuan, S.S., Cox, L.A., Bradley, A., Lee, W.H., and Herrup, K. (1994). Dual roles of the retinoblastoma protein in cell cycle regulation and neuron differentiation. Gene Dev *8*, 2008–2021.

Lee, E.Y., Cam, H., Ziebold, U., Rayman, J.B., Lees, J.A., and Dynlacht, B.D. (2002b). E2F4 loss suppresses tumorigenesis in Rb mutant mice. Cancer Cell *2*, 463–472.

Lee, J.-O., Russo, A.A., and Pavletich, N.P. (1998). Structure of the retinoblastoma tumour-suppressor pocket domain bound to a peptide from HPV E7. Nature *391*, 859–865.

Lee, M.H., Williams, B.O., Mulligan, G., Mukai, S., Bronson, R.T., Dyson, N., Harlow, E., and Jacks, T. (1996). Targeted disruption of p107: functional overlap between p107 and Rb. Genes Dev *10*, 1621–1632.

Lee, N., Park, S.J., Haddad, G., Kim, D.-K., Park, S.-M., Park, S.K., and Choi, K.Y. (2016). Interactomic analysis of REST/ NRSF and implications of its functional links with the transcription suppressor TRIM28 during neuronal differentiation. Scientific Reports *6*, 1–14.

Lee, W.-H., Shew, J.-Y., Hong, F.D., Sery, T.W., Donoso, L.A., Young, L.-J., Bookstein, R., and Lee, E.Y.H.P. (1987). The retinoblastoma susceptibility gene encodes a nuclear phosphoprotein associated with DNA binding activity. Nature *329*, 642–645.

Lees, J.A., Saito, M., Vidal, M., Valentine, M., Look, T., Harlow, E., Dyson, N., and Helin, K. (1993). The retinoblastoma protein binds to a family of E2F transcription factors. Mol Cell Biol *13*, 7813–7825.

Leone, G., DeGregori, J., Yan, Z., Jakoi, L., Ishida, S., Williams, R.S., and Nevins, J.R. (1998). E2F3 activity is regulated during the cell cycle and is required for the induction of S phase. Gene Dev *12*, 2120–2130.

Leone, G., Nuckolls, F., Ishida, S., Adams, M., Sears, R., Jakoi, L., Miron, A., and Nevins, J.R. (2000). Identification of a Novel E2F3 Product Suggests a Mechanism for Determining Specificity of Repression by Rb Proteins. Mol Cell Biol *20*, 3626–3632.

Lepagnol-Bestel, A.-M., Zvara, A., Maussion, G., Quignon, F., Ngimbous, B., Ramoz, N., Imbeaud, S., Loe-Mie, Y., Benihoud, K., Agier, N., et al. (2009). DYRK1A interacts with the REST/NRSF-SWI/SNF chromatin remodelling complex to deregulate gene clusters involved in the neuronal phenotypic traits of Down syndrome. Hum Mol Genet *18*, 1405–1414.

Li, H., Collado, M., Villasante, A., Matheu, A., Lynch, C.J., Cañamero, M., Rizzoti, K., Carneiro, C., Martínez, G., Vidal, A., et al. (2012). p27(Kip1) directly represses Sox2 during embryonic stem cell differentiation. Cell Stem Cell *11*, 845–852.

Li, J., Ran, C., Li, E., Gordon, F., Comstock, G., Siddiqui, H., Cleghorn, W., Chen, H.-Z., Kornacker, K., Liu, C.-G., et al. (2008). Synergistic function of E2F7 and E2F8 is essential for cell survival and embryonic development. Developmental Cell *14*, 62–75.

Liban, T.J., Thwaites, M.J., Dick, F.A., and Rubin, S.M. (2016). Structural Conservation and E2F Binding Specificity within the Retinoblastoma Pocket Protein Family. Journal of Molecular Biology *428*, 1–25.

Lindeman, G.J., Dagnino, L., Gaubatz, S., Xu, Y., Bronson, R.T., Warren, H.B., and Livingston, D.M. (1998). A specific, nonproliferative role for E2F-5 in choroid plexus function revealed by gene targeting. Gene Dev *12*, 1092–1098.

Litovchick, L., Sadasivam, S., Florens, L., Zhu, X., Swanson, S.K., Velmurugan, S., Chen, R., Washburn, M.P., Liu, X.S., and DeCaprio, J.A. (2007). Evolutionarily Conserved Multisubunit RBL2/p130 and E2F4 Protein Complex Represses Human Cell Cycle-Dependent Genes in Quiescence. Mol Cell *26*, 539–551.

Liu, D.X., Nath, N., Chellappan, S.P., and Greene, L.A. (2005). Regulation of neuron survival and death by p130 and associated chromatin modifiers. Genes Dev *19*, 719–732.

Lledo, P.-M., and Valley, M. (2016). Adult Olfactory Bulb Neurogenesis. Csh Perspect Biol *8*, a018945.

Llorens-Bobadilla, E., Zhao, S., Baser, A., Saiz-Castro, G., Zwadlo, K., and Martin-Villalba, A. (2015). Single-Cell Transcriptomics Reveals a Population of Dormant Neural Stem Cells that Become Activated upon Brain Injury. Cell Stem Cell *17*, 329–340.

Loh, Y.-H., Wu, Q., Chew, J.-L., Vega, V.B., Zhang, W., Chen, X., Bourque, G., George, J., Leong, B., Liu, J., et al. (2006). The Oct4 and Nanog transcription network regulates pluripotency in mouse embryonic stem cells. Nat Genet *38*, 431–440.

López-Sánchez, N., Garrido-García, A., Ramón-Landreau, M., Cano-Daganzo, V., and Frade, J.M. (2021). E2F4-Based Gene Therapy Mitigates the Phenotype of the Alzheimer's Disease Mouse Model 5xFAD. Neurotherapeutics 1–20.

Lundberg, A.S., and Weinberg, R.A. (1998). Functional Inactivation of the Retinoblastoma Protein Requires Sequential Modification by at Least Two Distinct Cyclin-cdk Complexes. Mol Cell Biol *18*, 753–761.

MacPherson, D., Sage, J., Crowley, D., Trumpp, A., Bronson, R.T., and Jacks, T. (2003). Conditional Mutation of Rb Causes Cell Cycle Defects without Apoptosis in the Central Nervous System. Molecular and Cellular Biology *23*, 1044–1053.

Mampay, M., and Sheridan, G.K. (2019). REST: An epigenetic regulator of neuronal stress responses in the young and ageing brain. Front Neuroendocrin *53*, 100744.

Marqués-Torrejón, M.Á., Porlan, E., Banito, A., Gómez-Ibarlucea, E., Lopez-Contreras, A.J., Fernández-Capetillo, Ó., Vidal, A., Gil, J., Torres, J., and Fariñas, I. (2013). Cyclin-dependent kinase inhibitor p21 controls adult neural stem cell expansion by regulating Sox2 gene expression. Cell Stem Cell *12*, 88–100.

McClellan, K.A., and Slack, R.S. (2006). Novel functions for cell cycle genes in nervous system development. Cell Cycle (Georgetown, Tex.) *5*, 1506–1513.

McClellan, K.A., Ruzhynsky, V.A., Douda, D.N., Vanderluit, J.L., Ferguson, K.L., Chen, D., Bremner, R., Park, D.S., Leone, G., and Slack, R.S. (2007). Unique Requirement for Rb/E2F3 in Neuronal Migration: Evidence for Cell Cycle-Independent Functions. Molecular and Cellular Biology *27*, 4825–4843.

McClellan, K.A., Vanderluit, J.L., Julian, L.M., Andrusiak, M.G., Dugal-Tessier, D., Park, D.S., and Slack, R.S. (2009). The p107/E2F Pathway Regulates Fibroblast Growth Factor 2 Responsiveness in Neural Precursor Cells. Molecular and Cellular Biology *29*, 4701–4713.

McClelland, S., Brennan, G.P., Dubé, C., Rajpara, S., Iyer, S., Richichi, C., Bernard, C., and Baram, T.Z. (2014). The transcription factor NRSF contributes to epileptogenesis by selective repression of a subset of target genes. Elife *3*, e01267.

Meyer, K., Feldman, H.M., Lu, T., Drake, D., Lim, E.T., Ling, K.-H., Bishop, N.A., Pan, Y., Seo, J., Lin, Y.-T., et al. (2019). REST and Neural Gene Network Dysregulation in iPSC Models of Alzheimer's Disease. Cell Reports *26*, 1112-1127.e9.

Mich, J.K., Signer, R.A., Nakada, D., Pineda, A., Burgess, R.J., Vue, T.Y., Johnson, J.E., and Morrison, S.J. (2014). Prospective identification of functionally distinct stem cells and neurosphere-initiating cells in adult mouse forebrain. Elife *3*, e02669.

Ming, G.-L., and Song, H. (2011). Adult neurogenesis in the mammalian brain: significant answers and significant questions. Neuron *70*, 687–702.

Mirzadeh, Z., Merkle, F.T., Soriano-Navarro, M., Garcia-Verdugo, J.M., and Alvarez-Buylla, A. (2008). Neural Stem Cells Confer Unique Pinwheel Architecture to the Ventricular Surface in Neurogenic Regions of the Adult Brain. Cell Stem Cell *3*, 265–278.

Moberg, K., Starz, M.A., and Lees, J.A. (1996). E2F-4 switches from p130 to p107 and pRB in response to cell cycle reentry. Mol Cell Biol *16*, 1436–1449.

Moreno, E., Pandit, S.K., Toussaint, M.J.M., Bongiovanni, L., Harkema, L., Essen, S.C. van, Liere, E.A. van, Westendorp, B., and Bruin, A. de (2021). Atypical E2Fs either Counteract or Cooperate with RB during Tumorigenesis Depending on Tissue Context. Cancers *13*, 2033.

Moreno-Jiménez, E.P., Flor-García, M., Terreros-Roncal, J., Rábano, A., Cafini, F., Pallas-Bazarra, N., Ávila, J., and Llorens-Martín, M. (2019). Adult hippocampal neurogenesis is abundant in neurologically healthy subjects and drops sharply in patients with Alzheimer's disease. Nat Med *25*, 554–560.

Morris, E.J., and Dyson, N.J. (2001). Retinoblastoma protein partners. Adv Cancer Res *82*, 1–54.

Morshead, C., and Kooy, D. van der (1992). Postmitotic death is the fate of constitutively proliferating cells in the subependymal layer of the adult mouse brain. J Neurosci *12*, 249–256.

Morshead, C.M., Reynolds, B.A., Craig, C.G., McBurney, M.W., Staines, W.A., Morassutti, D., Weiss, S., and Kooy, D. van der (1994). Neural stem cells in the adult mammalian forebrain: A relatively quiescent subpopulation of subependymal cells. Neuron *13*, 1071–1082.

Morshead, C.M., Craig, C.G., and Kooy, D. van der (1998). In vivo clonal analyses reveal the properties of endogenous neural stem cell proliferation in the adult mammalian forebrain. Development *125*, 2251–2261.

Mortazavi, A., Thompson, E.C.L., Garcia, S.T., Myers, R.M., and Wold, B. (2006). Comparative genomics modeling of the NRSF/REST repressor network: From single conserved sites to genome-wide repertoire. Genome Research *16*, 1208–1221.

Mu, L., Berti, L., Masserdotti, G., Covic, M., Michaelidis, T.M., Doberauer, K., Merz, K., Rehfeld, F., Haslinger, A., Wegner, M., et al. (2012). SoxC Transcription Factors Are Required for Neuronal Differentiation in Adult Hippocampal Neurogenesis. J Neurosci *32*, 3067–3080.

Mukherjee, S., Brulet, R., Zhang, L., and Hsieh, J. (2016). REST regulation of gene networks in adult neural stem cells. Nature Communications *7*, 1–14.

Müller, H., Moroni, M.C., Vigo, E., Petersen, B.O., Bartek, J., and Helin, K. (1997). Induction of S-phase entry by E2F transcription factors depends on their nuclear localization. Mol Cell Biol *17*, 5508–5520.

Mulligan, G., and Jacks, T. (1998). The retinoblastoma gene family: cousins with overlapping interests. Trends Genet *14*, 223–229.

Narasimha, A.M., Kaulich, M., Shapiro, G.S., Choi, Y.J., Sicinski, P., and Dowdy, S.F. (2014). Cyclin D activates the Rb tumor suppressor by mono-phosphorylation. Elife *3*, e02872.

Naser, R., Vandenbosch, R., Omais, S., Hayek, D., Jaafar, C., Lafi, S.A., Saliba, A., Baghdadi, M., Skaf, L., and Ghanem, N. (2016). Role of the Retinoblastoma protein, Rb, during adult neurogenesis in the olfactory bulb. Scientific Reports *6*, 20230.

Nechiporuk, T., McGann, J., Mullendorff, K., Hsieh, J., Wurst, W., Floss, T., and Mandel, G. (2016). The REST remodeling complex protects genomic integrity during embryonic neurogenesis. Elife *5*, e09584.

Nesti, E., Corson, G.M., McCleskey, M., Oyer, J.A., and Mandel, G. (2014). C-terminal domain small phosphatase 1 and MAP kinase reciprocally control REST stability and neuronal differentiation. Proc National Acad Sci *111*, E3929–E3936.

Nishihara, S., Tsuda, L., and Ogura, T. (2003). The canonical Wnt pathway directly regulates NRSF/REST expression in chick spinal cord. Biochem Bioph Res Co *311*, 55–63.

Obernier, K., Cebrian-Silla, A., Thomson, M., Parraguez, J.I., Anderson, R., Guinto, C., Rodriguez, J.R., García-Verdugo, J.M., and Alvarez-Buylla, A. (2018). Adult Neurogenesis Is Sustained by Symmetric Self- Renewal and Differentiation. Stem Cell *22*, 221-234.e8.

O'Leary, T.P., Askari, B., Lee, B., Darby, K., Knudson, C., Ash, A.M., Seib, D.R., Espinueva, D.F., and Snyder, J.S. (2021). Inhibiting adult neurogenesis differentially affects spatial learning in females and males. Biorxiv 2021.10.27.466135.

Opavsky, R., Tsai, S.-Y., Guimond, M., Arora, A., Opavska, J., Becknell, B., Kaufmann, M., Walton, N.A., Stephens, J.A., Fernandez, S.A., et al. (2007). Specific tumor suppressor function for E2F2 in Myc-induced T cell lymphomagenesis. Proc National Acad Sci *104*, 15400–15405.

Oshikawa, M., Okada, K., Nakajima, K., and Ajioka, I. (2013). Cortical excitatory neurons become protected from cell division during neurogenesis in an Rb family-dependent manner. Development *140*, 2310–2320.

Otsuki, L., and Brand, A.H. (2018). Cell cycle heterogeneity directs the timing of neural stem cell activation from quiescence. Science (New York, N.Y.) *360*, 99–102.

Pajcini, K.V., Corbel, S.Y., Sage, J., Pomerantz, J.H., and Blau, H.M. (2010). Transient inactivation of Rb and ARF yields regenerative cells from postmitotic mammalian muscle. Cell Stem Cell *7*, 198–213.

Palm, K., Belluardo, N., Metsis, M., and Timmusk, T. õnis (1998). Neuronal Expression of Zinc Finger Transcription Factor REST/NRSF/XBR Gene. J Neurosci *18*, 1280–1296.

Pan, H., Yin, C., Dyson, N.J., Harlow, E., Yamasaki, L., and Dyke, T.V. (1998). Key Roles for E2F1 in Signaling p53-Dependent Apoptosis and in Cell Division within Developing Tumors. Mol Cell *2*, 283–292.

Paredes, M.F., Sorrells, S.F., Cebrian-Silla, A., Sandoval, K., Qi, D., Kelley, K.W., James, D., Mayer, S., Chang, J., Auguste, K.I., et al. (2018). Does Adult Neurogenesis Persist in the Human Hippocampus? Cell Stem Cell *23*, 780–781.

Pechnick, R.N., Zonis, S., Wawrowsky, K., Pourmorady, J., and Chesnokova, V. (2008). p21Cip1 restricts neuronal proliferation in the subgranular zone of the dentate gyrus of the hippocampus. Proceedings of the National Academy of Sciences of the United States of America *105*, 1358–1363.

Pilz, G.-A., Bottes, S., Betizeau, M., Jörg, D.J., Carta, S., Simons, B.D., Helmchen, F., and Jessberger, S. (2018). Live imaging of neurogenesis in the adult mouse hippocampus. Science (New York, N.Y.) *359*, 658–662.

Poiana, G., Gioia, R., Sineri, S., Cardarelli, S., Lupo, G., and Cacci, E. (2020). Transcriptional regulation of adult neural stem/progenitor cells: tales from the subventricular zone. Neural Regen Res *15*, 1773–1783.

Porlan, E., Morante-Redolat, J.M., Marqués-Torrejón, M.Á., Andreu-Agulló, C., Carneiro, C., Gómez-Ibarlucea, E., Soto, A., Vidal, A., Ferrón, S.R., and Fariñas, I. (2013). Transcriptional repression of Bmp2 by p21(Waf1/Cip1) links quiescence to neural stem cell maintenance. Nat Neurosci *16*, 1567–1575.

Praag, H. van, Schinder, A.F., Christie, B.R., Toni, N., Palmer, T.D., and Gage, F.H. (2002). Functional neurogenesis in the adult hippocampus. Nature *415*, 1030–1034.

Previll, L.A., Crosby, M.E., Castellani, R.J., Bowser, R., Perry, G., Smith, M.A., and Zhu, X. (2007). Increased Expression of p130 in Alzheimer Disease. Neurochem Res *32*, 639–644.

Redmond, S.A., Silla, A.C., Nascimento, M.A., Mansky, B., Wu, D., Obernier, K., Rodriguez, R.R., Lim, D.A., and Alvarez-Buylla, A. Single-cell analysis of the ventricular-subventricular zone reveals signatures of dorsal and ventral adult neurogenic lineages.

Rempel, R.E., Saenz-Robles, M.T., Storms, R., Morham, S., Ishida, S., Engel, A., Jakoi, L., Melhem, M.F., Pipas, J.M., Smith, C., et al. (2000). Loss of E2F4 Activity Leads to Abnormal Development of Multiple Cellular Lineages. Mol Cell *6*, 293–306.

Ren, B., Cam, H., Takahashi, Y., Volkert, T., Terragni, J., Young, R.A., and Dynlacht, B.D. (2002). E2F integrates cell cycle progression with DNA repair, replication, and G2/M checkpoints. Gene Dev *16*, 245–256.

Reynolds, B., and Weiss, S. (1992). Generation of neurons and astrocytes from isolated cells of the adult mammalian central nervous system. Science (New York, N.Y.) *255*, 1707–1710.

Richards, B.A., and Frankland, P.W. (2017). The Persistence and Transience of Memory. Neuron *94*, 1071–1084.

Robertson, K.D., Ait-Si-Ali, S., Yokochi, T., Wade, P.A., Jones, P.L., and Wolffe, A.P. (2000). DNMT1 forms a complex with Rb, E2F1 and HDAC1 and represses transcription from E2F-responsive promoters. Nat Genet *25*, 338–342.

Roopra, A., Sharling, L., Wood, I.C., Briggs, T., Bachfischer, U., Paquette, A.J., and Buckley, N.J. (2000). Transcriptional Repression by Neuron-Restrictive Silencer Factor Is Mediated via the Sin3-Histone Deacetylase Complex. Mol Cell Biol *20*, 2147–2157.

Rotgers, E., Rivero-Müller, A., Nurmio, M., Parvinen, M., Guillou, F., Huhtaniemi, I., Kotaja, N., Bourguiba-Hachemi, S., and Toppari, J. (2014). Retinoblastoma protein (RB) interacts with E2F3 to control terminal differentiation of Sertoli cells. Cell Death Dis *5*, e1274.

Saavedra, H.I., Wu, L., Bruin, A. de, Timmers, C., Rosol, T.J., Weinstein, M., Robinson, M.L., and Leone, G. (2002). Specificity of E2F1, E2F2, and E2F3 in mediating phenotypes induced by loss of Rb. Cell Growth & Differentiation : The Molecular Biology Journal of the American Association for Cancer Research *13*, 215–225.

Sage, J. (2000). Targeted disruption of the three Rb-related genes leads to loss of G1 control and immortalization. Genes Dev *14*, 3037–3050.

Sage, J. (2012). The retinoblastoma tumor suppressor and stem cell biology. Genes Dev *26*, 1409–1420.

Sage, J., Miller, A.L., Pérez-Mancera, P.A., Wysocki, J.M., and Jacks, T. (2003). Acute mutation of retinoblastoma gene function is sufficient for cell cycle re-entry. Nature *424*, 223–228.

Sahay, A., Scobie, K.N., Hill, A.S., O'Carroll, C.M., Kheirbek, M.A., Burghardt, N.S., Fenton, A.A., Dranovsky, A., and Hen, R. (2011). Increasing adult hippocampal neurogenesis is sufficient to improve pattern separation. Nature *472*, 466–470.

Sangwan, M., McCurdy, S.R., Livne-bar, I., Ahmad, M., Wrana, J.L., Chen, D., and Bremner, R. (2012). Established and New Mouse Models Reveal E2f1 and Cdk2 Dependency of Retinoblastoma and Expose Strategies to Block Tumor Initiation. Oncogene *31*, 5019–5028.

Schade, A.E., Fischer, M., and DeCaprio, J.A. (2019). RB, p130 and p107 differentially repress G1/S and G2/M genes after p53 activation. Nucleic Acids Res.

Schoenherr, C.J., and Anderson, D.J. (1995). The Neuron-Restrictive Silencer Factor (NRSF): A Coordinate Repressor of Multiple Neuron-Specific Genes. Science *267*, 1360–1363.

Sheehy, R.N., Quintanilla, L.J., and Song, J. (2021). Epigenetic Regulation in the Neurogenic Niche of the Adult Dentate Gyrus. Neurosci Lett 136343.

Shimojo, H., Ohtsuka, T., and Kageyama, R. (2008). Oscillations in Notch Signaling Regulate Maintenance of Neural Progenitors. Neuron *58*, 52–64.

Shirodkar, S., Ewen, M., DeCaprio, J.A., Morgan, J., Livingston, D.M., and Chittenden, T. (1992). The transcription factor E2F interacts with the retinoblastoma product and a p107-cyclin A complex in a cell cycle-regulated manner. Cell *68*, 157–166.

Smart, I. (1961). The subependymal layer of the mouse brain and its cell production as shown by radioautography after thymidine-H3 injection. J Comp Neurol *116*, 325–347.

Smith, E.J., Leone, G., DeGregori, J., Jakoi, L., and Nevins, J.R. (1996). The accumulation of an E2F-p130 transcriptional repressor distinguishes a G0 cell state from a G1 cell state. Molecular and Cellular Biology *16*, 6965–6976.

Soldati, C., Caramanica, P., Burney, M.J., Toselli, C., Bithell, A., Augusti-Tocco, G., Stanton, L.W., Biagioni, S., Buckley, N.J., and Cacci, E. (2015). RE1 silencing transcription factor/neuron-restrictive silencing factor regulates expansion of adult mouse subventricular zone-derived neural stem/progenitor cells in vitro. J Neurosci Res *93*, 1203–1214.

Song, J., Sun, J., Moss, J., Wen, Z., Sun, G.J., Hsu, D., Zhong, C., Davoudi, H., Christian, K.M., Toni, N., et al. (2013). Parvalbumin interneurons mediate neuronal circuitry–neurogenesis coupling in the adult hippocampus. Nat Neurosci *16*, 1728–1730.

Sorrells, S.F., Paredes, M.F., Cebrian-Silla, A., Sandoval, K., Qi, D., Kelley, K.W., James, D., Mayer, S., Chang, J., Auguste, K.I., et al. (2018). Human hippocampal neurogenesis drops sharply in children to undetectable levels in adults. Nature *124*, 319–381.

Spalding, K.L., Bergmann, O., Alkass, K., Bernard, S., Salehpour, M., Huttner, H.B., Boström, E., Westerlund, I., Vial, C., Buchholz, B.A., et al. (2013). Dynamics of Hippocampal Neurogenesis in Adult Humans. Cell *153*, 1219–1227.

Stefano, L.D. (2003). E2F7, a novel E2F featuring DP-independent repression of a subset of E2F-regulated genes. The EMBO Journal *22*, 6289–6298.

Stengel, K.R., Thangavel, C., Solomon, D.A., Angus, S.P., Zheng, Y., and Knudsen, E.S. (2009). Retinoblastoma/p107/p130 Pocket Proteins: PROTEIN DYNAMICS AND INTERACTIONS WITH TARGET GENE PROMOTERS. Journal of Biological Chemistry *284*, 19265–19271.

Su, X., Gopalakrishnan, V., Stearns, D., Aldape, K., Lang, F.F., Fuller, G., Snyder, E., Eberhart, C.G., and Majumder, S. (2006). Abnormal Expression of REST/NRSF and Myc in Neural Stem/Progenitor Cells Causes Cerebellar Tumors by Blocking Neuronal Differentiation. Mol Cell Biol *26*, 1666–1678.

Sueda, R., Imayoshi, I., Harima, Y., and Kageyama, R. (2019). High Hes1 expression and resultant Ascl1 suppression regulate quiescent vs. active neural stem cells in the adult mouse brain. Genes Dev 1–14.

Suh, H., Consiglio, A., Ray, J., Sawai, T., D'Amour, K.A., and Gage, F.H. (2007). In Vivo Fate Analysis Reveals the Multipotent and Self-Renewal Capacities of Sox2+ Neural Stem Cells in the Adult Hippocampus. Cell Stem Cell *1*, 515–528.

Sun, Y.-M., Greenway, D.J., Johnson, R., Street, M., Belyaev, N.D., Deuchars, J., Bee, T., Wilde, S., and Buckley, N.J. (2005). Distinct profiles of REST interactions with its target genes at different stages of neuronal development. Molecular Biology of the Cell *16*, 5630–5638.

Thored, P., Arvidsson, A., Cacci, E., Ahlenius, H., Kallur, T., Darsalia, V., Ekdahl, C.T., Kokaia, Z., and Lindvall, O. (2006). Persistent Production of Neurons from Adult Brain Stem Cells During Recovery after Stroke. Stem Cells *24*, 739–747.

Tirosh, I., Izar, B., Prakadan, S.M., II, M.H.W., Treacy, D., Trombetta, J.J., Rotem, A., Rodman, C., Lian, C., Murphy, G., et al. (2016). Dissecting the multicellular ecosystem of metastatic melanoma by single-cell RNA-seq. Science *352*, 189–196.

Tobin, M.K., Musaraca, K., Disouky, A., Shetti, A., Bheri, A., Honer, W.G., Kim, N., Dawe, R.J., Bennett, D.A., Arfanakis, K., et al. (2019). Human Hippocampal Neurogenesis Persists in Aged Adults and Alzheimer's Disease Patients. Stem Cell *24*, 1–13.

Toda, T., and Gage, F.H. (2017). Review: adult neurogenesis contributes to hippocampal plasticity. Cell and Tissue Research *12*, 1–17.

Tsai, K.Y., Hu, Y., Macleod, K.F., Crowley, D., Yamasaki, L., and Jacks, T. (1998). Mutation of E2f-1 Suppresses Apoptosis and Inappropriate S Phase Entry and Extends Survival of Rb-Deficient Mouse Embryos. Mol Cell *2*, 293–304.

Urbach, A. (2019). Divide or Commit – Revisiting the Role of Cell Cycle Regulators in Adult Hippocampal Neurogenesis. Fcell-07-00055.Tex *7*, 1–22.

Urban, N., Berg, D.L.C. van den, Forget, A., Andersen, J., Demmers, J.A.A., Hunt, C., Ayrault, O., and Guillemot, F. (2016). Return to quiescence of mouse neural stem cells by degradation of a proactivation protein. Science (New York, N.Y.) *353*, 292–295.

Urbán, N., Blomfield, I.M., and Guillemot, F. (2019a). Quiescence of Adult Mammalian Neural Stem Cells: A Highly Regulated Rest. Neuron *104*, 834–848.

Urbán, N., Blomfield, I.M., and Guillemot, F. (2019b). Quiescence of Adult Mammalian Neural Stem Cells: A Highly Regulated Rest. Neuron *104*, 834–848.

Vandenbosch, R., Clark, A., Fong, B.C., Omais, S., Jaafar, C., Dugal-Tessier, D., Dhaliwal, J., Lagace, D.C., Park, D.S., Ghanem, N., et al. (2016). RB regulates the production and the survival of newborn neurons in the embryonic and adult dentate gyrus. Hippocampus *26*, 1379–1392.

Vanderluit, J.L., Ferguson, K.L., Nikoletopoulou, V., Parker, M., Ruzhynsky, V., Alexson, T., McNamara, S.M., Park, D.S., Rudnicki, M., and Slack, R.S. (2004). p107 regulates neural precursor cells in the mammalian brain. J Cell Biol *166*, 853–863.

Vanderluit, J.L., Wylie, C.A., McClellan, K.A., Ghanem, N., Fortin, A., Callaghan, S., MacLaurin, J.G., Park, D.S., and Slack, R.S. (2007). The Retinoblastoma family member p107 regulates the rate of progenitor commitment to a neuronal fate. J Cell Biol *178*, 129–139.

Venugopal, N., Ghosh, A., Gala, H., Aloysius, A., Vyas, N., and Dhawan, J. (2020). The primary cilium dampens proliferative signaling and represses a G2/M transcriptional network in quiescent myoblasts. Bmc Mol Cell Biology *21*, 25.

Verdugo-Sivianes, E.M., and Carnero, A. (2021). Role of the Holoenzyme PP1-SPN in the Dephosphorylation of the RB Family of Tumor Suppressors During Cell Cycle. Cancers *13*, 2226.

Verona, R., Moberg, K., Estes, S., Starz, M., Vernon, J.P., and Lees, J.A. (1997). E2F activity is regulated by cell cycle-dependent changes in subcellular localization. Mol Cell Biol *17*, 7268–7282.

Viatour, P., Somervaille, T.C., Venkatasubrahmanyam, S., Kogan, S., McLaughlin, M.E., Weissman, I.L., Butte, A.J., Passegué, E., and Sage, J. (2008). Hematopoietic stem cell quiescence is maintained by compound contributions of the retinoblastoma gene family. Cell Stem Cell *3*, 416–428.

Viatour, P., Ehmer, U., Saddic, L.A., Dorrell, C., Andersen, J.B., Lin, C., Zmoos, A.-F., Mazur, P.K., Schaffer, B.E., Ostermeier, A., et al. (2011a). Notch signaling inhibits hepatocellular carcinoma following inactivation of the RB pathway. The Journal of Experimental Medicine *208*, 1963–1976.

Viatour, P., Ehmer, U., Saddic, L.A., Dorrell, C., Andersen, J.B., Lin, C., Zmoos, A.-F., Mazur, P.K., Schaffer, B.E., Ostermeier, A., et al. (2011b). Notch signaling inhibits hepatocellular carcinoma following inactivation of the RB pathway. J Exp Medicine *208*, 1963–1976.

Vicidomini, C., Guo, N., and Sahay, A. (2020). Communication, Cross Talk, and Signal Integration in the Adult Hippocampal Neurogenic Niche. Neuron *105*, 220–235.

Walker, T.L., Overall, R.W., Vogler, S., Sykes, A.M., Ruhwald, S., Lasse, D., Ichwan, M., Fabel, K., and Kempermann, G. (2016). Lysophosphatidic Acid Receptor Is a Functional Marker of Adult Hippocampal Precursor Cells. Stem Cell Rep *6*, 552–565.

Walkley, C.R., and Orkin, S.H. (2006). Rb is dispensable for self-renewal and multilineage differentiation of adult hematopoietic stem cells. Proceedings of the National Academy of Sciences *103*, 9057–9062.

Wang, D., Russell, J.L., and Johnson, D.G. (2000). E2F4 and E2F1 Have Similar Proliferative Properties but Different Apoptotic and Oncogenic Properties In Vivo. Mol Cell Biol *20*, 3417–3424.

Winner, B., and Winkler, J. (2015). Adult Neurogenesis in Neurodegenerative Diseases: Figure 1. Cold Spring Harbor Perspectives in Biology *7*, a021287.

Wirt, S.E., and Sage, J. (2010). p107 in the public eye: an Rb understudy and more. Cell Div *5*, 9–9.

Wirt, S.E., Adler, A.S., Gebala, V., Weimann, J.M., Schaffer, B.E., Saddic, L.A., Viatour, P., Vogel, H., Chang, H.Y., Meissner, A., et al. (2010). G1 arrest and differentiation can occur independently of Rb family function. J Cell Biol *191*, 809–825.

Ye, F., Kang, E., Yu, C., Qian, X., Jacob, F., Yu, C., Mao, M., Poon, R.Y.C., Kim, J., Song, H., et al. (2017). DISC1 Regulates Neurogenesis via Modulating Kinetochore Attachment of Ndel1/Nde1 during Mitosis. Neuron *96*, 1–20.

Yeh, C.-Y., Asrican, B., Moss, J., Quintanilla, L.J., He, T., Mao, X., Cassé, F., Gebara, E., Bao, H., Lu, W., et al. (2018). Mossy Cells Control Adult Neural Stem Cell Quiescence and Maintenance through a Dynamic Balance between Direct and Indirect Pathways. Neuron.

Yun, S., Tran, F., Soler, I., Reynolds, R., Suarez, M., and Eisch, A. (2019). GABAergic entorhinal cortex control of hippocampal function in stress-related disorder: Cellular and circuitry mechanisms. Ibro Reports *6*, S504–S505.

Zacksenhaus, E., Jiang, Z., Chung, D., Marth, J.D., Phillips, R.A., and Gallie, B.L. (1996). pRb controls proliferation, differentiation, and death of skeletal muscle cells and other lineages during embryogenesis. Genes Dev *10*, 3051–3064.

Zhao, C. (2006). Distinct Morphological Stages of Dentate Granule Neuron Maturation in the Adult Mouse Hippocampus. J Neurosci *26*, 3–11.

Zheng, W., ZhuGe, Q., Zhong, M., Chen, G., Shao, B., Wang, H., Mao, X., Xie, L., and Jin, K. (2013). Neurogenesis in Adult Human Brain after Traumatic Brain Injury. J Neurotraum *30*, 1872–1880.

Ziebold, U., Lee, E.Y., Bronson, R.T., and Lees, J.A. (2003). E2F3 Loss Has Opposing Effects on Different pRB-Deficient Tumors, Resulting in Suppression of Pituitary Tumors but Metastasis of Medullary Thyroid Carcinomas. Mol Cell Biol *23*, 6542–6552.

Zini, N., Trimarchi, C., Claudio, P.P., Stiegler, P., Marinelli, F., Maltarello, M.C., Sala, D.L., Falco, G.D., Russo, G., Ammirati, G., et al. (2001). pRb2/p130 and p107 control cell growth by multiple strategies and in association with different compartments within the nucleus*. J Cell Physiol *189*, 34–44.

APPENDIX I: THE RB/E2F AXIS AND 3xTG-AD MICE

Figure 1

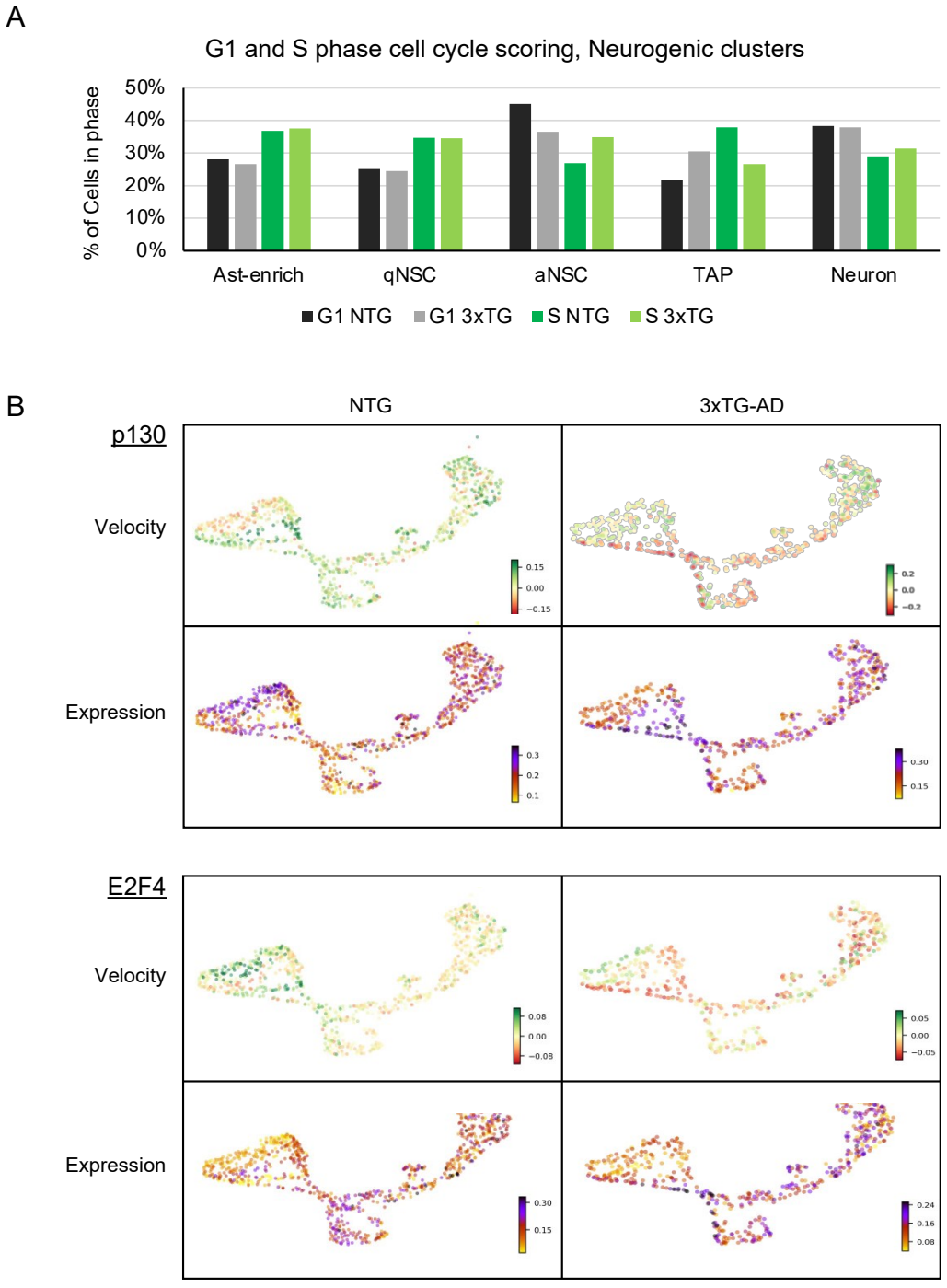

Figure Legend

Figure 1: Cluster-specific alterations to cell cycle proteins in response to 3xTG

(H) Quantification of cell portion in either G1 or S phase, expressed as a percentage of each cluster, separated by indicated genotype.
(I) Plots of RNA velocity and expression for p130 and E2F4, separated by indicated genotype.

APPENDIX II: PERMISSIONS

Permission to reprint (Vandenbosch et al., 2016)

JOHN WILEY AND SONS LICENSE
TERMS AND CONDITIONS

Oct 29, 2021

This Agreement between Mr. Bensun Fong ("You") and John Wiley and Sons ("John Wiley and Sons") consists of your license details and the terms and conditions provided by John Wiley and Sons and Copyright Clearance Center.

License Number	5178340573056
License date	Oct 29, 2021
Licensed Content Publisher	John Wiley and Sons
Licensed Content Publication	Hippocampus
Licensed Content Title	RB regulates the production and the survival of newborn neurons in the embryonic and adult dentate gyrus
Licensed Content Author	Ruth S. Slack, Noël Ghanem, David S. Park, et al
Licensed Content Date	Jul 8, 2016
Licensed Content Volume	26
Licensed Content Issue	11
Licensed Content Pages	14
Type of use	Dissertation/Thesis
Requestor type	Author of this Wiley article
Format	Print and electronic
Portion	Full article
Will you be translating?	No
Title	REGULATION OF ADULT NEUROGENESIS BY RB FAMILY PROTEINS
Institution name	University of Ottawa
Expected presentation date	Nov 2021
Requestor Location	Mr. Bensun Fong [redacted] Ottawa, ON K1H8M5 Canada Attn: Mr. Bensun Fong
Publisher Tax ID	EU826007151
Total	0.00 CAD

Terms and Conditions

TERMS AND CONDITIONS

This copyrighted material is owned by or exclusively licensed to John Wiley & Sons, Inc. or one of its group companies (each a"Wiley Company") or handled on behalf of a society with which a Wiley Company has exclusive publishing rights in relation to a particular work (collectively "WILEY"). By clicking "accept" in connection with completing this licensing transaction, you agree that the following terms and conditions apply to this transaction (along with the billing and payment terms and conditions established by the Copyright Clearance Center Inc., ("CCC's Billing and Payment terms and conditions"), at the time that you opened your RightsLink account (these are available at any time at http://myaccount.copyright.com).

Terms and Conditions

- The failure of either party to enforce any term or condition of this Agreement shall not constitute a waiver of either party's right to enforce each and every term and condition of this Agreement. No breach under this agreement shall be deemed waived or excused by either party unless such waiver or consent is in writing signed by the party granting such waiver or consent. The waiver by or consent of a party to a breach of any provision of this Agreement shall not operate or be construed as a waiver of or consent to any other or subsequent breach by such other party.

- This Agreement may not be assigned (including by operation of law or otherwise) by you without WILEY's prior written consent.

- Any fee required for this permission shall be non-refundable after thirty (30) days from receipt by the CCC.

- These terms and conditions together with CCC's Billing and Payment terms and conditions (which are incorporated herein) form the entire agreement between you and WILEY concerning this licensing transaction and (in the absence of fraud) supersedes all prior agreements and representations of the parties, oral or written. This Agreement may not be amended except in writing signed by both parties. This Agreement shall be binding upon and inure to the benefit of the parties' successors, legal representatives, and authorized assigns.

- In the event of any conflict between your obligations established by these terms and conditions and those established by CCC's Billing and Payment terms and conditions, these terms and conditions shall prevail.

- WILEY expressly reserves all rights not specifically granted in the combination of (i) the license details provided by you and accepted in the course of this licensing transaction, (ii) these terms and conditions and (iii) CCC's Billing and Payment terms and conditions.

- This Agreement will be void if the Type of Use, Format, Circulation, or Requestor Type was misrepresented during the licensing process.

- This Agreement shall be governed by and construed in accordance with the laws of the State of New York, USA, without regards to such state's conflict of law rules. Any legal action, suit or proceeding arising out of or relating to these Terms and Conditions or the breach thereof shall be instituted in a court of competent jurisdiction in New York County in the State of New York in the United States of America and each party hereby consents and submits to the personal jurisdiction of such court, waives any objection to venue in such court and consents to service of process by registered or certified mail, return receipt requested, at the last known address of such party.

WILEY OPEN ACCESS TERMS AND CONDITIONS

Wiley Publishes Open Access Articles in fully Open Access Journals and in Subscription journals offering Online Open. Although most of the fully Open Access journals publish open access articles under the terms of the Creative Commons Attribution (CC BY) License only, the subscription journals and a few of the Open Access Journals offer a choice of Creative Commons Licenses. The license type is clearly identified on the article.

The Creative Commons Attribution License

The Creative Commons Attribution License (CC-BY) allows users to copy, distribute and transmit an article, adapt the article and make commercial use of the article. The CC-BY license permits commercial and non-

Creative Commons Attribution Non-Commercial License

The Creative Commons Attribution Non-Commercial (CC-BY-NC)License permits use, distribution and reproduction in any medium, provided the original work is properly cited and is not used for commercial purposes.(see below)

Creative Commons Attribution-Non-Commercial-NoDerivs License

The Creative Commons Attribution Non-Commercial-NoDerivs License (CC-BY-NC-ND) permits use, distribution and reproduction in any medium, provided the original work is properly cited, is not used for commercial purposes and no modifications or adaptations are made. (see below)

Use by commercial "for-profit" organizations

Permission to reprint Fig. 2 from (Bonaguidi et al., 2016)

From: Brown, Carol brown@cshl.edu
Subject: FW: CSHL Press Reprint Permission Request Form

Date: October 28, 2021 at 12:51 PM **To:** [redacted]

Permission is granted for the use of Fig 2, p. 4 in the article detailed below in your PhD thesis only. Please include complete reference and copyright to Cold Spring Harbor Laboratory Press.

Best wishes for success with your thesis,

Carol C. Brown
Books Development, Marketing and Sales Cold Spring Harbor Laboratory Press
[redacted]
Woodbury NY 11797
[redacted]
-----Original Message-----
From: reprint@cshlpress.org <reprint@cshlpress.org> Sent: Thursday, October 28, 2021 12:38 PM
To: Reprint <Reprint@cshl.edu>
Subject: CSHL Press Reprint Permission Request Form

Name: Bensun Fong
CompanyInstitution: University of Ottawa Library Address: [redacted] Library Address (line 2):
City: Ottawa
State (US and Canada): Ontario Country: Canada
Zip: K1H8M5
Title: Doctoral Candidate Lab/Department: Dr. Ruth Slack Phone: [redacted]
Fax:
Email: [redacted]

Title of Publication:
Authors/Editors:
Date of Publication:
Publisher: University of Ottawa
Title of CSHLP Journal/Book: Cold Spring Harbor Perspectives in Biology

English Canada

Print

REGULATION OF ADULT NEUROGENESIS BY RB FAMILY PROTEINS Bensun C Fong

November 2021

Diversity of Neural Precursors in the Adult Mammalian Brain
Michael A. Bonaguidi1,2,3,7, Ryan P. Stadel1,4, Daniel A. Berg1,2, Jiaqi Sun1,5, Guo-li Ming1,2,3,6 and 4

Language:
Territory:
Format:
Additional comments: For use in PhD Thesis. Will cite original as Bonaguidi et al., 2016.

Permission to reprint Figure from Box 2, (Dick and Rubin, 2013)

SPRINGER NATURE LICENSE
TERMS AND CONDITIONS

Oct 29, 2021

This Agreement between Mr. Bensun Fong ("You") and Springer Nature ("Springer Nature") consists of your license details and the terms and conditions provided by Springer Nature and Copyright Clearance Center.

License Number	5177760966950
License date	Oct 28, 2021
Licensed Content Publisher	Springer Nature
Licensed Content Publication	Nature Reviews Molecular Cell Biology
Licensed Content Title	Molecular mechanisms underlying RB protein function
Licensed Content Author	Frederick A. Dick et al
Licensed Content Date	Apr 18, 2013
Type of Use	Thesis/Dissertation
Requestor type	academic/university or research institute
Format	print and electronic
Portion	figures/tables/illustrations
Number of figures/tables/illustrations	1
High-res required	no
Will you be translating?	no
Circulation/distribution	50000 or greater
Author of this Springer Nature content	no
Title	REGULATION OF ADULT NEUROGENESIS BY RB FAMILY PROTEINS
Institution name	University of Ottawa
Expected presentation date	Nov 2021
Portions	Figure in Box 2, page 300
Requestor Location	Mr. Bensun Fong [redacted] Ottawa, ON K1H8M5 Canada Attn: Mr. Bensun Fong
Total	0.00 CAD

Terms and Conditions

Springer Nature Customer Service Centre GmbH
Terms and Conditions

This agreement sets out the terms and conditions of the licence (the **Licence**) between you and **Springer Nature Customer Service Centre GmbH** (the **Licensor**). By clicking 'accept' and completing the transaction for the material (**Licensed Material**), you also confirm your acceptance of these terms and conditions.

1. **Grant of License**

    1. The Licensor grants you a personal, non-exclusive, non-transferable, world-wide licence to reproduce the Licensed Material for the purpose specified in your order only. Licences are granted for the specific use requested in the order and for no other use, subject to the conditions below.

    2. The Licensor warrants that it has, to the best of its knowledge, the rights to license reuse of the Licensed Material. However, you should ensure that the material you are requesting is original to the Licensor and does not carry the copyright of another entity (as credited in the published version).

3. If the credit line on any part of the material you have requested indicates that it was reprinted or adapted with permission from another source, then you should also seek permission from that source to reuse the material.

2. **Scope of Licence**

1. You may only use the Licensed Content in the manner and to the extent permitted by these Ts&Cs and any applicable laws.

2. A separate licence may be required for any additional use of the Licensed Material, e.g. where a licence has been purchased for print only use, separate permission must be obtained for electronic re-use. Similarly, a licence is only valid in the language selected and does not apply for editions in other languages unless additional translation rights have been granted separately in the licence. Any content owned by third parties are expressly excluded from the licence.

3. Similarly, rights for additional components such as custom editions and derivatives require additional permission and may be subject to an additional fee. Please apply to Journalpermissions@springernature.com/bookpermissions@springernature.com for these rights.

4. Where permission has been granted **free of charge** for material in print, permission may also be granted for any electronic version of that work, provided that the material is incidental to your work as a whole and that the electronic version is essentially equivalent to, or substitutes for, the print version.

5. An alternative scope of licence may apply to signatories of the STM Permissions Guidelines, as amended from time to time.

Duration of Licence

1. A licence for is valid from the date of purchase ('Licence Date') at the end of the relevant period in the below table:

Scope of Licence	Duration of Licence
Post on a website	12 months
Presentations	12 months
Books and journals	Lifetime of the edition in the language purchased

Acknowledgement

1. The Licensor's permission must be acknowledged next to the Licenced Material in print. In electronic form, this acknowledgement must be visible at the same time as the figures/tables/illustrations or abstract, and must be hyperlinked to the journal/book's homepage. Our required acknowledgement format is in the Appendix below.

Restrictions on use

1. Use of the Licensed Material may be permitted for incidental promotional use and minor editing privileges e.g. minor adaptations of single figures, changes of format, colour and/or style where the adaptation is credited as set out in Appendix 1 below. Any other changes including but not limited to, cropping, adapting, omitting material that affect the meaning, intention or moral rights of the author are strictly prohibited.

2. You must not use any Licensed Material as part of any design or trademark.

3. Licensed Material may be used in Open Access Publications (OAP) before publication by Springer Nature, but any Licensed Material must be removed from OAP sites prior to final publication.

Ownership of Rights

1. Licensed Material remains the property of either Licensor or the relevant third party and any rights not explicitly granted herein are expressly reserved.

Warranty

IN NO EVENT SHALL LICENSOR BE LIABLE TO YOU OR ANY OTHER PARTY OR ANY OTHER PERSON OR FOR ANY SPECIAL, CONSEQUENTIAL, INCIDENTAL OR INDIRECT DAMAGES, HOWEVER CAUSED, ARISING OUT OF OR IN

CONNECTION WITH THE DOWNLOADING, VIEWING OR USE OF THE MATERIALS REGARDLESS OF THE FORM OF ACTION, WHETHER FOR BREACH OF CONTRACT, BREACH OF WARRANTY, TORT, NEGLIGENCE, INFRINGEMENT OR OTHERWISE (INCLUDING, WITHOUT LIMITATION, DAMAGES BASED ON LOSS OF PROFITS, DATA, FILES, USE, BUSINESS OPPORTUNITY OR CLAIMS OF THIRD PARTIES), AND
WHETHER OR NOT THE PARTY HAS BEEN ADVISED OF THE POSSIBILITY OF SUCH DAMAGES. THIS LIMITATION SHALL APPLY NOTWITHSTANDING ANY FAILURE OF ESSENTIAL PURPOSE OF ANY LIMITED REMEDY PROVIDED HEREIN.

Limitations

1. ***BOOKS ONLY:***Where **'reuse in a dissertation/thesis'** has been selected the following terms apply: Print rights of the final author's accepted manuscript (for clarity, NOT the published version) for up to 100 copies, electronic rights for use only on a personal website or institutional repository as defined by the Sherpa guideline (www.sherpa.ac.uk/romeo/).

2. For content reuse requests that qualify for permission under the STM Permissions Guidelines, which may be updated from time to time, the STM Permissions Guidelines supersede the terms and conditions contained in this licence.

Termination and Cancellation

1. Licences will expire after the period shown in Clause 3 (above).

2. Licensee reserves the right to terminate the Licence in the event that payment is not received in full or if there has been a breach of this agreement by you.

Appendix 1 — Acknowledgements:

For Journal Content:
Reprinted by permission from [**the Licensor**]: [**Journal Publisher** (e.g. Nature/Springer/Palgrave)] [**JOURNAL NAME**] [**REFERENCE CITATION**(Article name, Author(s) Name), [**COPYRIGHT**] (year of publication)
For **Advance Online Publication papers:**
Reprinted by permission from [**the Licensor**]: [**Journal Publisher** (e.g. Nature/Springer/Palgrave)] [**JOURNAL NAME**] [**REFERENCE CITATION**(Article name, Author(s) Name), [**COPYRIGHT**] (year of publication), advance online publication, day month year (doi: 10.1038/sj.[JOURNAL ACRONYM].)
For Adaptations/Translations:
Adapted/Translated by permission from [**the Licensor**]: [**Journal Publisher** (e.g. Nature/Springer/Palgrave)] [**JOURNAL NAME**] [**REFERENCE CITATION**(Article name, Author(s) Name), [**COPYRIGHT**] (year of publication)
Note: For any republication from the British Journal of Cancer, the following credit line style applies:
Reprinted/adapted/translated by permission from [**the Licensor**]: on behalf of Cancer Research UK: : [**Journal Publisher** (e.g. Nature/Springer/Palgrave)] [**JOURNAL NAME**] [**REFERENCE CITATION** (Article name, Author(s) Name), [**COPYRIGHT**] (year of publication)
For **Advance Online Publication** papers:
Reprinted by permission from The [**the Licensor**]: on behalf of Cancer Research UK: [**Journal Publisher** (e.g. Nature/Springer/Palgrave)] [**JOURNAL NAME**] [**REFERENCE CITATION** (Article name, Author(s) Name), [**COPYRIGHT**] (year of publication), advance online publication, day month year (doi: 10.1038/sj.[JOURNAL ACRONYM])
For Book content:
Reprinted/adapted by permission from [**the Licensor**]: [**Book Publisher** (e.g. Palgrave Macmillan, Springer etc) [**Book Title**] by [**Book author**(s)] [**COPYRIGHT**] (year of publication)

Other Conditions:
Version 1.3

Questions? customercare@copyright.com or +1-855-239-3415 (toll free in the US) or +1-978-646-2777.